

Modeling GSH Metabolism in Diabetes to Study the Role of Redox Status in Anti-diabetic Treatment

विद्या वाचस्पति की
उपाधि की अपेक्षाओं की आंशिक पूर्ति में प्रस्तुत शोध प्रबंध

A thesis submitted in partial fulfillment of the requirements of the
degree of Doctor of Philosophy

द्वारा / By

छात्र का नाम / Name of Student: अर्जुन कोलप्पुरत्त मठतिल /
Arjun Kolappurath Madathil

पंजीकरण सं. / Registration No.: **20173569**

शोध प्रबंध पर्यवेक्षक / Thesis Supervisor: डॉ. प्रणय गोयल /
Dr. Pranay Goel



भारतीय विज्ञान शिक्षा एवं अनुसंधान संस्थान पुणे
INDIAN INSTITUTE OF SCIENCE EDUCATION AND RESEARCH PUNE

2023

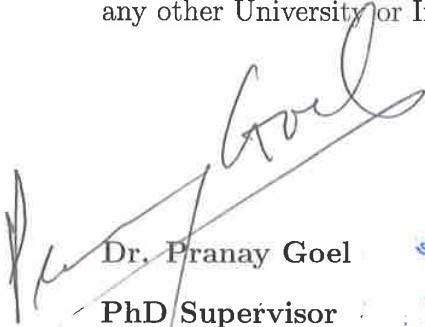
Dedication

To my mother and sister

Thank you for being there, always.

Certificate

I hereby certify that the thesis entitled “**Modeling GSH Metabolism in Diabetes to Study the Role of Redox status in Anti-diabetic Treatment**” presented by Mr. Arjun Kolappurath Madathil was carried out completely by him under my supervision. The work presented here is original and has not been included previously for the award of any degree or diploma from any other University or Institution.



Dr. Pranay Goel

PhD Supervisor

Dept. of Biology

IISER Pune

डॉ. प्रणय गोयल / Dr. Pranay Goel
सहयोगी प्राध्यापक / Associate Professor
भारतीय विज्ञान शिक्षा एवं अनुसंधान संस्थान
Indian Institute of Science Education & Research
पुणे / Pune - 411 008, India

Date:

13 July 2023

Declaration

I hereby declare that the work in this thesis is my original work and has not been submitted for any other degree or professional qualification. Any sources used in preparing this thesis have been fully acknowledged and referenced by the academic conventions of my field of study.



Mr. Arjun Kolappurath Madathil

Reg. ID: 20173569

Dept. of Biology

IISER Pune

Date: 14/7/2023

Acknowledgements

I hereby want to express my sincere gratitude to the following individuals and entities who have played significant roles directly and indirectly in the completion of my PhD thesis:

Firstly, I am grateful to my supervisor, Dr. Pranay Goel, for his invaluable guidance, constant support, and insightful discussions throughout the PhD period. His expertise has been crucial in shaping the direction of my work. He has motivated me to pursue a career as an independent researcher and enlightened me about the significance of critical reasoning in research. I am truly indebted for his instrumental role in my academic and personal growth. The impact of his guidance and insights will resonate with me in my future endeavors as well. Thank you for everything.

I sincerely thank my Research Advisory Committee members, namely Professor Saroj Ghaskadbi, Dr. Collins Assisi, and Dr. Chetan Gadgil, for their interest in my work, valuable insights, constructive criticism, and continuous encouragement. In particular, I would like to extend my special gratitude to Professor Saroj Ghaskadbi, a mentor and collaborator who played a significant role in my research. I am thankful to Professor Ghaskadbi for generously sharing different diabetic datasets, which greatly contributed to the success of my work. Additionally, their guidance has been invaluable to this research.

I want to sincerely thank Professor James Sneyd for his invaluable mentor-

ship, support, and enlightening discussions. His guidance has played a crucial role in enhancing the clarity and rigor of my research findings. I am grateful for the time and effort he dedicated to mentoring in this journey.

Special thanks to IISER Pune and DST Inspire for funding me through PhD fellowship.

I am grateful to my colleagues and friends for their understanding and support throughout my PhD journey, especially during the tough times. In particular, Prashasti, Sandy, Sai, Pranoti, members of the GIT Travel group, and IISER Badminton groups for their continuous support and the beautiful memories shared in Pune. Their diverse perspectives and intellectual contributions have significantly enhanced my research experience.

Last but not least, I express my deepest appreciation to the family for their unwavering support and admiration of my efforts throughout my journey. Thank you for standing by me, particularly during challenging moments.

Abstract

Hyperglycemia-induced oxidative stress leads to the development and progression of complications associated with type 2 diabetes (T2D). The cellular antioxidant glutathione (GSH) is crucial in maintaining systemic redox balances. Studies have reported low GSH concentration in individuals with T2D, and alleviating systemic oxidative stress through GSH supplementation could help control the complications. A six-month-long pragmatic prospective clinical trial was conducted to investigate the effect of oral GSH supplementation on erythrocytic GSH stores and glucose homeostasis in individuals with T2D undergoing anti-diabetic treatment. GSH supplementation was observed to improve body stores of GSH and offered protection from oxidative damage in these individuals. It also helped maintain lower HbA1c and improved fasting insulin in elder individuals with T2D. Inter-individual variations of biochemical changes were observed to be very evident in this clinical study. In order to understand the dynamics of biochemical responses and their inter-individual variation for elucidating effective personalized interventions with GSH, we analyzed the clinical trial data with the framework of linear mixed-effects (LME) models. We modeled longitudinal changes in individuals with T2D and obtained the distribution of subject-wise trajectories and overall rates of changes across various study groups of GSH supplementation. We modeled the serial changes in elder and younger individuals with T2D during the study period

separately to investigate the variations in their progression. The model-derived average linear trajectories elucidate the progression of biochemical parameters in individuals with T2D over the six-month study period. The response to GSH supplementation was observed to differ between elder and younger individuals with T2D. GSH was observed to replenish faster in younger than in elder individuals with T2D. It enhances the reduction rates in HbA1c and boosts fasting insulin levels in elder individuals with T2D. The reduction in 8-OHdG occurred at a faster rate in older individuals compared to their younger counterparts. Further, we monitored imbalances in cellular GSH and their turnover to provide quantitative insights into the recovery path of individuals with T2D. We propose a minimal mathematical model based on physiology for describing erythrocytic GSH turnover under varying extracellular conditions. This model was used to understand the glutathione response profiles in erythrocytic treatment experiments conducted in nondiabetic, prediabetic, and diabetic individuals. Model estimates of relevant parameters described the restoration of cellular GSH pools and stress under varying extracellular conditions, thereby allowing us to demonstrate patient recovery as a quantal response to GSH supplementation. Therefore, the research conducted in this thesis indicates that oral GSH supplementation has the potential to complement anti-diabetic therapy, leading to improved glycemic targets, particularly in the elderly. Model results and predictions assist in evaluating treatment progress and personalizing treatment goals for using oral GSH supplementation as an adjunct therapy in T2D.

Contents

1	Introduction	19
1.1	Datasets	25
1.2	Thesis Outline	26
1.3	Methodological Approaches	31
2	Problem foundations: Understanding GSH metabolism and oxidative stress in T2D	34
2.1	Roles of ROS in the pathophysiology of T2D complications . .	37
2.2	GSH: the master antioxidant and implications in T2D care . .	40
2.2.1	Targeting OS in T2D: can GSH-based therapy be promising?	42
2.3	Quantitative approaches for T2D care	44
2.3.1	Modeling GSH metabolism in erythrocytes	46
2.3.2	Modeling to tailor individualized targets for GSH supplementation in T2D treatment	48
3	Investigating the effect of GSH supplementation on individuals with T2D: a randomized controlled trial	51
3.1	Introduction	52
3.2	Methodology	55
3.2.1	The design of clinical trial	55

3.2.2	Clinical trial participants and measured data	56
3.2.3	Statistical analysis of the clinical data	58
3.2.4	Effect size analysis between D and DG groups	59
3.3	Results	60
3.3.1	Covariate balance between the study arms	60
3.3.2	Effect of GSH supplementation on 6-month biochemical changes	62
3.3.3	Serial biochemical changes in the study groups	62
3.3.4	Effect size analysis in different age groups	66
3.3.5	Effect size analysis on treatment subgroups	71
3.4	Discussion	74
3.5	Appendix	79
3.5.1	Biochemical changes in elder diabetic individuals	79
4	Multilevel modeling of longitudinal biochemical changes in in- dividuals with T2D on GSH supplementation	83
4.1	Introduction	84
4.2	Methodology	87
4.2.1	Summary of clinical trial data	87
4.2.2	Linear mixed-effects models	89
4.2.3	Modeling clinical trial data with LME models	90
4.2.4	Formulation of linear mixed-effects models	90
4.2.5	Design matrix of model equations	92
4.2.6	Covariance matrices in the model	94
4.2.7	Model derivation for BLUE and BLUP	96
4.2.8	Iterative schemes of optimization	98
4.2.9	Model parameters and fitting	99
4.2.10	Data preparation for fitting with LME models	100

4.2.11	Independent LME models for two age classes	101
4.2.12	LME models to study age effects	102
4.2.13	Correlation analysis with LME models	104
4.2.14	Making predictions for new individuals	105
4.3	Results	106
4.3.1	Results from LME models	106
4.3.2	Results from the analysis of two independent age classes	111
4.3.3	Results from analyzing age effects	116
4.3.4	Results of correlation analysis with LME models	118
4.3.5	Predictions for virtual individuals	121
4.4	Discussion	126
4.5	Appendix	132
4.5.1	Sample structure of the data for LME analysis	132
4.5.2	Results of RIFS models	133
4.5.3	Results of RIFS models for different age classes	135
4.5.4	RIRS models for anti-diabetic treatment groups	136

**5 Mathematical modeling of erythrocytic glutathione turnover
in T2D 138**

5.1	Introduction	138
5.2	Methodology	141
5.2.1	Statement of contribution	141
5.2.2	Funding	142
5.2.3	Ethics Statement	142
5.2.4	Data Availability Statement	142
5.2.5	Acknowledgments	142
5.2.6	Conflict of Interest	142
5.2.7	Erythrocyte experiments	143

5.2.8	Measured data from erythrocyte experiments	144
5.2.9	Modelling GSH turnover in human erythrocytes	144
5.2.10	Minimal mathematical model for GSH turnover	145
5.2.11	Model parameters	146
5.2.12	Model fitting and parameter optimization	147
5.2.13	GSH influx and H ₂ O ₂ estimates from clinical trial data	148
5.3	Results	149
5.3.1	Fitted model parameters and steady states	149
5.3.2	Geometry of minimal model and implications	149
5.3.3	Results of stimulation with extracellular GSH	152
5.3.4	Results of stimulation with extracellular H ₂ O ₂	152
5.3.5	Results of stimulation with extracellular GSSG	156
5.3.6	Estimated α - H ₂ O ₂ traces on GSH supplementation and clinical implications	160
5.4	Discussion	170
5.5	Appendix	176
5.5.1	Detailed models for <i>GPx</i> and <i>GR</i> enzyme kinetics	176
5.5.2	Glutathione Reductase	177
5.5.3	Glutathione Peroxidase	179
5.5.4	Use of $\frac{GSSG}{GSH^2}$ ratio: perspectives	183
5.5.5	Model-derived relationships for $\frac{GSSG}{GSH^2}$ ratio	184
5.5.6	8-OHdG and G-ratio comparisons	186
6	Conclusions and future directions	189
A	Copyrights and License	224
B	List of Publications	227
B.1	Publications	227

B.2	Conference Abstracts	228
B.3	Preprints	228
C	Ethics statement	256

List of Figures

2.1	Oxidative stress pathways involved in T2D complications . . .	38
3.1	Depiction of the clinical study design	57
3.2	Effect size of changes in blood biochemical parameters	63
3.3	Longitudinal changes in GSH and GSSG concentrations	65
3.4	Longitudinal changes in 8-OHdG and HbA1c concentrations .	67
3.5	Longitudinal changes in FPG and FPI levels	68
3.6	Longitudinal changes in PPG and PPI levels	69
3.7	The effect size of changes in different age classes	70
3.8	The effect size of biochemical changes in different anti-diabetic treatment groups	73
3.9	Serial changes of GSH and GSSG in elderly diabetic subjects .	79
3.10	Serial changes of 8-OHdG and HbA1c in elderly diabetic subjects	80
3.11	Serial changes of FPG and FPI in elderly diabetic subjects . .	81
3.12	Serial changes of PPG and PPI in elderly diabetic subjects . .	82
4.1	Longitudinal biochemical changes of individuals with T2D in the clinical trial	88
4.2	Treatment effects of GSH supplementation on biochemical changes estimated using LME models	109

4.3	Treatment effects of GSH supplementation on glycemia estimated using LME models	110
4.4	Average treatment effects of GSH supplementation in younger diabetic subjects	112
4.5	Average treatment effects of GSH supplementation in elder diabetic subjects	113
4.6	Correlation analysis with LME Models	122
4.7	Correlation analysis with LME Models for elder diabetic subjects	123
4.8	Correlation analysis with LME Models for younger diabetic subjects	124
4.9	Model predictions for virtual individuals.	125
4.10	Fitted results of RIFS models for biochemical changes.	134
5.1	Reaction diagram for building the minimal mathematical model for glutathione turnover	145
5.2	The geometry of minimal GSH model and implications for different groups	150
5.3	Effects of extracellular GSH treatments in nondiabetic individuals	153
5.4	Effects of extracellular GSH treatments in prediabetic individuals	154
5.5	Effects of extracellular GSH treatments in diabetic individuals	155
5.6	Effects of extracellular H ₂ O ₂ treatments in nondiabetic, individuals	157
5.7	Effects of extracellular H ₂ O ₂ treatments in prediabetic individuals	158
5.8	Effects of extracellular H ₂ O ₂ treatments in diabetic individuals	159
5.9	Effects of extracellular GSSG treatments in nondiabetic individuals	161
5.10	Effects of extracellular GSSG treatments in prediabetic individuals	162

5.11	Effects of extracellular GSSG treatments in diabetic individuals	163
5.12	Longitudinal changes in the GSH influx and H_2O_2 in different groups	165
5.13	Longitudinal changes in the GSH influx and H_2O_2 in elder diabetic subjects	166
5.14	Trajectories of control group individuals in the clinical trial . .	167
5.15	Trajectories of D group individuals in the clinical trial	168
5.16	Trajectories of DG group individuals in the clinical trial	169
5.17	Reaction pathways for GSH turnover in RBCs.	176
5.18	Enzymatic kinetics for Glutathione Reductase	177
5.19	Enzymatic kinetics for Glutathione Peroxidase.	180
5.20	Regression between 8-OHdG and G-ratio in the control group at the first and third visits	187
5.21	Regression between 8-OHdG and G-ratio in the D group at the first and third visits	187
5.22	Regression between 8-OHdG and G-ratio in the DG group at the first and third visits	188
6.1	Reaction diagram for transport, intracellular synthesis, and turnover of GSH in RBCs.	195
A.1	Copyright information for Kalamkar et al. (2022) reused in chapter 3	225
A.2	Copyright information for Madathil et al. (2023) reused in chapter 4	226

List of Tables

3.1	Baseline characteristics of Control, D, and DG groups	61
4.1	Results from LME Models	108
4.2	Results from LME models for younger adults	116
4.3	Results from LME models for elder adults	117
4.4	Results from Model 2 for analyzing age-effects	118
4.5	Results from Model 3 for analyzing age-effects	119
4.6	Results obtained from Model 4 for analyzing age-effects	119
4.7	Comparison between models for studying age-effects using AIC estimates	120
4.8	Comparison between models for studying age-effects using BIC estimates	120
4.9	Baseline values assumed for virtual individuals.	121
4.10	The structure of sample data from D and DG groups.	132
4.11	Results of fixed-effect parameters from RIFS models.	133
4.12	Results of random-effect parameters from RIFS models.	133
4.13	Results from RIFS models fitted for elderly diabetic subjects.	135
4.14	Results from RIFS models fitted for younger diabetic subjects.	136
4.15	Results from RIRS models fitted for B and BS subgroups.	137

5.1	Parameter values obtained from model optimization from the three study groups.	149
-----	---	-----

Chapter 1

Introduction

Diabetes mellitus is a non-communicable metabolic disorder characterized by elevated levels of glucose in the bloodstream (ADA [1], Rockefeller [2], DeFronzo *et al.* [3]). It has already become a global epidemic, with the number of diabetic adults already exceeding 415 million and projected to rise to cross 642 million in the next two decades (CDC [4], NCD Risk Factor Collaboration [5], IDF Diabetes Atlas [6], Saklayen *et al.* [7], Unnikrishnan *et al.* [8], Wild *et al.* [9], Saeedi *et al.* [10]). Notably, India is outracing other countries to become an epicenter of diabetes worldwide (Shetty [11], Kaveeshwar and Cornwall [12]). Diabetes is primarily classified into three types: type 1 and type 2, both representing the chronic forms of diabetes, and gestational diabetes, a short-term condition. Among them, type 2 diabetes (T2D) is the most prevalent, and it has detrimental effects on various bodily systems, potentially leading to severe and life-threatening complications, including atherosclerosis, neuropathy, retinopathy, coronary artery diseases, etc. Due to the complexity of disease conditions, multiple strategies are also required for the efficient management of diabetes (Martín-Timón *et al.* [13], Rask-Madsen and King [14]).

Over six decades after the discovery of reactive oxygen species (ROS) in skeletal muscles (Commoner *et al.* [15]), the scientific community has been comprehending the effect of the unpaired electron of ROS molecules in physiological pathways (Juan *et al.* [16], Zorov *et al.* [17], Roy *et al.* [18]). ROS plays various roles as secondary messengers and influences normal physiological functions in the body (Valko *et al.* [19], Bardaweel *et al.* [20], Magder [21]). Several clinical and experimental reports have shown beneficial and detrimental characteristics of ROS which help it in performing its specific roles at T2D conditions in different biological compartments (Mero *et al.* [22], Bardaweel *et al.* [20], Giacco *et al.* [23], Marchioli *et al.* [24]). The excessive production of superoxides triggers five different pathways predominant in the progression of complications. These pathways not only included the increase in polyol pathway flux and advanced glycation end-products (AGEs) but also enhanced AGE receptor expressions, activation of protein kinase C (PKC) isoforms, and excessive activity in the hexosamine pathways (Lazo-de-la-Vega *et al.* [25], Evans *et al.* [26], Espinosa-Diez *et al.* [27]). The state of imbalance between ROS production and their neutralization in the presence of antioxidants is known as **oxidative stress**. Notably, this leads to a disruption of oxidation-reduction (redox) reactions and redox control that are fundamental in cell signaling and physiological regulation (Baynes [28], Birben *et al.* [29], Kurutas *et al.* [30]). Oxidative stress tremendously affects health in individuals with T2D, as it causes inflammation and migration of smooth muscle cells and impacts the function of vascular wall cells. These subsequently contribute to both microvascular and macrovascular complications (Pizzino *et al.* [31], Bennett *et al.* [32]).

Glutathione is the most abundant cellular endogenous antioxidant, which plays a vital role in determining their redox status (Wu *et al.* [33], Sies [34]).

Glutathione forms a prominent redox couple with reduced and oxidized species, GSH and GSSG, respectively. The glutathione reductase enzyme reduces oxidized glutathione (GSSG) to GSH, whereas the glutathione peroxidase enzyme (GPx) catalyzes the reverse reaction. The development of oxidative stress increases GSSG, which stimulates reductase and regenerates glutathione using reducing equivalents from NADPH (Wu *et al.* [33]). GSH is mainly synthesized from glutamate, cysteine, and glycine amino acids with the help of two cytosolic enzymes, γ -glutamylcysteine synthetase and GSH synthetase. The activity of γ -glutamylcysteine synthetase enzyme, availability of cysteine pools, and feedback inhibition are the major regulators of GSH synthesis (Townsend *et al.* [35], Lu [36]). Glutathione is compartmentalized in the cell, with the majority found in the cytoplasmic pool functioning in detoxification (Griffith *et al.* [37]). Several reports have shown that erythrocyte stores of GSH are significantly low in individuals with T2D (Lutchmansingh *et al.* [38], Gawlik *et al.* [39], Thornalley *et al.* [40]). These studies have indicated that a decrease in the concentration of GSH makes individuals with T2D more susceptible to oxidative damage and leads to the formation of glycation products, which are the primary precursors of T2D complications. Additionally, Acharya *et al.* [41] showed that controlling hyperglycemia over two months increased GSH stores and reduced oxidative damage significantly regardless of the anti-diabetic treatment. When different oxidative stress markers were measured, GSH best explained the glucose recovery, which was apparently exhibiting a rapid response within eight weeks to variations in HbA1c levels (Kulkarni *et al.* [42]). This data indicated that altering hyperglycemia leads to changes in GSH. So, it is essential to ask whether changes in GSH would impact glucose homeostasis in T2D. Furthermore, there is a need to investigate the role of these factors in the emergence of T2D complications and the possibility

of preventing them by administering GSH supplements. It is reasonable to believe that replenishing GSH could be a potentially promising strategy to improve systemic redox status in individuals with T2D (Forman *et al.* [43]).

Strong clinical evidence is still lacking on the effects of GSH supplementation, and this is an important open area in improving T2D care. Clinical trials are designed to answer these questions about GSH-based interventions and improve health and quality of life. Only after well-designed trials have established the evidence will it be possible to claim whether a GSH-assisted treatment is effective and safe for individuals with T2D. Without that, there is a great risk that people will be given treatments that do not work and may even be harmful. American Diabetes Association (ADA) also shares the same view towards the use of antioxidant supplementation in their standards of diabetes care (ADA, [44]). So, taking antioxidant supplements may not be advisable for everyone. However, it is also important to examine the effects of supplementation in T2D, and if it does benefit, who might benefit better, and what effective ways or doses of administration are. Well-designed and adequately powered clinical trials are necessary to determine whether GSH supplementation has any harmful effects or is beneficial for individuals with T2D. Moreover, biochemical changes in individuals with T2D are shown to have inter-individual variations in their response to interventions due to differences in their physiology and T2D conditions (Kulkarni *et al.* [42]).

The progression and pathophysiology of T2D are unique in individuals, and it is crucial to address these differences while designing the treatment and care (Shrivastava *et al.* [45], Adu *et al.* [46], Chiou and Shang-Jyh [47]). This indicates personalized management plans are essential to address the specific needs of each individual with T2D. A personalized approach considering factors such as age, lifestyle, and overall health status to create a tailored diabetes

management plan can potentially work best for them and can achieve better health treatment outcomes (Inzucchi *et al.* [48]). Quantitatively analyzing the imbalances in cellular GSH stores, their restoration patterns, and responses to other blood biochemical parameters can potentially provide insights into the recovery path of individuals with T2D from the complications. Statistically modeling longitudinal changes of individuals with T2D in a clinical trial would help analyze and quantify the outcomes of GSH supplementation and forecast the individual trajectories and variation between individuals in the different study arms. This would be necessary for clinicians to customize treatment strategies by understanding the patient response and improving it efficiently. Moreover, developing effective GSH supplementation strategies to improve health and interventions in T2D requires a thorough quantitative understanding of GSH metabolism. Mechanistic models, which are predictive in nature, can be utilized to describe these dynamics, evaluate a cellular response in individuals with T2D compared to average population-level responses, and further determine the effectiveness of a treatment strategy. Model-derived insights about the parameters and model predictions can be incorporated while designing personalized anti-diabetic therapies based on the redox status of individual patients.

We primarily designed this project to study GSH metabolism in diabetes and how controlling redox status influences and improves anti-diabetic treatment outcomes. Our objectives are to evaluate the effectiveness of GSH supplementation in regulating the redox status and improving the efficiency of treatment, with a particular focus on personalized goals, by exploring adequate quantitative approaches. Our lab at IISER Pune has been collaborating with the group led by Prof. Saroj Ghaskadbi from SPPU Pune for over a decade on various aspects of diabetes and the impacts of glutathione on healthcare in

T2D. In this thesis project, we mainly work with datasets collected from two major studies in this collaboration. These datasets are described in the section below. To develop effective strategies for GSH-assisted anti-diabetic interventions with personalization goals, we adopted a comprehensive multiscale modeling framework that utilizes these two datasets. Firstly, we performed a population-level analysis to examine the effects of GSH supplementation on the biochemical parameters of individuals with T2D. Further, we formulated statistical models for the longitudinal analysis of biochemical changes observed in T2D patients during the clinical trial duration. These models provided estimates to predict the trajectory of progression of individuals with T2D and the impact of GSH supplementation, which further facilitates personalized treatment goal setting. These results establish new standards of GSH supplementation that are directly useful for clinical applications in T2D. Secondly, we formulated mathematical models for describing the dynamics of cellular GSH turnover and examining how it responds to extracellular stimuli under different diabetic conditions. These model estimates and insights derived from these models help identify the individual-specific recovery on GSH supplementation in T2D patients. Overall, these findings, derived from the clinical trial and modeling approaches to improving the standards of personalized T2D care with GSH, are the main outcomes of this thesis research.

1.1 Datasets

The datasets utilized in this thesis are briefly described below.

1. A randomized controlled clinical trial was conducted on Indian diabetic patients who were already under anti-diabetic treatment and recruited by physician Dr. Uma Divate from JCDC at Jehangir Hospital, Pune. All subjects provided signed informed consent upon enrollment in the study. Serial collection of blood samples was performed by Dr. Divate and colleagues on the study subjects at the first visit, three months, and six months after the first visit. Ghaskadbi group measured blood biochemical parameters, erythrocytic glutathione, and oxidative DNA damage markers (8-OHdG) from these samples. After the data collection, the de-identified data was shared with us for analysis. These datasets have been utilized for the research work conducted in Chapters 3 and 4. Refer to Appendix Section C for the ethical clearance document and details for this study (numbered 1).
2. A study with cellular treatment experiments was conducted to study the response behavior of erythrocytic glutathione-dependent systems on different extracellular conditions. Nondiabetic, prediabetic, and diabetic subjects were recruited from the Savitribai Phule Pune University (SPPU) health center, Pune. Signed informed consent was obtained from the subjects for participating in the study. In vitro experiments on the collected blood samples were conducted by Prof. Ghasbkadbi and colleagues. The blood samples were treated with different doses of GSH and hydrogen peroxide extracellularly. The de-identified datasets were shared for modeling and analysis. These datasets have been used for the research work conducted in Chapter 5. Refer to Appendix Section C for

the ethical clearance details (numbered 2).

1.2 Thesis Outline

This research is carried out to investigate GSH metabolism in T2D conditions and gain a deeper understanding of how the redox state plays a role in improving anti-diabetic interventions. This research can shed light on enhancing treatment options, ultimately developing more effective approaches to managing T2D. The project utilized a systematic framework incorporating various quantitative modeling approaches to analyze clinical and experimental data at *population-, patient-, and cellular-levels*. This thesis aims to evaluate the effectiveness of GSH-based interventions in diabetic patients and develop personalized treatment goals through a population-level analysis of extensive clinical trial data, a longitudinal analysis of patient-level data, and mechanistic modeling of cellular behavior related to GSH systems in different chapters. The underlying rationale and motivation for different parts of the project are presented below. A detailed introduction with technical aspects is provided before the corresponding chapter.

In **Chapter 2**, we begin by reviewing the existing literature to understand the theories underlying the development of oxidative stress arising from excessive ROS production. We emphasize how it plays a central role in the pathophysiology of complications arising from hyperglycemia in T2D. We thoroughly examine the evidence about the effectiveness of antioxidant supplementation in T2D. It is highlighted that the standards of diabetes care by the ADA do not recommend routine antioxidant supplementation due to insufficient evidence about their safety and efficacy. We motivate the role of the most vital and abundant endogenous antioxidant, GSH, in T2D complications. We also stress

the previous studies in the literature that attempted GSH supplementation and the limited evidence available. With strong literature support, we emphasize the potential of using GSH as a viable strategy for relieving oxidative stress and managing complications in T2D. We have developed fundamental directions for this project by thoroughly reviewing the relevant literature. We ask whether changes in GSH could affect glucose homeostasis in individuals with T2D. Evaluating the impact of oral GSH supplementation on body GSH stores and the regulation of glucose homeostasis among T2D patients through a well-designed clinical trial would help greatly resolve the literature gap and provide evidence. By identifying specific phenotypes that may benefit most from GSH supplementation during the trial, we hope to understand better the potential utility of this approach for managing T2D. More importantly, the effects of supplementation in T2D benefit patients differently. So, we elaborate on why identifying effective and safer ways of administration in a patient-centered manner is the key to achieving efficient T2D care. Furthermore, we review previous studies to understand the relevance of quantitative approaches toward developing personalization goals. We emphasize some of the previous models of GSH metabolism in the literature. We specifically motivate the scope and potential of mechanistic modeling to obtain insights for predicting personalized treatment targets and interventions in T2D.

In **Chapter 3**, we present the randomized controlled clinical trial conducted in our collaboration with the Ghaskadbi lab from SPPU Pune to investigate the effects of oral GSH supplementation on improving GSH stores and glucose homeostasis in T2D patients. This is the most extensive longitudinal study on the effects of GSH supplementation reported in the literature. We provide the results from a detailed population-level effect size analysis of the biochemical data from the clinical trial subjects and offer compelling evidence

of the beneficial effects of GSH supplementation. Results from this study show a systemic improvement of the redox state in diabetes on GSH supplementation, and further, the augmented antioxidant reserves may help relieve oxidative assault. We also inquire whether supplementing with GSH enhances the efficacy of standard anti-diabetic treatment for maintaining normoglycemia in individuals with T2D. Important evidence shows that supplemented GSH is tolerated very well by patients, making it a beneficial therapeutic strategy to add to the clinician’s arsenal. Additionally, it is known in the literature that elder T2D subjects are prone to have more complications. We have also conducted a posthoc analysis to find differences in the effects of GSH supplementation between subgroups of individuals above and below the median age. Our study will be a milestone study of GSH supplementation in clinical practices. Not only do we believe that our results can be directly used clinically, but we also outline ways in which GSH supplementation can potentially be personalized. We point out that factors such as age, type of anti-diabetic interventions or medications, and dietary modifications may influence the effectiveness of GSH supplementation. Therefore, the development of more personalized strategies that take into account these factors is essential. Our study can serve as the foundation for future studies investigating the finer nuances of supplementation in different patient populations.

In **Chapter 4**, we present a longitudinal analysis of the biochemical changes in the participants in the clinical trial with diabetes. To the best of our knowledge, this marks **the first inter-individual examination of the impacts of GSH supplementation in individuals with T2D**. The primary findings of this study involve delineating the variability in inter-individual biochemical responses, notably influenced by an individual’s age group. We studied how T2D individuals responded to oral GSH supplementation and estimated the

effects brought in by the particular dose of GSH supplementation. A class of statistical models known as linear mixed effects (LME) models are used here to analyze and investigate the longitudinal data available from the clinical trial. These models allow consideration of a subject as an individual with unique characteristics and not just as a population member with an average value to estimate. Using mixed effects models, we assess the individual trajectories of GSH supplementation and estimate the average treatment effects of GSH supplementation. We provide model estimates of the effect of GSH supplementation on different blood biochemical parameters in T2D individuals. We also examine the differential effects of GSH supplementation in different age groups independently using LME models. We provide clinically helpful schemes for making predictions about the response of T2D individuals to GSH supplementation. This chapter focuses on developing approaches to addressing more personalized goals of GSH supplementation.

In **Chapter 5**, we formulate mathematical models for the dynamics of cellular-level GSH turnover under extracellular stimuli on different diabetic conditions. We present our approaches to developing a minimal mathematical model for the dynamics of erythrocytic GSH turnover. To support our cellular-level observations in the clinical trial, an experimental study of cellular treatments was further designed in collaboration with the Ghaskadbi group. Data of erythrocytic GSH response was collected from extracellular treatments with different concentrations of H_2O_2 and reduced, oxidized forms of glutathione in the three study groups in control, prediabetic, and diabetic individuals. We formulate physiology-based models and analyze cellular glutathione response profiles from these treatments. By modeling the cellular treatment data, we describe how erythrocytic GSH is altered under different conditions and how GSH supplementation affects this turnover in T2D. Re-

sults from these analyses help monitor the dynamics of cellular changes and further identify personalized strategies for employing GSH supplementation in anti-diabetic interventions.

In **Chapter 6**, we summarize the major findings and outcomes from different parts of this project. We then elaborate on the results and how the findings of our study contribute to an overall improvement in the standards of personalized care in Type 2 Diabetes. Our clinical study provides conclusive evidence of the effect of GSH supplementation on improving the body stores of GSH and their potential benefits in attaining glucose control targets in diabetic patients. Results from the population-level analysis of the clinical trial data are further investigated through inter-individual analysis at the patient level with LME models. This provides more robust evidence on the effects of GSH supplementation and studies how individuals respond relatively to the average population responses. LME models capture longitudinal biochemical changes in diabetic patients due to GSH supplementation. The prediction schemes using LME model estimates can predict individual-specific trajectories expected for newly recruited subjects with diabetes. These schemes will be of great translational potential for academic and clinical uses in forecasting the average time for patient responses and the extent of their responses. Further, the cellular-level model described how GSH turnover responds to different conditions. The analysis of the experimental data supports the evidence on the effects of GSH supplementation obtained from the clinical trial. By understanding the mechanisms of biochemical changes and the dynamics of their imbalances under different diabetic conditions, we can determine how recovery progresses in individuals. The model estimates and insights are pivotal in advancing the personalized treatment of T2D, providing valuable insights for clinical decision-making and improving patient outcomes. Together, the

results at these three levels establish the effects of GSH supplementation in T2D and provide ways to personalize and improve anti-diabetic interventions with it.

By comprehending how oxidants act and the potential and restrictions of antioxidant treatments, this work provides evidence and formulation of reasonable approaches with GSH to enhance therapeutic interventions in T2D. The framework of quantitative tools in this thesis project at different scales, including mechanistic components based on physiology, represent a promising form of decision support that can predict outcomes and patient progress in T2D treatment. The unifying theme of the chapters in this thesis is to investigate the effects of GSH-mediated interventions with quantitative approaches on improving the standards of personalized care for T2D. Moreover, this thesis ensures tangible outcomes with clinical utility in T2D, for which ready-to-deploy methods for digital tools can be formulated based on our findings.

1.3 Methodological Approaches

Throughout this research, we have attempted to constitute the problem into a part of the coherent multi-scale framework. This framework consists of conducting a clinical trial, analyzing different trends in the clinical data at the population level, understanding the dynamics down to their basic mechanisms at the individual levels, and then connecting them to fundamental ideas of metabolic dynamics at cellular levels.

The clinical study was conducted as a **pragmatic-prospective randomized clinical trial designed in a case-control setting**. This study carefully and rigorously adhered to the principles of randomization in trials to correctly

attribute the effects to the intervention of GSH supplementation alone. We confirmed the baseline covariate balance once randomization had been carried out. Thus, we emphasize that there is no bias in recruiting subjects to either the intervention arm or the diabetic control group. The metabolic conditions of these groups are very nearly identical. Various mathematical and statistical models are used to make better quantitative insights into the problem, namely a class of **mixed-effects models** for modeling longitudinal biochemical changes of diabetic patients in the clinical trial (Sections 4.2.3). Further, we formulate **mechanistic models** of cellular-level biochemical changes (Section 5.2.3) in individuals with different T2D conditions. However, there are both positive aspects and drawbacks to the use of each of these methods. Firstly, we acknowledge some limitations of the clinical study, such as that although anti-diabetic treatments were not changed during the study period, patients used different medications. We have examined the complexity of combining treatments, but some may lack sufficient statistical power. Secondly, we note that for some variables in the dataset, nonlinear mixed-effect models could have been suitable to describe the dynamics of changes, probably for a longer time duration. However, we specifically used a simple, ‘linear’ class of mixed-effects models to describe average linear trajectories over six months for all variables. These linear ME models were also used to obtain clinically transferable estimates of the treatment effect of intervention and correlation analysis to establish the association between different biochemical changes. We consider LME estimates, which predict model trajectories within the interquartile ranges of the data at all visits, to be good descriptions of the data. The linear models were also a suitable choice, considering the limited data points. Thirdly, the minimal mathematical models used for describing mechanistic pathways of GSH turnover offer possibilities for the analytical treatment

of the problem and theory development based on observations from cellular treatment experiments and the clinical trial of GSH supplementation. However, constructing these models required significant intuition to accurately depict the requisite physiology and incorporate sufficient complexity to account for the constrained experimental data.

The research findings presented in this work will establish a solid foundation and evidence for developing new strategies for GSH-mediated interventions in patients with T2D. This accomplishment has been made possible by integrating insights gained from clinical observations, data obtained from laboratory experiments, and their comprehensive modeling using mathematical and statistical methods with the coherent framework in this study.

Chapter 2

Problem foundations:

Understanding GSH metabolism and oxidative stress in T2D

Despite advancements in clinical treatments and medications, the occurrence of T2D has witnessed a substantial rise over the past few decades. Current clinical practices primarily aim to slow the progression of hyperglycemia but lack sufficient guidance on preventing complications associated with T2D. There is an urgent need to gain better insights into efficient preventive measures for controlling oxidative stress-lead complications for T2D care and to develop clinical and theoretical strategies focusing on optimizing interventions. In this thesis, we attempt to investigate GSH metabolism in T2D and, particularly, the role of redox status in facilitating personalized anti-diabetic interventions with the help of quantitative approaches. This thesis research plays a critical role in bridging this gap and improving the standards of T2D care.

To provide context for this research, we discuss the literature linking oxidative stress to the major T2D complications caused by hyperglycemia. The

activation of various metabolic signaling pathways by hyperglycemia can lead to diabetic complications such as inflammation in the vessels and nerves, nephropathy, retinopathy, and cardiovascular diseases (Rask-Madsen *et al.* [14], Giri *et al.* [49], Volpe *et al.* [50], Demir *et al.* [51]). Therefore, managing diabetes is challenging due to its complex nature involving multiple metabolic pathways, and effective strategies to regulate these pathways and prevent complications are scarce. Factors such as diet, physical activity, and weight management can influence diabetes and must be considered when tailoring anti-diabetic therapy for individuals.

The physiological relevance of antioxidants is still uncertain in treating diabetes in the light of ADA position (ADA [52]). So, taking antioxidant supplements may not be advisable for everyone. However, it is also important to investigate the role of GSH, the master antioxidant in cellular systems, in redox status and in improving the standards of personalized anti-diabetic interventions. Our research aims to investigate the evidence on the role of GSH and its relevance in the context of T2D care. Defining individualized treatment targets to manage diabetic complications could be more efficient, however challenging. It involves understanding patient-specific factors that impact intervention efficacy and the mechanistic behavior of antioxidant pools that affect cellular redox status and hyperglycemia-mediated diabetic complications. The current approach to managing hyperglycemia relies on utilizing existing knowledge of the underlying mechanisms, and glucose targets in patients are also determined by the progression toward diabetic complications. This thesis is about a quantitative understanding of the fundamental physiology of GSH actions in controlling hyperglycemia-induced oxidative stress associated with T2D complications. Additionally, our approaches enable for development of tailored diabetes management plans to utilize GSH supplement-

tation as a protection against hyperglycemia-induced complications triggered by oxidative stress.

We begin this chapter by attempting to understand how hyperglycemia-lead ROS production and the development of OS act as the central cause of complications in diabetes (Section 2.1). Substantial evidence supports the notion that controlling increased glucose levels may not be enough to mitigate diabetic complications. Consequently, we intend to question whether current interventions adequately address the root cause of diabetic complications while focusing only on glucose targets. In addition, we elaborate on the evidence that supports the possible uses of GSH in advancing diabetic complications (Section 2.2). It is important to emphasize that utilizing GSH to regulate OS could be a significant therapeutic objective in managing these complications. Additionally, we emphasize the requirement to reassess the conventional approaches in treating T2D with the help of model-based, data-driven insights and implementing personalized intervention strategies with GSH to target OS-lead complications specifically (Section 2.3).

In summary, by providing an overview of the causal relationships between hyperglycemia and OS, mechanisms by which it contributes to diabetes-related complications, functions of antioxidant defenses, methods for boosting it by replenishing GSH stores, potentials of GSH-based interventions and motivations behind personalized approaches needs, this lays the foundation for rationales behind aims of this research project. Before going into the role of GSH and its potential in regulating redox balances and mitigating T2D complications, we begin by describing oxidative stress in the pathophysiology of diabetes itself. This will give an understanding and motivation for discussing the need for effective antioxidant-based interventions in achieving T2D treatment objectives.

2.1 Roles of ROS in the pathophysiology of T2D complications

The imbalance between the generation of oxidizing agents and antioxidant defenses in cellular systems was coined as **oxidative stress** (OS) and popularized by Helmut Sies in several works for more than three decades ([53], [54], [55], [56], [57], [58], [59], [60]). The increased ROS production leads to the OS. ROS not only include reactive molecules derived from O_2 such as superoxide (O_2^-), singlet oxygen but also derivatives like hydrogen peroxide (H_2O_2), and hydroxyl radical (OH) (Giacco and Brownlee [23], Collin [61], Nordberg *et al.* [62]). OS arise from both endogenous and exogenous agents. Oxidative stress has been extensively studied in both basic and applied fields of biology and medicine (Storey [63], Jones and Sies [64], Islam [65], Lushchak [66], Cadenas *et al.* [67]). The field of redox biology has advanced from studying the concept of oxidative stress in pathology to exploring redox signaling in physiology for various diseases.

Figure 2.1 illustrates how hyperglycemia leads to reactive oxygen species production through various pathways and further impact, resulting in the modification and damage of proteins, apoptosis, impairing mitochondrial function, oxidative DNA damage, and diabetic complications. These effects are known to disrupt various signaling pathways and often lead to an acceleration of pathological progression and increased expressions of disease symptoms (Forman and Zhang [43], Halliwell [68], Halliwell [69]). Hyperglycemia causes tissue damage through different mechanisms, as depicted in Figure 2.1. These routes primarily stem from increased glucose flux via the polyol pathway and cellular production of AGEs. Additionally, the enhanced activation of PKC isoforms and the activity of the hexosamine pathway also act as links, lead-

ing to complications (Giacco and Brownlee [23], Lazo-de-la-Vega *et al.* [25]). Evidence shows that all of these mechanisms are triggered by ROS overproduction. ROS readily reacts with most biomolecules, which leads to free radical formation reactions. To control these reactions, these free radicals should engage in reactions to eliminate the unpaired electrons or with any antioxidants (Nordberg *et al.* [62]). The current approaches for managing T2D are not

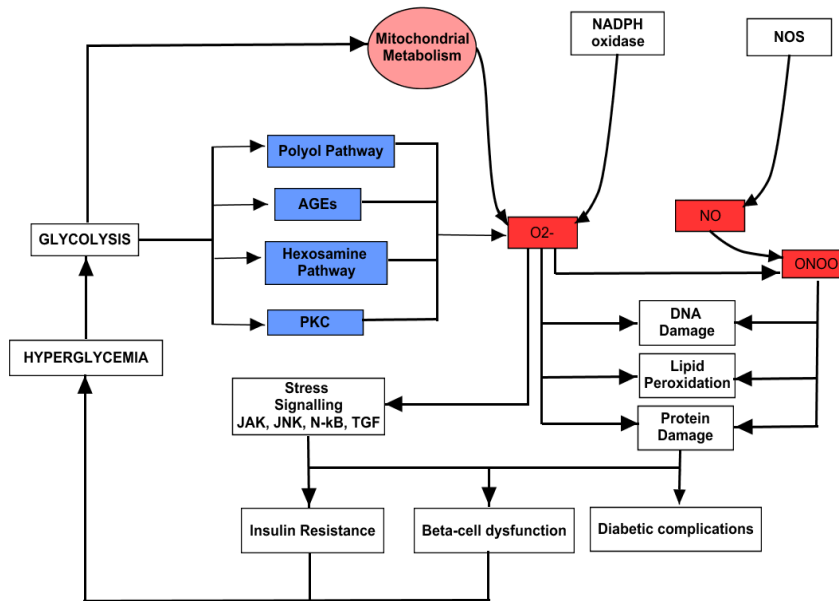


Figure 2.1: Oxidative stress pathways involved in T2D complications. This figure is adapted from Lazo-de-la-Vega *et al.* [25]. The overproduction of superoxides acts as the central causal link between hyperglycemia, leading to complications.

effective in preventing complications caused by oxidative stress. The excessive production of superoxides triggered by hyperglycemia is a continuous process with individual variations in its dynamics, making those practices unlikely to effectively counteract the detrimental effects of ROS molecules.

Evidence in the literature suggests that antioxidant-based approaches can

be crucial in relieving oxidative stress. Their ability to counteract the harmful effects of reactive oxygen species (ROS) and, thereby, oxidative stress could control the progression of T2D complications. Several animal studies have shown that antioxidants and antioxidant enzyme expressions have beneficial effects in inhibiting hyperglycemia-induced ROS production in diabetes. In turn this could prevent the progressions to diabetic retinopathy, nephropathy, and cardiomyopathy (Salvemini *et al.* [70], Vincent *et al.* [71]), Otero *et al.* [72], Zhang *et al.* [73], Kowluru *et al.* [74], DeRubertis *et al.* [75]). Several dietary constituents have been proposed to be major free radical scavengers inside the cellular systems; however, conclusive evidence is still lacking.

Developing effective antioxidant therapies is essential in managing T2D complications, given that oxidative stress is the major contributing factor. It is now widely recognized that the goal of antioxidant defense should not solely focus on preventing the formation of harmful ROS such as $\cdot\text{OH}$, ONOO^- , etc. H_2O_2 is a major precursor for ROS. Hence, a more nuanced approach would be needed to consider its importance in redox signaling. Increased awareness of this fact is crucial for developing effective antioxidant strategies. Here, we briefly reviewed the history and characteristics of ROS molecules and how they can adversely affect individuals with T2D. We also highlighted how this knowledge has contributed to our understanding of the pathophysiology of oxidative stress-induced T2D complications.

Additionally, we point out that the effectiveness of antioxidant therapies in T2D is complex and context-dependent, and detailed research is needed to understand their uses to tackle ROS developed in cellular systems. Nevertheless, incorporating antioxidant strategies into personalized T2D care plans is promising as a therapeutic approach to mitigate oxidative stress and improve overall patient outcomes.

2.2 GSH: the master antioxidant and implications in T2D care

The most common non-protein thiol observed in mammalian tissues, γ -glutamyl-cysteinyl-glycine, which is also known as GSH, acts as a molecule that performs various vital functions within the body (Meister and Anderson [76], Lu [77]). GSH is synthesized from glutamate, cysteine, and glycine amino acids, two consecutive reactions of γ -glutamyl cysteine synthase and glutathione synthase enzymes in the γ -glutamyl cycle (often referred to as the Meister cycle in the literature). The breakdown of GSH back into its constituent amino acids happens mainly through γ -glutamyl transpeptidase and cysteinyl-glycine dipeptidase (Lu [77], Sies [34], Wu *et al.* [33]). The antioxidant functions of GSH rely on GPx-catalyzed reactions that decrease hydrogen peroxide and lipid peroxide while GSH is oxidized to GSSG. This process creates a redox cycle in which GSSG is transformed back to GSH by GSSG reductase, requiring NADPH. Catalase can also reduce hydrogen peroxide but is exclusively in the peroxisome. Consequently, GSH is particularly crucial in protecting against oxidative stress generated. On severe OS conditions, if the conversion of GSSG into GSH gets difficult, GSSG may either be transported out of cells or combined with protein sulphhydryl groups to avoid significant shifts in the redox balance. This can cause depletion of cellular GSH supply. GSH plays a crucial role in redox signaling as it transfers electrons between molecules in the body and helps maintain a balanced cellular environment. Additionally, GSH detoxifies xenobiotics, which are foreign substances that can harm the body (Meister and Anderson [76], Lu [77]). It also modulates cell proliferation, apoptosis, immune function, and fibrogenesis, etc. Overall, glutathione is a critical component of many physiological processes and is essential for

maintaining optimal health (Meister and Anderson [76], Lu [77]).

Individuals with T2D are reported to have lower GSH levels in their red blood cells and plasma, which is associated with reduced expression of enzymes, including GCL, GS, and GGT (Lagman *et al.* [78]). The impaired synthesis of GSH contributes to its deficiency in patients with T2D, which is more pronounced in individuals with diabetic complications. There could have been elevated non-glycemic consumption of GSH, leading to its irreversible utilization. Furthermore, substrate availability also plays a role in controlling GSH synthesis rates, as demonstrated by another study that showed partial restoration of GSH pools and synthesis rates after supplementation (Sekhar [79]). Studies have also found that small pools of these compounds in individuals with T2D can undergo a higher turnover rate, similar to proteins (Gougeon *et al.* [80], Halvatsiotis *et al.* [81]). In cases of increased demand, augmenting the availability of GSH or its precursors could be crucial for managing the metabolism of diabetic patients. This approach was found to improve glucose disposal rate and insulin sensitivity (Nguyen *et al.* [82]). Additionally, GSH may prevent an increase in plasma cytokines induced by hyperglycemia (Esposito *et al.* [83]). Gaining a deeper understanding of the regulation of GSH metabolism is crucial for identifying effective approaches to enhance overall well-being and manage these T2D health conditions.

Studies have provided robust evidence about the potential benefits of GSH in managing T2D. However, precise mechanisms that affect GSH metabolism and turnover in patients with T2D complications remain unclear. This necessitates further investigations to evaluate the observed deficiency and establish new rationales for enhancing personalized T2D care.

2.2.1 Targeting OS in T2D: can GSH-based therapy be promising?

Extensive literature highlights that cellular defensive mechanisms mainly rely on antioxidant enzymes, supplying their substrates and repairing injury to protect themselves against oxidative injury. These defenses increase in response to oxidants and enhance the capacity to detoxify and repair oxidative damage (Forman and Zhang [43]). Consequently, the primary strategy for antioxidant therapy should be to enhance these defenses and thereby target OS-lead complications in individuals with T2D. However, due to a lack of evidence about the long-term safety and efficacy, routine anti-oxidant supplementation for treating diabetes is not recommended by the American Diabetes Association (ADA, [84]).

Despite cells generally having a millimolar range concentration of GSH, oxidative stress often leads to a significant decrease in these levels (Ballatori *et al.* [85], Waggiallah *et al.* [86]). Notably, methods to restore GSH through the supplementation of GSH or supply of precursor amino acids of GSH synthesis have demonstrated efficacy in treating diverse diseases (Sekhar *et al.* [87]). There have been several previous clinical and experimental studies to examine the effect of GSH supplementation with different doses and modes of administration (Paolisso *et al.* [88], Paolisso *et al.* [89], Sekhar *et al.* [79], Richie *et al.* [90], Allen and Bradley [91], Buonocore *et al.* [92], Bruggman *et al.* [93]). Paolisso *et al.* [88] demonstrated that 10mg/min GSH infusion potentiated beta-cell response in patients having impaired glucose tolerance, leading to increased glucose disposal. This highlighted the role of GSH in glucose homeostasis. Allen and Bradley [91] reported that oral GSH supplementation does not alter intracellular GSH levels. In addition, they have shown no changes in oxidative stress markers such as 8-OHdG and F2-isoprostanes. On the con-

trary, Richie *et al.* [90] used a range of oral GSH doses from 250 to 1000 mg for a longer duration and reported that oral GSH supplementation in not only dose- but also time-dependent manner increases intracellular GSH in healthy adult subjects. Studies carried out on different animal models demonstrated that the treatment of antioxidants partly improves glucose homeostasis and ameliorates diabetic complications (Ueno *et al.* [94]). Studies investigating the use of GSH for treating certain medical conditions have tested different dosages. However, the optimal dosage for GSH remains undetermined due to insufficient evidence. Several factors, such as age, sex, and medical history, may influence the appropriate dosage for an individual. There needs to be more information on potential interactions between glutathione, specific medications, and other supplements.

In light of these studies, supplementation of GSH, GSH precursors, and antioxidant enzyme mimics could be a major strategy to enhance the synthesis of antioxidant enzymes and cellular GSH synthesis. Therefore, formulating anti-diabetic treatment effectively could be promising to replenish cellular GSH levels and provide protection against hyperglycemia induced by oxidative stress. We note that GSH dietary supplements are not subject to the same regulatory standards as drugs, which means the Food and Drug Administration (FDA) does not assess their safety and efficacy prior to their release on the market (Dwyer *et al.* [95]). Nonetheless, opting for supplements that have undergone testing by reputable third-party organizations like USP or NSF can offer a safer alternative (Dwyer *et al.* [95]). Glutathione supplements are considered safe for consumption, but their potential side effects are not well-established due to insufficient research. However, it is worth noting that no adverse effects have been documented with regard to a high GSH intake from dietary sources alone. Notably, there is an alarming requirement for more compelling

evidence to confirm the efficacy of GSH supplementation-based interventions in addressing the rising graphs of diabetic complications.

2.3 Quantitative approaches for T2D care

The utilization of quantitative approaches has become essential for comprehending diverse aspects of diabetes, such as the glucose-insulin dynamics, complications associated with diabetes, and the effectiveness of treatment approaches (Bergman *et al.* [96], De Gaetano and Arino [97], Topp *et al.* [98], Cobelli *et al.* [99], Jauslin *et al.* [100], Malka *et al.* [101], Ackerman *et al.* [102], Corte *et al.* [103], Segre *et al.* [104], Srinivasan *et al.* [105]). A range of mathematical, statistical, and computational models have studied the biochemical mechanisms underlying diabetes pathophysiology and the effectiveness of different interventions. These models are mechanistic or phenomenological in nature and capable of generating physiologically realistic descriptions in T2D. Cobelli *et al.* developed approaches for mathematically modeling endocrine systems ([106]) and blood glucose control ([107]). The FDA has approved this model as a replacement for animal testing in preclinical trials due to its high physiological accuracy. Topp *et al.* [98] provided a mathematical model for describing β cell mass and glucose-insulin dynamics, which theoretically predicted the pathways in prolonged hyperglycemia. These models offered more quantified insights into medicine prescription and a better understanding of designing trials to test the efficacy of drugs to delay or prevent T2D.

By focusing on clinical significance, analyses of these models have significantly aided in uncovering insights towards improving patient responses to glucose-control therapy. Furthermore, these models have even been utilized for the personalized prescription tool as Continuous Glucose Monitoring (CGM) in

T2D management research (Goel *et al.* [108], Goel [109], Kulkarni *et al.* [42]). This evidence supports our perspectives on developing quantitative models to create a structural depiction of the relevant physiological processes in the development of T2D complications and their heterogeneity, which aid in comprehending the fundamental mechanisms resulting in different characteristics of T2D individuals.

Getting precise parameter estimates to describe the evolution of these systems in T2D and resulting patient-specific characteristics is very difficult. This is because of the long time scales associated with the phenomenon, difficulties with longitudinal studies, and the ethical concerns that arise with the progression of T2D severity (Fritzen *et al.* [110]). However, the availability of more clinical data is rising, and it holds promises for better understanding in both diagnosis and patient-specific therapy. Modeling approaches must be employed adequately to support a functional understanding of the mechanisms and factors driving certain T2D complications. They aptly enable the design of personalized treatment strategies to address key clinical questions in T2D.

Before going further into the modeling approaches to tailor individualized targets for GSH supplementation in controlling T2D complications, we describe modeling attempts for understanding metabolic pathways involving GSH in the next section. Our main focus here is on Red blood cells (RBCs) due to their crucial role in inter-organ communication functions, such as regulating systemic nitric oxide metabolism, redox cycles, and blood rheology. As previously mentioned, measurements of erythrocytic GSH stores are a significant component of this research. We provide a brief overview of modeling studies conducted to replicate molecular processes in erythrocytic systems based on the kinetics of metabolic pathways. This provides a current understanding of the field and the scope of modeling GSH metabolism in erythrocytes.

2.3.1 Modeling GSH metabolism in erythrocytes

Several studies have employed mathematical modeling and computational simulations to elucidate the functions and dynamic behaviors of cellular biochemical changes (Bailey *et al.* [111], Fell [112], and Reich and Sel'kov [113]). Developing quantitative models for the metabolism of erythrocytes has garnered significant attention over the years due to relative simplicity and knowledge of their functioning metabolic networks. Detailed models of erythrocyte metabolism have been developed over several studies with varying levels of abstraction (Rapoport *et al.* [114], Ataullakhanov *et al.* [115], Holzhutter *et al.*, Jamshidi *et al.* [116], Palsson and Joshi [117], Nakayama *et al.* [118]). Many of these models have utilized ordinary differential equations to describe the systems and elucidate various functions in erythrocyte metabolism. For instance, Rapoport *et al.* [114] proposed a model for glycolytic pathways, which was modified later by Ataullakhanov *et al.* [115] by combining model descriptions for pentose phosphate pathways as well. Further, Holzhutter *et al.* [119] mathematically modeled glycolysis, pentose phosphate pathway, and 2,3-BPG shunts for explaining the experimental data from patients with pyruvate kinase deficiency.

Palsson and Joshi proposed the most comprehensive model of RBC metabolism in a series of articles to investigate different metabolic networks and properties of erythrocytes, such as components and characteristics of membranes, electroneutrality, osmotic regulations, interactions with the environment and enzyme kinetics, etc. ([117], [120], [121], [122]). This detailed model of differential equations comprising 33 dynamic mass balances and 41 reaction rates provided a theoretical framework for integrating and consistently interpreting data from the literature. In 1996, the E-cell project built a sophisticated platform for modeling whole-cell level biochemical changes ([123]). Several studies

utilized E-cell with different focuses to explain problems related to metabolic dynamics in erythrocytes. Nakayama *et al.* [118] modified the model proposed by Palsson and Joshi ([117]) on the E-cell platform by including the GSH synthesis and transport pathways to explain the disease conditions that arise due to glucose-6-phosphate deficiency. Modeling erythrocytic metabolism has also been shown useful in realistic predictions at the cellular level of changes and different pathological conditions (Jamshidi *et al.* [116], Mulquiney *et al.* [124]).

Only a few reported studies theoretically investigated the dynamics of cellular GSH metabolism and its role in maintaining the cellular redox balance. Notably, Reed *et al.* [125] formulated a model for GSH metabolism in hepatic cells by combining the reaction kinetics of enzymes involved in one-carbon metabolism, trans-sulfuration pathway and breakdown to amino acids. This model consisted of 34 differential equations formulated from these mass balances, which were further used to explain the regulation of GSH synthesis and its fluctuations on amino acid inputs. Later, Raftos *et al.* [126] published a depiction of GSH metabolism in human erythrocytes with a mathematical model encompassing the major enzymatic pathways helped in gaining better insights into its synthesis and turnover. This model was able to capture the experimental erythrocyte data decently. To the best of our knowledge, models for the aspects of GSH turnover relevant to T2D conditions of high oxidative load that could describe diabetes clinical data are lacking in the literature. Elucidation of the models for specific components of GSH turnover metabolism in T2D is required to explain the erythrocytic GSH relevant to planning therapeutic interventions. Model-derived insights can also help develop GSH strategies based on oxidative stress status in T2D.

We understand that obtaining an accurate and comprehensive understanding of the experimental data using model parameterization can be challenging

sometimes, primarily due to limited data points and the highly complex and dynamic nature of these metabolic networks, which are subject to various regulatory mechanisms. We also note that there is a general agreement in the field about using models for system dynamics with minimal complexity, and several identifiable parameters are recommended (Bergman *et al.* [96], Bergman [127]). Developing simple and minimal mathematical models is favored to effectively capture the essential dynamics of GSH turnover. The insights derived from such models are our first-hand choice to interpret the data for direct clinical uses.

Next, we attempt to understand the scope and potential of modeling methods in planning personalized goals for GSH supplementation, aiming to enhance T2D management efficiency.

2.3.2 Modeling to tailor individualized targets for GSH supplementation in T2D treatment

Developing effective T2D care plans that consider individual requirements, including factors such as age, lifestyle, and overall health status, to improve health outcomes for individuals with T2D under treatment (Davidson *et al.* [128], Galaviz *et al.* [129], and Inzucchi *et al.* [48]). As evidenced by several works in the literature, quantitative approaches and analysis have played a pivotal role in advancing T2D care, especially in the context of personalized goals.

Modeling studies undoubtedly benefit the transition of T2D healthcare from conventional population-based approaches to personalized treatment strategies. This is primarily because such models assist in quantifying the physiological differences and dynamics of systems involved in the progression of T2D complications. Identifying model-derived estimates specific to patients

also helps set an appropriate treatment target for patients in the progress of therapy in T2D. Formulating physiology-based models with meaningful interpretations and parameters, which can also be estimated with reasonable precision, is of great interest. Notably, Graham and Adler [130] provided a foundation for comprehending the chronic development of insulin resistance and T2D, revealing that glucose overload-induced oxidative stress slows irreversible mitochondrial impairment. There have been approaches that utilize the model knowledge to effectively target intervention strategies in individuals ([130]). Kulkarni *et al.* [42] developed a mechanistic model to mathematically describe serial changes in oxidative stress over time with the measurements of glutathione in newly diagnosed type 2 diabetes patients undergoing anti-diabetic treatment. By employing this model [42], distinct recovery paths for each individual characterized by a quantal response were identified. Kulkarni *et al.* demonstrated the potential of model-derived estimates in assessing the extent of individual patient response to treatment and reevaluating treatment strategies.

Additionally, we understand that designing personalized treatments is complex and involves multiple factors affecting disease progression in T2D; leveraging insights from the model may help ease some of its complexities. Here, we believe those modeling methods are important when they successfully combine mathematical sophistication with practical applications for analyzing data in T2D and provide clinically useful outcomes. This is especially because it highlights the ability of mathematical modeling to offer insightful explanations for T2D complications and the ways of recovery. Earlier, we discussed how administering GSH to diabetic patients could be a beneficial strategy to protect them from DNA damage and oxidative stress-induced T2D complications. A subsequent analysis of the underlying systems with mechanistic models would

help to understand intracellular GSH response profiles and how they can be used for clinical uses better. Model simulations can be performed to obtain a theoretical understanding of the behavior in GSH systems under different extracellular conditions arising from stress, interventions, etc. This also allows us to ask how GSH responses alter under different T2D conditions. Using these models and their estimations could potentially assist in creating personalized approaches for managing diabetes through GSH-based interventions by tracking recovery.

To summarize, this chapter provided a concise literature review and discussed the experimental and clinical significance of oxidative stress in the pathophysiology of T2D and the importance to continue exploring the field of oxidative stress and GSH-based treatments to customize medical management based on individual T2D patient characteristics with the help of quantitative approaches. This chapter supports the idea that restoring GSH levels can effectively enhance overall redox status and mitigate oxidative stress during the progression of diabetic complications associated with hyperglycemia. Furthermore, we highlighted the necessity for individualized treatments and examined the literature on quantitative approaches for anti-diabetic intervention goals.

We outline the development of evidence-based modeling methods for comprehending the effects of GSH-mediated interventions toward achieving personalized T2D targets, aiming to improve the efficiency of anti-diabetic therapy. We believe that the concepts presented in this chapter will help elucidate the rationale behind our approaches in the subsequent chapters of this work.

Chapter 3

Investigating the effect of GSH supplementation on individuals with T2D: a randomized controlled trial

Published as and adapted from:

Kalamkar, S.; Acharya, J.; **Kolappurath Madathil, A.**; Gajjar, V.; Divate, U.; Karandikar Iyer, S.; Goel, P.; Ghaskadbi, S. *Randomized Clinical Trial of How Long-Term Glutathione Supplementation Offers Protection from Oxidative Damage and Improves HbA1c in Elderly Type 2 Diabetic Patients.* Antioxidants 2022, 11, 1026. doi:10.3390/antiox11051026.

Results in the paper were revised by correcting for a typographical error in the dataset, and the details are given in section 3.1.

3.1 Introduction

Persistent hyperglycemia in T2D leads to oxidative stress, which further results in microvascular and macrovascular complications (Brownlee [131], Volpe *et al.* [50], Giacco and Brownlee [23], Marchioli *et al.* [24]). The ADA position statement suggests that using antioxidant supplements is not advisable for everyone due to insufficient evidence of their long-term safety and effectiveness in T2D (ADA [44]). Despite being the most abundant cellular endogenous antioxidant, studies have indicated low levels of GSH in T2D make them more susceptible to the formation of AGEs, oxidative damage, and T2D complications (Lutchmansingh *et al.*, 2018, Gawlik *et al.*, 2016, Thornalley *et al.*, 1996). GSH was also shown to be the best covariate of glucose recovery, and their body stores were increased while controlling hyperglycemia over two months (Acharya *et al.* [41], Kulkarni *et al.* [42]). So, it is important to understand whether changes in GSH would impact glucose homeostasis in T2D. Replenishing GSH may be a promising approach to improving the overall redox status in individuals with T2D. However, stronger evidence needs to be established on the effective ways of administration and also on the effects of GSH supplementation in T2D.

Various studies have explored different approaches to the administration of GSH, including variations in dosage, duration, and method of administration, such as oral administration in different forms, such as sublingual (Schmitt *et al.* [132]), orobuccal (Buonocore *et al.* [92]), Bruggeman *et al.* [93]) and liposomal (Sinha *et al.* [133]) for rapid absorption. We note that these forms of GSH are not only not easily available commercially but also sublingual and orobuccal formulations that include GSH as one of the (primary) ingredients, which makes it difficult to attribute the effects to GSH alone. Richie *et al.* [90] demonstrated that oral GSH supplementation in 20 healthy individuals

significantly increased blood GSH. In a somewhat larger study conducted on 40 healthy American adults, however, Allen and Bradly [91] reported that oral GSH supplementation did not change GSH levels and biomarkers of oxidative stress. Precursor amino acids of GSH administered orally have also demonstrated enhanced body stores of GSH (Sekhar *et al.* [87]) in humans. GSH has an added advantage over its precursor amino acids, for instance, cysteine, which has an unpleasant taste, in ensuring better patient compliance. Paolisso *et al.* [88] reported that GSH infusion led to increased GSH and total body glucose disposal in 10 Italian diabetic subjects; this effect was more pronounced in elderly individuals with impaired glucose tolerance (Paolisso *et al.* [89]). Infusion is clearly difficult to implement in clinical practice. Despite efforts in the literature, the effects of GSH supplementation are not sufficiently understood, especially in the context of T2D. In addition to that, we note most of these clinical studies have been carried out with small sample sizes and are often inconclusive. Discrepancies in the outcomes of these studies could be due to differences in the dose and duration of GSH and the site of measurement of GSH being plasma instead of an erythrocyte fraction. **Consequently, conducting a stronger-powered study to investigate the potential benefits of GSH supplementation is crucial for generating empirical evidence on its effectiveness in individuals with T2D.**

In this chapter, we present an investigation conducted as a clinical trial conducted in our collaboration with the Ghaskadbi group from SPPU Pune and Jehangir Hospital, Pune, to assess the effect of oral GSH supplementation on improving body stores of GSH and glucose homeostasis in individuals with T2D. We claim this is the most extensive longitudinal clinical study to date reported for examining the effects of GSH supplementation in individuals with T2D. We begin this chapter by briefly describing the design of this clinical trial

and the biochemical data measured from the participants. We then present the population-level analysis of this data and assess the effectiveness of GSH supplementation on the blood biochemical parameters in individuals with T2D. Previous reports in the literature have indicated that the levels of GSH decline with age in humans. As a posthoc analysis, we further investigated whether the response to oral GSH supplementation differed between different age groups, younger and older sub-groups of individuals with T2D. These findings potentially answer whether oral GSH administration can complement anti-diabetic treatments and help achieve better glycemic targets, particularly among the elderly population. We also analyze the effect of GSH supplementation on the subgroup of individuals with T2D who are receiving different anti-diabetic treatments. This chapter provides evidence on the impact of GSH supplementation on individuals with T2D under anti-diabetic treatment, elucidates safer administration methods, and determines which phenotypes may benefit better.

Presented here is also a commentary on the work which has already been published in the *Antioxidants* journal under the title "Randomized Clinical Trial of How Long-Term Glutathione Supplementation Offers Protection from Oxidative Damage and Improves HbA1c in Elderly Type 2 Diabetic Patients" (Kalamkar *et al.* [134]). A medRxiv version of this paper is also available online (Kalamkar *et al.* [135]). **We hereby report a typographical error in the datasheet while entering the patient test reports for a subject ID of DG50. In the dataset used for analysis, Fasting Insulin (FPI) for this patient DG50 was found to be entered incorrectly as 222.7 $\mu\text{U}/\text{mL}$ instead of 18.3 $\mu\text{U}/\text{mL}$. We have made this correction during analysis, and the updated results are incorporated in the revised figures presented here.** The figures presented in this chapter are reproduced

under the Creative Commons attribution license.

3.2 Methodology

We carried out a pragmatic-prospective clinical trial to investigate the effect of oral GSH supplementation in restoring body GSH levels and maintaining glucose homeostasis in Indian Type 2 diabetes patients who were already on anti-diabetic treatment at Jehangir Hospital, Pune. This trial was registered with Clinical Trials Registry-India (CTRI/2018/01/011257) and approved by the Institutional Ethical Committee of Jehangir Hospital Development Center, Pune, Institutional Biosafety Committee of SPPU, Pune, and the Institutional Ethics Committee of IISER, Pune, India. The clinical study details and results are briefly described next.

3.2.1 The design of clinical trial

This study was a pragmatic-prospective clinical trial designed as a case-control cohort study to assess the effect of oral GSH supplementation in individuals with T2D. The study design is depicted in Figure 3.1. Healthy nondiabetic controls ($n = 104$) with $\text{HbA1c} < 6.5\%$, and known T2D subjects ($n = 250$) with $\text{HbA1c} \geq 6.5\%$ visiting Jehangir Hospital and Iyer clinic, Pune were recruited for this study. Pregnant women, heavy smokers, individuals with excessive alcohol intake, individuals with any clinical infection or a history of a recent cardiovascular event, and those receiving antioxidants or herbal formulations were excluded from the study. We recruited known diabetic subjects ($n = 250$) already on an anti-diabetic regimen. The study physician randomly categorized them into two groups based on a coin-toss method: 125 diabetic patients were advised to continue with their anti-diabetic regimen (Group D),

and the other 125 diabetic patients were given oral 500 mg glutathione (Jarrow Formulas, USA) supplementation once daily in addition to their anti-diabetic treatment for a period of six months (Group DG) (Figure 3.1). At the time of randomization, concentrations of covariates, fasting and postprandial glucose, fasting, postprandial insulin, HbA1c, reduced and oxidized glutathione (GSSG), and 8-OHdG were unavailable. They, therefore, did not influence the assignment of diabetic patients in D or DG groups.

Compliance with medical treatment by patients of the D and DG groups and consumption of GSH by patients of the DG was emphasized by maintaining continuous communication between the physician and patients. Out of 125 diabetic patients in D and DG groups, 23 were lost to follow-up in the D group and 21 in the DG group for not complying with the treatment regimen. We also recruited healthy, nondiabetic control subjects who were followed for six months and were advised to continue their regular diet and exercise regimen. Blood samples were collected at the time of enrollment 0 (α -visit), 3 (β -visit), and 6 (γ -visit) months after the date of enrollment. Sample Size ($n = 100$) is calculated based on a two-sided t-test, at 0.1 type 1 error and 80% power, to detect a mean difference of 35 in GSH with a standard deviation of 100.

Details of participants in the clinical trial and biochemical data measured are described further.

3.2.2 Clinical trial participants and measured data

The study consisted of known type 2 diabetic subjects visiting Jehangir Hospital, Pune, and Iyer Clinic, Pune. During the study, we recruited 250 diabetic subjects undergoing anti-diabetic treatment and assigned them randomly into two groups. Diabetic subjects in one group (Group D, $n=125$) were asked to pursue their anti-diabetic treatment, while subjects in the other group (Group

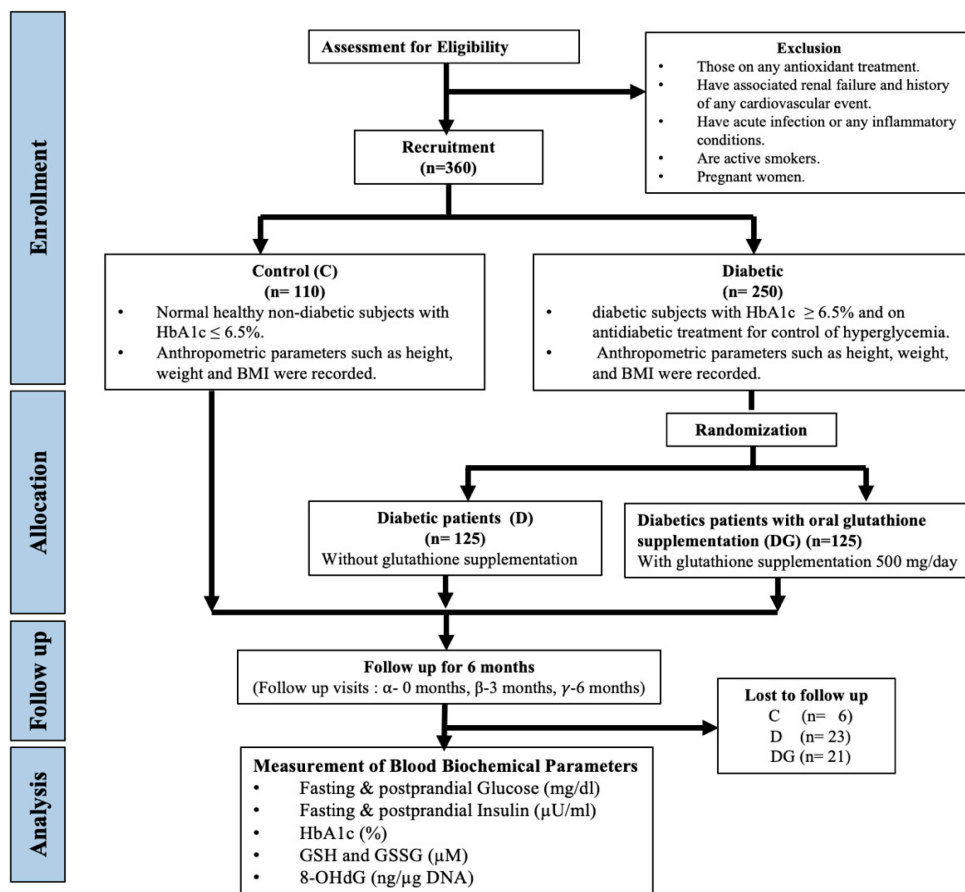


Figure 3.1: Depiction of the clinical study design. This figure is reproduced from Kalamkar *et al.* [134], published as Figure 1 in the main text.

DG, n=125) were given 500mg glutathione supplementation daily in conjunction with their anti-diabetic treatment for six months. nondiabetic healthy subjects were also recruited as the control group and asked to continue their diet and exercise. Subjects in D and DG groups maintained continuous communication with the physicians during the study period. Twenty-three subjects in the D group and 21 subjects in the DG group were lost to follow-up during this period. Details of the sample collection, measurements of various biochemical parameters, and further analysis are described next.

Demographic information like age, height, weight, and sex from subjects was recorded at the first visit. Blood samples from all subjects were collected at the time of enrollment (α visit), 3 (β visit), and 6 (γ visit) months after the enrollment date. S. Ghaskadbi et al. planned and carried out the measurements of fasting and post-prandial glucose, fasting and post-prandial insulin, glycated hemoglobin (HbA1c), erythrocytic levels of glutathione (GSH), and oxidized glutathione (GSSG) from the collected blood samples.

We analyzed this measured biochemical data and examined the effects of GSH supplementation during the clinical trial. Details of the analysis are described below.

3.2.3 Statistical analysis of the clinical data

Biochemical levels at different visits are compared using permutation tests in R with the “Coin” package (Hothorn *et al.* [136]). Two-sample, two-sided t-tests were used to confirm the comparison results with permutation tests. The statistical significance of comparisons was set at a p-value < 0.05 . The difference between biochemical changes in D and DG groups during the 6-month period was quantified using effect sizes. Comparisons and effect size calculations were also performed between elder subgroups of D and DG subjects with an age

of more than 55 years. All effect size calculations and parametric t-tests for comparisons were carried out using Matlab version 2019. All figures shown in this report consist of significance levels based on permutation test results (p-values of comparisons are not shown). Corresponding figures with t-test results and their p-values are also not shown in this report.

3.2.4 Effect size analysis between D and DG groups

Measurements of a biochemical variable, X at α , β and γ visits of the D group subjects are represented by X_α^D , X_β^D , X_γ^D and measurements from DG group subjects by X_α^{DG} , X_β^{DG} , X_γ^{DG} , respectively. The variables, X are HbA1c, FPG (Fasting glucose), FPI (Fasting insulin), PPG (PP glucose), PPI (PP insulin), GSH, and GSSG. Changes from α visit to γ visit in the D group were estimated using their paired differences as $X_{\gamma-\alpha}^D = X_\gamma^D - X_\alpha^D$. Similarly, $X_{\gamma-\alpha}^{DG}$ represents the paired changes from α to γ visit (6 month period). The group-wise mean of paired difference in D and DG groups are $\bar{X}_{\gamma-\alpha}^D$ and $\bar{X}_{\gamma-\alpha}^{DG}$ respectively. The effect size between 6-month changes in the concentration of a particular biochemical variable, X , in D and DG groups are estimated using Cohen's d as

$$d = \frac{\bar{X}_{\gamma-\alpha}^D - \bar{X}_{\gamma-\alpha}^{DG}}{s} \quad (3.1)$$

where the pooled standard deviation of biochemical changes in D and DG (s) is given by

$$s = \sqrt{\frac{(N_D - 1)s_1^2 + (N_{DG} - 1)s_2^2}{N_D + N_{DG} - 2}} \quad (3.2)$$

where s_1 is the standard deviation of $X_{\gamma-\alpha}^D$, s_2 is the standard deviation of $X_{\gamma-\alpha}^{DG}$. Where N_C , N_D , N_{DG} are the number of individuals in control, D, and DG groups, respectively. Cohen [137] described an effect size of 0.2, 0.5, and 0.8 as ‘‘Small,’’ ‘‘Medium,’’ and ‘‘Large’’ effects, respectively, and Sawilowsky

[138] classified an effect of size 1.2 as “Very large” and 2 as a “Huge” effect.

Next, we analyzed the blood biochemical parameters at the baseline to verify the covariate balance and serial changes across different visits. We also performed an effect-size analysis on the clinical trial study arms for estimating the effects of GSH supplementation. We also performed post hoc analyses of clinically relevant subgroups in the study to identify the evidence about GSH supplementation. We present the results from this analysis in the next section below.

3.3 Results

3.3.1 Covariate balance between the study arms

The study population consisted of diabetic participants who had an average age of 54 years and a BMI of 26.9 kg/m^2 . The Control group comprised individuals with an average age of 41 years and a BMI of 26 kg/m^2 . The D group had 57 male and 45 female participants, while the DG group had 49 male and 55 female participants. The Control group had 62 male and 42 female participants. Table 3.1 displays the baseline characteristics of each group. The study found that compared to the Control group ($p < 0.001$, for all parameters), D and DG groups had significantly higher levels of FPG, PPG, FPI, HbA1c, and 8-OHdG, and significantly lower levels of GSH. However, the levels of PPI were not significantly different among the groups (Table 3.1). Additionally, no significant differences in FPG, PPG, FPI, PPI, HbA1c, and GSH were observed within the D and DG groups, indicating a covariate balance between the two groups at baseline (Table 3.1).

Variable	Control Group
Age (years)	39.5 (33.5–49)
BMI (kg/m^2)	26.1 (23.5–28.2)
HbA1c (%)	5.6 (5.4–5.8)
Fasting Glucose (mg/dL)	90 (85–95)
Fasting Insulin ($\mu\text{U}/\text{mL}$)	9.4 (6.8–12.3)
PP Glucose (mg/dL)	104 (96–117)
PP Insulin ($\mu\text{U}/\text{mL}$)	36 (18.1–71.7)
GSH (μM)	801 (548–1068)
GSSG (μM)	205 (124–303)
8-OHdG (ng/ μg DNA)	129.97 (97.2–175.2)

Variable	D Group
Age (years)	55.5 (47–61)***
BMI (kg/m^2)	26.3 (22.7–29.2)
HbA1c (%)	8.1 (7.1–9.6) ***
Fasting Glucose (mg/dL)	147 (120–190) ***
Fasting Insulin ($\mu\text{U}/\text{mL}$)	11.9 (7.4–17.1)**
PP Glucose (mg/dL)	220 (169–285) ***
PP Insulin ($\mu\text{U}/\text{mL}$)	36.2 (24–54.8)
GSH (μM)	379 (243–533)* * *
GSSG (μM)	215 (139–326)
8-OHdG (ng/ μg DNA)	442.33 (340.26–514)***

Variable t	DG Group
Age (years)	56 (48–61)***
BMI (kg/m^2)	26.8 (23.8–29.8)
HbA1c (%)	8 (7.1–9.7) ***
Fasting Glucose (mg/dL)	140.5 (109–182) ***
Fasting Insulin ($\mu\text{U}/\text{mL}$)	10.4 (7.5–16.1)*
PP Glucose (mg/dL)	209 (168–258)***
PP Insulin ($\mu\text{U}/\text{mL}$)	32.4 (18.1–60.4)
GSH (μM)	440 (176–635)* * *
GSSG (μM)	137 (89–209) ***,###
8-OHdG (ng/ μg DNA)	481.71 (412.23–535.11) **,##

Table 3.1: **Baseline characteristics of Control, D, and DG groups.** Data from each group at three visits are presented here as median and inter-quartile ranges (25th –75th percentile). Significance levels of Control versus D comparisons are $*p < 0.05$, $**p < 0.01$, and $***p < 0.001$. Similarly, comparisons between D versus DG groups are denoted with ##, or ### for $p < 0.05$, $p < 0.01$, and $p < 0.001$, respectively. This table is adapted from Kalamkar *et al.* [134].

3.3.2 Effect of GSH supplementation on 6-month biochemical changes

We conducted an analysis of the effect size of GSH supplementation within the diabetic groups, which revealed a "Large" effect size (Cohen's $d = 1.01$; $p < 0.001$), indicating a significant increase in GSH levels in the DG group compared to the D group (Figure 3.2). Similarly, GSSG was increased in DG compared to D (Cohen's $d = 0.61$, $p < 0.001$). Additionally, we observed a significant decrease in 8-OHdG concentrations from the α to γ visit with a "Large" effect in DG (Cohen's $d = -1.07$; $p < 0.001$), but not in the D and Control groups ($p > 0.05$) (Figure 3.2). We then examined the effect of oral GSH supplementation on glycemic parameters in diabetic patients. We found that while HbA1c levels decreased significantly over six months in both D and DG groups, the extent of decrease in DG was comparable to the D group, with a small Cohen's $d = -0.16$ ($p > 0.05$) (Figure 3.2). Furthermore, FPG, PPG, FPI, and PPI all decreased over six months in D and DG, with no significant difference between the two groups ($p > 0.05$, Cohen's $d < 0.2$, all parameters). Our results demonstrate that GSH supplementation leads to a significant increase in erythrocyte GSH and GSSG levels and a decrease in 8-OHdG in diabetic patients but has similar effects on glycemic parameters in both D and DG groups.

3.3.3 Serial biochemical changes in the study groups

We examined whether GSH supplementation had an immediate and sustained effect or if the changes in GSH levels occurred gradually over the six-month study period. Figure 3.3 illustrates the changes in GSH and GSSG concentrations in the three study groups at visits α , β , and γ . The Control group

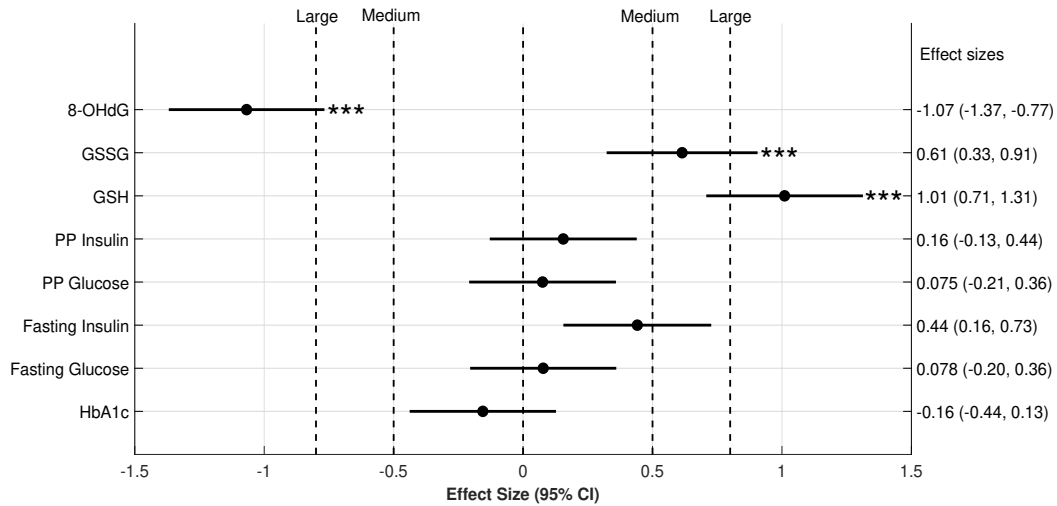
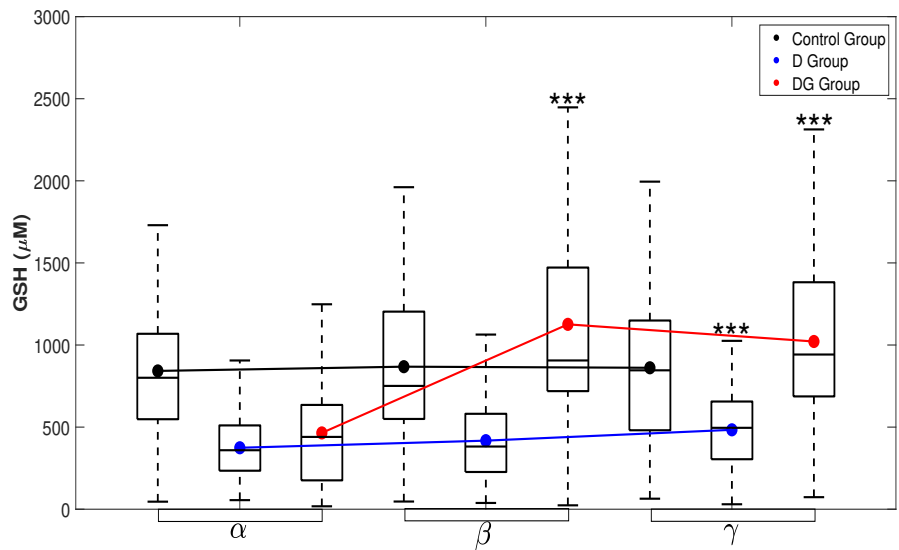


Figure 3.2: **Effect size of changes in blood biochemical parameters.** Six-month changes in the biochemical parameters of D and DG groups were compared here on a forest plot with effect size and corresponding 95% confidence intervals (CI). Effect size (Cohen's d) calculated between six-month changes in the concentration of biochemical variables are denoted on the x-axis. The groupwise means of 6-month changes in the concentration of these variables were compared using two-sample permutation tests. The significance of these comparisons is denoted by the p values mentioned to the right of horizontal lines for CI. The significance level for respective comparisons is *** $p < 0.001$. Effect size takes either a positive or negative sign based on the direction of change: a positive effect size increases towards the right, and a negative effect towards the left. Vertical dotted lines represent different classifications of effect size. In particular, Medium effects are labeled at 0.5 and -0.5, and Large effects at 0.8 and -0.8. Abbreviations used here are HbA1c - glycated hemoglobin, GSH - reduced glutathione, PP glucose - postprandial glucose, PP insulin - postprandial insulin, and 8-OHdG- 8-hydroxy-2-deoxy guanosine. This figure is reproduced from Kalamkar *et al.* [134], published as Figure 2 in the main text after incorporating the correction for Fasting Insulin.

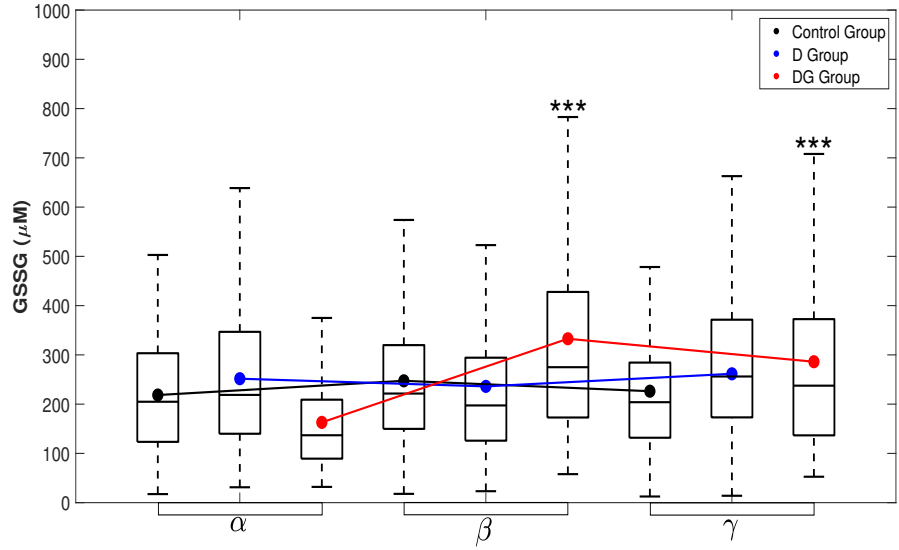
showed no significant change in GSH and GSSG over the six-month period. In the DG group, oral GSH supplementation resulted in a significant increase in GSH within three months ($p < 0.001$), which remained stable for up to six months (Figure 3.3a). On the other hand, the D group only exhibited a slight increase in GSH at three and six months. GSSG levels also significantly increased within the first three months of oral GSH supplementation in the DG group ($p < 0.001$) but did not change further (Figure 3.3b). Meanwhile, GSSG levels in the D group remained unchanged throughout the study. **These findings suggest that oral GSH supplementation can significantly enhance GSH levels within three months and maintain them for up to six months in diabetic patients.** In contrast, anti-diabetic therapy alone resulted in only a minor increase in GSH levels.

While the concentrations of 8-OHdG remained unchanged over six months in the Control group, the supplementation of GSH in diabetic patients caused a significant reduction in 8-OHdG within the initial three months, and this effect continued to decrease significantly thereafter ($p < 0.001$) (Figure 3.4a). Conversely, in the D group, the concentrations of 8-OHdG did not change significantly.

We conducted a detailed analysis of changes in glycemic parameters in the D and DG groups. Within three months, FPG levels significantly decreased in both groups ($p < 0.01$ for D and $p = 0.05$ for DG), but they returned to baseline by the end of six months (Figure 3.5a). However, PPG levels did not change significantly in either group over the six-month study period ($p > 0.05$ for both) (Figure 3.6a). HbA1c levels rapidly decreased from 0 to 3 months in both groups ($p < 0.01$ for D and $p < 0.001$ for DG) (Figure 3.4b), and in the DG group, they remained stable up to six months. In contrast, HbA1c levels in the D group returned to baseline. FPI levels changed significantly from 0 to 3



(a) GSH



(b) GSSG

Figure 3.3: **Longitudinal changes in the concentration of (a) GSH and (b) GSSG in different groups.** The measured data for (a) GSH and (b) GSSG concentrations from Control, D, and DG groups at $\alpha, \beta,$ and γ visits are shown here with box and whiskers plots. The mean data (black circles for Control, blue for D, and red for DG groups, respectively) and inter-quartile ranges (IQR) are overlaid over the corresponding box plots. The group-wise means at different visits are connected using solid lines with the same color. Significance levels displayed above β and γ and visits denote the comparisons with α visits using permutation tests. Significance level are $*p < 0.05, **p < 0.01, ***p < 0.001$ for respective comparisons. This figure is reproduced from Kalamkar *et al.*[134], published as Figure 3 in the main text.

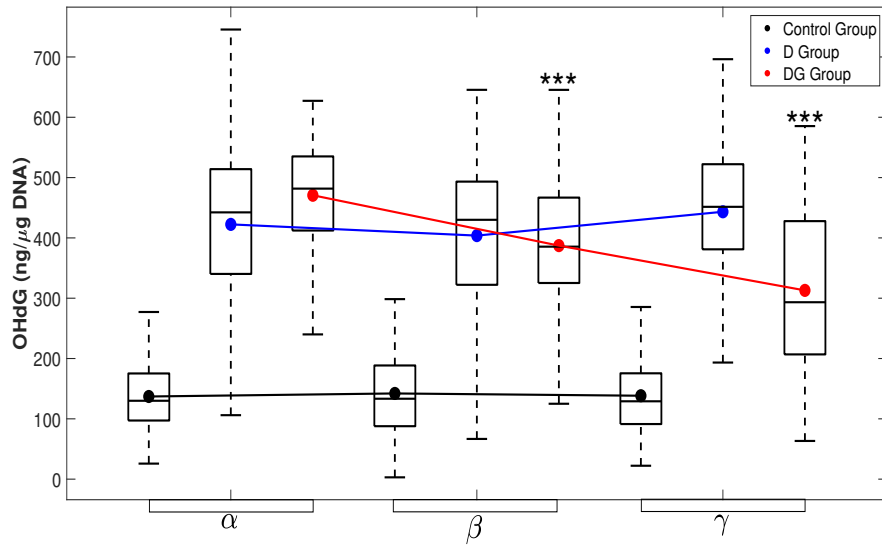
and 6 months in the D group ($p < 0.05$), while they remained unchanged in the DG group ($p > 0.05$) (Figure 3.5b). PPI levels remained unchanged in both groups throughout the study period (Figure 3.6b). **Overall, our findings suggest that oral GSH supplementation has a stabilizing effect on HbA1c, meaning that it rapidly decreases within three months and remains low thereafter.**

3.3.4 Effect size analysis in different age groups

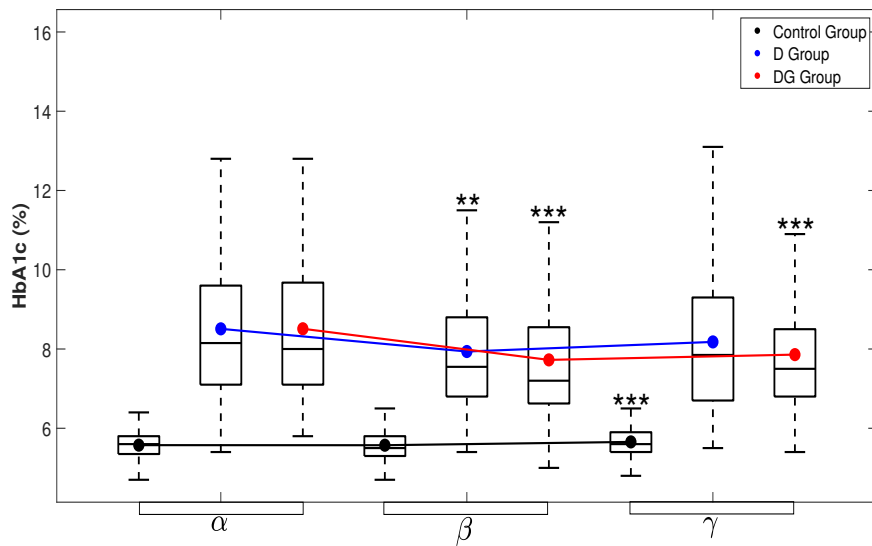
Previous studies have reported a decline in GSH concentration with age in healthy adults (Sekhar *et al.* [79], Erden-Inal *et al.* [139]). Therefore, we aimed to investigate the impact of GSH supplementation on elderly diabetic patients, as the age range of our study participants was from 31 to 78 years old. The median age of the diabetic patients in the D and DG groups was approximately 55 years. To further explore the response to oral GSH supplementation in the elderly subgroup, we used the age of 55 as a threshold to isolate this group and re-evaluated the effect of GSH supplementation.

Mean values for all the biochemical parameters and serial changes from 0 to 3 and 6 months in their concentrations in the D ($n = 44$) and DG ($n = 54$) groups are shown in the appendix (Figure 3.9-3.11). As observed in the overall diabetic population, the concentration of GSH and GSSG increased significantly over six months in both D and DG subgroups (Figure 3.7a). Additionally, the mean changes in GSH and GSSG concentrations over six months were significantly higher in the DG group compared to the D group (Cohen's $d = 1.14$ and 0.67 for GSH and GSSG, respectively, $p < 0.001$) (Figure 3.7).

Oral GSH supplementation in the elderly sub-group of diabetic patients showed a "Very large" effect (Cohen's $d = -1.45$, $p < 0.001$) in reducing the accumulation of oxidative DNA damage, as evidenced by a significant reduc-

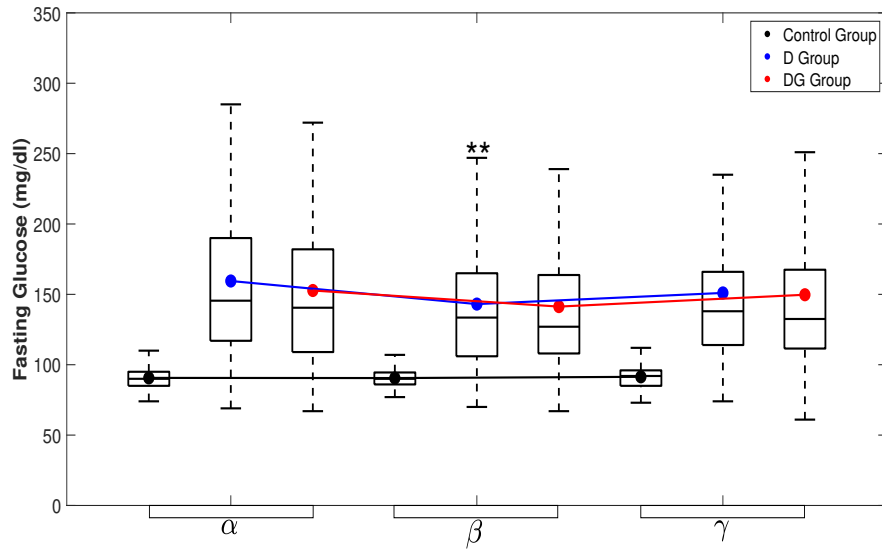


(a) 8-OHdG

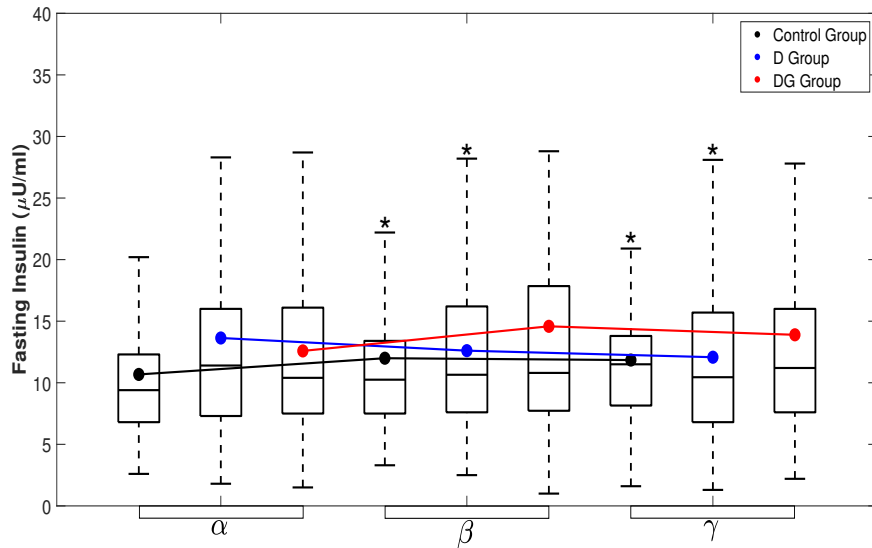


(b) HbA1c

Figure 3.4: **Longitudinal changes in the concentration of (a) 8-OHdG and (b) HbA1c in different groups.** The measured data for (a) 8-OHdG and (b) HbA1c concentrations from Control, D, and DG groups at α , β and γ visits are shown here with box and whiskers plots. Significance levels are $*p < 0.05$, $**p < 0.01$, $***p < 0.001$ for respective comparisons. Abbreviations used here are 8-OHdG - 8-hydroxy-2-deoxy guanosine and HbA1c - glycated hemoglobin. This figure is reproduced from Kalamkar *et al.* [134], published as Figure 4 in the main text.

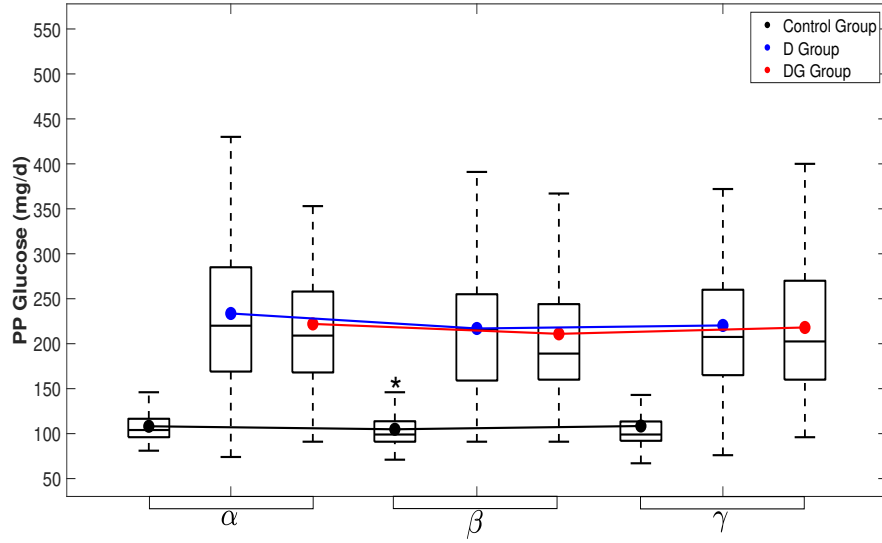


(a) Fasting Glucose

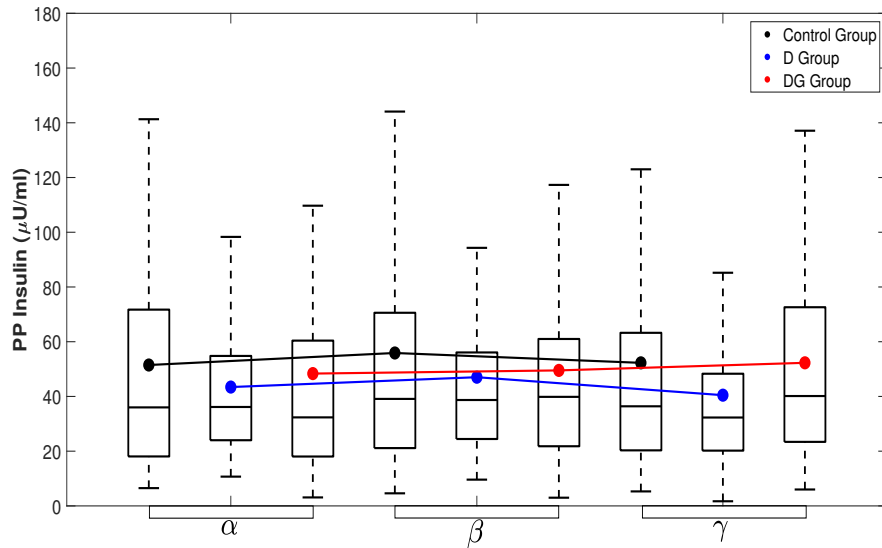


(b) Fasting Insulin

Figure 3.5: **Longitudinal changes in the concentration of (a) Fasting Glucose and (b) Fasting Insulin in different groups.** The measured data for (a) Fasting Glucose and (b) Fasting Insulin concentrations from Control, D, and DG groups at α, β and γ visits are shown here with box and whiskers plots. Significance level are $*p < 0.05, **p < 0.01, ***p < 0.001$ for respective comparisons. Abbreviations used here are FPG - fasting glucose and FPI - fasting insulin. This figure is reproduced from Kalamkar *et al.* [134], published as Figure 4 in the main text after incorporating the correction for Fasting Insulin.

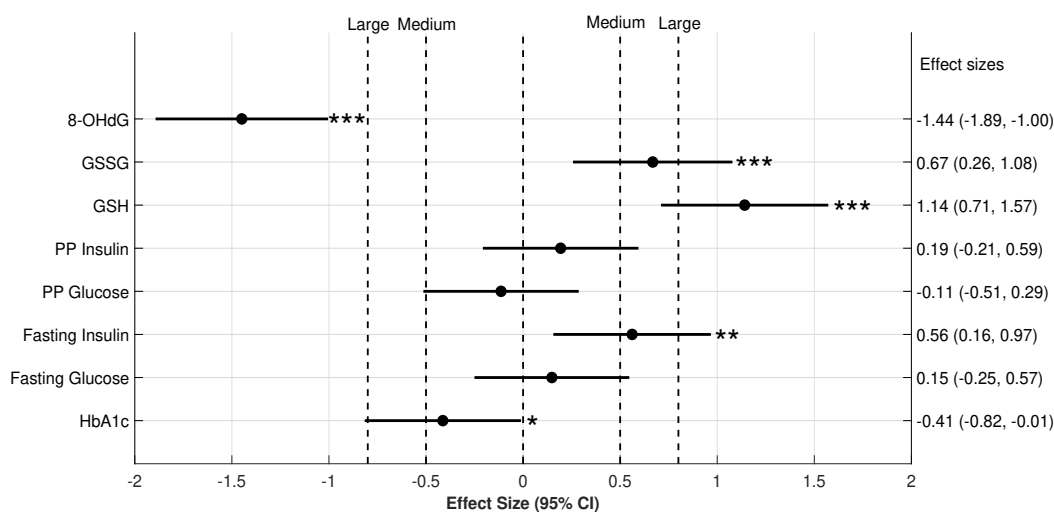


(a) Postprandial Glucose

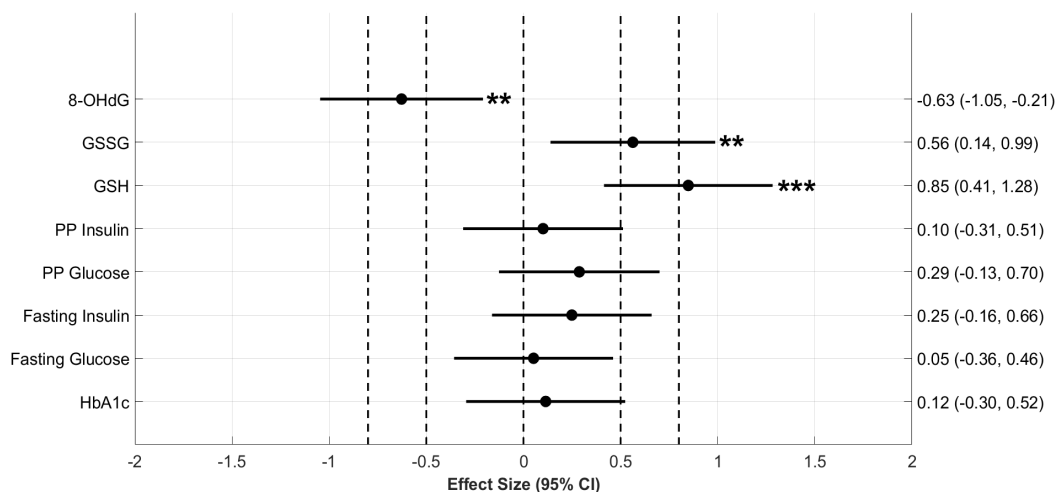


(b) Postprandial Insulin

Figure 3.6: **Longitudinal changes in the concentration of (a) Postprandial Glucose and (b) Postprandial Insulin in different groups.** The measured data for (a) Postprandial Glucose and (b) Postprandial Insulin concentrations from Control, D, and DG groups at α, β and γ visits are shown here with box and whiskers plots. Significance level are $*p < 0.05$, $**p < 0.01$, $***p < 0.001$ for respective comparisons. Abbreviations used here are PPG - postprandial glucose and PPI - postprandial insulin. This figure is reproduced from Kalamkar *et al.* [134], published as Figure 4 in the main text.



(a) Elder diabetic adults



(b) Younger diabetic adults

Figure 3.7: The effect size of changes in blood biochemical parameters of (a) elder and (b) younger diabetic adults. Six-month changes in the biochemical parameters of those in D and DG subgroups were compared here on a forest plot with effect size and 95 % confidence intervals. Effect size (Cohen's d) calculated between six-month changes in the concentration of biochemical variables are denoted on the x-axis. Groupwise means of six-month changes in the concentration of these variables were compared using two sample permutation tests. The significance of these comparisons is denoted by the p values mentioned to the right of horizontal lines for CI. Significance level are $*p < 0.05$, $**p < 0.01$, $***p < 0.001$ for respective comparisons. This figure is reproduced from Kalamkar *et al.* [134], published as Figure 5 in the main text and Figure S5 in the supplementary data after incorporating the correction for Fasting Insulin.

tion in 8-OHdG (Figure 3.7a). Furthermore, we investigated the effect of GSH supplementation on blood glyceemic parameters in the elderly sub-group of diabetic patients (Figure 3.7a). Unlike the findings observed in the overall diabetic population, GSH supplementation resulted in a significant reduction in HbA1c over a period of 6 months in the DG sub-group compared to D (Cohen's $d = -0.41$, $p < 0.05$).

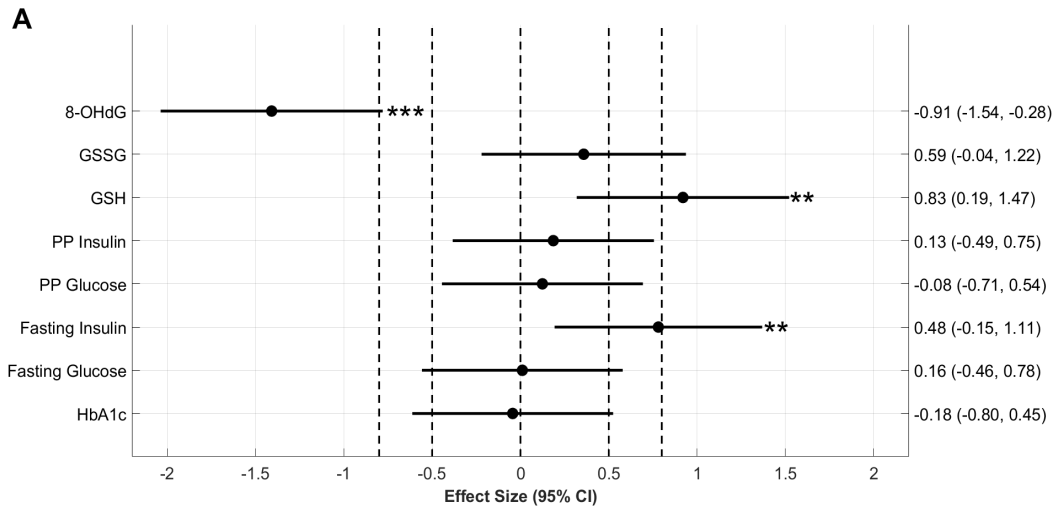
Intriguingly, the DG sub-group showed a significant increase in FPI levels from the α to γ visit compared to D (Cohen's $d = 0.56$, $p < 0.05$). GSH supplementation had a minimal effect on FPG, PPG, and PPI levels in the DG sub-group (Cohen's $d < 0.2$, $p < 0.05$, all parameters). Consequently, the administration of GSH in conjunction with anti-diabetic therapy led to a noteworthy elevation in erythrocyte GSH, GSSG, and FPI levels and a decrease in HbA1c and 8-OHdG levels in the elderly diabetic sub-group (Figure 3.7a), implying that the elderly diabetic population is more responsive to GSH supplementation.

Furthermore, we evaluated the effect of GSH supplementation in the younger sub-groups of D and DG, and the outcomes are presented in Figure 3.7b. Although HbA1c levels changed significantly in the younger sub-group of DG from the baseline (Figure 3.7b), the 6-month changes in the younger sub-group of DG were not significantly different from those in the younger sub-group of D following GSH supplementation (Figure 3.7b).

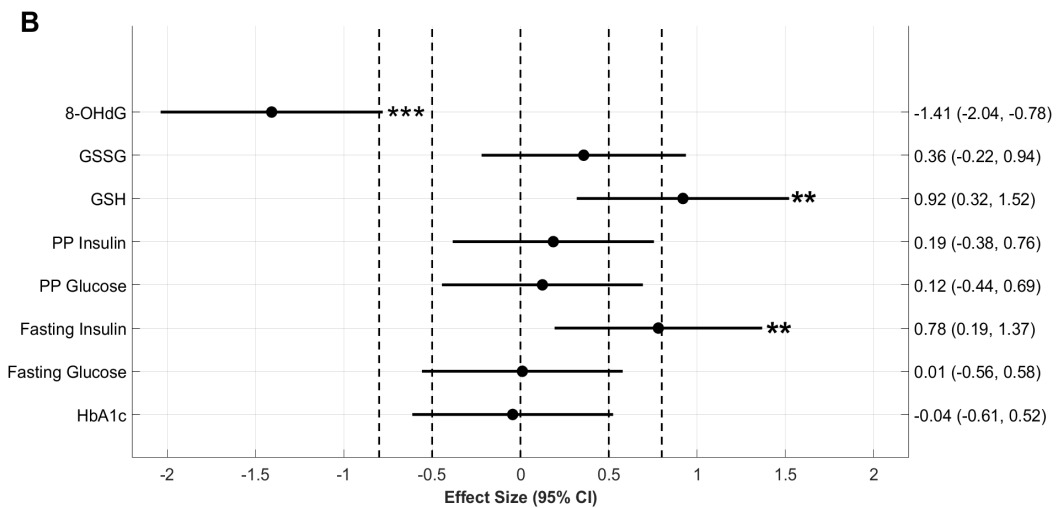
3.3.5 Effect size analysis on treatment subgroups

In this study, the diabetic patients were receiving different anti-diabetic treatments as prescribed by their physicians. A **post-hoc analysis** was performed to examine the effect size of biochemical changes between the D and DG sub-groups receiving different anti-diabetic treatments. The two major types of

treatments were Biguanides alone (B subgroup) and Biguanide-Sulphonylurease combination (BS subgroup). The results of this analysis are presented in Figure 3.8. The analysis of the B subgroup indicated significant changes in GSH, GSSG, 8-OHdG, and FPI as a result of GSH supplementation (Figure 3.8a). However, significant effects were only observed for the BS subgroup on GSH and 8-OHdG (Figure 3.8b).



(a) Elder diabetic adults



(b) Younger diabetic adults

Figure 3.8: **The effect size of changes in blood biochemical parameters of in diabetic subjects with (a) biguanides and sulphonylureas and (b) biguanides alone treatments.** Six-month changes in the biochemical parameters of those in D and DG subgroups were compared here on a forest plot with effect size and 95% confidence intervals. Effect size (Cohen's d) calculated between six-month changes in the concentration of biochemical variables are denoted on the x-axis. The group-wise means of six-month changes in the concentration of these variables were compared using two sample permutation tests. The significance of these comparisons is denoted by the p values mentioned to the right of horizontal lines for CI. Significance levels are *** $p < 0.001$ for respective comparisons

3.4 Discussion

The primary approach to treating individuals with T2D has been controlling hyperglycemia. Previous research from our group has shown GSH to have a strong correlation with changes in HbA1c among various oxidative stress markers (Kulkarni *et al.* [42]), and GSH levels changing rapidly in response to hyperglycemia modifications. However, it was uncertain whether improving the redox status with GSH supplementation could counteract the oxidative stress induced by hyperglycemia. Although clinical trials examining the impact of oral GSH supplementation have produced conflicting and controversial results, our recent clinical study [134] offers conclusive evidence that long-term oral GSH supplementation not only increases the body GSH stores of GSH but also significantly reduces oxidative DNA damage in Indian T2D patients. It enhances the efficiency of anti-diabetic treatment in maintaining normal blood glucose levels in diabetic patients.

The design of the clinical trial was planned and carried out by our clinical collaborators to investigate the effect of long-term GSH supplementation on various biomarkers in T2D patients already under antidiabetic treatment. The duration of the clinical trial and between visits were decided based on the physiology and understanding of previous studies in the field. In particular, very few studies describe GSH supplementation of T2D patients in the literature. Most studies in the literature were typically conducted for short durations, such as 2-4 weeks. To the best of our knowledge, the only previous study to be carried out for six months was Richie *et al.* [90]; however, this was not comparable to this study as it included only healthy, non-diabetic subjects.

HbA1c was measured as a primary marker in the study, which shows the average blood sugar (glucose) level for the past two to three months. The RBC

lifespan is typically known as 120 days. The overall study duration was chosen to be six months, which allowed two measurements of change in HbA1c three months apart. This allowed the investigators to establish long-term effects and study the stability of the observations to prolonged supplementation.

It is known that GSH can be transported intact from intestinal epithelial cells into the blood lumen (Nolan *et al.* [140]), or it can be broken down into its constituent amino acids by gamma-glutamyl transferase (Hanigman *et al.* [141]). However, it remains unclear whether GSH is absorbed directly or broken down and then re-synthesized by glutathione synthetase. In addition, our study found a significant increase in the concentration of erythrocytic GSSG, possibly due to the conversion of erythrocytic GSH into GSSG, as reported in previous studies. For example, Nolan *et al.* [140] demonstrated that GSH administered to mice is rapidly converted to GSSG and accumulates in red blood cells and the liver. Therefore, oral GSH supplementation increases the body stores of GSH and stores a portion as GSSG. Our findings are strongly indicating GSH supplementation leads to a systemic improvement in the redox state of individuals with T2D. By augmenting antioxidant reserves through elevated GSH, a significant reduction in the accumulation of oxidative DNA damage is attained, which indicates an improvement in the pathophysiology of T2D complications. Despite regular anti-diabetic treatment, HbA1c levels in diabetic patients usually fluctuate. However, our study found that GSH supplementation over three months helped to maintain lowered HbA1c levels, particularly in elderly patients over 55 years of age. The characteristics of the glycemic state, including FPG, PPG, FPI, and PPI, did not change in the diabetic patients as a whole. However, we observed an increase in FPI levels in elderly diabetic patients, which was an interesting finding. The exact mechanism by which GSH helps maintain normoglycemia in diabetic patients

remains unclear and requires further investigation.

Preserving adequate β -cell function is crucial for controlling glucose levels in diabetic patients, as their ability to secrete insulin in response to glucose depends on intracellular thiols (Anjaneyulu *et al.* [142]). Due to their low antioxidant capacity and poor ability to repair oxidatively damaged DNA, β -cells are particularly vulnerable to ROS, and thus, providing antioxidant support to pancreatic β -cells is a potential strategy for improving β -cell function (Modak *et al.* [143], Lenzen *et al.* [144]). Extracellular GSH levels have been shown to enhance β -cell response to glucose in rats (Ammon *et al.* [145]) and improve glucose disposal in patients with impaired glucose tolerance (Bruggeman *et al.* [93]). Our results also suggest that oral GSH supplementation can support anti-diabetic treatment in reducing hyperglycemia, particularly in elderly patients. However, the exact mechanism underlying these observations requires further investigation. It is worth noting that while Southeast Asian diabetic patients are believed to exhibit poor insulin resistance, recent reports indicate that a significant subgroup of patients has insulin deficiency (Prasad *et al.* [146]). Additionally, as only a small number of patients in our study were on insulin, it remains unclear if our observations apply to those with severe insulin insufficiency.

The concentration of GSH is known to decrease with age, and this decline may be even more pronounced in elderly diabetic patients, as indicated by previous research (Sekhar *et al.* [79], Erdennal *et al.* [139]). Our study found that GSH supplementation significantly reduced oxidative DNA damage and improved glycemic control in elderly diabetic patients. Interestingly, we also observed a significant increase in FPI in these patients. Recent research by Zhang *et al.* [147] demonstrated that oral GSH administration improved β -cell function and reduced oxidative damage markers in diabetic rats. Similarly,

treating islets from T2D cadaveric organ donors with GSH improved their functionality and reduced oxidative damage markers (Del Guerra *et al.* [148]), suggesting that reducing OS in islets may be a viable approach to treating diabetes. Our findings suggest that the systemic increase in GSH levels may have reduced oxidative DNA damage, improved pancreatic β -cell function, and lowered HbA1c, especially in elderly diabetic patients. We recognize that the study was not designed to evaluate this analysis explicitly, and as such, it is a weaker form of evidence. Independent clinical trials need to be designed to understand and provide stronger evidence with sufficient statistical power on the age effects for the effectiveness of GSH supplementation.

We have recruited 250 diabetic subjects in our study. Even larger studies can be designed if we are to stratify various subgroups to understand the specific effects of GSH supplementation. We feel that the clues to the effectiveness of GSH supplementation may lie in diet, physical activity, the stage, and nature (if any) of pathology. It is not prudent in the present study to analyze our data based on factors such as diet, physical activity, weight reduction, etc., since such subdivisions of the data would lead to loss of statistical power due to insufficient sample size and, therefore, weaken the analysis. In the present study, we have chosen to remain modest in our description of the study results. We now remark in some detail on the several ways in which the present work can be extended to personalize GSH therapy. Therefore, further clinical trials must be designed to investigate these effects and obtain stronger evidence with sufficient statistical power.

It would be valuable to investigate the duration of the effects of GSH intervention, as individual antioxidant status can vary greatly, potentially affecting the efficacy of exogenous supplementation. This might even explain why the changes in HbA1c observed in DG have shown limited effect sizes. It is also

conceivable that longer intervention with GSH may show further improvements in glycemic parameters such as fasting glycemia. In our study, due to sample size limitations, we do not have enough statistical power to do such analyses.

However, our results lay the foundation for further studies with various population cohorts to understand these effects better. Our findings provide evidence of GSH supplementation's significant yet modest effects on HbA1c. This is very important, especially in light of the ADA position (Inzucchi *et al.* [48]), which highlights the importance of personalizing anti-diabetic therapy to achieve successful glycemic targets, instead of relying on a one-size-fits-all approach. However, few algorithms exist to facilitate this complex objective despite the need for personalized therapy. Consequently, GSH supplementation is a safe and valuable treatment option that clinicians should consider, despite the lack of algorithms to guide this effort.

3.5 Appendix

The longitudinal biochemical changes in elder individuals with T2D are detailed in the next section below.

3.5.1 Biochemical changes in elder diabetic individuals

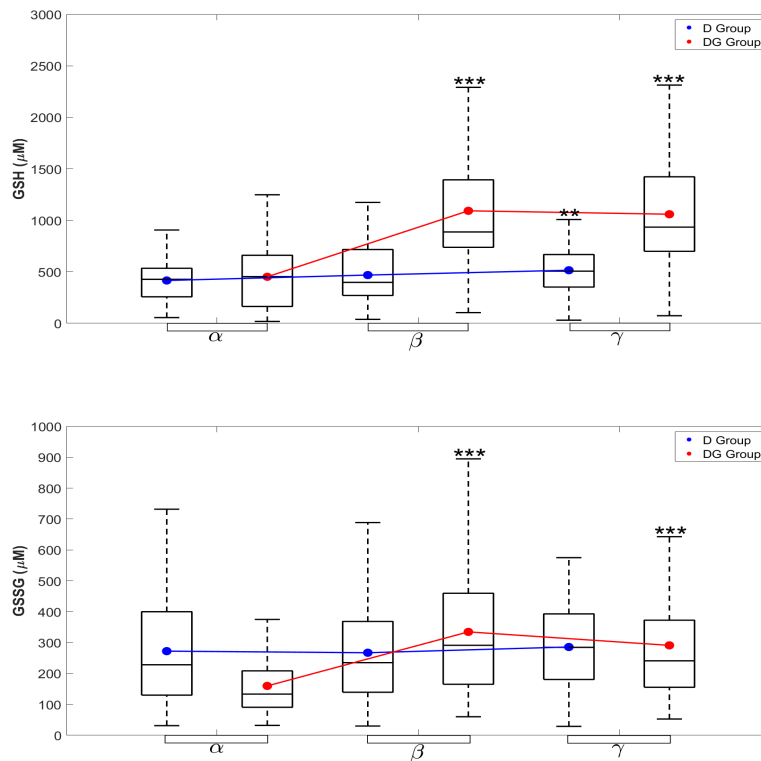


Figure 3.9: Serial changes in the concentration of (A) GSH and (B) GSSG of elderly diabetic subjects in D (blue) and DG (red) groups are shown here with box and whiskers plots. Significance levels shown here are * $p < 0.05$, ** $p < 0.01$, *** $p < 0.001$ for respective comparisons. This figure is reproduced from Kalamkar *et al.* [134], published as Figure S1 in the supplementary data.

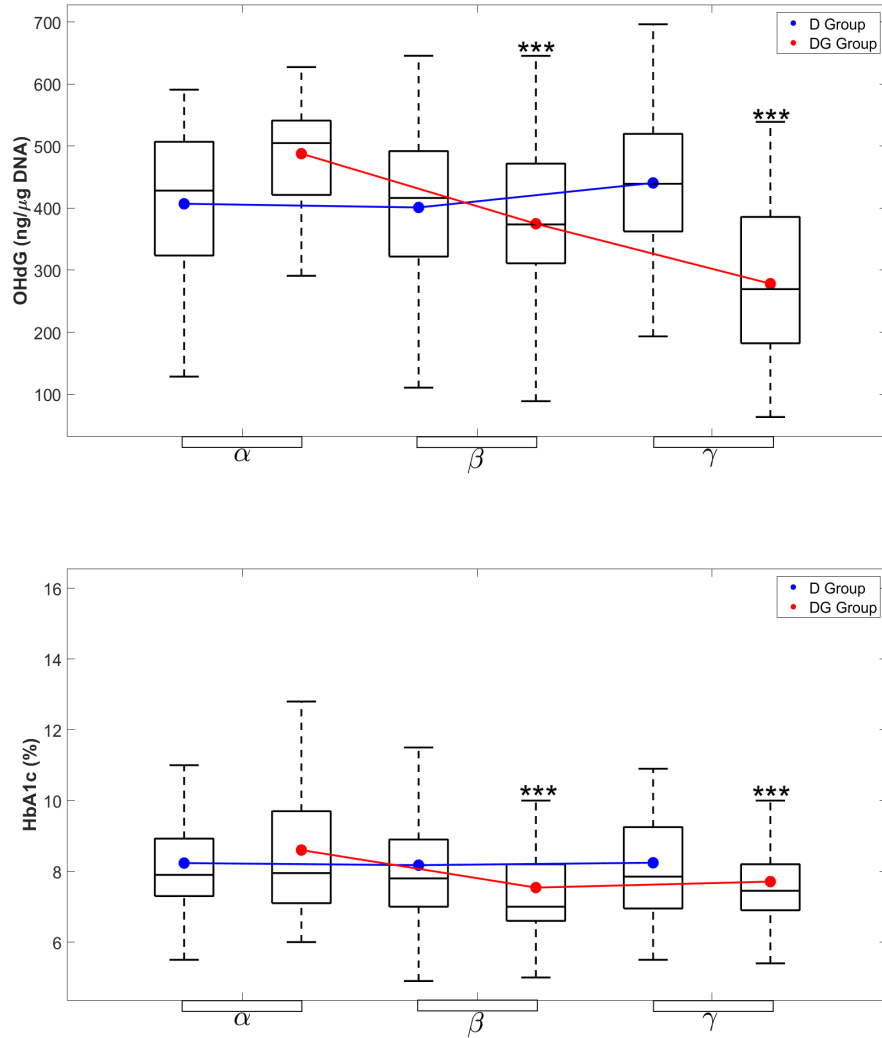


Figure 3.10: Serial changes in the concentration of (A) 8-OHdG and (B) HbA1c of elderly diabetic subjects in D (blue) and DG (red) groups are shown here with box and whiskers plots. Significance levels shown here are $*p < 0.05$, $**p < 0.01$, $***p < 0.001$ for respective comparisons. This figure is reproduced from Kalamkar *et al.* [134], published as Figure S2 in the supplementary data.

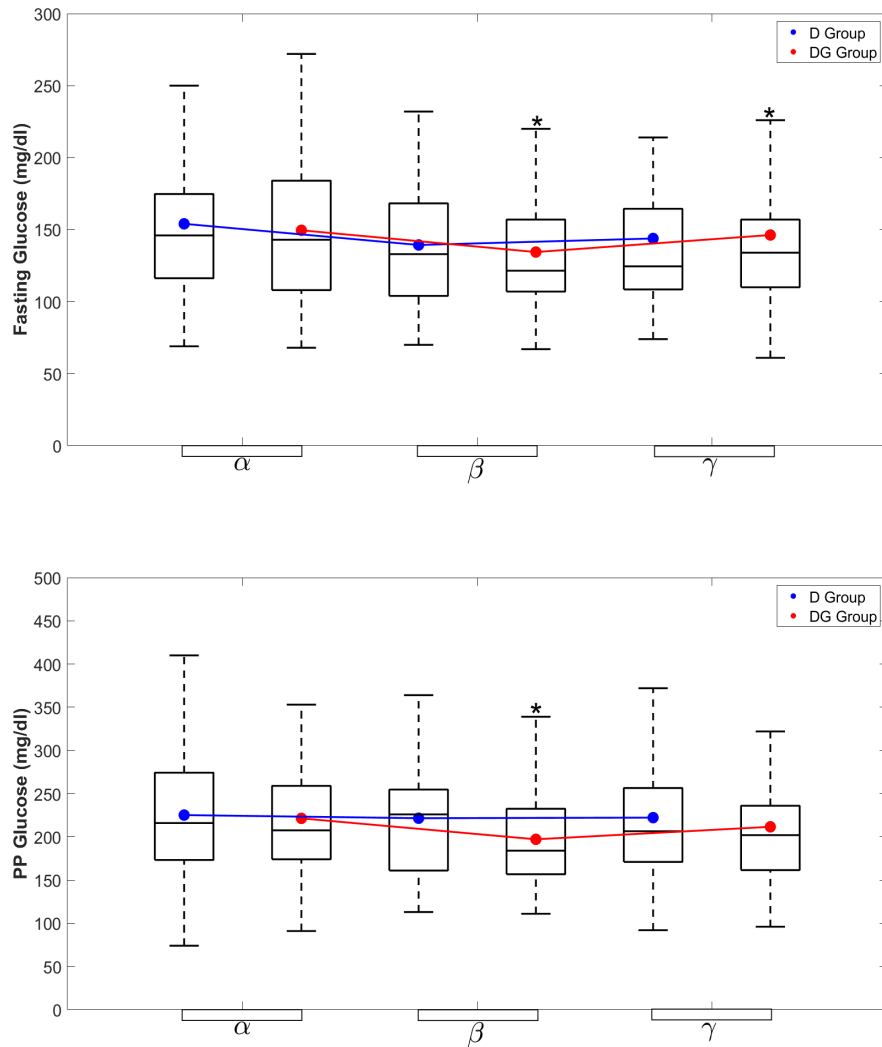


Figure 3.11: Serial changes in the concentration of (A) FPG and (B) FPI in elderly diabetic subjects in D (blue) and DG (red) groups are shown here with box and whiskers plots. Significance levels shown here are $*p < 0.05$, $**p < 0.01$, $***p < 0.001$ for respective comparisons. This figure is reproduced from Kalamkar *et al.* [134], published as Figure S2 in the supplementary data.

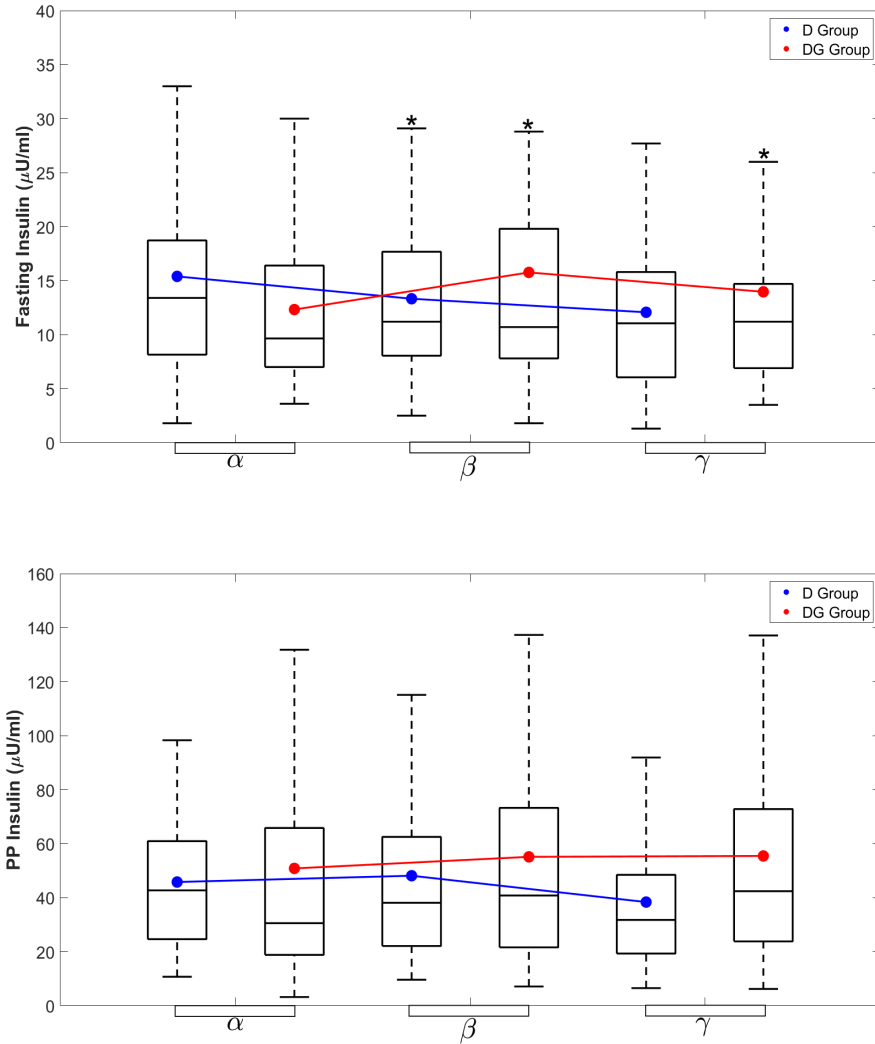


Figure 3.12: Longitudinal changes in the concentration of (A) PPG and (B) PPI in elderly diabetic subjects in D (blue) and DG (red) groups are shown here with box and whiskers plots. Significance levels shown here are $*p < 0.05$, $**p < 0.01$, $***p < 0.001$ for respective comparisons. This figure is reproduced from Kalamkar *et al.* [134], published as Figure S2 in the supplementary data.

Chapter 4

Multilevel modeling of longitudinal biochemical changes in individuals with T2D on GSH supplementation

Published as and adapted from:

Kolappurath Madathil, A.; Ghaskadbi, S.; Kalamkar, S.; Goel, P. Pune
GSH supplementation study: *Analyzing longitudinal changes in type 2 diabetic
patients using linear mixed-effects models.* *Frontiers in Pharmacology* 2023,
14:1139673. doi:10.3389/fphar.2023.1139673.

4.1 Introduction

The clinical trial results presented in the previous chapter showed that GSH supplementation for six months improved erythrocytic stores of GSH and offered protection from oxidative damage in individuals with T2D. We have shown the benefits of GSH supplementation on HbA1c and fasting insulin in elder individuals with T2D. With this evidence, we proposed using GSH supplementation as an adjunct therapy during regular anti-diabetic treatment for individuals with T2D. Notably, our data reveals significant variations in individual responses to GSH supplementation, which may be influenced by factors such as age, diet, physical activity, dosage, duration of intervention, baseline levels of endogenous GSH, etc. Based on these factors, we emphasize the importance of personalizing GSH supplementation for T2D patients, as this could be a valuable addition to current clinical practices. ADA has also recognized the need for personalized anti-diabetic therapy, rather than a one-size-fits-all treatment approach, to achieve optimal glycemic targets (Inzucchi et al. [48]). However, limited algorithms are available to guide the implementation of such personalized approaches in T2D care.

Quantitative models for quantification identifying personalized treatment goals are becoming increasingly important in modern healthcare (Mathur and Sutton [149], Johnson *et al.* [150], Gasparini *et al.* [151]). Models can be designed to incorporate a wide range of patient-specific data, including physiological measurements and medical history, to create a personalized treatment plan tailored to the unique needs of each patient. By accounting for individual differences, these models can help healthcare providers make more accurate predictions about personalized treatment outcomes, identify potential risks or complications, and optimize treatment strategies to improve patient outcomes. Additionally, personalized models can help reduce healthcare costs by mini-

mizing the need for trial-and-error approaches to treatment and identifying the most effective treatment options early on in the process. As such, models for personalization goals are rapidly becoming essential in modern healthcare, potentially transforming how we approach disease prevention, diagnosis, and treatment.

Repeatedly examining the same subjects to identify the changes that occurred over a period of time is an integral part of designing clinical research. In this chapter, we use the terminology of 'longitudinal data' to indicate repeated observations of the same variables over a period of time. Longitudinal studies have designs that involve correlational research with these repeated observations (Laird and Ware [152], Brown and Prescott [153], Verbeke *et al.* [154]). We note that understanding the dynamics of longitudinal biochemical change and variations in individual response to GSH supplementation is critical for developing effective personalized interventions for GSH with anti-diabetic treatment. This would be largely useful in evaluating the progress of treatment and understanding the glucose control targets for diabetic individuals. Longitudinal studies are necessary to monitor the changes in GSH concentration and other relevant blood biochemical markers over time to identify whether GSH supplementation has a long-lasting effect on glucose control or if its effects diminish over time. Therefore, personalized interventions should be designed with careful consideration of the individual's specific needs and health status. Developing algorithms that can predict an individual's response to GSH supplementation would be beneficial, enabling clinicians to develop more personalized treatment plans based on their unique characteristics and needs.

In this chapter, we present the **Pune Glutathione Supplementation Study** carried out for examining finer nuances of individualized GSH sup-

plementation by analyzing the longitudinal data collected from the clinical trial (Kalamkar *et al.*[134]) using a framework of multilevel models. We particularly focus on developing the goals of using GSH supplementation as an adjunct therapy in a personalized manner for individuals with T2D in this chapter. We formulated multilevel models, also known as mixed-effects models, to analyze the clinical data of diabetic individuals. Our mixed-effects (ME) models are hierarchical models, where the units of analysis are subject-level predictors (level two) with fixed and random effects (Laird and Ware [152], Brown and Prescott [153], Verbeke *et al.* [154]). The framework of linear mixed-effects (LME) models also performs ‘shrinkage’ for estimating model parameters; that is, individual estimates obtained from mixed-effects models are shrunk towards a grand mean of the population level estimate compared to fitting separate linear models to each subject’s data (Gelman *et al.* [155], Bell *et al.* [156]). Mixed-effects models have a long history of use in health and medicine since these models treat each patient not only as a member of a population but as an individual with unique characteristics (Gelman *et al.* [155], Barr *et al.* [157], Baldwin *et al.* [158], Wang *et al.* [159], Schober and Vetter [160]). Thereby mixed-effects models allow estimating model parameters that describe between- and within-subject variability of individual responses. A two-level mixed-effects model will be able to provide reliable estimates in absolute, not just relative, physical units of the variables.

Further, we addressed our insights from our earlier study, suggesting that age is a very important covariate of the effectiveness of GSH supplementation. We analyzed how the longitudinal changes in biochemical parameters of elder and younger diabetic individuals differ with GSH supplementation independently using LME models. Center for Disease Control (CDC) reports indicate that as the average world population ages, the number of older adults affected

by diabetes also increases [4]. It is, therefore, necessary to improve the understanding of effective interventions, especially in elder individuals with T2D. Elderly adults often have one or more co-existing disease conditions or microvascular complications that might impact their diabetes control. Therefore, special considerations should be given to support their overall health. The predictability of glycemic variables and markers for oxidative DNA damage gives more information about the physiology and treatment to be tailored for each individual with time. This also helps in deciding the interventions for elder individuals with T2D better. Considering the translational aspects of our results and their direct clinical and academic uses, we formulate a basic scheme for making predictions of the trajectory of individuals on GSH supplementation using the fitted LME models.

The work presented in this chapter has been published as Madathil *et al.* [161] under the title, **Pune GSH supplementation study: Analyzing longitudinal changes in type 2 diabetic patients using linear mixed-effects models** in the *Frontiers in Pharmacology* journal. The figures in this chapter are reproduced under the creative commons attribution license.

4.2 Methodology

Next, we describe the methods and analysis used in the multilevel modeling of longitudinal biochemical changes in T2D.

4.2.1 Summary of clinical trial data

The dataset published in the trial comprised 250 known Indian diabetic individuals recruited between February 2016 and January 2018 who were already on anti-diabetic treatment. The clinical trial consisted of three groups: a con-

trol group comprising healthy, nondiabetic subjects and two groups of diabetic patients; in one of those, GSH supplementation (500 mg/day for six months) was carried out, namely the DG group, and the other group without supplementation, the D group. The only difference between this D and DG group is the intervention and supplementation with GSH. More importantly, D and DG are similar in nearly all respects, and covariate balance at the baseline has already been observed Kalamkar *et al.* [134]. As shown in Figure 4.1, inter-individual variation is evident in both groups' longitudinal data of GSH concentration. Similar depictions for other measured variables are not shown in the thesis.

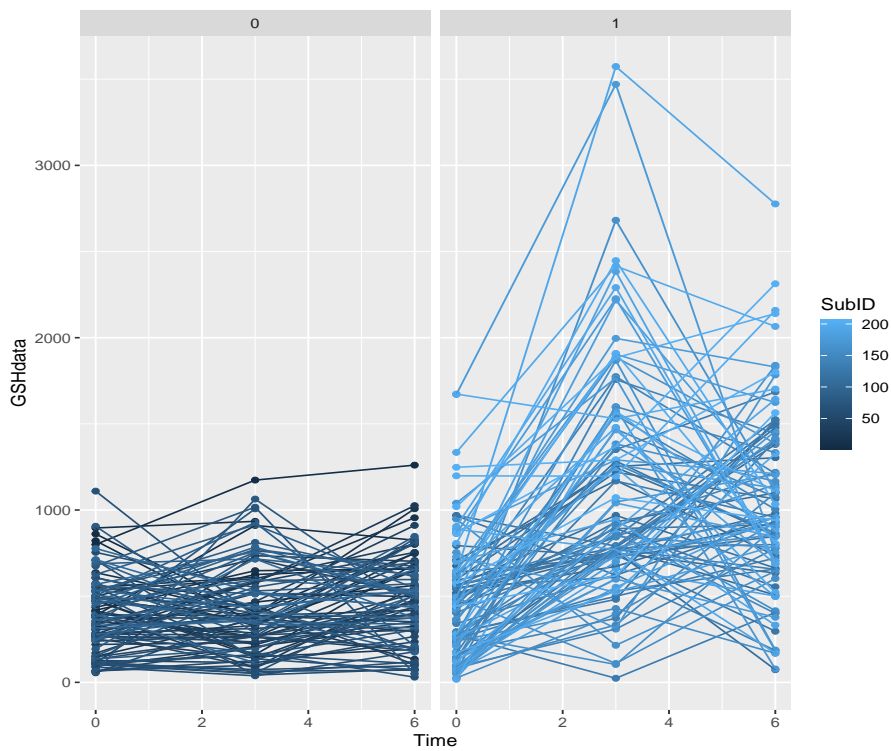


Figure 4.1: **Longitudinal biochemical changes of individuals with T2D in the clinical trial.** GSH measurements from subjects in D (n=100) and DG (n=101) groups at three visits in the study are depicted here. The individual lines connecting three visits represent the trajectory of each subject during the clinical trial.

4.2.2 Linear mixed-effects models

Mixed effects models, which are also known as hierarchical or multilevel models, have a fairly long history and have been widely used in the health and medicine fields (Laird and Ware [152], Brown and Prescott [153], Verbeke *et al.* [154]). These models consist of both *fixed* and *random effects*. Fixed effects in these models are often used to obtain the groupwise or population-level fits. In contrast, random effects are used to explain the subject-specific distribution of parameters and residual errors. The framework of mixed effects models allows considering that the observations within a subject may be correlated and estimate the model parameter along with estimates of between- and within-subject variability. These models identify different levels in the data by allowing for residual components at each level in the structure. Thus, the residual variance is partitioned into a between-subject component and a within-subject component. The unobserved variables also lead to a correlation between outcomes from the same subjects. Thus, the residual variance is partitioned into a between-subject component and within-subject components in mixed-effects models (Bates *et al.* [162]). Therefore, the methods are suitable for assessing and comparing the individual effects of treatments rather than just the average effects (Gelman *et al.* [155]).

A feature of mixed effects models, which allows the consideration of random coefficients for parametrizing the characteristic of a particular patient, is so useful for personalizing an intervention. This variability in a coefficient across patients could also result from real variation arising from biological or experimental factors. These models allow consideration of a subject as an individual with unique characteristics and not just as a population member with an average value to estimate. Therefore, estimates of treatment effects obtained from these mixed effects models are more reliable and with direct

clinical uses than the population-level estimate (Gelman *et al.* [155]).

4.2.3 Modeling clinical trial data with LME models

We use mixed-effects models for analyzing the clinical data over classic regression-based models, which treat the units of analysis as independent observations. Data available from diabetic subjects have a hierarchical or clustered structure. For instance, subjects in the same group might change longitudinally similar in their biochemical characteristics compared to individuals chosen randomly from the population in general. Individuals may be further nested within different treatment types. We understand that the classical regression models fail to recognize hierarchical structures, and the standard errors of regression coefficients will be underestimated. This might lead to an overstatement of the statistical significance of interested model parameters. We think classical regression models are a good choice to make inferences beyond average population estimates through fixed-effect models. The units of analysis are treated as independent observations in conventional multiple regression approaches. Hierarchical structures are not considered, so the standard errors of regression coefficients could be underestimated. This can cause the statistical significance of the relevant model parameters to be overstated. At the same time, mixed effects models recognize different levels in the data by allowing for residual components at each level in the structure.

The formulation of these models and further analysis are detailed next.

4.2.4 Formulation of linear mixed-effects models

Linear mixed-effect (LME) models were formulated independently for biochemical response variables, GSH, GSSG, HbA1c, 8-OHdG, FPG, FPI, PPG, and PPI by assuming fixed effect and random effect parameters at different

levels (Level 1: time, Level 2: individuals). Then the composite form of the model equations was obtained by substituting the Level 2 equations with Level 1. This form of the model was further used to study the dependency of each effect at different levels and their nested structure in one another. Now, the response variable Y from subject i on the j^{th} visit can be modeled with a Random Intercept and Random Slope (RIRS) model as

$$\text{Level 1: } Y_{ij} = b_{i0}^* + b_{i1}^* \times t_{ij} + \epsilon_{ij} \quad (4.1)$$

The random variables for slope or intercepts in the model can be written as

$$\text{Level 2: } b_{i0}^* = \beta_0 + b_{i0}$$

$$b_{i1}^* = \beta_1 + \beta_2 \times T_i + b_{i1}$$

Where the treatment indicator variable T_i takes the value 0 for the D group, and 1 for the DG group, and b_{i0}, b_{i1} are distributed as

$$\begin{pmatrix} b_{i0} \\ b_{i1} \end{pmatrix} \sim N \left(\begin{bmatrix} 0 \\ 0 \end{bmatrix}, \begin{bmatrix} \sigma_0 & \sigma_{01} \\ \sigma_{01} & \sigma_1 \end{bmatrix} \right) \quad (4.2)$$

Here in this model, fixed effects are $\beta_0, \beta_1, \beta_2$ and random effects are b_{i0}, b_{i1} . The RIRS model equation can be rewritten as

$$Y_{ij} = \beta_0 + b_{i0} + (\beta_1 + \beta_2 \times T_i + b_{i1}) \times t_{ij} + \epsilon_{ij} \quad (4.3)$$

Similarly, a Random Intercept and Fixed Slope (RIRS) model can be formulated at two levels as

$$\text{Level 1: } Y_{ij} = b_{i0}^* + b_{i1}^* \times t_{ij} + \epsilon_{ij} \quad (4.4)$$

at level 2, random intercept and fixed slope are given by

$$\text{Level 2: } b_{i0}^* = \beta_0 + b_{i0}$$

$$b_{i1}^* = \beta_1 + \beta_2 \times T_i$$

b_{i0} are distributed as

$$b_{i0} \sim N(0, \sigma_0) \quad (4.5)$$

Here the fixed effects are $\beta_0, \beta_1, \beta_2$ and random effect is b_{i0} . The RIFS model equation can be written as

$$Y_{ij} = \beta_0 + b_{i0} + (\beta_1 + \beta_2 \times T_i + b_{i1}) \times t_{ij} + \epsilon_{ij} \quad (4.6)$$

Parameters from these RIRS and RIFS formulations can be interpreted as:

β_0 : Overall intercept (Mean expected GSH) when all predictors are 0

β_1 : Average rate of change in GSH in for the control group (D)

β_2 : Difference in the rate of change between D and DG (treatment effect)

b_{i0} : Random effect for person-specific differences at baseline

b_{i1} : Random effect for person-specific differences in the rate of change

We express the individual-specific parameters and data points in the form of matrices for writing the model equations in matrix forms. The descriptions of design matrices are given next.

4.2.5 Design matrix of model equations

The matrix version of the model equations was used to explain the estimates for all subjects

$$Y = X\beta + Zb + \epsilon \quad (4.7)$$

where the data column vector (Y) and matrices X, Z, β, b, ϵ for RIRS models are of the form

$$Y = \begin{pmatrix} Y_{11} \\ Y_{12} \\ Y_{13} \\ Y_{21} \\ Y_{22} \\ Y_{23} \\ \dots \\ \dots \\ Y_{N1} \\ Y_{N2} \\ Y_{N3} \end{pmatrix} \quad X = \begin{pmatrix} 1 & t_{11} & T_1 \times t_{11} \\ 1 & t_{12} & T_1 \times t_{12} \\ 1 & t_{13} & T_1 \times t_{13} \\ 1 & t_{21} & T_2 \times t_{11} \\ 1 & t_{22} & T_2 \times t_{12} \\ 1 & t_{23} & T_2 \times t_{13} \\ \dots & \dots & \dots \\ \dots & \dots & \dots \\ 1 & t_{N1} & T_N \times t_{11} \\ 1 & t_{N2} & T_N \times t_{12} \\ 1 & t_{N3} & T_N \times t_{13} \end{pmatrix} \quad \beta = \begin{pmatrix} \beta_0 \\ \beta_1 \\ \beta_2 \end{pmatrix}$$

$$Z = \begin{pmatrix} 1 & t_{11} & 0 & 0 & \dots & 0 & 0 \\ 1 & t_{12} & 0 & 0 & \dots & 0 & 0 \\ 1 & t_{13} & 0 & 0 & \dots & 0 & 0 \\ 0 & 0 & 1 & t_{21} & \dots & 0 & 0 \\ 0 & 0 & 1 & t_{22} & \dots & 0 & 0 \\ 0 & 0 & 1 & t_{23} & \dots & 0 & 0 \\ \dots & \dots & \dots & \dots & \dots & \dots & \dots \\ \dots & \dots & \dots & \dots & \dots & \dots & \dots \\ 0 & 0 & 0 & 0 & \dots & 1 & t_{N1} \\ 0 & 0 & 0 & 0 & \dots & 1 & t_{N2} \\ 0 & 0 & 0 & 0 & \dots & 1 & t_{N3} \end{pmatrix} \quad b = \begin{pmatrix} b_{10} \\ b_{11} \\ b_{20} \\ b_{21} \\ \dots \\ \dots \\ b_{N0} \\ b_{N1} \end{pmatrix} \quad \epsilon = \begin{pmatrix} \epsilon_{11} \\ \epsilon_{12} \\ \epsilon_{13} \\ \epsilon_{21} \\ \epsilon_{22} \\ \dots \\ \dots \\ \epsilon_{N1} \\ \epsilon_{N2} \\ \epsilon_{N3} \end{pmatrix}$$

Similarly, the design matrices for RIFS models, Y, X, β , will be similar to those for RIRS models. But b, Z, ϵ are different. They are of the form

$$Z = \begin{pmatrix} 1 & 0 & \dots & 0 & 0 \\ 1 & 0 & \dots & 0 & 0 \\ 1 & 0 & \dots & 0 & 0 \\ 0 & 1 & \dots & 0 & 0 \\ 0 & 1 & \dots & 0 & 0 \\ 0 & 1 & \dots & 0 & 0 \\ \dots & \dots & \dots & \dots & \dots \\ \dots & \dots & \dots & \dots & \dots \\ 0 & 0 & 0 & \dots & 1 \\ 0 & 0 & 0 & \dots & 1 \\ 0 & 0 & 0 & \dots & 1 \end{pmatrix} \quad b = \begin{pmatrix} b_{10} \\ b_{20} \\ \dots \\ \dots \\ b_{N0} \end{pmatrix} \quad \epsilon = \begin{pmatrix} \epsilon_{11} \\ \epsilon_{12} \\ \epsilon_{13} \\ \epsilon_{21} \\ \epsilon_{22} \\ \dots \\ \dots \\ \epsilon_{N1} \\ \epsilon_{N2} \\ \epsilon_{N3} \end{pmatrix}$$

Further, we formulate the expressions for the covariance matrix using these matrix forms in the next section.

4.2.6 Covariance matrices in the model

The covariance matrix for the data vector Y (from N subjects), V for an LME model of the form $Y = X\beta + Zb + \epsilon$, is obtained as $V = ZGZ^T + R$, where $\mathbb{E}(b) = 0$, $\mathbb{E}(\epsilon) = 0$, covariance matrix of random effects, $Var(b) = G$, and the covariance matrix for residual error, $Var(\epsilon) = R$ (Laird and Ware [152],

Henderson [163]). The variance matrix of G is of a block diagonal matrix form

$$G = \begin{pmatrix} \sigma_0^2 & \sigma_{01} & 0 & 0 & \dots & \dots & 0 & 0 \\ \sigma_{01} & \sigma_1^2 & 0 & 0 & \dots & \dots & 0 & 0 \\ 0 & 0 & \sigma_0^2 & \sigma_{01} & \dots & \dots & 0 & 0 \\ 0 & 0 & \sigma_{01} & \sigma_1^2 & \dots & \dots & 0 & 0 \\ \dots & \dots & \dots & \dots & \dots & \dots & \dots & \dots \\ \dots & \dots & \dots & \dots & \dots & \dots & \dots & \dots \\ 0 & 0 & 0 & 0 & \dots & \dots & \sigma_0^2 & \sigma_{01} \\ 0 & 0 & 0 & 0 & \dots & \dots & \sigma_{01} & \sigma_1^2 \end{pmatrix}$$

This matrix is composed of N identical blocks $\begin{pmatrix} \sigma_0^2 & \sigma_{01} \\ \sigma_{01} & \sigma_1^2 \end{pmatrix}$ corresponding random effects from N subjects. Similarly, the structure of the covariance matrices for the RIFS model looks like

$$G = \begin{pmatrix} \sigma_0^2 & 0 & 0 & \dots & \dots & 0 \\ 0 & \sigma_0^2 & \dots & \dots & 0 & 0 \\ \dots & \dots & \dots & \dots & \dots & \dots \\ \dots & \dots & \dots & \dots & \dots & \dots \\ 0 & 0 & 0 & \dots & \dots & \sigma_0^2 \end{pmatrix}$$

which was composed of N identical blocks of $\begin{pmatrix} \sigma_0^2 \end{pmatrix}$. The structure of R was assumed to be a diagonal matrix, with $R = \sigma_e^2 \mathbb{I}_{3N \times 3N}$, where $\mathbb{I}_{3N \times 3N}$ is a block diagonal matrix with N identical blocks of identity matrices for N subjects with 3×3 dimension. The individual entries of the variance matrix (V) for

an RIRS model are of the following form:

$$\begin{aligned}
cov(y_{ij}, y_{ij'}) &= cov(\beta_0 + b_{i0} + \beta_1 \times t_{ij} + \beta_2 \times T_i \times t_{ij} + b_{i1} \times t_{ij} + \epsilon_{ij}, \beta_0 + b_{i0} \\
&\quad + \beta_1 \times t_{ij'} + \beta_2 \times T_i \times t_{ij'} + b_{i1} \times t_{ij'} + \epsilon_{ij'}) \\
&= cov(b_{i0} + b_{i1} \times t_{ij}, b_{i0} + b_{i1} \times t_{ij'}) + cov(\epsilon_{ij}, \epsilon_{ij'}) \\
&= cov(b_{i0}, b_{i0}) + cov(b_{i0}, b_{i1} \times t_{ij}) + cov(b_{i0}, b_{i1} \times t_{ij'}) \\
&\quad + cov(b_{i1} \times t_{ij}, b_{i1} \times t_{ij'}) \\
&= Var(b_{i0}) + cov(b_{i0}, b_{i1}) \times (t_{ij} + t_{ij'}) + Var(b_{i1}) \times t_{ij}t_{ij'} \\
cov(y_{ij}, y_{ij'}) &= \sigma_0^2 + (t_{ij} + t_{ij'}) \times \sigma_{01} + t_{ij}t_{ij'}\sigma_1^2 + cov(\epsilon_{ij}, \epsilon_{ij'})
\end{aligned} \tag{4.8}$$

which can be written as

1. For $j = j'$, $cov(y_{ij}, y_{ij'}) = Var(y_{ij}) = \sigma_0^2 + 2t_{ij} \times \sigma_{01} + t_{ij}^2\sigma_1^2 + \sigma_e^2$
2. For $j \neq j'$, $cov(y_{ij}, y_{ij'}) = \sigma_0^2 + (t_{ij} + t_{ij'}) \times \sigma_{01} + t_{ij}t_{ij'}\sigma_1^2$

Next, we discuss how these formulations derive model estimates and further analyze the datasets.

4.2.7 Model derivation for BLUE and BLUP

The Maximum Likelihood-based derivations obtain expressions for the model estimates for β and b given by Henderson equations or Mixed Model Equations (Henderson [163]). The details are described below.

For the model equations of the form $Y = X\beta + Zb + \epsilon$ with covariance matrices described in section 3.2.1, the joint likelihood for Y can be written in terms of probability densities of b and ϵ , $g(\cdot)$ and $h(\cdot)$ respectively, as

$$f(Y, b) = g(Y/b)h(b) = g(\epsilon)h(b) \tag{4.9}$$

Therefore, $f(Y, b)$ has the form

$$f(Y, b) = \left(\frac{1}{2\pi}\right)^{\frac{N}{2}} |R|^{-1/2} e^{-\frac{1}{2}\epsilon^T R^{-1} \epsilon} \times \left(\frac{1}{2\pi}\right)^{\frac{N}{2}} |G|^{-1/2} e^{-\frac{1}{2}b^T G^{-1} b} \quad (4.10)$$

Then likelihood function (L) can be written as

$$L = f(Y, b) = c e^{-\frac{1}{2}\epsilon^T R^{-1} \epsilon} e^{-\frac{1}{2}b^T G^{-1} b}$$

Log-likelihood function will be given by

$$\begin{aligned} \ln(L) &= \ln(f(Y, b)) \\ &= \ln(c) - \frac{1}{2}\epsilon^T R^{-1} \epsilon - \frac{1}{2}b^T G^{-1} b \\ &= \ln(c) - \frac{1}{2}(Y - X\beta - Zb)^T R^{-1} (Y - X\beta - Zb) - \frac{1}{2}b^T G^{-1} b \end{aligned} \quad (4.11)$$

Taking the partial derivatives of $\ln(L)$ with respect to β , b and setting them to zero provides

$$\frac{\partial(\ln L)}{\partial \beta} = 0 \quad \text{and} \quad \frac{\partial(\ln L)}{\partial b} = 0$$

\implies

$$\begin{aligned} -2X^T R^{-1} X\beta + 2X^T R^{-1} Zb &= X^T R^{-1} Y \\ Z^T R^{-1} X\beta + Z^T R^{-1} Zb + G^{-1} b &= Y^T R^{-1} Z \end{aligned} \quad (4.12)$$

These equations are known as **Henderson equations or Mixed Model Equations** (Henderson [163]) for the estimation of the parameters and are written in matrix form below.

$$\begin{pmatrix} X^T R^{-1} X & X^T R^{-1} Z \\ Z^T R^{-1} X & G^{-1} + Z^T R^{-1} Z \end{pmatrix} \begin{pmatrix} \beta \\ b \end{pmatrix} = \begin{pmatrix} X^T R^{-1} y \\ Z^T R^{-1} y \end{pmatrix} \quad (4.13)$$

The solutions of these equations are BLUE (Best Linear Unbiased Estimator) of $\hat{\beta}$, and BLUE (Best Linear Unbiased Predictor) of \hat{b} .

$$\hat{\beta} = (X^T V^{-1} X)^{-1} X^T V^{-1} Y \quad (4.14)$$

$$\hat{b} = G Z^T V^{-1} (Y - X \beta) \quad (4.15)$$

Further, we provide a description of how a sequential optimization for estimating $\hat{\beta}$ and \hat{b} from the data is performed.

4.2.8 Iterative schemes of optimization

The variance matrix was unknown and can be assumed as $V(\theta)$, a function of θ , the parameter vector from the covariance matrices, G and R . A brief description of the steps involved in the steps of iterative optimization is the following:

1. Set the iteration counter $k = 0$. Assign initial values to covariance parameters for $\theta^{(0)} = (\theta_1, \dots, \theta_n)^T$
2. At each m^{th} iteration, substitute $\theta^{(m-1)}$ and obtain $\hat{V} = V(\theta^{(m-1)})$. Then obtain

$$\beta^{(m)} = (X^T V^{-1} X)^{-1} X^T V^{-1} Y$$

3. Obtain $\theta^{(m)}$ by maximizing the likelihood function

$$L(\theta; y) = -\frac{1}{2} [\log(|V(\theta)|) + (Y - X \beta_\theta^{(m)})^T V^{-1}(\theta) (Y - X \beta_\theta^{(m)})]$$

4. Repeat steps 1, 2, and 3 until convergence or a predetermined number of iterations k .

5. Keep $\theta^{(k)}$ fixed. Use them to obtain the estimates $\hat{\beta}^{(k)}$ of $\hat{\beta}$ and $\hat{b}^{(k)}$ of \hat{b} using the equations

$$\hat{\beta} = (X^T V^{-1} X)^{-1} X^T V^{-1} Y$$

The details of model parameter optimization and fitting tools are described in the next section.

4.2.9 Model parameters and fitting

RIFS and RIRS models were fitted for GSH, GSSG, 8-OHdG, HbA1c, FPG, FPI, PPG, and PPI and compared based on best AIC values and by avoiding the singularity arising while model fitting (Barr *et al.* [157]). RIFS models were fitted to obtain five parameters, $\beta_0, \beta_1, \beta_2, \sigma_0, \sigma_e$, and RIRS models were fitted with seven parameters, $\beta_0, \beta_1, \beta_2, \sigma_0, \sigma_1, \sigma_{01}, \sigma_e$. The fitted estimates for β and b are given by the BLUE of $\hat{\beta}$, and BLUP of \hat{b} Henderson [164] can be written as

$$\hat{\beta}_{\text{BLUE}} = (X^T V^{-1} X)^{-1} X^T V^{-1} Y \quad (4.16)$$

$$\hat{b}_{\text{BLUP}} = G Z^T V^{-1} (Y - X \hat{\beta}_{\text{BLUE}}) \quad (4.17)$$

The components of \hat{b} , b_{i0} , and b_{i1} , random effects represent person-specific intercepts (in both RIFS and RIRS) at the baseline and person-specific differences in the rate of change in the slopes (in RIRS only), respectively. The formulated models have been tested and fitted using the lme4 package in R [165]; these calculations were confirmed using the fitlme package in Matlab and the mimosa package (Titz *et al.* [166]) for mixed effects models. Other packages, ggplot2 and tidyverse in R were used for analysis and plots. A suitable RIFS or RIRS model was selected for each response variable using the

best AIC and non-singularity criteria (Bates *et al.*[162]).

The statistical significance of the results of the LME estimates was determined as $p < 0.05$. We have followed the uncorrected p-value to interpret the results throughout. To ensure completeness, we have performed corrections for multiple comparisons using the Bonferroni method (Bonferroni [167]). We applied these corrections for the estimates from LME models for each variable and across all main and supplementary analysis results. Those results, which continued to be statistically significant even after the corrections, were marked with a # in the corresponding tables. The reader should consider this when evaluating the statistical findings.

The details of the data preparation for fitting with LME models are described next.

4.2.10 Data preparation for fitting with LME models

A sample structure of the long format of the data from the GSH clinical trial prepared for fitting with the LME model is shown in Table 4.10. A depiction of the GSH measurements from D (N=102) and DG group (N=104) subjects on the first, second, and third visits (0, 3, and 6 months of the study) are shown below. Measurements from an individual are connected with solid lines. The Group IDs, 0 for the D group and 1 for the DG group, are encoded on each panel. RIRS and RIFS models were used independently to fit datasets for different variables. Notably, these trajectories have evident inter-individual and intra-individual variations.

Further, we describe LME models formulated in the subsequent analyses to study the age-related effects of GSH supplementation on individuals with T2D. We begin by analyzing the two age classes discussed in the previous chapter using independent LME models in the next section.

4.2.11 Independent LME models for two age classes

Diabetes is an age-onset disease; an early diagnosis leads to an increased chance for complications to set in relatively early. We subdivided the DG population above and below age 55, namely that this is the median age of either group. This is purely a statistical criterion and does not reflect any value judgments on our part. Thus, we coined the term ‘elder’ subgroup for subjects above the median age. We note that our criterion of the age of 55 coincides with a similar choice in the literature (Kannel and McGee [168], Duckworth *et al.* [169]), which reports diabetes-related complications in elder individuals; individuals of age around 55 years are reported to have a markedly increased risk. We have earlier demonstrated that the effectiveness of GSH supplementation differed between the younger and elder populations using an age cutoff of 55 years, which was the median age of the study population (Kalamkar *et al.* [134]). This was done through a post hoc subgroup analysis in our study. LME models provided a more formal way of comparing their differential responses in the two age classes.

We assumed two independent LME models to analyze the treatment effects of GSH supplementation in the elder and younger adults of D and DG separately. An RIRS model for elder adults (EA) was formulated at the subject level as

$$\text{Level 1: } Y_{ij} = b_{i0}^* + b_{i1}^* \times t_{ij} + \epsilon_{ij} \quad (4.18)$$

with a random slope and intercepts in the model given by

$$\text{Level 2: } b_{i0}^* = \beta_0 + b_{i0}$$

$$b_{i1}^* = \beta_1 + \beta_2 \times T_i + b_{i1}$$

where the treatment indicator variable, T_i takes a value of 0 for EA of D D group and 1 for EA of DG group. The assumptions on the random effects and covariance parameters are similar to the model formulations in (model 4). Similarly, we formulated the model for YA subgroups as well. We fit a separate LME for each of these two age groups. Model estimates obtained by fitting LME models independently for EA and YA will be presented in the results.

Next, we formulate different LME models for studying the effects of age considered as model variables.

4.2.12 LME models to study age effects

We studied the effects of the age of individuals on the outcome variables Y with different LME models by incorporating age in two ways: (i) a continuous variable for the age of individuals at the recruitment and (ii) a categorical variable for elder and younger age groups. To do this, we formulated four different models described below.

Model 1: The original RIRS model in the study without age variables

The outcome (Y) was modeled as

$$Y_{ij} = b_{i0}^* + b_{i1}^* \times t_{ij} + \epsilon_{ij} \quad (4.19)$$

where subject-specific random slopes and intercepts b_{i0}^* and b_{i1}^* defined by

$$b_{i0}^* = \beta_0 + b_{i0}$$

$$b_{i1}^* = \beta_1 + \beta_2 \times T_i + b_{i1}$$

Model 2: RIRS model with a treatment-time interaction term and three-way interaction term with age, treatment indicator, and time at the patient level.

The outcome (Y) was modeled with a three-way interaction term of age (Age_i), treatment (T_i), and time (t_{ij}) below as:

$$Y_{ij} = b_{i0}^* + b_{i1}^* \times t_{ij} + \epsilon_{ij} \quad (4.20)$$

where subject-specific random slopes and intercepts b_{i0}^* and b_{i1}^* defined by

$$b_{i0}^* = \beta_0 + b_{i0}$$

$$b_{i1}^* = \beta_1 + \beta_2 \times T_i Age_i + b_{i1}$$

Model 3: RIRS model with a three-way interaction term with age, treatment indicator, and time at the patient level (Level 2).

The outcome (Y) was modeled with a treatment and time interaction term and a three-way interaction term of age (Age_i), treatment (T_i), and time (t_{ij}) below as:

$$Y_{ij} = b_{i0}^* + b_{i1}^* \times t_{ij} + \epsilon_{ij} \quad (4.21)$$

where subject-specific random slopes and intercepts b_{i0}^* and b_{i1}^* defined by

$$b_{i0}^* = \beta_0 + b_{i0}$$

$$b_{i1}^* = \beta_1 + \beta_2 \times T_i + \beta_3 \times T_i Age_i + b_{i1}$$

Model 4: RIRS model with age groups as a categorical variable for pooling EA and YA at the patient level.

The outcome (Y) was modeled with categorical treatment variables for $Age \geq 55$ and $Age < 55$ as

$$Y_{ij} = b_{i0}^* + b_{i1}^* \times t_{ij} + \epsilon_{ij} \quad (4.22)$$

where subject-specific random slopes and intercepts b_{i0}^* and b_{i1}^* defined by

$$b_{i0}^* = \beta_0 + b_{i0}$$

$$b_{i1}^* = \beta_1 + \beta_2 \times T_i^{Age \geq 55} + \beta_3 \times T_i^{Age < 55} + b_{i1}$$

These four models are used to fit GSH, GSSG, 8-OHdG, HbA1c, FPG, FPI, PPG, and PPI data, and fit results were further compared using AIC and BIC estimates to identify best-fit models for the longitudinal data. The model-fit results and comparisons are presented in the Results section.

4.2.13 Correlation analysis with LME models

The correlation between individual-specific slopes of variables obtained from RIRS models was estimated using the Pearson correlation coefficient (Pearson [170]). Correlation diagrams were obtained between all variables using the slopes for RIRS models fitted with (i) the whole data sets and (ii) the unpooled data sets from elder and younger individuals. The circle size in each cell of the correlation diagram represents the extent of correlation between compared variables. Blue represents a positive correlation, and brown represents a negative correlation.

Further, we describe possible ways to utilize the formulated LME models for making predictions with clinical potentials.

4.2.14 Making predictions for new individuals

The fitted model estimates were utilized to predict responses in virtual individuals with diabetes. We considered three new virtual individuals (V1, V2, and V3) and assumed arbitrary but reasonable baseline measurements of GSH, 8-OHdG, and HbA1c. We thus predicted trajectories in these subjects over six months.

We make predictions for the trajectories of new virtual subjects by assuming their baseline measurements of GSH, 8-OHdG, and HbA1c using the following steps.

1. Obtain the model estimates of fixed-effects, $\hat{\beta} = (\beta_0, \beta_1, \beta_2)$, random effects and covariance parameters σ_0, σ_e .
2. Random-intercepts for new subjects estimated based on the baseline data (Y^{New}) for subjects VS1, VS2, and VS3 as

$$b_i^{New} = GZ^T V^{-1} (Y^{New} - X\hat{\beta}) \quad (4.23)$$

3. Predict the average trajectories for new subjects using the subject-specific random-effects b^{New} and design matrices, X^{Pred} and Z^{Pred} with fixed-effects and random-effects parameters, respectively, as

$$Y^{Pred} = X^{Pred}\beta + Z^{Pred}b^{New} \quad (4.24)$$

In this scheme, the baseline values assumed for virtual subjects are shrunk towards the average intercept estimated by the LME model, and the individual-

specific random effects are obtained. Further, using the model estimates of the average intercept, the random effect of the intercept, and the rate of changes in the slopes, we obtain the average linear trajectory for each virtual individual in the presence and absence of GSH supplementation.

Results obtained from the LME analysis of biochemical changes in individuals with T2D on GSH supplementation during the clinical trial are presented in the next section.

4.3 Results

4.3.1 Results from LME models

We fit RIRS and RIFS models for GSH, GSSG, 8-OHdG, HbA1c, FPG, PPG, FPI, and PPI (as described in Model parameters and fitting). These subject-wise trajectories obtained from RIRS models are shown in Figure 4.1. Individual trajectories are distributed around the group-wise average trajectory. Group-wise average intercepts are determined by β_0 ; these are equal for both D and DG. The average slopes in D and DG are β_1 and $\beta_1 + \beta_2$, respectively. This β_2 denotes the difference between the average slopes in the two groups: the treatment effect of GSH supplementation on outcomes. These estimates (β_0 , β_1 , and β_2) and estimated random effects are given in Table 4.1.

We find that β_2 is significant for GSH, GSSG, and 8-OHdG Table4.1. Among the glyceic variables, β_2 is significant only for FPI and PPI but not for HbA1c, FPG, and PPG. The mean erythrocytic GSH is estimated as 492 μM in individuals with diabetes. It increased slightly, at an average rate of 0.04 μM per month from the baseline during the study period in D. In DG, GSH increased at an average rate of 107.7 μM per month. Therefore, GSH supplementation significantly improved GSH by about 22 percent (107.7

μM , $p < 0.001$) per month relative to baseline. Mean GSSG is estimated as $221 \mu\text{M}$. In D and DG, GSSG increased at average rates of 4.7 and $17.7 \mu\text{M}$ per month, respectively, from the baseline (Figure 4.2). Thus, GSSG rates are significantly improved ($p < 0.001$) by about six percent per month of the baseline ($13.02 \mu\text{M}$, $p < 0.001$). 8-OHdG is estimated to be $442 \text{ ng}/\mu\text{g DNA}$ in diabetic individuals. It decreased in D and DG at average rates of 2.8 and $21.3 \text{ ng}/\mu\text{g DNA}$ per month, respectively. Thus the effect of GSH supplementation significantly reduced 8-OHdG by four percent per month of the baseline ($18.5 \text{ ng}/\mu\text{g DNA}$, $p < 0.001$).

HbA1c, FPG, and PPG changed at similar rates in D and DG (Figure 4.3), suggesting that the effect was negligible ($p > 0.05$). FPI and PPI are found to be affected significantly. Mean FPI is estimated as $13.4 \mu\text{U}/\text{mL}$. FPI decreased at an average rate of $0.3 \mu\text{U}/\text{mL}$ per month in D. GSH supplementation significantly improved FPI at a rate of $0.2 \mu\text{U}/\text{mL}$ in DG. The average PPI is estimated as $48.8 \mu\text{U}/\text{mL}$ in individuals with diabetes. It decreased at average rates of 0.8 and $4.9 \mu\text{U}/\text{mL}$ per month in D and DG, respectively (Figure 4.3). GSH supplementation significantly enhanced FPI by four percent ($0.5 \mu\text{U}/\text{mL}$, $p < 0.001$) and reduced PPI rates by eight percent ($4.1 \mu\text{U}/\text{mL}$, $p < 0.001$) of the baseline per month.

Results obtained from RIFS models are shown in Table 4.11 and Table 4.12. The parameter estimates of β_2 from RIFS models are also found to be significant for GSH, GSSG, 8-OHdG, FPI, and PPI, leading to similar conclusions about the effects of GSH supplementation as in RIRS models. We note that these results largely coincide with the results from previous work (Kalamkar *et al.* [134]). However, FPI and PPI, which were earlier reported not to be affected by GSH supplementation, are found to have a significant effect through the LME model-based analysis.

Variables	β_0 (SE)	β_1 (SE)	β_2 (SE)
GSH	492.2(27.4) ^{***} #	0.04 (8.6)	107.7(10.3) ^{***} #
GSSG	221(10.1) ^{***} #	4.7 (3.3)	13.02(4.2) ^{***} #
8-OHdG	442.02(7.5) ^{***} #	-2.8 (2.6)	-18.5(2.9) ^{***} #
HbA1c	8.4(0.1) ^{***} #	-0.06 (0.03)	-0.05 (0.04)
FPG	152.9(3.9) ^{***} #	-1.33 (1.09)	0.4 (1.3)
FPI	13.4(0.66) ^{***} #	-0.3(0.14)*	0.5(0.2)**
PPG	224.4(5.4) ^{***} #	-1.6 (1.6)	0.3 (2)
PPI	48.8(2.8) ^{***} #	-0.8 (0.6)	-4.1(0.6) ^{***} #

(A) Fixed-effects parameter estimates

Variables	σ_0	σ_1	σ_{01}	σ_e
<i>GSH</i>	162.3	14.1	2286.3	386.8
<i>GSSG</i>	66.3	9.4	621.3	139.6
<i>8 - OHdG</i>	55.95	17.04	-551.2	98.5
<i>HbA1c</i>	1.53	0.21	-0.17	0.96
<i>FPG</i>	46.07	8.71	-215.2	33.2
<i>FPI</i>	7.8	0.07	0.53	5.7
<i>PPG</i>	59.68	11.38	-296	51.6
<i>PPI</i>	32.54	3.31	-107.9	23.8

(B) Random-effects parameter estimates

Table 4.1: **Results from LME Model analysis** Fixed-effects and random-effects parameter values obtained by fitting LME models of RIRS form for GSH, GSSG, 8-OHdG, HbA1c, FPG, FPI, PPG, and PPI variables are presented here with standard error associated with the estimates. The fitted results from the corresponding RIFS model are shown in Table 4.11 and Table 4.12. The average treatment effects (β_2) of GSH supplementation were significant on the rate of changes (slopes) for GSH, GSSG, 8-OHdG, FPI, and PPI levels. Significance levels shown here are * $p < 0.05$, ** $p < 0.01$, *** $p < 0.001$ for respective comparisons. Statistically, significance after Bonferroni corrections are marked with # symbols here. This table is adapted from Madathil *et al.* [161], published as Table 2 in the main text and Table S2 in the supplementary data.

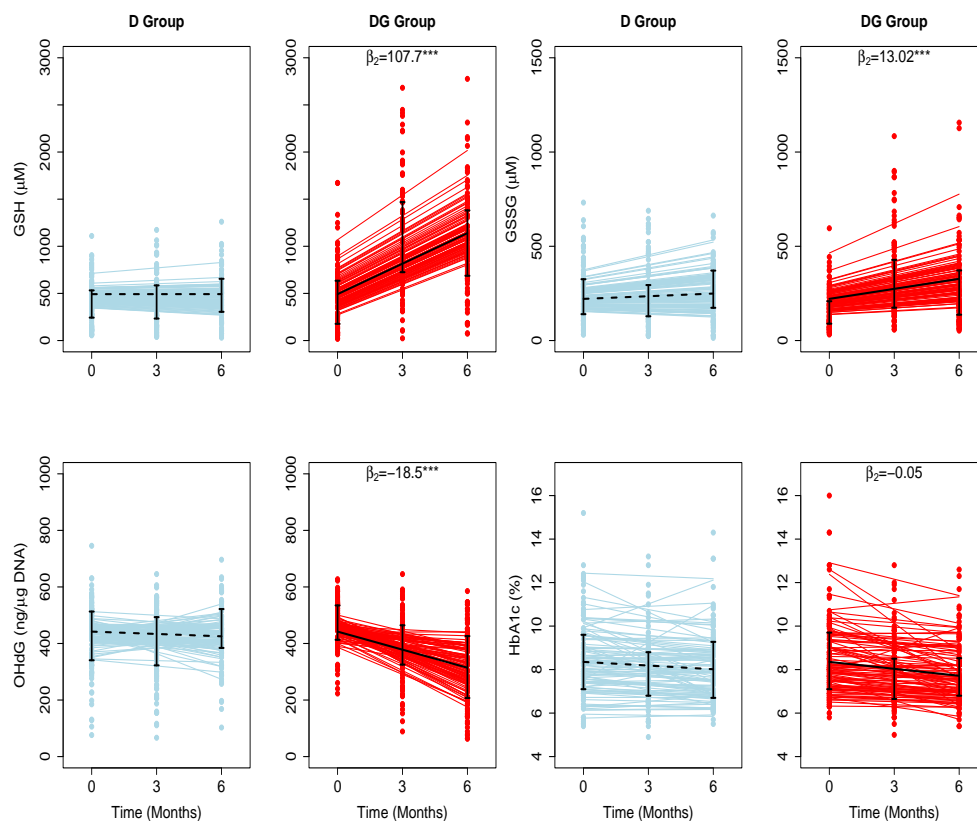


Figure 4.2: **Treatment effects of GSH supplementation on biochemical changes estimated using LME Models.** The fitted results of RIRS models for GSH, GSSG, 8-OHdG, and HbA1c in D and DG groups (figure panels marked with titles D and DG) are overlaid here with the longitudinal data from 201 individuals (100 D subjects in blue circles, 101 DG subjects in red circles) at three visits (RIFS model fits are shown in Figure 4.10). Solid blue and red lines depict the fitted subject-specific mean trajectories in the D and DG groups, respectively. The black dotted and solid lines represent the group-wise means for D and DG, respectively. Interquartile ranges of the data for D and DG groups are shown with vertical interval plots (25th-75th quartiles) at each visit. The average treatment effects of GSH supplementation (β_2) are denoted on top of each panel corresponding to the DG group. Significance of these parameter estimates are given by $*p < 0.05$, $**p < 0.01$, and $***p < 0.001$. This figure is reproduced from Madathil *et al.* [161], published as Figure 2 in the main text.

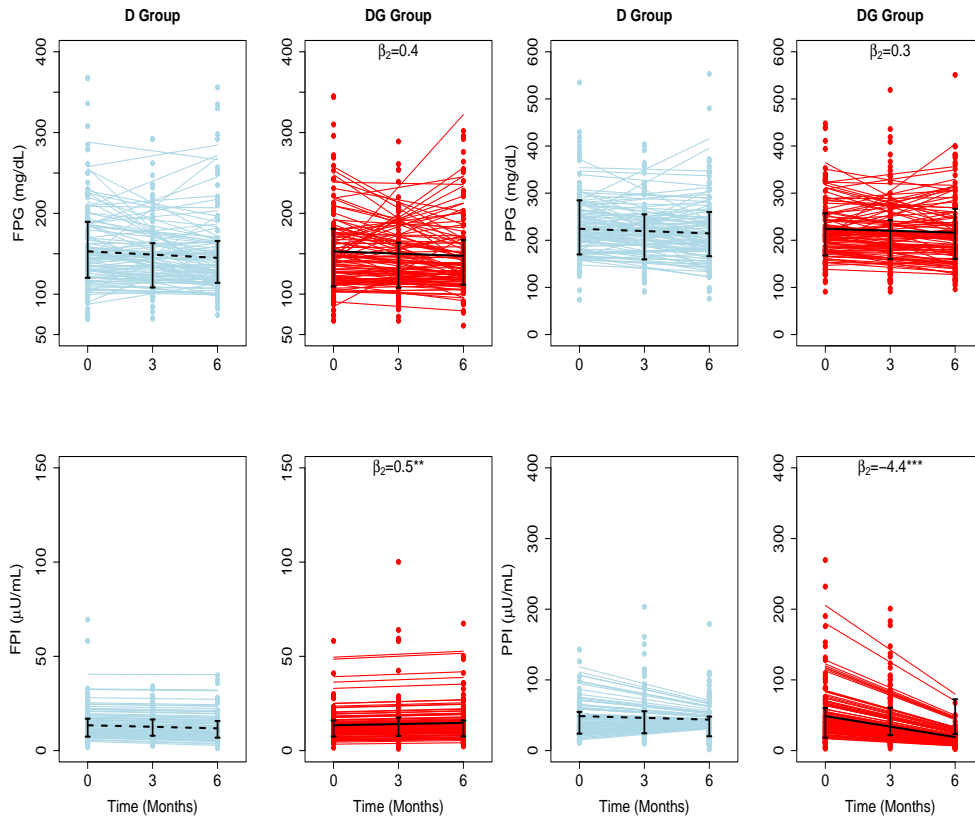


Figure 4.3: **Treatment effects of GSH supplementation on glycemia estimated using LME Models.** The fitted results of RIRS models for glycemic variables, FPG, FPI, PPG, and PPI in D and DG groups (figure panels marked with titles D and DG) are overlaid here with the longitudinal data from 201 individuals (100 D subjects in blue circles, 101 DG subjects in red circles) at three visits (RIFS model fits are shown in Figure 4.10). Solid blue and red lines depict the fitted subject-specific mean trajectories in the D and DG groups. The black dotted and solid lines represent the group-wise means for D and DG, respectively. Interquartile ranges of the data for D and DG groups are shown with vertical interval plots (25th-75th quartiles) at each visit. The average treatment effects of GSH supplementation (β_2) are denoted on top of each panel corresponding to the DG group. Significance of these parameter estimates are given by $*p < 0.05$, $**p < 0.01$, and $***p < 0.001$. This figure is reproduced from Madathil *et al.* [161], published as Figure 2 in the main text.

In the next section, we describe the results obtained from analyzing the two age classes, namely, elder and younger adults, using two independent LME models.

4.3.2 Results from the analysis of two independent age classes

Diabetes is an age-onset disease; an early diagnosis leads to an increased chance for complications to set in relatively early. We have earlier demonstrated that the effectiveness of GSH supplementation differed between the younger and elder populations using an age cutoff of 55 years, which was the median age of the study population (Kalamkar *et al.* [134]). We fit a separate LME for each of these two age groups. Model estimates obtained by fitting LME models independently for EA and YA are detailed in Table 4.2 and Table 4.3, respectively.

GSH supplementation significantly affected GSH, 8-OHdG, HbA1c, FPI, and PPI in EA, and GSH, GSSG, 8-OHdG, and PPI in YA (β_2 in Table 4.2, $p < 0.001$).

GSH: Mean erythrocytic GSH in EA (488 μM) is estimated to be less than YA (497 μM). In YA of D, GSH decreased at an average rate of 6.9 μM per month, whereas in DG, GSH increased at an average rate of 104 μM per month (Figure 4.4). In EA of D and DG, GSH increased at average rates of 6.5 and 111 μM per month, respectively (Figure 4.5). This clearly indicates that GSH supplementation resulted in a significant improvement in GSH by about 21 percent per month of their baseline in YA (111 μM , $p < 0.001$) and 22 percent per month in EA (105 μM , $p < 0.001$) with diabetes.

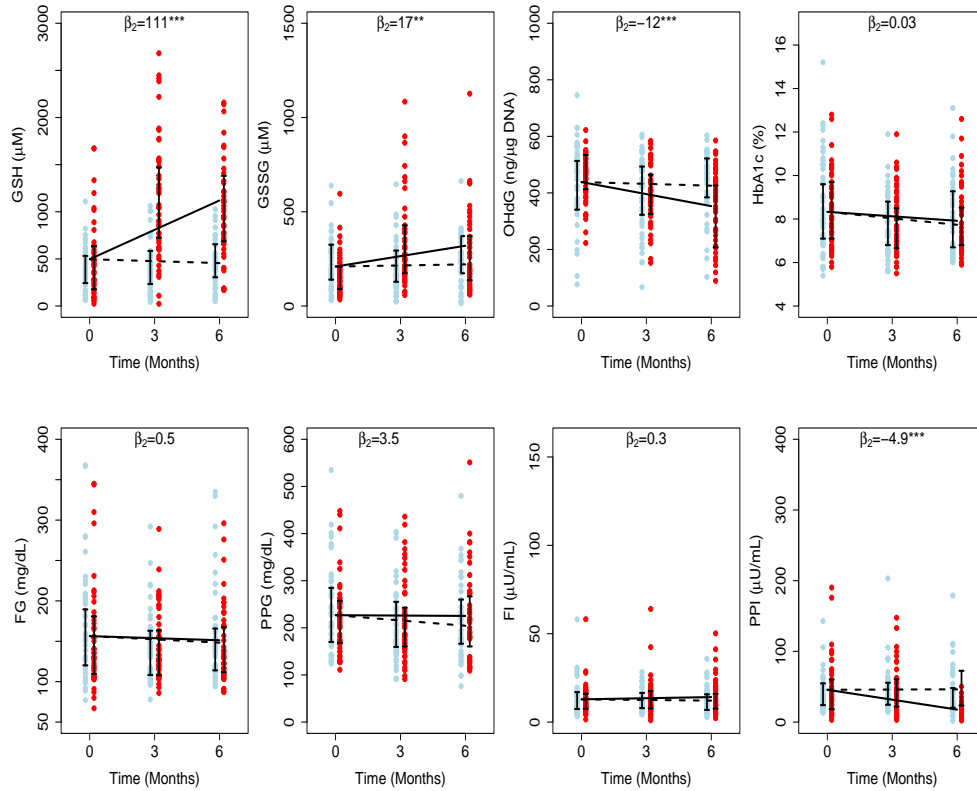


Figure 4.4: **Average treatment effects of GSH supplementation in younger diabetic subjects.** The fitted results of RIRS models for GSH, GSSG, 8-OHdG, HbA1c, FPG, FPI, PPG, and PPI variables of younger adults (YA) with diabetes are shown on different panels here with the longitudinal data (blue circles for D individuals and red circles for DG individuals) at different visits. The data from 107 elder adults (52 from D and 55 from DG) are overlaid with group-wise mean trajectories for D and DG groups represented by black dotted lines and solid lines, respectively. Interquartile data ranges for individuals (from D and DG) are shown with vertical interval plots (25th-75th quartiles) at each visit. The average treatment effects of GSH supplementation (β_2) on the rate of changes (slope) denoted on top of corresponding panels which are significant on GSH ($\beta_2 = 105\mu M$ per month), 8-OHdG ($\beta_2 = -24ng/\mu g$ DNA per month), HbA1c ($\beta_2 = -0.6\%$ per month), FPI ($\beta_2 = 0.6\mu U/mL$ per month) and PPI ($\beta_2 = -4.9\mu U/mL$ per month) levels of younger adults. Significance of these parameter estimates are given by $*p < 0.05$, $**p < 0.01$, and $***p < 0.001$. This figure is reproduced from Madathil *et al.* [161], published as Figure S2 in the supplementary data.

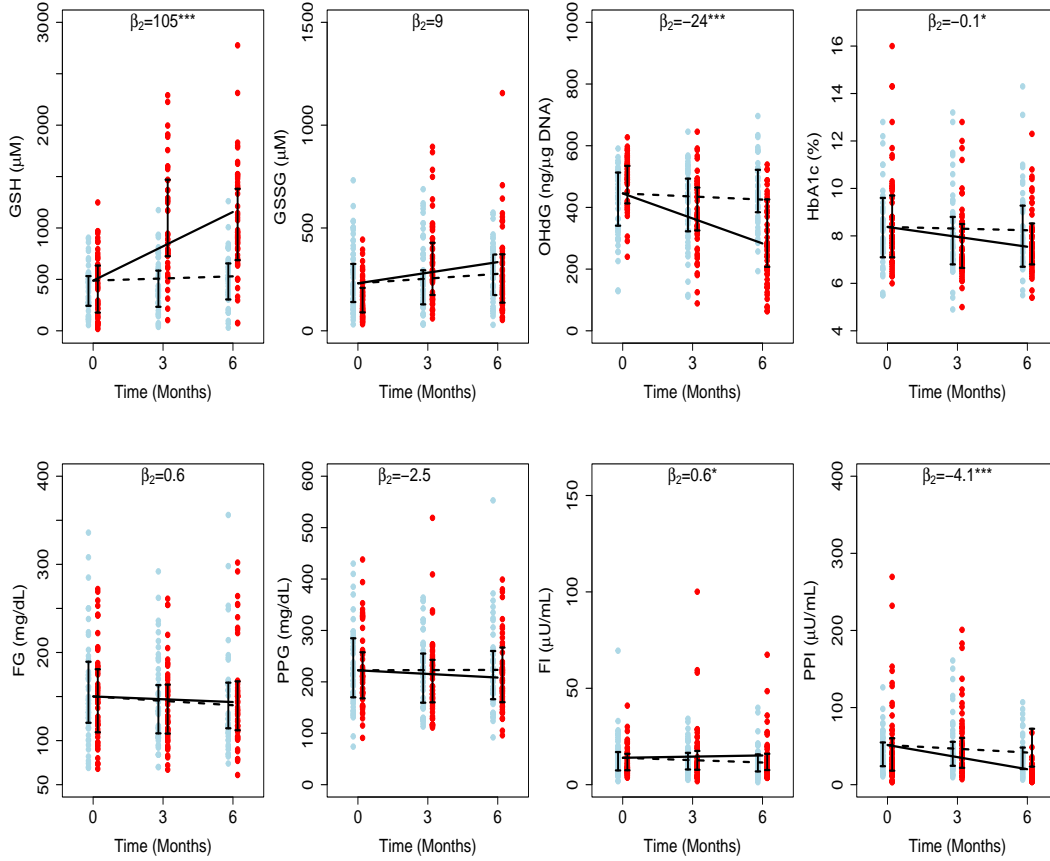


Figure 4.5: **Average treatment effects of GSH supplementation in elder diabetic subjects.** The fitted results of RIRS models for GSH, GSSG, 8-OHdG, HbA1c, FPG, FPI, PPG, and PPI variables of elder adults (EA) with diabetes are shown on different panels here with the longitudinal data (blue circles for D individuals and red circles for DG individuals) at different visits. The data from 107 elder adults (52 from D and 55 from DG) are overlaid with group-wise mean trajectories for D and DG groups represented by black dotted lines and solid lines, respectively. Interquartile data ranges for individuals (from D and DG) are shown with vertical interval plots (25th-75th quartiles) at each visit. The average treatment effects of GSH supplementation (β_2) on the rate of changes (slope) denoted on top of corresponding panels which are significant on GSH ($\beta_2 = 105\mu M$ per month), 8-OHdG ($\beta_2 = -24ng/\mu g$ DNA per month), 8-OHdG ($\beta_2 = -24ng/\mu g$ DNA per month), HbA1c ($\beta_2 = -0.1\%$ per month), FPI ($\beta_2 = 0.6\mu U/mL$ per month) and PPI ($\beta_2 = -4.1\mu U/mL$ per month) levels of younger adults. Significance of these parameter estimates are given by $*p < 0.05$, $**p < 0.01$, and $***p < 0.001$. This figure is reproduced from Madathil *et al.* [161], published as Figure 2 in the main text.

GSSG: Interestingly, the effect on GSSG was significant in YA ($p < 0.01$) but not in EA. The mean GSSG in EA (231 μM) was estimated to be higher than YA (209 μM). When YA of D and DG were examined, GSSG increased at average rates of 1.9 and 18.4 μM per month, respectively (Figure 4.4). It increased at average rates of 7.6 and 17.1 μM per month in EA of D and DG, respectively. (Figure 4.5). This shows that GSH supplementation enhanced GSSG significantly per month by eight percent of the baseline (17.5 μM , $p < 0.001$) per month only in YA.

8-OHdG: The average 8-OHdG estimate is higher in EA (445 ng/ μg DNA) than in YA (438 ng/ μg DNA). In EA of both D and DG, 8-OHdG decreased at average rates of 3.3 and 27 ng/ μg DNA per month during the study period (Figure 4.5). Similarly, it decreased at average rates of 2.1 and 14.16 ng/ μg DNA per month in the YA of D and DG groups (Figure 4.3). Thus, we find that GSH supplementation significantly reduced 8-OHdG from the baseline by 12.06 ng/ μg DNA per month (3%) in YA and 23.7 ng/ μg DNA per month (5%) in EA. These results suggest that oral GSH administration rapidly offers better protection from oxidative DNA damage in EA compared to YA.

HbA1c: GSH supplementation was earlier reported to affect the HbA1c in the elder cohort significantly (Kalamkar *et al.* [134]). We examined LME estimates of both YA and EA to quantify the effect on HbA1c. The average HbA1c is estimated at 8.3% and 8.4% in YA and EA, respectively. In EA of D, HbA1c decreased at an average rate of 0.02% per month, while in DG, it decreased at an average rate of 0.12% per month (Figure 4.5), suggesting that GSH supplementation improved HbA1c rates significantly by about 0.1% per month in EA. Estimated HbA1c rates are not significantly different between

YA of D and DG (Figure 4.4).

Fasting Insulin: Our earlier work [134] found that oral GSH supplementation significantly changed FPI in elder patients. We quantitated the effect on FPI using LME model estimates (Table 4.2). The average FPI is estimated to be 12.9 $\mu\text{U}/\text{mL}$ in YA and 14 $\mu\text{U}/\text{mL}$ in EA. In both EA and YA of D, FPI decreased at rates of 0.4 $\mu\text{U}/\text{mL}$ and 0.1 $\mu\text{U}/\text{mL}$ per month, respectively (Figure 4.5). The estimated rates were similar between the YA of the D and DG, indicating that the effect on FPI is negligible ($p > 0.05$). On the other hand, in EA of DG, FPI increased at a rate of 0.2 $\mu\text{U}/\text{mL}$ per month, suggesting that GSH supplementation improved FPI rates significantly by 0.6 $\mu\text{U}/\text{mL}$ per month. FPI increased by 4.3 % of the baseline per month in EA and negligibly in YA.

Postprandial Insulin: Using LME models to fit the data, PPI was found to decrease in both YA and EA. The average PPI in YA and EA is estimated to be 46 and 51 $\mu\text{U}/\text{mL}$, respectively. In YA of D, PPI increased at a rate of 0.1 $\mu\text{U}/\text{mL}$ per month, whereas in DG, it decreased at a rate of 4.7 $\mu\text{U}/\text{mL}$ per month. PPI decreased at average rates of 1.6 $\mu\text{U}/\text{mL}$ and 5.2 $\mu\text{U}/\text{mL}$ per month in EA of D and DG, respectively.

Fasting and Postprandial Glucose: The average FPG estimated in YA and EA are 156 and 150 mg/dL, respectively. In both YA and EA, the GSH supplementation effect wasn't found to be significant. In both EAs of D and DG, FPG decreased at average rates of 1.7 and 0.9 mg/dL per month, respectively. Similarly, YAs of D and DG decreased at average rates of 1.3 and 0.8 mg/dL per month, respectively. PPG estimated in YA and EA at the

time of recruitment is 227 and 223 mg/dL, respectively. GSH supplementation decreased PPG by 2.5 mg/dL per month in EAs and increased PPG by 3.5 mg/dL per month in YA.

Variable	Fixed effect parameters (YA)		
	β_0 (SE)	β_1 (SE)	β_2 (SE)
GSH	496.6(44.9) ^{***} #	-6.9 (13.07)	111(15.3) ^{***} #
GSSG	209.4(14.03) ^{***} #	1.9 (4.9)	16.5(6.2) ^{**}
8-OHdG	438.3(11) ^{***} #	-2.1 (3.6)	-12.06(4.2) ^{**} #
HbA1c	8.3(0.2) ^{***} #	-0.1(0.04) [*]	0.03(0.06)
FPG	156.4(5.9) ^{***} #	-1.3 (1.8)	0.5(2.1)
FPI	12.9(0.9) ^{***} #	-0.12 (0.15)	0.3(0.2)
PPG	226.8(8.3) ^{***} #	-3.7 (2.5)	3.5(3.1)
PPI	45.7(3.3) ^{***} #	0.1 (0.7)	-4.8(0.9) ^{***} #

Table 4.2: **Results from LME models for younger adults** The fixed-effect parameter values were obtained by fitting the data from the subgroup of younger adults (YA) using the RIRS models for GSH, GSSG, 8-OHdG, HbA1c, FPG, FPI, PPG, and PPI variables are shown here with the standard errors (SE). The average treatment effects (β_2) of GSH supplementation are significant on GSH, GSSG, 8-OHdG, and PPI levels for YA. Significance levels shown here are ^{*} $p < 0.05$, ^{**} $p < 0.01$, ^{***} $p < 0.001$ for respective comparisons. Statistical significance continued after Bonferroni corrections were marked with # symbols here. This table is adapted from Madathil *et al.* [161], published as Table S4 in the supplementary data.

Next, we describe the results obtained from different LME models for analyzing the age effects on the observed biochemical changes during the clinical trial.

4.3.3 Results from analyzing age effects

For exploratory purposes, we also analyzed the effects of the age using new candidate models as incorporated with age as a model variable (Model 2, Model 3, and Model 4) for GSH, GSSG, 8-OHdG, HbA1c, FPG, FPI, PPG, and PPI. Results obtained by fitting with these models are shown in Table 4.4,

Variable	Fixed effect parameters (EA)		
	β_0 (SE)	β_1 (SE)	β_2 (SE)
GSH	488.1(33.4) ^{***} #	6.5 (11.5)	104(14.05) ^{***} #
GSSG	231(14.5) ^{***} #	7.6 (4.5)	9.5 (5.6)
8-OHdG	445.3(10.2) ^{***} #	-3.3 (3.5)	-23.7(3.9) ^{***} #
HbA1c	8.4(0.2) ^{***} #	-0.02 (0.04)	-0.1(0.05) [*]
FPG	150.1(5.2) ^{***} #	-1.7 (1.2)	0.6 (1.6)
FPI	14(1.002) ^{***} #	-0.4 (0.2)	0.6(0.3) [*]
PPG	222.5(6.9) ^{***} #	0.14 (1.97)	-2.5 (2.4)
PPI	51.4(4.3) ^{***} #	-1.6(0.82) [*]	-3.6(0.77) ^{***} #

Table 4.3: **Results from LME models for elder adults.** The fixed-effect parameter values were obtained by fitting the data from the subgroup of elder adults (EA) using the RIRS models for GSH, GSSG, 8-OHdG, HbA1c, FPG, FPI, PPG, and PPI variables are shown here with the standard errors (SE). The average treatment effects (β_2) of GSH supplementation are significant on GSH, 8-OHdG, HbA1c, FPI, and PPI levels for EA. Significance levels shown here are ^{*} $p < 0.05$, ^{**} $p < 0.01$, ^{***} $p < 0.001$ for respective comparisons. Statistical significance continued after Bonferroni corrections were marked with # symbols here. This table is adapted from Madathil *et al.* [161], published as Table S4 in the supplementary data.

Table 4.5, and Table 4.6. When we compared model fits from all four models using AIC and BIC estimates, our original RIRS model (Model 1) was found to be the better-fit model for all variables (Table 4.7, Table 4.8).

Variable	Fixed effect parameters		
	β_0 (SE)	β_1 (SE)	β_2 (SE)
GSH	492.1(27.5) ^{***} #	3.4 (8.5)	1.9(0.2) ^{***} #
GSSG	221(10.1) ^{***} #	5.1 (3.2)	0.2(0.07) ^{**}
8-OHdG	442(7.5) ^{***} #	-2.5 (2.5)	-0.3(0.05) ^{***} #
HbA1c	8.4(0.1) ^{***} #	-0.05 (0.03)	-1.05 (0.0006)
FPG	152.9(3.9) ^{***} #	-1.1 (1.07)	2(0.02)
FPI	13.4(0.7) ^{***} #	-0.3(0.13) [*]	0.008(0.003) ^{**}
PPG	224.4(5.4) ^{***} #	-1.2 (1.5)	-0.009 (0.03)
PPI	48.8(2.8) ^{***} #	-1 (0.6)	-0.07(0.01) ^{***} #

Table 4.4: **Results from Model 2 for analyzing age-effects.** The fixed-effect parameter values were obtained by fitting Model 2 for GSH, GSSG, 8-OHdG, HbA1c, FPG, FPI, PPG, and PPI variables are shown here with the standard errors (SE). Significance levels shown here are ^{*} $p < 0.05$, ^{**} $p < 0.01$, ^{***} $p < 0.001$ for respective comparisons. Statistical significance continued after Bonferroni corrections were marked with # symbols here. This table is adapted from Madathil *et al.* [161], published as Table S5 in the supplementary data.

Results obtained from the correlation analysis of slopes from the fitted LME models are discussed next.

4.3.4 Results of correlation analysis with LME models

We estimated pairwise correlations between subject-specific slopes of GSH, GSSG, 8-OHdG, HbA1c, FPG, FPI, PPG, and PPI obtained from RIRS models. These correlation diagrams for the full population (pooled data) are shown in Figure 4.6. Changes in GSH are found to be strongly correlated positively with GSSG ($r > 0.6$) and FPI ($r > 0.9$). Changes in GSH correlated negatively with 8-OHdG and PPI ($r < -0.6$). The other correlations are found to be relatively weaker.

Variable	Fixed effect parameters			
	β_0 (SE)	β_1 (SE)	β_2 (SE)	β_3 (SE)
GSH	492.2(27.4) ^{***} #	-0.03 (8.6)	82.1(38.5) [*]	0.5 (0.7)
GSSG	221(10.1) ^{***} #	4.7 (3.3)	9.7(15.6)	0.06 (0.3)
8-OHdG	442(7.5) ^{***} #	-2.7 (2.5)	3.9(10.8) ^{***} #	-0.4(0.2) [*]
HbA1c	8.4(0.1) ^{***} #	-0.06 (0.03)	0.1 (0.14)	-0.003 (0.002)
FPG	152.9(3.9) ^{***} #	-1.3 (1.1)	5.5 (4.9)	-0.09 (0.09)
FPI	13.4(0.7) ^{***} #	-0.3(0.13) [*]	0.2 (0.7)	0.005 (0.01)
PPG	224.4(5.4) ^{***} #	-1.6 (1.6)	10.7 (7.3)	-0.2 (0.1)
PPI	48.8(2.8) ^{***} #	-0.8 (0.6)	-3.8 (2.1)	-0.007 (0.04)

Table 4.5: **Results from Model 3 for analyzing age-effects** The fixed-effect parameter values were obtained by fitting Model 3 for GSH, GSSG, 8-OHdG, HbA1c, FPG, FPI, PPG, and PPI variables are shown here with the standard errors (SE). Significance levels shown here are ^{*} $p < 0.05$, ^{**} $p < 0.01$, ^{***} $p < 0.001$ for respective comparisons. Statistical significance continued after Bonferroni corrections were marked with # symbols here. This table is adapted from Madathil *et al.* [161], published as Table S5 in the supplementary data.

Variable	Fixed effect parameters			
	β_0 (SE)	β_1 (SE)	β_2 (SE)	β_3 (SE)
GSH	492.2(27.4) ^{***} #	0.08 (8.6)	110.8(12.2) ^{***} #	104(12.9) ^{***} #
GSSG	221(10.1) ^{***} #	4.7 (3.3)	13.7(4.9) ^{**}	12.2(5.2) [*]
8-OHdG	442(7.5) ^{***} #	-2.6 (2.5)	-24.5(3.4) ^{***} #	-12.2(3.6) ^{***} #
HbA1c	8.4(0.1) ^{***} #	-0.06 (0.03)	-0.08 (0.04)	-0.01 (0.05)
FPG	152.9(3.9) ^{***} #	-1.3 (1.09)	-0.19 (1.6)	1.1 (1.7)
FPI	13.4(0.7) ^{***} #	-0.3(0.1) [*]	0.4(0.2) [*]	0.5(0.2) [*]
PPG	224.4(5.4) ^{***} #	-1.6 (1.6)	-1 (2.3)	1.7 (2.4)
PPI	48.8(2.8) ^{***} #	-0.8 (0.6)	-4.1(0.7) ^{***} #	-4.2(0.7) ^{***} #

Table 4.6: **Results from Model 4 for analyzing age-effects** The fixed-effect parameter values were obtained by fitting Model 4 for GSH, GSSG, 8-OHdG, HbA1c, FPG, FPI, PPG, and PPI variables are shown here with the standard errors (SE). Significance levels shown here are ^{*} $p < 0.05$, ^{**} $p < 0.01$, ^{***} $p < 0.001$ for respective comparisons. Statistical significance continued after Bonferroni corrections were marked with # symbols here. This table is adapted from Madathil *et al.* [161], published as Table S5 in the supplementary data.

Variable	AIC			
	Model 1	Model 2	Model 3	Model 4
GSH	8870.5	8874.5	8872	8872.3
GSSG	7718.1	7718.4	7720	7720
8-OHdG	7331.1	7326.6	7328.5	7323.8
HbA1c	2149	2148.2	2149.7	2149.3
FPG	6323	6323.1	6323.9	6324.5
FPI	4139.6	4139.5	4141.4	4141.5
PPG	6740.8	6740.8	6740.6	6741.8
PPI	5708.9	5712	5710.9	5710.9

Table 4.7: Comparison between four models for studying age-effects (Model 1, Model 2, Model 3, and Model 4) using their AIC estimates. Model 1 was found to be the better-fit model across all eight endpoints. This table is adapted from Madathil *et al.* [161], published as Table S5 in the supplementary data.

Variable	BIC			
	Model 1	Model 2	Model 3	Model 4
GSH	8901.2	8905.2	8907.1	8907.3
GSSG	7748.8	7749.1	7755.1	7755.1
8-OHdG	7361.8	7357.3	7363.6	7358.9
HbA1c	2179.7	2178.9	2184.8	2184.4
FPG	6353.7	6353.8	6359	6359.6
FPI	4170.3	4170.1	4176.4	4176.6
PPG	6771.5	6771.4	6775.6	6776.9
PPI	5739.6	5742.6	5745.9	5745.9

Table 4.8: Comparison between four models to study age-effects (Model 1, Model 2, Model 3, Model 4) using their BIC estimates. Model 1 was found to be the better-fit model across all eight endpoints. This table is adapted from Madathil *et al.* [161], published as Table S5 in the supplementary data.

Correlation plots for EAs alone are shown in Figure 4.7. GSH slopes are strongly negatively correlated with 8-OHdG slopes ($r = -0.71$) and HbA1c slopes at moderate levels ($r = -0.43$). GSH slopes are strongly negatively correlated with PPI slopes ($r = -0.74$, Figure 4.7); however, they are strongly positively correlated with FPI ($r = 0.75$). In YAs (Figure 4.8), GSH slopes are negatively correlated at moderate levels with 8-OHdG ($r = -0.43$) and PPI ($r = -0.57$) slopes. The correlation between GSH slopes and HbA1c slopes is negligibly small. Taken together, the strengths of the correlations between the changes in GSH and outcome variables are evidently different between EAs and YAs. We next use LME model estimates to help quantify the overall rates of changes that individuals can expect.

We further present the results of sample predictions made with LME models for virtual individuals.

4.3.5 Predictions for virtual individuals

We make sample predictions obtained for three virtual individuals (V1, V2, and V3) using RIFS models. Baseline values assumed for these virtual individuals are given in Table 4.9.

SubID	V1	V2	V3
GSH (μM)	200	500	10
8-OHdG (ng/ μg DNA)	500	400	8
HbA1c (%)	800	300	6

Table 4.9: The baseline values of three virtual subjects (VS1, VS2, and VS3) assumed for predictions. This table is adapted from Madathil *et al.* [161], published as Table 3 in the main text.

The trajectories of GSH, 8-OHdG and HbA1c obtained if they were with or without GSH supplementation are shown in Figure 4.9. RIFS models predicted

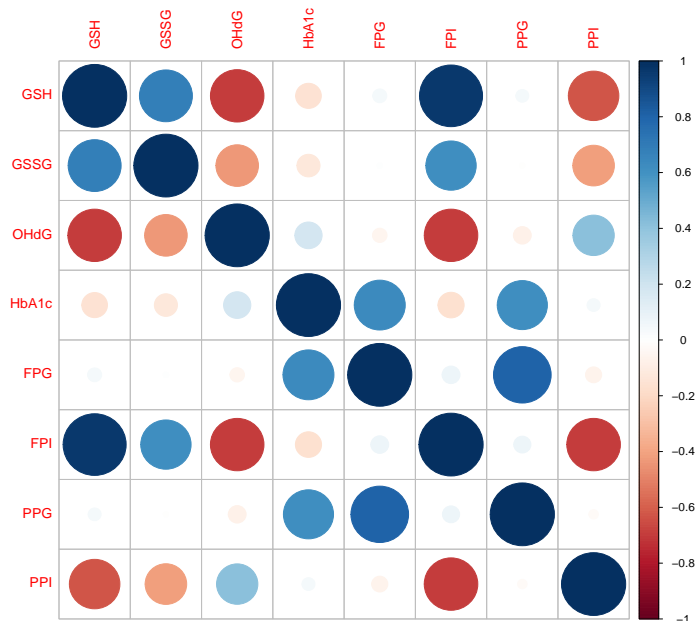


Figure 4.6: The correlation diagrams obtained between subject-specific random slopes from fitted RIRS models for different biochemical measures (GSH, GSSG, 8-OHdG, HbA1c, FPG, FPI, PPG, and PPI) are shown here. The strength and direction of correlation between subject-specific slopes are reflected in both the color and size of the circular markers. The scales of Pearson’s correlation coefficient have been classified as low ($r < 0.4$), moderate ($r < 0.6$), strong ($r > 0.6$), or very strong ($r > 0.8$). Blue indicates a strong positive correlation, and red indicates a strong negative correlation. This figure is reproduced from Madathil *et al.* [161], published as Figure 3 in the main text.

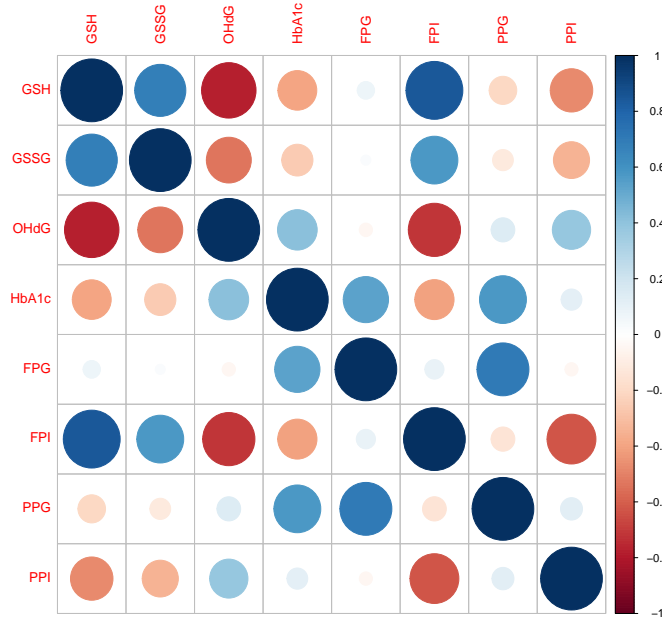


Figure 4.7: Correlation diagram between subject-specific random slopes fitted for outcome measures in elder diabetic subjects. The strength and direction of correlation between subject-specific slopes are reflected in both the color and size of the circular markers. The scales of Pearson's correlation coefficient have been classified as low ($r < 0.4$), moderate ($r < 0.6$), strong ($r > 0.6$), or very strong ($r > 0.8$). Blue indicates a strong positive correlation, and red indicates a strong negative correlation. This figure is reproduced from Madathil *et al.* [161], published as Figure 3 in the main text.

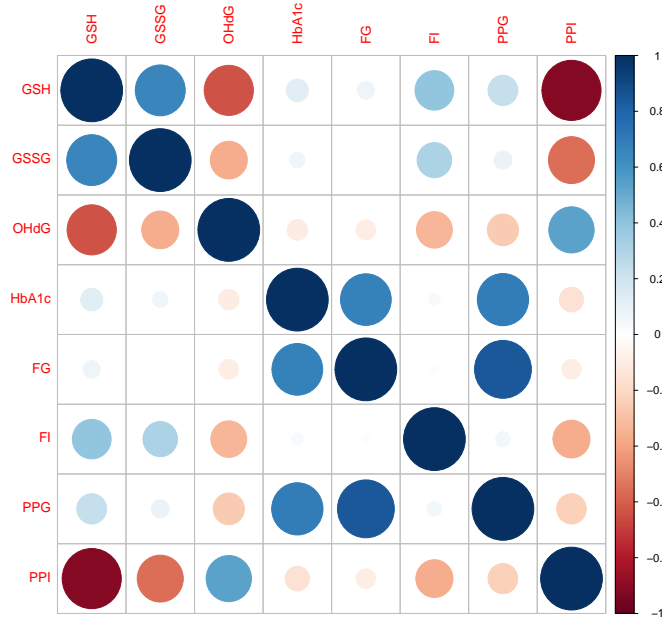


Figure 4.8: Correlation diagram between subject-specific random slopes fitted for outcome measures in younger diabetic subjects. The strength and direction of correlation between subject-specific slopes are reflected in both color and size of the circular markers. The scales of Pearson's correlation coefficient have been classified as low ($r < 0.4$), moderate ($r < 0.6$), strong ($r > 0.6$), or very strong ($r > 0.8$). Blue indicates a strong positive correlation, and red indicates a strong negative correlation. This figure is reproduced from Madathil *et al.* [161], published as Figure S3 in the supplementary data.

the GSH of V1 close to $429 \mu\text{M}$ by the end of 6 months, whereas, on GSH supplementation, V1 ended up at $1079 \mu\text{M}$. Similar predictions were made for 8-OHdG and HbA1c for all these individuals (Figure 4.9). This can also be modified to estimate (i) the average time required for a recruited individual to reach a particular level of a biochemical parameter given the baseline value and (ii) the expected change in the level of a particular biochemical parameter with time. Finding a patient’s potential trajectory has direct clinical and academic uses. This method, therefore, can be used on newly added subjects to predict different outcomes during six months, with or without GSH supplementation.

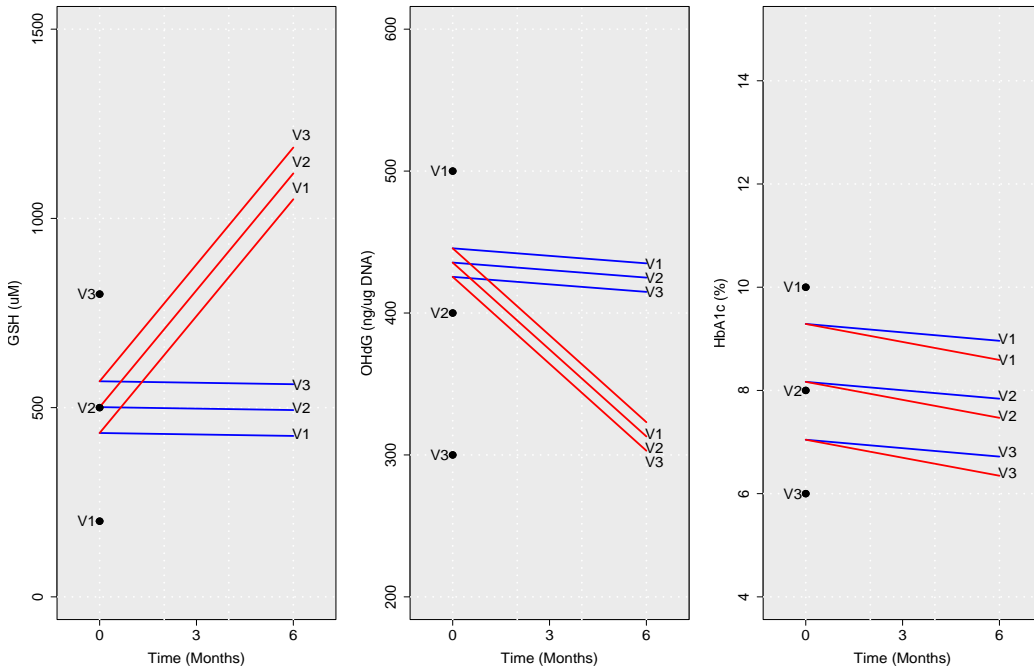


Figure 4.9: **Model predictions for virtual individuals.** Average trajectories of the concentration of (A) GSH, (B) 8-OHdG, and (C) HbA1c predicted using RIFS models in virtual individuals (V1, V2, and V3) if they were to be followed up with GSH supplementation (red) and without GSH supplementation (blue) are shown for six months are depicted here. The baseline values assumed and values predicted after six months are also marked for V1, V2, and V3. This figure is reproduced from Madathil *et al.* [161], published as Figure 4 in the main text.

4.4 Discussion

Results from our clinical trial in the **Chapter 3** demonstrated population-level changes in GSH, GSSG, HbA1c, 8-OHdG, FPG, FPI, PPG, and PPI; these changes were further studied for younger and elder subgroups of the patients. The response in individual patients is, unsurprisingly, considerably varied; however, analyzing individual responses was beyond the scope of that study. This chapter focused on studying individual-level responses to GSH supplementation over the full study period of six months using mixed-effects models. The major results here are to characterize the variability in the inter-individual biochemical response, in particular, determined by an individual's age group. To the best of our knowledge, this is the first inter-individual analysis of the effects of GSH supplementation in patients with diabetes.

The response to GSH supplementation was analyzed in the previous chapter by comparing 6-month changes in D and DG groups through population-level Cohen's-d-based estimates. GSH supplementation significantly affected GSH, GSSG, and 8-OHdG levels (at moderate levels of Cohen's $d > 0.6$) and not for HbA1c, FPG, FPI, and PPG variables. The LME model framework helped analyze biochemical responses longitudinally and obtain more refined estimates for inter-individual and within-individual variations at two levels of hierarchy. We note that LME models describe linear trajectories over a six-month duration. The estimates show that D and DG average trajectories lie between the 25th and 75th percentiles of the data at all visits; these models are a good description of the data. Model estimates were consistent with the effect size estimates in the study Kalamkar *et al.* [134] for GSH, GSSG, 8-OHdG, HbA1c, FPG, FPI, and PPG variables but not for PPI. LME estimates determined that the GSH supplementation markedly enhanced the rate of replenishments in erythrocytic GSH stores by about 22%, GSSG stores by

about 6%, and reduced oxidative DNA damage by about 4% of the baseline month in diabetic patients. Importantly, these estimates are in the actual (not relative) physical units and are, therefore, directly interpretable for use in clinical applications.

We identified an older subgroup separate from a younger diabetic population that benefits better from GSH supplementation through a post hoc subgroup analysis in our previous chapter. That clinical study was not pre-designed to evaluate this analysis explicitly, and as such, it was a weaker form of evidence. LME models provided a formal way of comparing their differential responses; two independent models described the responses in each age class. GSH supplementation improved the rates of 8-OHdG and HbA1c reduction in elder diabetic individuals more than in younger diabetic cohorts. LME models estimated the effect to be significant for FPI in elderly patients, supporting our claims of a beneficial elder cohort. Model estimates for GSSG suggested a significant effect of GSH supplementation in younger patients (by 17 μ M per month) but not in elder ones. In contrast to the earlier results, PPI model estimates were found to be significant in both elder and younger cohorts. Thus, our model-based analysis describes the extent to which diabetic patients above 55 can be expected to benefit from GSH supplementation. LME model estimates further allow for examining the strength of the association between covariates. The results of the correlation analysis show to what extent GSH intervention improves erythrocytic GSH stores and reduces DNA damage. Estimates from the elder and younger individuals also revealed that GSH changes were correlated strongly with changes in HbA1c and 8-OHdG in elder adults.

Finally, we have formulated a scheme that makes individual-specific predictions for newly recruited subjects with diabetes, given a baseline measurement by using the LME model estimates of the fixed-effects and random-effects pa-

rameters. In particular, this scheme can be utilized to predict what changes might be expected in the biochemical levels. Alternatively, the average time required for a recruited patient to reach a particular range of biochemical parameters in diabetic subjects can be estimated. The fitted LME model estimates can be used to identify the extent of each subject's response, whether they are in a better or worse condition than the average population response (Kirkman *et al.* ([171], Inzucchi *et al.* [48]). These schemes are of direct clinical and academic use to predict prospective trajectories, which can be a powerful addition to the clinician's toolbox.

The strengths of these results include that it is based on the data available from diabetic individuals on a well-conducted, randomized control trial, which is one of the most extensive GSH supplementation studies so far. Using LME models, we evaluated the individual trajectories and associated variations within and between individuals, which has yet to be done before in GSH intervention studies.

It is particularly important to remember that our understanding of the results is based on the uncorrected p-values. The practice of correcting for multiple comparisons has been a topic of debate among statisticians for several years now. Various opinions were found in the literature in opposition regarding the conditions under which a correction for multiple testing should be applied. We note that several highly cited reports over the years (Poole [172], Perneger [173], Cabin and Mitchell [174]) recommend dismissing the usage of corrections with multiple comparisons. It was shown that trying to reduce the rate of false positives (Type I error) for null associations often leads to an increase in the rate of false negatives (Type II error) for those that are not null (Rothman [175]). Also, these comparisons were often complained of being unnecessarily conservative, making this approach frequently fail to iden-

tify actual differences. However, for the interest of all readers, we have also incorporated significance levels after corrections for each comparison. Those readers who prefer statistically corrected results should follow the corresponding tables to determine which findings still retain significance and which did not after correction for multiple comparisons.

We had earlier identified the differential effects of GSH supplementation in elder and younger subgroups (Kalamkar *et al.* [134]). This study analyzed the longitudinal responses of GSH supplementation observed in these subgroups of diabetic individuals rigorously with a framework of the LME models. The subgroup of subjects above the median age of 55 years is consistent with previous studies that show an increased risk of diabetes-related complications in individuals around this age. Several organizations have already developed guidelines specific to, or including, older adults on their annual Standards of Medical Care in Diabetes (ADA [84]). These reports also discuss the severity of diabetes complications in elders and the lack of high-level evidence on the effectiveness of different medications in diabetics. We think the onset of diabetes and complications should be addressed differently for elder and younger diabetic individuals, and treatments need to be planned separately from each other. The two independent LME models formulated for analyzing the longitudinal trajectories of elder, and younger adults provided estimates of the treatment effect of GSH supplementation on each endpoint separately. This helps identify their extent of recovery and examine whether individuals are in a better or worse condition than the average profile in these subgroups on GSH supplementation for direct clinical use. We recommend planning large-scale clinical trials to examine these insights about GSH supplementation, especially in elder diabetic individuals. This could help in establishing novel benchmarks for caring for elder patients with diabetes. We have also ana-

lyzed different possible models to study the effect of the age of individuals on GSH supplementation. This will form the basis and motivate a number of future studies to examine many of the finer nuances of the effect of age on supplementation.

Although anti-diabetic treatments were not changed during the study period, patients used different medication types. We have not analyzed the complexity of the different combinations of all treatments further due to a lack of sufficient statistical power for such analysis. This we point out as a limitation of the clinical study. However, we have provided the results of LME analysis on two major subgroups of the study, individuals with Biguanides alone and (ii) Biguanides and Sulphonylureas treatment. It is possible that future work and larger clinical trials may uncover if GSH supplementation is particularly more effective with certain treatments than others. The results presented here can be the basis for future GSH intervention studies that advance precision diabetes research.

With the available three-point dataset, we designed our approaches to understand the effect of GSH supplementation on the observed biochemical changes. A preliminary effect size analysis was carried out earlier in Chapter 3, using the data from the baseline visit and visit after six months to estimate the size of the effects at the population level. In this chapter, we used LME (linear mixed-effects) models to study the dynamics of longitudinal biochemical changes. The LME framework allowed us to estimate GSH supplementation effects after accounting for inter- and intra-individual variability in the observed changes. LME framework-based analysis adequately captured the average trend in the trajectories of different study groups and subject-specific trajectories. The correlation estimates from model-fitted biochemical parameters provided stronger evidence of the effect of GSH supplementation.

In summary, the three-point data was sufficient for the analysis designed to address the goals of this study.

However, we think that if more measurements were available in addition to the three-point datasets, it would have been beneficial for achieving the personalization goals of GSH supplementation. Analyzing more frequent measurements in addition to the available datasets may be for longer durations could unravel the nonlinearities associated with the biochemical changes resulting from GSH supplementation. For instance, the biochemical changes driven by several enzymes and other key players in the system follow Michaelis Menten-like kinetics. In addition to that, the thesis has already discussed various covariates influencing the effects of GSH supplementation. So, by employing Nonlinear Mixed Effects Modeling frameworks on rich longitudinal datasets, we might gain deeper insights into the dynamics associated with the biochemical changes and these interaction effects of covariates, ultimately aiding in the pursuit of personalized GSH therapy objectives.

4.5 Appendix

4.5.1 Sample structure of the data for LME analysis

Subject ID	Time	Groups	Age	Y (eg: GSH in μM)
1	0	0	56	408
1	3	0	56	860
1	6	0	56	608
..
..
102	0	0	48	434
102	3	0	48	655
102	6	0	48	533
103	0	1	55	..
103	3	1	55	..
103	6	1	55	..
..
..
206	0	1	47	..
206	3	1	47	..
206	6	1	47	..

Table 4.10: **The structure of sample data from D and DG groups.** The available data consists of measurements from 102 subjects in D and 104 subjects in DG on three visits during the study period (0, 3, and 6 months of the study). The Group IDs for subjects in D and DG are encoded as 0 and 1. The models are fitted using these data sets. This table is adapted from Madathil *et al.* [161], published as Table S1 in the supplementary data.

4.5.2 Results of RIFS models

Results from RIFS models are shown below.

Variable	Fixed effect parameters		
	β_0 (SE)	β_1 (SE)	β_2 (SE)
GSH	492.2(28.9) ^{***} #	-0.2 (8.4)	108.2(9.8) ^{***} #
GSSG	221(11.3) ^{***} #	4.9 (3.1)	12.7(3.8) ^{***} #
8-OHdG	441.9(7.7) ^{***} #	-2.04 (2.3)	-19.8(2.6) ^{***} #
HbA1c	8.4(0.1) ^{***} #	-0.06 (0.03)	-0.05 (0.04)
FPG	152.9(3.7) ^{***} #	-1.3 (0.95)	0.46 (1.2)
FPI	13.4(0.7) ^{***} #	-0.3 (0.13)	0.48(0.2) ^{**} #
PPG	224.4(5.4) ^{***} #	-1.6 (1.4)	0.37 (1.7)
PPI	48.8(2.3) ^{***} #	-0.7 (0.6)	-4.4(0.7) ^{***} #

Table 4.11: The estimated fixed effect parameters obtained by fitting RIFS models are given here. Significance of parameter estimates are given by $*p < 0.05$, $**p < 0.01$, and $***p < 0.001$. Statistical significance continued after Bonferroni corrections marked with # symbols. This table is adapted from Madathil *et al.* [161], published as Table S3 in the supplementary data.

Variable	Random-effect parameters	
	σ_0	σ_e
GSH	200.9	389.9
GSSG	91.82	142.8
8-OHdG	40.35	110.6
HbA1c	1.27	1.15
FPG	35.95	42.17
FPI	8.01	5.7
PPG	50.68	61.72
PPI	22	25.86

Table 4.12: The estimated random effects parameters obtained by fitting RIFS models are given here. This table is adapted from Madathil *et al.* [161], published as Table S3 in the supplementary data.

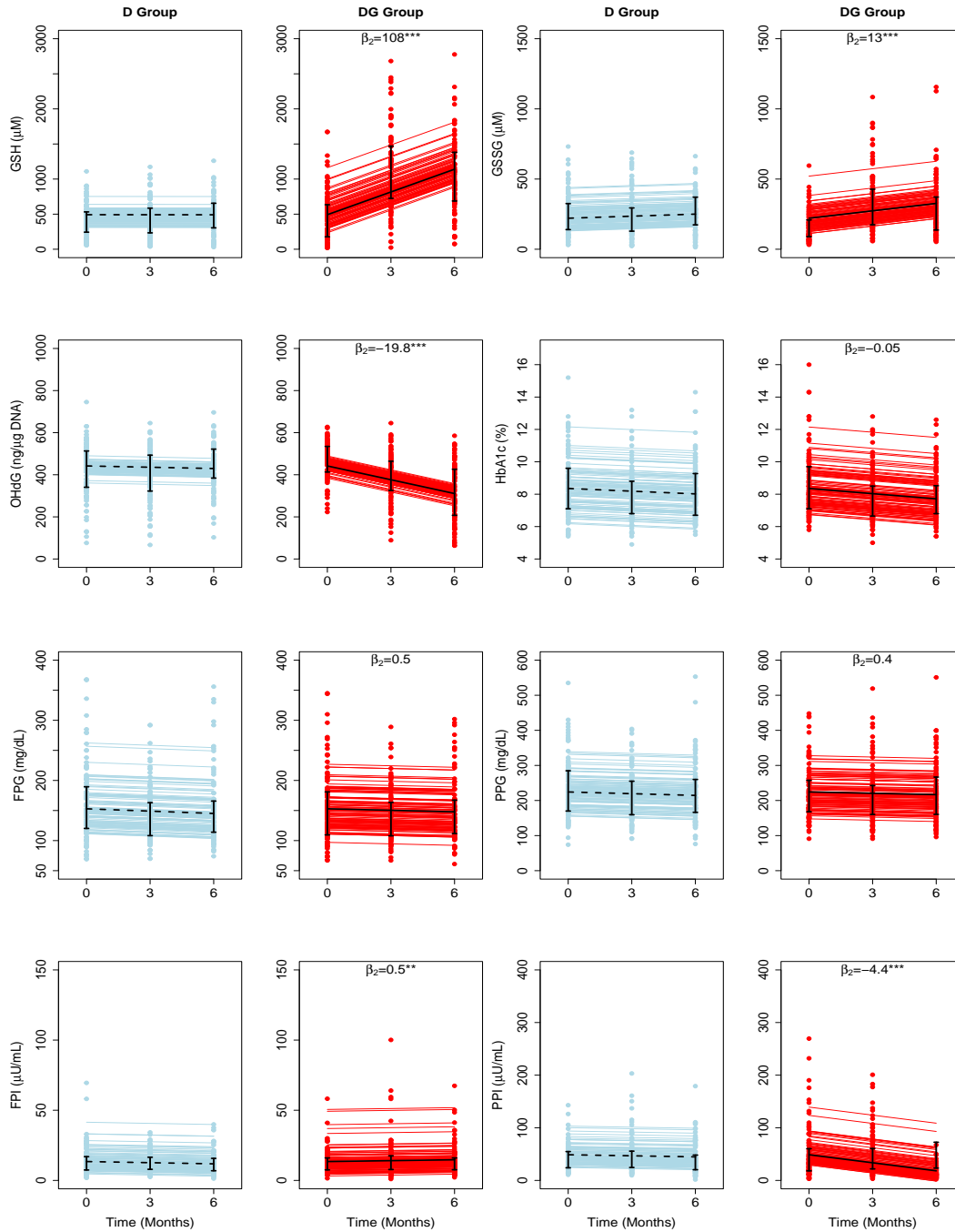


Figure 4.10: The fitted results of RIFS models for GSH, GSSG, 8-OHdG, HbA1c, FPG, FPI, PPG, and PPI variables in D group and DG groups. The average treatment effects of GSH supplementation (β_2) are denoted on each panel corresponding to the DG group. The estimated β_2 was significant on the rate of changes in GSH ($\beta_2 = 108\mu\text{M}$ per month), GSSG ($\beta_2 = 13\mu\text{M}$ per month), 8-OHdG ($\beta_2 = -12.1\text{ng}/\mu\text{g}$ DNA per month), FPI ($\beta_2 = 0.5\mu\text{U}/\text{mL}$ per month) and PPI ($\beta_2 = -4.4\mu\text{U}/\text{mL}$ per month) levels. Significance levels shown here are * $p < 0.05$, ** $p < 0.01$, *** $p < 0.001$. This figure is reproduced from Madathil *et al.* [161], published as Figure S1 in the main text.

4.5.3 Results of RIFS models for different age classes

Variable	Fixed effect parameters (EA)		
	β_0 (SE)	β_1 (SE)	β_2 (SE)
GSH	488.1(37.1) ^{***} #	6.5 (10.8)	105(12.6) ^{***} #
GSSG	230.9(15.6) ^{***} #	7.9 (4.3)	9.04 (5.2)
8-OHdG	445.2(10.3) ^{***} #	-2.2 (3.5)	-25.8(3.5) ^{***} #
HbA1c	8.4(0.2) ^{***} #	-0.02 (0.04)	-0.1(0.05) ^{**}
FPG	150.1(4.9) ^{***} #	-1.7 (1.1)	0.7 (1.5)
FPI	14(1.002) ^{***} #	-0.4 (0.2)	0.6(0.3) [*]
PPG	222.5(6.8) ^{***} #	0.1 (1.8)	-2.5 (2.2)
PPI	51.4(3.4) ^{***} #	-1.3 (0.9)	-4.1(1.07) ^{***} #

Table 4.13: **Results from RIFS models fitted for elderly diabetic subjects** The fixed-effects parameter values obtained by fitting RIFS models for GSH, GSSG, 8-OHdG, HbA1c, FPG, FPI, PPG, PPI variables are shown here with the standard errors (SE). The average treatment effects (β_2) of GSH supplementation are significant on GSH, 8-OHdG, HbA1c, FPI, and PPI levels for EA. Significance of parameter estimates are given by $*p < 0.05$, $**p < 0.01$, and $***p < 0.001$. Statistical significance continued after Bonferroni corrections marked with # symbols. This table is adapted from Madathil *et al.* [161], published as Table S4 in the supplementary data.

Variable	Fixed effect parameters (YA)		
	β_0 (SE)	β_1 (SE)	β_2 (SE)
GSH	496.6(45)***#	-6.9 (13.06)	110.8(15.3)***#
GSSG	209.5(16.06)***#	1.8 (4.5)	16.5(5.4)**
8-OHdG	438.3(11.2)***#	-1.8 (3.3)	-12.5(3.8)**#
HbA1c	8.3(0.2)***#	-0.1(0.04)*	0.03(0.05)
FPG	156.2(5.6)***#	-1.1 (1.5)	0.4 (1.9)
FPI	12.9(0.9)***#	-0.12 (0.14)	0.3(0.2)
PPG	226.6(8.3)***#	-3.6 (2.1)	3.5 (2.7)
PPI	45.7(3)***#	0.1 (0.8)	-4.9(1)***#

Table 4.14: **Results from RIFS models fitted for younger diabetic subjects** The fixed-effects parameter values obtained by fitting the data from the subgroup of younger adults (YA) using the RIFS models for GSH, GSSG, 8-OHdG, HbA1c, FPG, FPI, PPG, PPI variables are shown here with the standard errors (SE). The average treatment effects (β_2) of GSH supplementation are significant on GSH, GSSG, 8-OHdG, and PPI levels for YA. Significance of parameter estimates are given by * $p < 0.05$, ** $p < 0.01$, and *** $p < 0.001$. Statistical significance continued after Bonferroni corrections marked with # symbols. This table is adapted from Madathil *et al.* [161], published as Table S4 in the supplementary data.

4.5.4 RIRS models for anti-diabetic treatment groups

Variable	Fixed effect parameters (B)			Fixed effect parameters (BS)		
	β_0	β_1	β_2	β_0	β_1	β_2
GSH	502.83***	-2.35	114.47***	517.83***	-20.81	146.59***
GSSG	227.71***	-1.57	15.4	229.4***	8.59	3.96
8-OHdG	446.22***	-7.07	-13.26*	439.38***	-1.41	-16.57*
HbA1c	8.52***	-0.11	-0.002	8.23***	0.016	-0.19*
FPG	163.56***	-5.62*	2.048	148.44***	0.90	-3.64
FPI	13.08***	-0.12	0.23	12.98***	-0.54**	0.69**
PPG	234.64***	-8.37***	4.93	218.10***	3.36	-10.28***
PPI	49.64***	-1.93	-3.55	47.87***	-1.24	-4.01

Table 4.15: **Results from RIRS models fitted for B and BS subgroups**
The fixed-effects parameter values obtained by fitting the data from the subgroup of subjects with Biguanides only (B) and Biguanides-Sulphonylurease (BS) treatments using the RIRS models for GSH, GSSG, 8-OHdG, HbA1c, FPG, FPI, PPG, PPI variables are shown here with the standard errors (SE). The average treatment effects (β_2) of GSH supplementation are significant on GSH and 8-OHdG for B and on GSH, 8-OHdG, HbA1c, FPI, and PPG for BS subgroups. Significance of parameter estimates are given by * $p < 0.05$, ** $p < 0.01$, and *** $p < 0.001$. Statistical significances after Bonferroni correction is marked with # symbols.

Chapter 5

Mathematical modeling of erythrocytic glutathione turnover in T2D

5.1 Introduction

As discussed earlier in **Chapter 3** and **Chapter 4**, several prior studies have indicated that prolonged hyperglycemia causes OS, which subsequently results in complications associated with T2D (Brownlee [131], Volpe *et al.* [50], Giacco and Brownlee [23], Marchioli *et al.* [24]). We re-emphasize that it is crucial to understand the mechanisms and pathophysiology of oxidative stress in T2D to prevent or minimize its complications. We provided evidence in **Chapter 3** that compensating for a deficiency in GSH through supplementation improves erythrocytic glutathione stores and helps to enhance the redox state and slow the progression of complications in T2D individuals (Kalamkar *et al.* [134], Madathil *et al.* [161]). Our clinical trial data have revealed significant variations in cellular biochemical responses between individuals, highlighting

the complexity of the underlying biological processes. Therefore, understanding the dynamics of cellular-level biochemical changes and the regulation of GSH metabolism is crucial for developing effective, personalized anti-diabetic treatments that incorporate GSH and are tailored to individual patients.

As discussed earlier in **Chapter 2**, mechanistic models play a pivotal role in advancing the personalized treatment of diabetes by providing valuable knowledge for optimizing strategies for T2D management and care. Models can quantitatively describe how cellular and systemic responses differ in subjects with different diabetic conditions, providing insights into the production, utilization, and degradation of GSH. These models can identify key enzymes and pathways involved in GSH metabolism, predicting how changes in these pathways may affect GSH stores and, thereby, oxidative conditions in cells. These models can also be used to study the recovery progress of individuals and determine if their cellular response is better or worse than the average population, allowing for the evaluation of treatment progress and setting personalized targets for patients. Model-derived insights can be used to optimize treatment plans for maximum effectiveness and improved patient outcomes by targeting GSH metabolism to control oxidative stress-related complications in individuals with T2D.

Cellular pathways for GSH turnover are complex as they encompass different syntheses, interconversions, and transport processes, and their dynamics are susceptible to changes with disease conditions. This complexity is a challenge in modeling the dynamics of GSH within the body. While existing erythrocytic models such as Palsson and Joshi [176] and Reed *et al.* [125] outline various GSH-dependent metabolic pathways, the complexity of these models makes it difficult to determine their parameters and understand GSH turnover in situations where data is limited. Furthermore, despite their high

relevance, there is a lack of comprehensive models in the literature that can elucidate cellular GSH metabolism in the context of T2D conditions.

In this chapter, our main focus is to develop mathematical models of cellular and systemic level changes and explain the clinical observations, thereby, the role of redox status in hyperglycemia. We specifically aim to obtain model estimates that help identify the extent of response in individuals with T2D compared to the average population and to plan effective anti-diabetic interventions. To support the clinical observations, S. Ghaskadbi and collaborators designed an experimental study entitled “Estimation of the threshold for GSH/GSSG transport in erythrocytes.” This study was performed to analyze the thresholds for the transport of GSH and GSSG supplied extracellularly consisting of five nondiabetic control subjects, five prediabetic subjects, and five diabetic individuals from our previous study. We analyze the erythrocytic glutathione profiles of the subjects from control, prediabetic, and diabetic groups, thereby understanding the effect of extracellular treatments with GSH, GSSG, and Hydrogen peroxide. By applying the formulated model to the measured data from these experiments, we assess the impact of external stimuli on the oxidized and reduced forms of intracellular glutathione. This model obtains cellular parameters that measure the amount of available GSH and their ability to clear H_2O_2 -induced stress under various external conditions. We compute these crucial cellular parameters for describing GSH supply and H_2O_2 clearance capacity in erythrocytic GSH stores and compare them between normal and diabetic cases. This chapter provides a minimal mathematical model of GSH turnover that could help to understand how the intracellular metabolism of GSH is affected by extracellular conditions in diabetes and is potentially useful in developing personalized goals.

Furthermore, we used this model to analyze the erythrocytic GSH mea-

sured from our GSH supplementation clinical trial (Kalamkar *et al.* [134]). We estimated GSH influx and H_2O_2 values in the model at different visits for individuals in control and treatment groups of GSH supplementation and, thereby, obtaining the trajectory of changes in these individuals during the study period. This approach is of great clinical significance as it can assist in identifying individual trajectories of improvements and tailoring treatment objectives to improve cellular redox status through GSH. Moreover, these model findings can potentially assess individuals relative to the average population and indicate whether more effective interventions are required to alter GSH stores or H_2O_2 clearance capacity, leading to better cellular redox health.

During this work, we have also formulated and studied mathematical models for different components of GSH-dependent systems and enzymatic pathways in human cells. This modeling approach aimed to investigate questions raised by experiments or experimentalists on GSH metabolism and turnover mechanisms. Although these models were not the main focus of our work, brief descriptions are given in the appendix for the reader. Given the limited availability of experimental data, we have utilized the minimal model that incorporates essential components.

5.2 Methodology

5.2.1 Statement of contribution

Prof. Saroj Ghaskadbi and Dr. Saurabh Kalamkar from the Department of Zoology, Savitribai Phule Pune University, Pune, India, recruited the subjects and conducted the erythrocyte experiments for this study. Ghaskadbi group provided us with the anonymized data after data collection. These datasets were utilized for the analysis presented in this chapter. Arjun K M, Dr. Pranay

Goel, and Prof. James Sneyd designed the modeling study and performed the computations. All the above collaborators have contributed to the analysis and results emerging from this work.

5.2.2 Funding

During the study, A.K.M. received financial support through a Senior Research Fellowship provided by DST-Inspire, Government of India. The Senior Research Fellowship from CSIR, Government of India supported S.K.

5.2.3 Ethics Statement

This study was approved by the Institutional Ethical Committee (IEC) of SPPU Pune (Ref. No.: SPPU/IEC/2020/85), Institutional Biosafety Committee of SPPU Pune (IBSC20120235) and Institutional Ethical Committee of IISER Pune (IECHR/Admin/2021/009).

5.2.4 Data Availability Statement

All datasets used for the analysis in this study can be obtained from the following figshare link: <https://figshare.com/s/25af0855061f1a468d1b>

5.2.5 Acknowledgments

We express our sincere gratitude to the mentioned funding agencies for their financial support during the study.

5.2.6 Conflict of Interest

The authors of this article declare no conflict of interest. The funding sources had no role in the design or execution of this study, in the analyses or data

interpretation, in the manuscript preparation, or in the decision to publish the results.

5.2.7 Erythrocyte experiments

In order to study the response behavior of erythrocytic glutathione-dependent systems on different extracellular conditions, we collaborated with the Ghaskadbi group from SPPU Pune and conducted different cellular treatment experiments. The details of the experiments and measured data are described below. Five healthy nondiabetic individuals (ND) with HbA1c $< 5.7\%$, five prediabetic individuals (PD) with HbA1c between 5.7 to 6.4 %, and five T2D diabetic patients (D) with HbA1c $\geq 6.5\%$ (ADA, [52]) visiting the health center of Savitribai Phule Pune University (SPPU), Pune during February to March 2021 were recruited for this study. The study excluded pregnant women, individuals with alcohol consumption, smokers, those with any clinical infection or recent cardiovascular event history, and individuals receiving antioxidants. These exclusion criteria aimed to ensure a more homogeneous study population. The intention was to eliminate potential confounding factors associated with these specific characteristics or conditions. The study excluded pregnant women, individuals with alcohol consumption, smokers, those with any clinical infection or recent cardiovascular event history, and individuals receiving antioxidants. These exclusion criteria aimed to ensure a more homogeneous study population. The intention was to avoid potential confounding factors associated with these specific characteristics or conditions. Complete medical history of all individuals was noted, including their anti-diabetic treatment, exercise regimen, and family history of diabetes. Anthropometric parameters such as body weight, height, and waist: hip ratio were also recorded for all individuals.

5.2.8 Measured data from erythrocyte experiments

A trained phlebotomist collected 10 ml of blood from each study participant. Biochemical tests were performed on an autoanalyzer at AG Diagnostics Pvt. Ltd, Pune, following Clinical and Laboratory Standards, USA guidelines. 2 ml of whole blood was incubated in the presence of different concentrations of GSH (10, 100, and 1000 μM), or GSSG (1, 10, and 100 μM) for 30 min. at 37° C or H_2O_2 (1, 10, and 100 μM) for 10 minutes at 37°C. The blood samples underwent centrifugation at 3000 rpm for 10 minutes. This facilitated the separation of plasma and erythrocyte fractions. Concentrations of GSH, GSSG, and NADP^+ from erythrocyte lysate were measured by following the protocols of Veskoukis *et al.* [177] and Baker *et al.* [178].

5.2.9 Modelling GSH turnover in human erythrocytes

As seen in **Chapter 2**, there are various pathways that influence GSH turnover in different physiological and pathological conditions. Including all these reactions was beyond the scope of this modeling study. We adopted a minimal model approach for representing the dynamics of the erythrocytic GSH turnover by incorporating the following reactions: Firstly, a constant flux into the intracellular pool of GSH resulting from intracellular GSH synthesis using precursor amino acids. Secondly, GSH oxidation into GSSG on reaction with H_2O_2 , lead by glutathione peroxidase (GPx) enzyme. Thirdly, GSSG reduction into GSH on reaction with NADPH, lead by glutathione reductase (GR) enzyme. Lastly, an export for GSSG outwards the cell through membrane-bound transporters. The model formulations and parameters are described next.

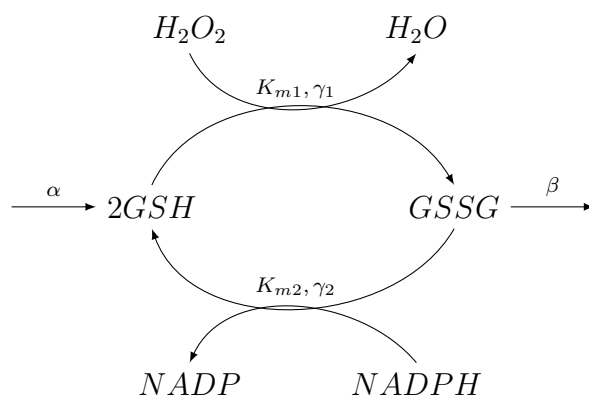


Figure 5.1: Reaction diagram for building the minimal mathematical model for glutathione turnover. The four major reactions considered here are GSH influx, GSH oxidation to GSSG, GSSG to GSH reduction, and GSSG export reactions. The parameters K_{m1} , K_{m2} , γ_1 , γ_2 , and β are marked on the associated reactions.

5.2.10 Minimal mathematical model for GSH turnover

An illustration of the reactions considered is shown in Figure 5.1. The model describes a constant GSH influx into the pool, denoted by α , which acts as the primary source for intracellular GSH. The oxidation of GSH to GSSG was assumed to follow Michaelis Menten (MM) kinetics with parameters K_{m1} and γ_1 . Similarly, the reduction of GSSG to GSH was modeled with parameters K_{m2} and γ_2 . GSSG export was assumed to be a concentration-dependent reaction through first-order kinetics with a constant β . The dynamic behavior of species involved in Figure 5.1 is described by a set of non-linear ordinary differential equations (Eq 5.1-5.2). The rates of changes in the concentration of species are given by

$$\frac{d[GSH]}{dt} = \alpha - 2 \frac{\gamma_1[GSH].[H_2O_2]}{K_{m1} + GSH} + 2 \frac{\gamma_2[GSSG].[NADPH]}{K_{m2} + GSSG} \quad (5.1)$$

$$\frac{d[GSSG]}{dt} = \frac{\gamma_1[GSH].[H_2O_2]}{K_{m1} + GSH} - \frac{\gamma_2[GSSG].[NADPH]}{K_{m2} + GSSG} - \beta[GSSG] \quad (5.2)$$

Using steady state assumptions, $\frac{d[GSH]}{dt} = 0$ and $\frac{d[GSSG]}{dt} = 0$, we obtained expressions for GSH and GSSG steady states, GSH^* and $GSSG^*$ respectively, as

$$[GSH]^* = \frac{K_{m1}}{\gamma_1 \frac{[H_2O_2]}{(\alpha)} \frac{1}{\left(\frac{1}{2} + \frac{\gamma_2[NADPH]}{2\beta K_{m2} + (\alpha)}\right)} - 1} \quad (5.3)$$

$$[GSSG]^* = \frac{\alpha}{2\beta} \quad (5.4)$$

These model equations (5.4-5.3) are further used for the optimization and parameter fitting in the next section.

5.2.11 Model parameters

The model optimization was performed independently for different study groups. The goals of optimization procedures were primarily to obtain the best fit for the parameters K_{m1} , K_{m2} , α , β , γ_1 , γ_2 , and H_2O_2 which estimates predicts the model steady states close to the data available from different treatments in each group. The physiological conditions and prolonged glycemic stress levels could have altered enzymatic activities and transporters across different groups. Therefore, it was reasonable to allow different values for these parameters across the study groups with different diabetic statuses. However, we assumed the same values for the enzymatic parameters K_{m1} , K_{m2} , γ_1 , γ_2 and the constant of GSSG export, β for different treatments in a group. The trends in the observed data across different treatments could possibly be resulting from the combined effects of available GSH and their efficiency in clearing the H_2O_2 induced stress in erythrocytes. Therefore, we allowed only α and H_2O_2 to vary across different treatments, and the other parameters were kept the same. Further, the trends observed in GSH and GSSG steady states were analyzed through the fitted values for α and H_2O_2 . It is particularly important

to note that the conditions with high α and low H_2O_2 levels could be used to qualitatively indicate low stress.

5.2.12 Model fitting and parameter optimization

The parameter optimization was performed individually for each group. This optimization determines the fitted values for the parameters $K_{m1}, K_{m2}, \alpha, \beta, \gamma_1, \gamma_2,$ and H_2O_2 based on the data available from different treatments in a group. Let the parameter vector of interest be,

$$d = [K_{m1}, K_{m2}, \alpha, \beta, \gamma_1, \gamma_2, H_2O_2]$$

The optimization problem for finding the fitted parameters d for a group, g where (g : Control, Prediabetic, Diabetic) can be stated as

$$d_{min}^g = \min_d \text{Cost}^g \quad (5.5)$$

$$\text{Cost}^g = \sum_{\text{Treatments}} (\text{Cost}_{GSH} + \text{Cost}_{GSSG}) \quad (5.6)$$

where the cost function in a group, Cost^g , is calculated as the sum of Cost_{GSH} and Cost_{GSSG} , which are defined as the squared differences between the data and model-predicted steady states of GSH and GSSG in different treatments respectively. These individual cost functions are calculated

$$\text{Cost}_{GSH} = \left\| [GSH]_{data} - GSH_{model}^* \right\|^2 \quad (5.7)$$

$$\text{Cost}_{GSSG} = \left\| [GSSG]_{data} - GSSG_{model}^* \right\|^2 \quad (5.8)$$

where $[GSH]_{data}$ and $[GSSG]_{data}$ are GSH, GSSG measurements from the different experiments. These data vectors, $[GSH]_{data}$ and $[GSSG]_{data}$ consist of

different treatments in a group; control sample, treatments with 1, 10, 100 μM of H_2O_2 , treatments with 10, 100, 1000 μM of GSH, treatments with 1, 10, 100 μM of GSSG. The corresponding vectors of the model steady state, GSH^*_{model} , and $GSSG^*_{model}$ are obtained by running the model equations until the steady states. The parameter optimization and model fitting using the available datasets have been performed using *fmincon* and *patternsearch* algorithms in Matlab software, version 2022.

5.2.13 GSH influx and H_2O_2 estimates from clinical trial data

The data from the clinical trial consisted of nondiabetic control individuals and a total of 250 known T2D individuals under anti-diabetic treatment in two groups. Namely, the DG group with GSH supplementation and the D group without supplementation. This dataset consists of GSH and GSSG measurements from all individuals at three different visits during the study period. In order to understand the effect of GSH supplementation using the formulated model, we analyzed GSH and GSSG measurements available from the control diabetic subjects with and without GSH supplementation at different visits during the study period. We used K_{m1} , K_{m2} , γ_1 , γ_2 , β , and NADPH values for these groups from the fitted results and estimated GSH influx (α) and H_2O_2 from the steady state equations. Further, we analyzed the longitudinal changes in α and H_2O_2 in these study groups during the study period.

5.3 Results

5.3.1 Fitted model parameters and steady states

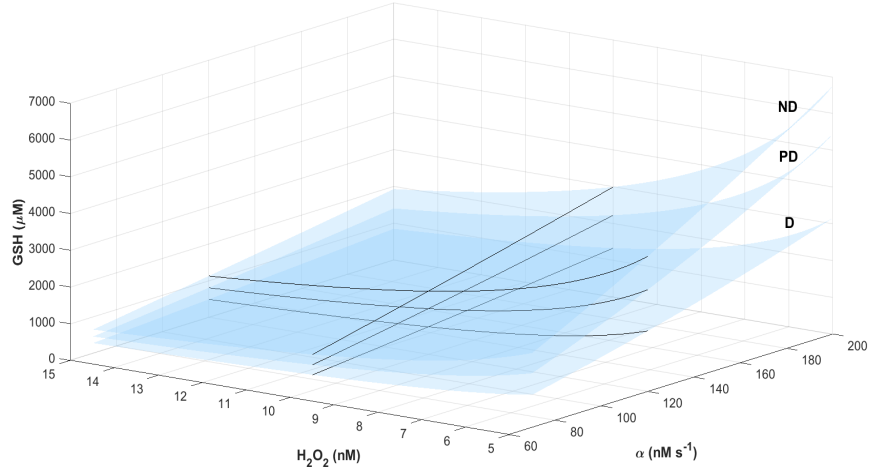
The fitted values of the model parameters, $K_{m1}, K_{m2}, \gamma_1, \gamma_2, \beta$ for different groups are listed in Table 5.1. The measured levels of erythrocytic GSH and GSSG model were depicted with estimated values for GSH and GSSG steady states at different treatments on the top and middle panels (Figure 5.2-5.11). These model predictions were successful in capturing the trends in the measured GSH and GSSG levels on different extracellular GSH stimuli. The steady states observed from the model lie close to the measured experimental data of GSH and GSSG. The fitted estimates of GSH influx and H_2O_2 for different treatments in these samples were analyzed further.

Parameter (Unit)	Nondiabetic	Prediabetic	Diabetic
K_{m1} (M)	2.64×10^{-2}	1.21×10^{-2}	0.84×10^{-2}
K_{m2} (M)	2.94×10^{-2}	2.54×10^{-2}	3.63×10^{-2}
γ_1 (s^{-1})	136.59	87.9	121.7
γ_2 (s^{-1})	152.67	130.34	254.81
β (s^{-1})	2.29×10^{-4}	2.30×10^{-4}	1.83×10^{-4}

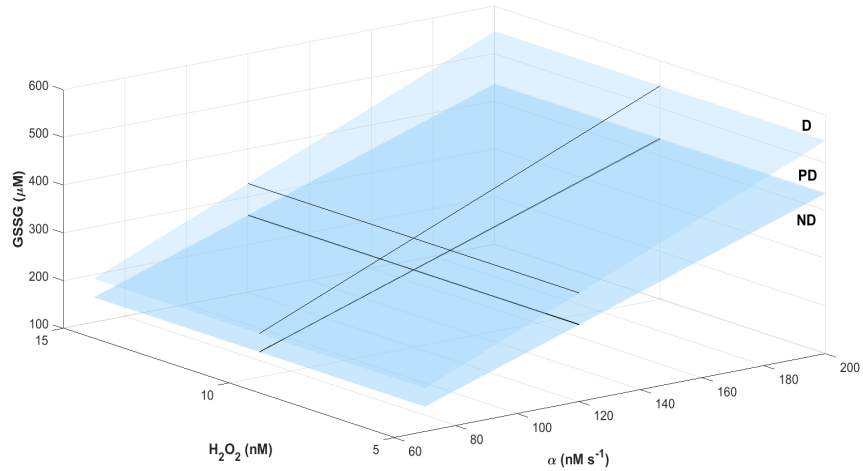
Table 5.1: Parameter values obtained from model optimization for nondiabetic, prediabetic, and diabetic study groups.

5.3.2 Geometry of minimal model and implications

The steady-state GSH and GSSG relationships in different groups were determined by the parameter estimates (Table 5.1) obtained from the model optimization. In Figure 5.2, these are represented geometrically as different surfaces for nondiabetic, prediabetic, and diabetic groups. The shapes of these surfaces for different groups were primarily characterized by their $K_{m1}, K_{m2}, \gamma_1, \gamma_2, \beta$, and NADPH values.



(a) Model predicted GSH surface



(b) Model predicted GSSG surface

Figure 5.2: **The geometry of minimal GSH model and implications for different groups.** Simulated surfaces describing the effect of GSH influx (α) and H_2O_2 on erythrocytic glutathione for nondiabetic (ND), prediabetic (PD), and diabetic (D) individuals are shown here with predicted erythrocytic GSH (a) and GSSG (b) steady states. These surfaces are plotted for α values in a range of 50-200 nM/s and H_2O_2 values in a 5-15 nM range. NADPH values of 17.5, 16.6, and 14.9 nM are used for simulating the surfaces for ND, PD, and D groups, respectively. GSH and GSSG steady states obtained by the model with an α value of 100 nM/s and varying H_2O_2 are marked (solid black curves) on these surfaces for the three groups. Similarly, steady states for fixed H_2O_2 of 10 nM for varying α values are also marked.

The data showed that erythrocytic GSH was larger in nondiabetic individuals than in prediabetic individuals and the lowest in diabetic individuals. Measured GSSG was larger in diabetic individuals than in prediabetic and diabetic individuals. This could be indicative of enzymatic activities prone to change under different diabetic conditions. As depicted in Figure 5.2, the parameter estimates were successful in capturing these trends in the basal GSH and GSSG from nondiabetic to prediabetic and then diabetic individuals.

Physiologically feasible ranges of GSH (Figure 5.2a) and GSSG (Figure 5.2b) steady states are simulated as surfaces for feasible ranges of α (50-200 nM/s) and H_2O_2 (5-15 nM). A given pair of values of α and H_2O_2 uniquely determines GSH and GSSG steady states on the surface corresponding to the diabetic status. To demonstrate the combinational effects of α and H_2O_2 , we have also shown the curves representing GSH and GSSG steady states with respect to one fixed and another varying parameter for all three groups. For instance, GSH steady states obtained by the model with a fixed α value (100 nM/s) are marked (solid black curves) on these surfaces and are observed to decrease with increasing H_2O_2 . Similarly, steady states for fixed H_2O_2 of 10 nM are also marked in the α direction, which is observed to increase with increasing α .

The geometrical representation of the model illustration describes the effect of changing extracellular conditions seen on GSH and GSSG steady states, primarily as changing GSH influx and H_2O_2 values on the surfaces. We used these surfaces for GSH and GSSG to describe their trajectories with estimates α and H_2O_2 for different treatments in the later section (Figure 5.3-5.5).

5.3.3 Results of stimulation with extracellular GSH

We fit the formulated GSH model with the data obtained from treatments with 10, 100, and 1000 μM of GSH. The simulation results obtained are shown in Figure 5.3. The measured and model-predicted levels of GSH and GSSG in response to these treatments are described in nondiabetic (Figure 5.3a), prediabetic (Figure 5.4a), and diabetic (Figure 5.5a) groups with the estimated results of GSH influx (α) and H_2O_2 .

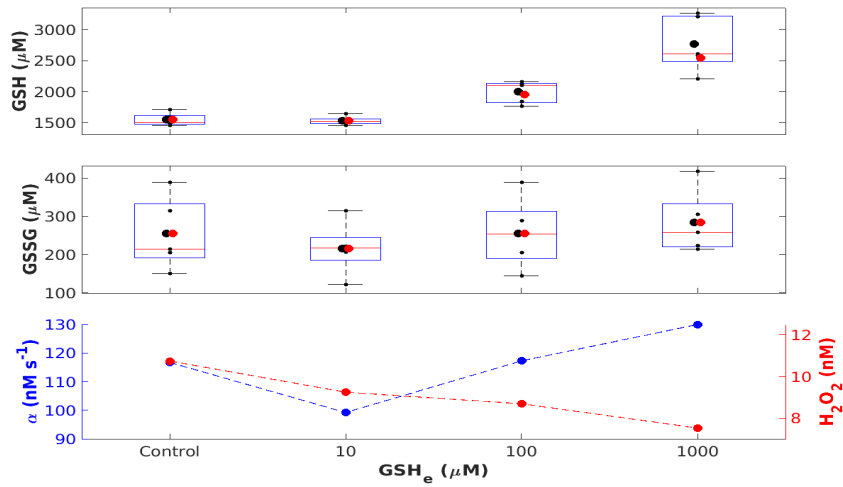
To geometrically understand the impact of changing α and H_2O_2 under different GSH treatments, we have also simulated 3-dimensional surfaces and highlighted the trace connecting model estimates of α and H_2O_2 with the predicted GSH and GSSG levels in nondiabetic (Figure 5.3b), prediabetic (Figure 5.4b), and diabetic (Figure 5.5b) erythrocytes.

We estimated α values of 117, 111, and 103 nM/s in the control samples for nondiabetic, prediabetic, and diabetic subjects, respectively. Interestingly, similar trends were observed in the fitted values of α and H_2O_2 with increasing extracellular GSH. Estimated GSH influx increased steadily in nondiabetic (100, 117 to 130 nM/s), prediabetic (112, 144 to 161 nM/s), and diabetic (119, 146 to 162 nM/s) samples with 10, 100, and 1000 μM GSH respectively.

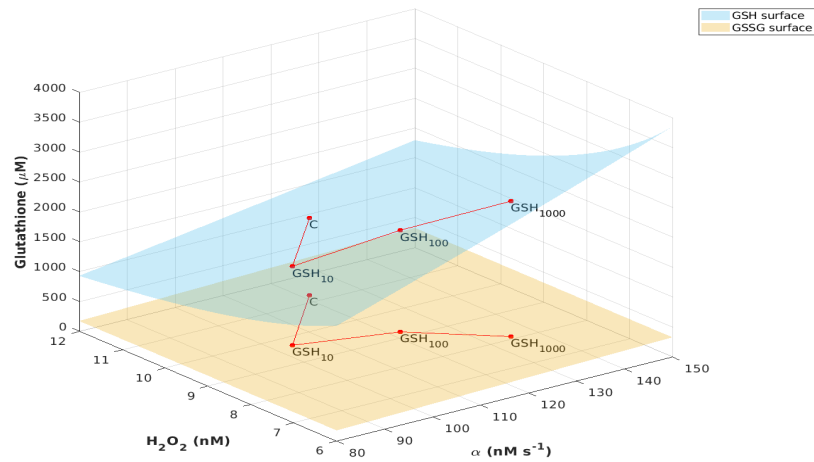
The fitted values for H_2O_2 were found to be steadily declining with increasing extracellular GSH (10, 100, and 1000 μM) in nondiabetic (9.24, 8.69, and 7.52 nM), prediabetic (11.2, 11.04, and 9.6 nM) and diabetic (10.51, 9.9, to 6.72 nM) respectively. Notably, the trends observed in the fitted H_2O_2 were seen to be closer in the nondiabetic and diabetic erythrocytes.

5.3.4 Results of stimulation with extracellular H_2O_2

Next, we fitted the model with the data obtained from extracellular treatments with 1, 10, and 100 μM of H_2O_2 . The measured and model-predicted levels

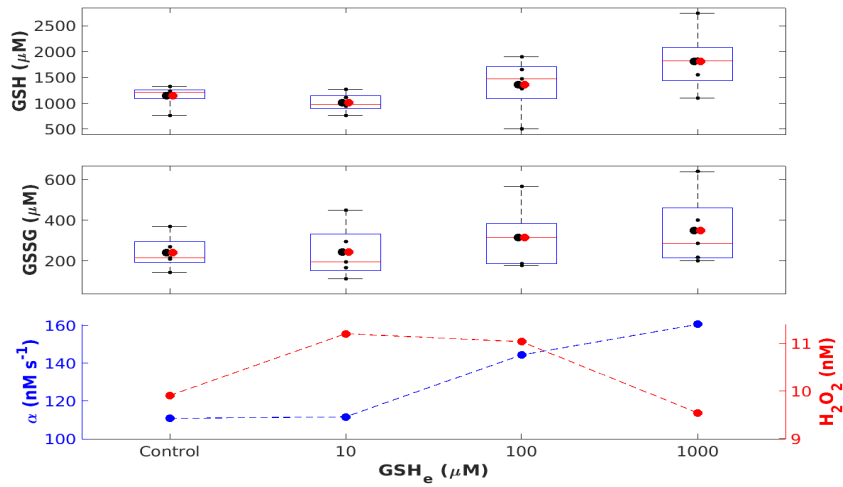


(a) Measured data and model predictions

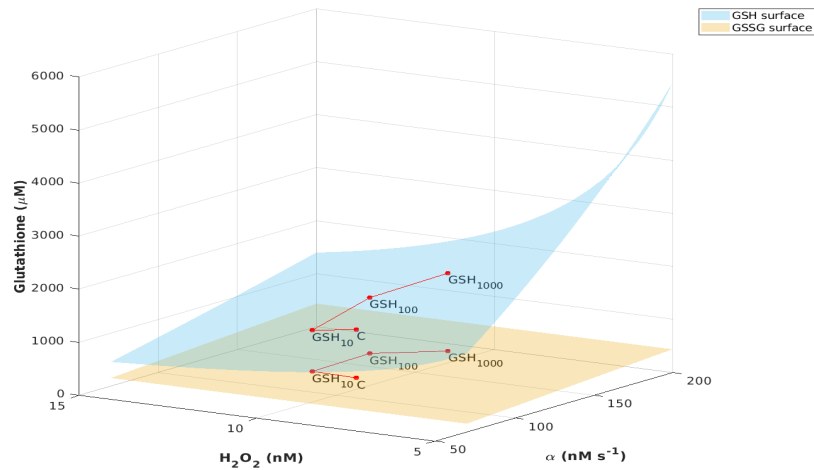


(b) Geometry of model-predicted values of GSH influx and H₂O₂

Figure 5.3: **Effects of extracellular GSH treatments in nondiabetic individuals.** The effects of extracellular treatments with 10, 100, and 1000 μM of GSH on erythrocytic GSH and GSSG concentrations are plotted here for nondiabetic individuals. (a) Box and whisker plots with data points are used to represent the median and interquartile ranges of the data ($n=5$) at each treatment. The mean measured (black circles) and model-predicted (red circle) concentrations of GSH (top panel) and GSSG (middle panel) are plotted against the concentration of treated GSH (10, 100, and 1000 μM). The model-fitted values GSH influx (α) and H₂O₂ are plotted on the left y-axis and right y-axis on the bottom panel against the treatment dose. (b) The model-simulated effect of GSH influx and H₂O₂ on the steady-state concentrations of erythrocytic GSH (blue surface) and GSSG (red surface) are shown. Red lines connect the points C, GSH₁₀, GSH₁₀₀, and GSH₁₀₀₀ representing the model estimates on treatments with 10, 100, 1000 μM GSH, respectively.

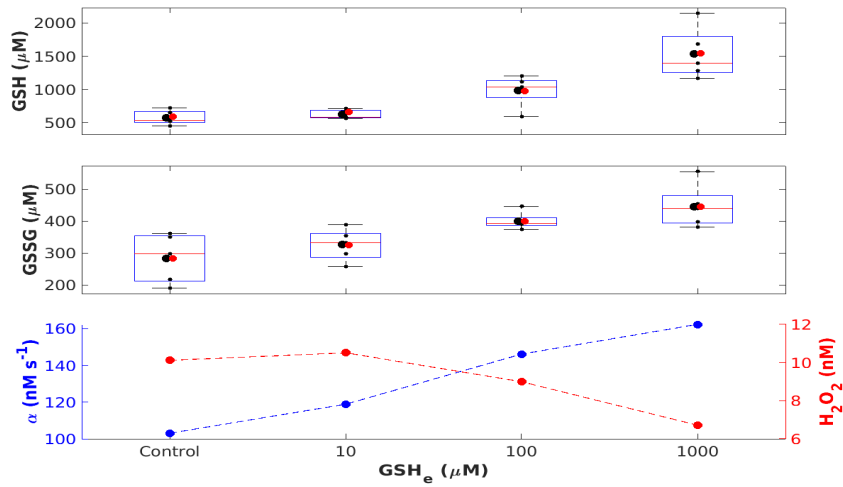


(a) Measured data and model predictions

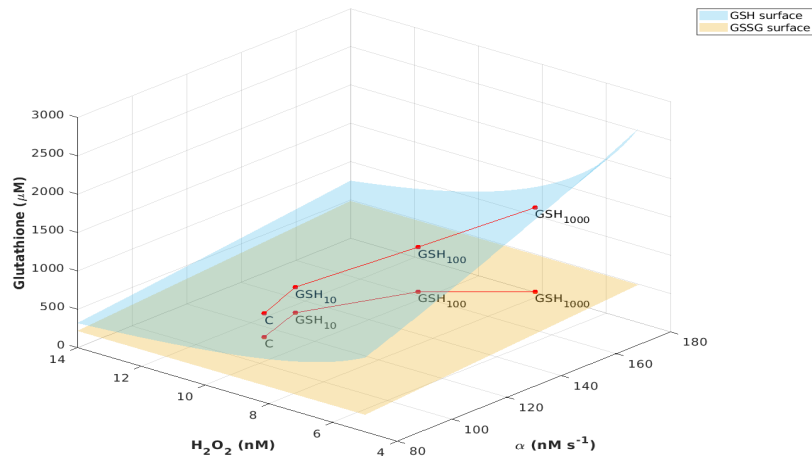


(b) Geometry of model-predicted values of GSH influx and H_2O_2

Figure 5.4: **Effects of extracellular GSH treatments in prediabetic individuals.** The effects of extracellular treatments with 10, 100, and 1000 μM of GSH on erythrocytic GSH and GSSG concentrations are plotted here for prediabetic individuals. (a) Box and whisker plots with data points are used to represent the median and interquartile ranges of the data ($n=5$) at each treatment. The mean measured (black circles) and model-predicted (red circle) concentrations of GSH (top panel) and GSSG (middle panel) are plotted against the concentration of treated GSH (10, 100, and 1000 μM). The model-fitted values GSH influx (α) and H_2O_2 are plotted on the left y-axis and right y-axis on the bottom panel against the treatment dose. (b) The model-simulated effect of GSH influx and H_2O_2 on the steady-state concentrations of erythrocytic GSH (blue surface) and GSSG (red surface) are shown. Red lines connect the points C, GSH_{10} , GSH_{100} , and GSH_{1000} representing the model estimates on treatments with 10, 100, 1000 μM GSH, respectively.



(a) Measured data and model predictions



(b) Geometry of model-predicted values of GSH influx and H_2O_2

Figure 5.5: **Effects of extracellular GSH treatments in diabetic individuals.** The effects of extracellular treatments with 10, 100, and 1000 μM of GSH on erythrocytic GSH and GSSG concentrations are plotted here for diabetic individuals. (a) Box and whisker plots with data points are used to represent the median and interquartile ranges of the data ($n=5$) at each treatment. The mean measured (black circles) and model-predicted (red circle) concentrations of GSH (top panel) and GSSG (middle panel) are plotted against the concentration of treated GSH (10, 100, and 1000 μM). The model-fitted values GSH influx (α) and H_2O_2 are plotted on the left y-axis and right y-axis on the bottom panel against the treatment dose. (b) The model-simulated effect of GSH influx and H_2O_2 on the steady-state concentrations of erythrocytic GSH (blue surface) and GSSG (red surface) are shown. Red lines connect the points C, GSH_{10} , GSH_{100} , and GSH_{1000} representing the model estimates on treatments with 10, 100, 1000 μM GSH respectively.

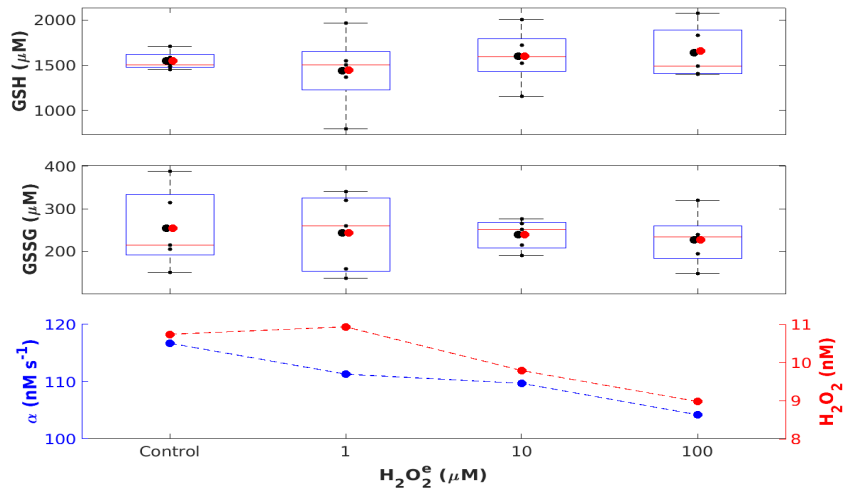
of GSH and GSSG on these treatments are described in nondiabetic (Figure 5.6a), prediabetic (Figure 5.7a), and diabetic (Figure 5.8a) erythrocytes with the estimated results of GSH influx (α) and H_2O_2 .

The model-simulated surface plots are shown here with a highlighted trace connecting model estimates of α , H_2O_2 , and predicted GSH and GSSG levels for different treatments in nondiabetic (Figure 5.6b), prediabetic (Figure 5.7b), and diabetic (Figure 5.8b) groups. Different patterns in the fitted values of GSH influx and H_2O_2 were observed across these erythrocytes with increasing extracellular H_2O_2 . Estimated GSH influx was observed to steadily decrease in nondiabetic (111, 110 to 104 nM/s) and increase in diabetic (89, 95 to 117 nM/s) erythrocytes with increasing extracellular H_2O_2 (1, 10, and 100 μ M) respectively. In the prediabetic erythrocytes, GSH influx was estimated to be 118, 112 to 119 nM/s for 1, 10, and 100 μ M, respectively. The fitted values for intracellular H_2O_2 were found to be steadily declining in nondiabetic samples (10.9, 9.8 to 9 nM). At the same time, they steadily increased in prediabetic samples (11.8, 11.5 to 12.5 nM) in response to increasing extracellular H_2O_2 (1, 10, and 100 μ M), respectively. The fitted H_2O_2 values of diabetic erythrocytes were found to be 9.1, 8.3, and 17.1 nM, respectively.

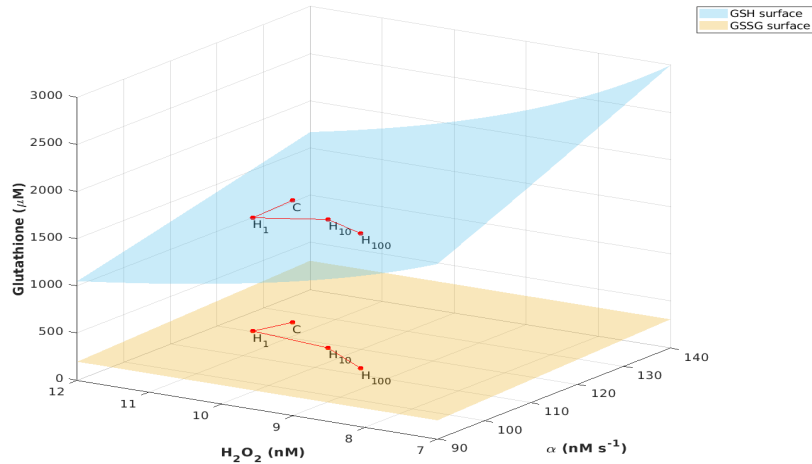
5.3.5 Results of stimulation with extracellular GSSG

Next, we fitted the data obtained for extracellular treatments with 1, 10, and 100 μ M of GSSG. The simulation results obtained are shown for nondiabetic (Figure 5.9), prediabetic (Figure 5.10), and diabetic (Figure 5.11) erythrocytes.

Different patterns in the fitted values of GSH influx and H_2O_2 were observed. Notably, we did not observe any steady changes as a result of increasing concentrations of GSSG. Estimated GSH influx increased in nondiabetic

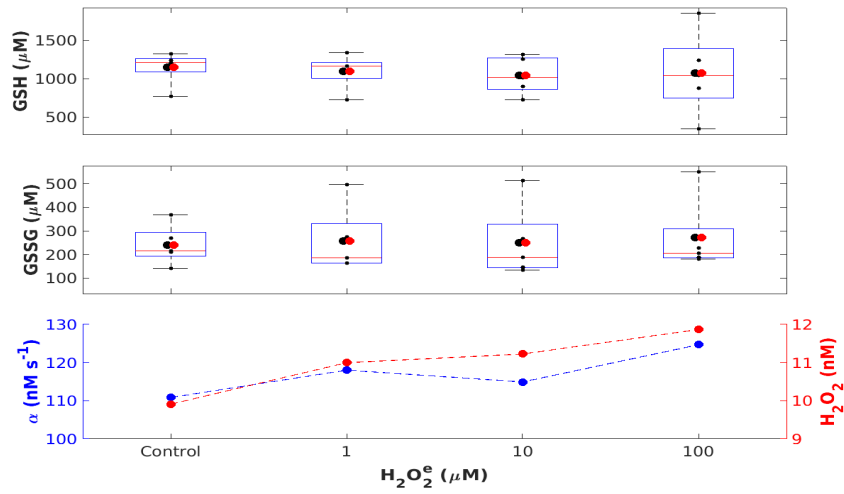


(a) Measured data and model predictions

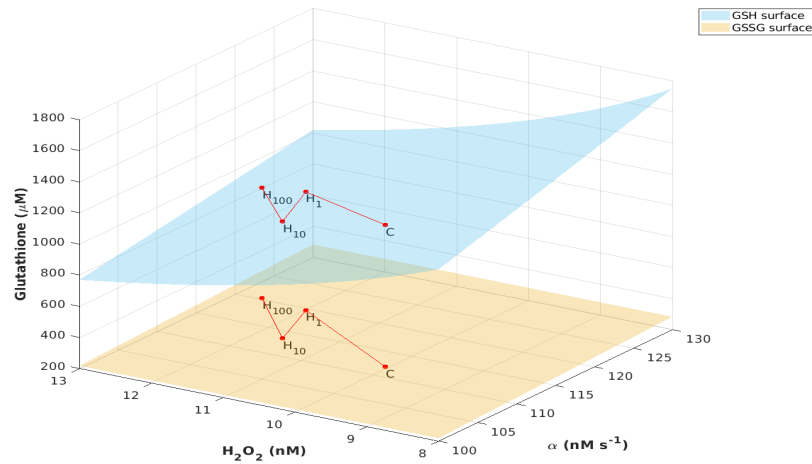


(b) Geometry of model-predicted values of GSH influx and H_2O_2

Figure 5.6: **Effects of extracellular H_2O_2 treatments in nondiabetic individuals.** The effects of extracellular treatments with 1, 10, and 100 μM of H_2O_2 on erythrocytic GSH and GSSG concentrations are plotted here for nondiabetic individuals. (a) Box and whisker plots with data points are used to represent the median and interquartile ranges of the data ($n=5$) at each treatment. The mean measured (black circles) and model-predicted (red circle) concentrations of GSH (top panel) and GSSG (middle panel) are plotted against the concentration of treated GSH (10, 100, and 1000 μM). The model-fitted values GSH influx (α) and H_2O_2 are plotted on the left y-axis and right y-axis on the bottom panel against the treatment dose. (b) The model-simulated effect of GSH influx and H_2O_2 on the steady-state concentrations of erythrocytic GSH (blue surface) and GSSG (red surface) are shown. Red lines connect the points C, H_1 , H_{10} , and H_{100} representing the model estimates on treatments with 1, 10, 100 μM of H_2O_2 respectively

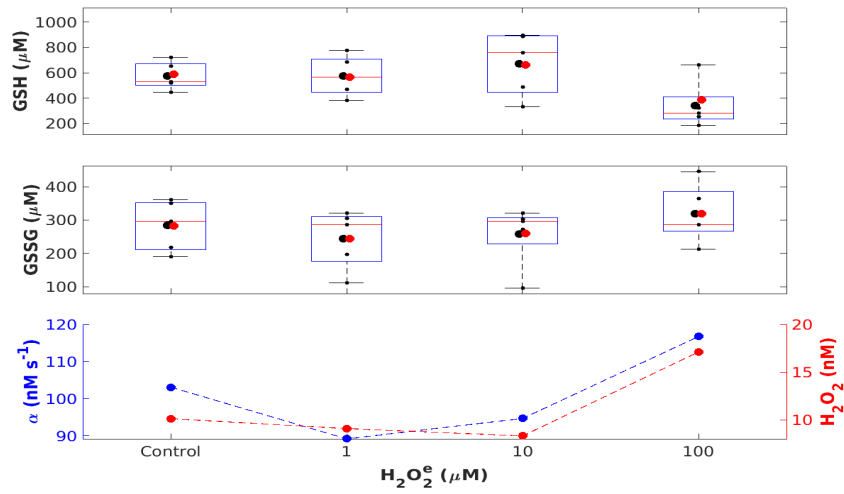


(a) Measured data and model predictions

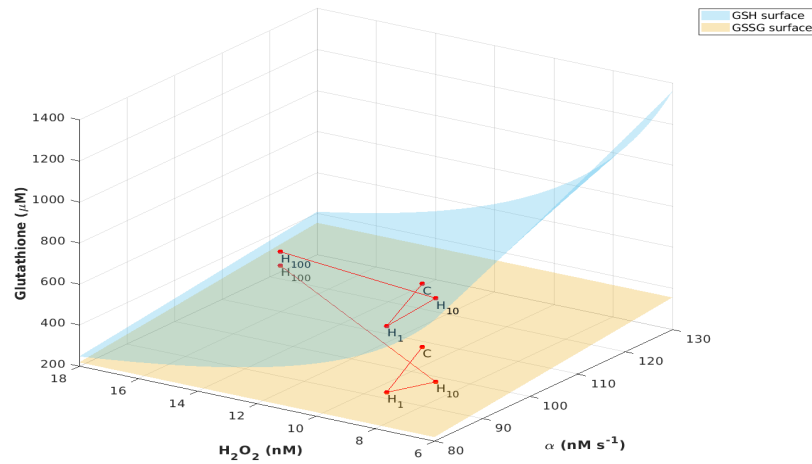


(b) Geometry of model-predicted values of GSH influx and H_2O_2

Figure 5.7: **Effects of extracellular H_2O_2 treatments in prediabetic individuals.** The effects of extracellular treatments with 1, 10, and 100 μM of H_2O_2 on erythrocytic GSH and GSSG concentrations are plotted here for prediabetic individuals. (a) Box and whiskers plots with data points are used to represent the median and interquartile ranges of the data ($n=5$) at each treatment. The mean measured (black circles) and model-predicted (red circle) concentrations of GSH (top panel) and GSSG (middle panel) are plotted against the concentration of treated GSH (10, 100, and 1000 μM). The model-fitted values GSH influx (α) and H_2O_2 are plotted on the left y-axis and right y-axis on the bottom panel against the treatment dose. (b) The model-simulated effect of GSH influx and H_2O_2 on the steady-state concentrations of erythrocytic GSH (blue surface) and GSSG (red surface) are shown. Red lines connect the points C, H_1 , H_{10} , and H_{100} representing the model estimates on treatments with 1, 10, 100 μM of H_2O_2 respectively



(a) Measured data and model predictions



(b) Geometry of model-predicted values of GSH influx and H_2O_2

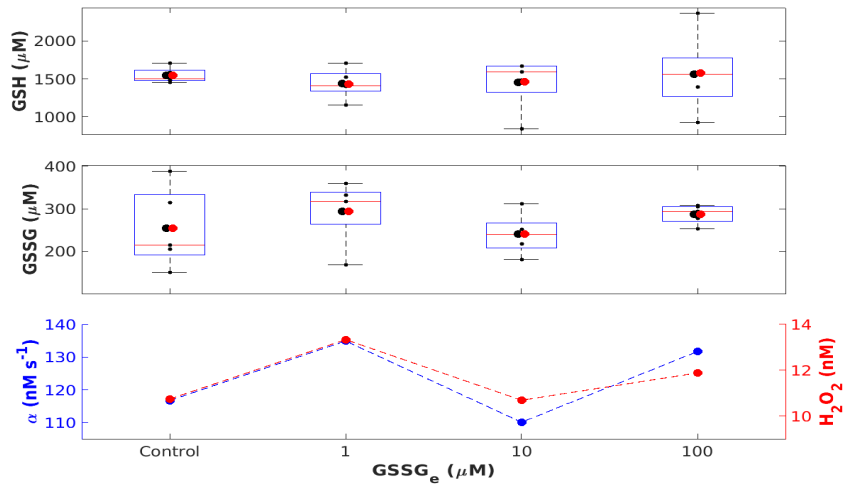
Figure 5.8: **Effects of extracellular H_2O_2 diabetic individuals.** The effects of extracellular treatments with 1, 10, and 100 μM of H_2O_2 on erythrocytic GSH and GSSG concentrations are plotted here for diabetic individuals. (a) Box and whiskers plots with data points are used to represent the median and interquartile ranges of the data ($n=5$) at each treatment. The mean measured (black circles) and model-predicted (red circle) concentrations of GSH (top panel) and GSSG (middle panel) are plotted against the concentration of treated GSH (10, 100, and 1000 μM). The model-fitted values GSH influx (α) and H_2O_2 are plotted on the left y-axis and right y-axis on the bottom panel against the treatment dose. (b) The model-simulated effect of GSH influx and H_2O_2 on the steady-state concentrations of erythrocytic GSH (blue surface) and GSSG (red surface) are shown. Red lines connect the points C, H_1 , H_{10} , and H_{100} representing the model estimates on treatments with 1, 10, 100 μM H_2O_2 respectively

(135, 110, 132 nM/s), prediabetic (119, 108, 106 nM/s), and diabetic (101, 115, 100 nM/s) samples with increasing extracellular GSSG (1, 10, and 100 μM) respectively. The fitted values for H_2O_2 showed nonsteady trends in non-diabetic (13.3, 10.7, 11.9 nM), prediabetic (12.1, 11, 10.6 nM), and diabetic (9.4, 11.1, 10.3 nM) erythrocytes with increasing extracellular GSSG (1, 10, and 100 μM) respectively.

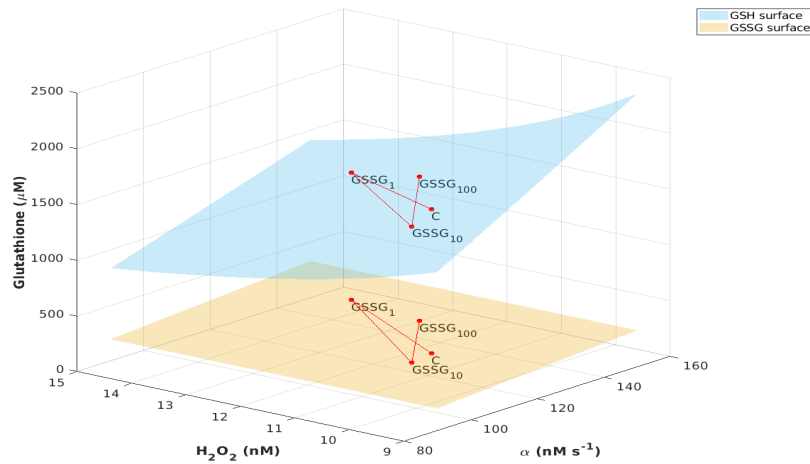
5.3.6 Estimated α - H_2O_2 traces on GSH supplementation and clinical implications

We further analyzed the clinical trial data from the study groups in the clinical trial (Kalamkar *et al.* [134]). The estimated GSH influx (α) and H_2O_2 values at three visits with connecting traces for each subject in control, D, and DG groups are shown in Figure 5.12. Over the period of six months, the model-estimated values of GSH influx and H_2O_2 did not change significantly in the Control and D groups. GSH influx in the DG group was observed to increase significantly within the first three months ($p < 0.001$). But the change was not significant for the next three months. In the DG group, estimated H_2O_2 did not change significantly within the first three months but was observed to have a significant decrease by the end of 6 months of GSH supplementation ($p < 0.001$). Additionally, 6-month changes in GSH influx were significantly larger in DG group individuals than in the D group individuals (Cohen's d effect size = 0.61 (large), $p < 0.001$). The effect of GSH supplementation on elder diabetic subjects is described in Figure 5.13. 6-month changes in GSH influx were significantly large in elder DG individuals than that in the D group individuals (Cohen's $d = 0.66$ (large), $p < 0.001$).

We analyzed the individual trajectories of all participants in the clinical trial. We note inter-individual variability in the trajectory during the clinical

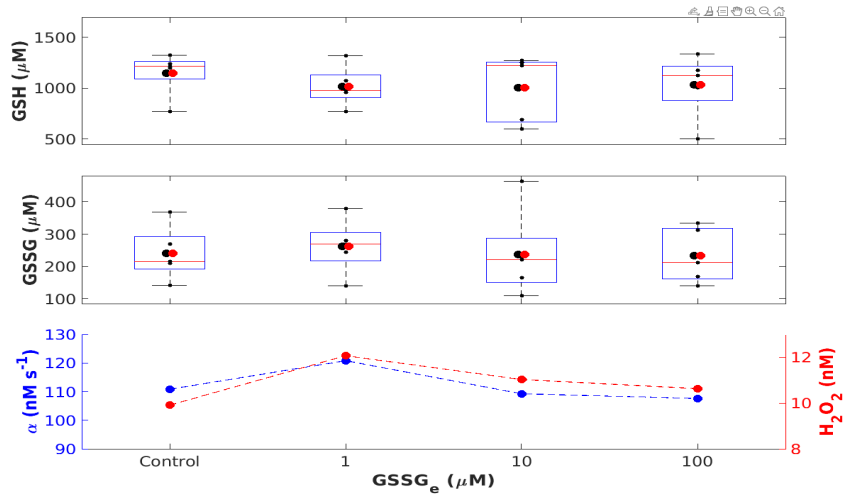


(a) Measured data and model predictions

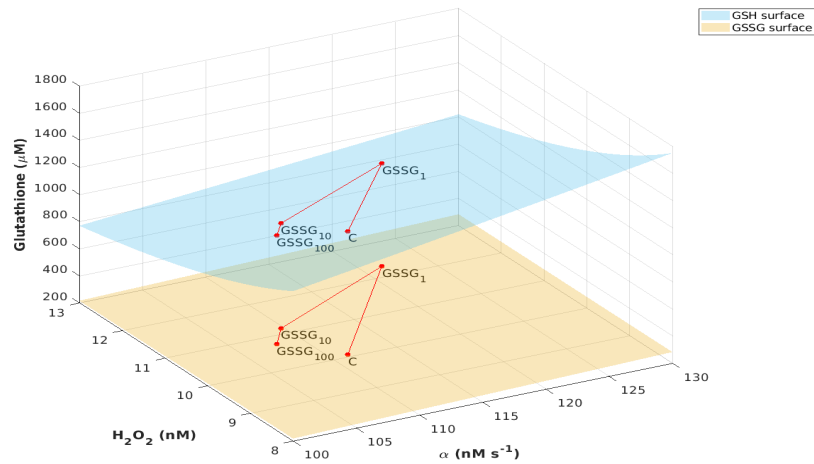


(b) Geometry of model-predicted values of GSH influx and H_2O_2

Figure 5.9: **Effects of extracellular GSSG treatments in nondiabetic individuals.** The effects of extracellular treatments with 1, 10, and 100 μM of GSSG on erythrocytic GSH and GSSG concentrations are plotted here for nondiabetic individuals. (a) Box and whiskers plots with data points are used to represent the median and interquartile ranges of the data ($n=5$) at each treatment. The mean measured (black circles) and model-predicted (red circle) concentrations of GSH (top panel) and GSSG (middle panel) are plotted against the concentration of treated GSH (10, 100, and 1000 μM). The model-fitted values GSH influx (α) and H_2O_2 are plotted on the left y-axis and right y-axis on the bottom panel against the treatment dose. (b) The model-simulated effect of GSH influx and H_2O_2 on the steady-state concentrations of erythrocytic GSH (blue surface) and GSSG (red surface) are shown. Red lines connect the points C, GSSG₁, GSSG₁₀, and GSSG₁₀₀ representing the model estimates on treatments with 1, 10, 100 μM GSSG respectively

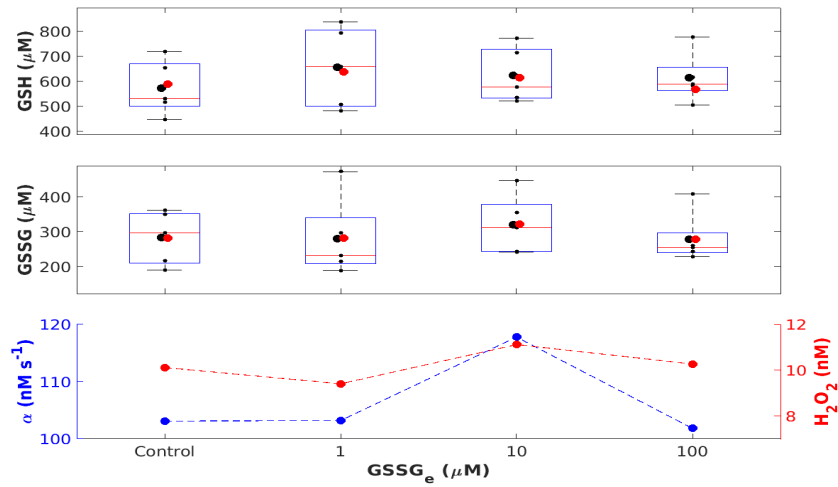


(a) Measured data and model predictions

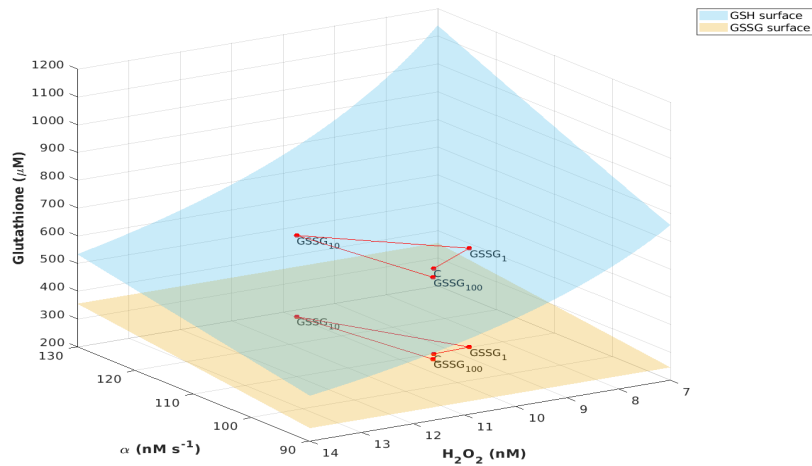


(b) Geometry of model-predicted values of GSH influx and H_2O_2

Figure 5.10: **Effects of extracellular GSSG treatments in prediabetic individuals.** The effects of extracellular treatments with 1, 10, and 100 μM of GSSG on erythrocytic GSH and GSSG concentrations are plotted here for prediabetic individuals. (a) Box and whiskers plots with data points are used to represent the median and interquartile ranges of the data ($n=5$) at each treatment. The mean measured (black circles) and model-predicted (red circle) concentrations of GSH (top panel) and GSSG (middle panel) are plotted against the concentration of treated GSH (10, 100, and 1000 μM). The model-fitted values GSH influx (α) and H_2O_2 are plotted on the left y-axis and right y-axis on the bottom panel against the treatment dose. (b) The model-simulated effect of GSH influx and H_2O_2 on the steady-state concentrations of erythrocytic GSH (blue surface) and GSSG (red surface) are shown. Red lines connect the points C, GSSG₁, GSSG₁₀, and GSSG₁₀₀ representing the model estimates on treatments with 1, 10, 100 μM GSSG respectively



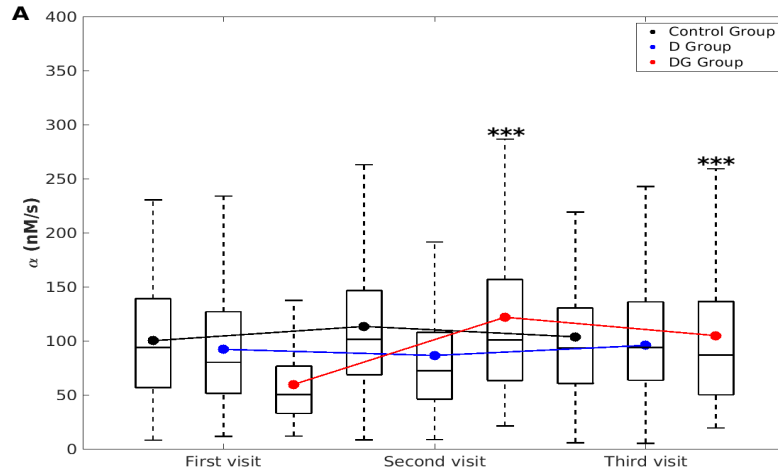
(a) Measured data and model predictions



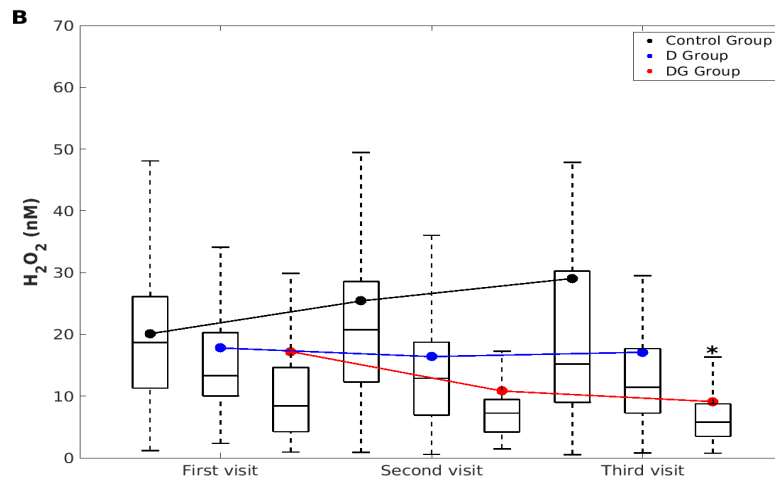
(b) Geometry of model-predicted values of GSH influx and H_2O_2

Figure 5.11: **Effects of extracellular GSSG treatments in diabetic individuals.** The effects of extracellular treatments with 1, 10, and 100 μM of GSSG on erythrocytic GSH and GSSG concentrations are plotted here for diabetic individuals. (a) Box and whiskers plots with data points are used to represent the median and interquartile ranges of the data ($n=5$) at each treatment. The mean measured (black circles) and model-predicted (red circle) concentrations of GSH (top panel) and GSSG (middle panel) are plotted against the concentration of treated GSH (10, 100, and 1000 μM). The model-fitted values GSH influx (α) and H_2O_2 are plotted on the left y-axis and right y-axis on the bottom panel against the treatment dose. (b) The model-simulated effect of GSH influx and H_2O_2 on the steady-state concentrations of erythrocytic GSH (blue surface) and GSSG (red surface) are shown. Red lines connect the points C, GSSG₁, GSSG₁₀, and GSSG₁₀₀ representing the model estimates on treatments with 1, 10, 100 μM GSSG respectively

trial period. Sample trajectories obtained for a few individuals from different groups are shown in Figure 5.14-5.16. Individuals with GSH supplementation (DG1, DG44, DG255) showed trajectories of gradual improvements in terms of GSH levels, GSH influx (α), and H_2O_2 during the clinical period (Figure 5.16) as compared to the trends observed in control (C1, C52, C96 in Figure 5.14), D groups (D1, D10, D12 in Figure 5.15). Improvements with high α and low H_2O_2 levels qualitatively indicate the improvement in stress conditions. The potential trajectory of subjects on the respective surface has direct clinical and academic uses in evaluating the effectiveness of clinical interventions and the extent of recovery.

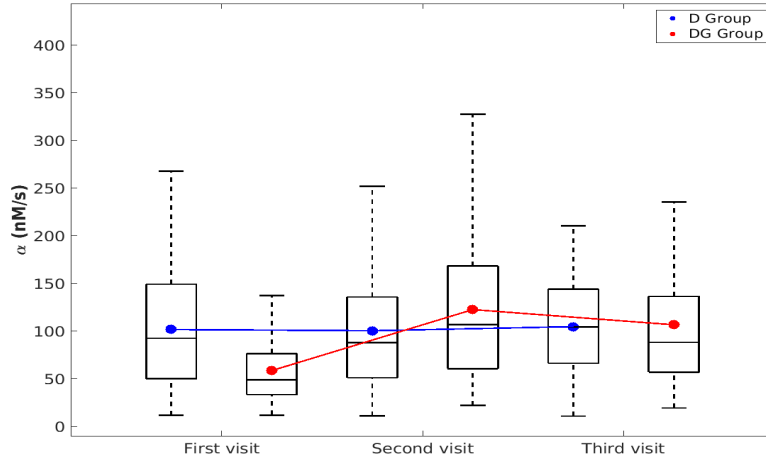


(a) Estimated GSH influx in the study groups

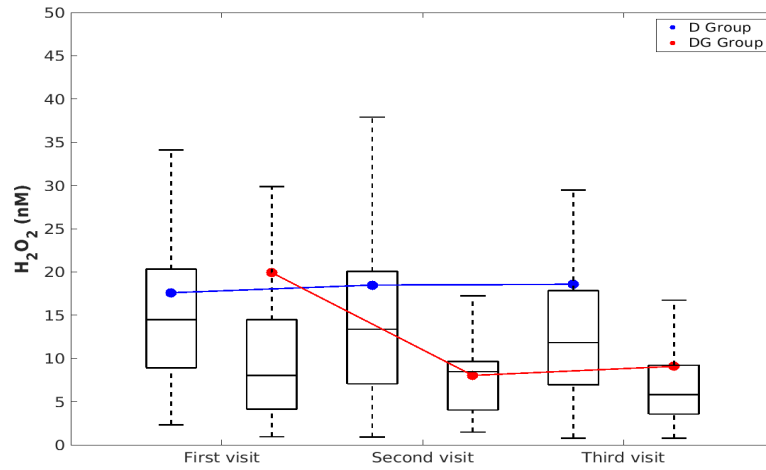


(b) Estimated H_2O_2 in the study groups

Figure 5.12: **Longitudinal changes in the GSH influx and H_2O_2 in different groups.** The model-fitted values for (a) GSH influx and (b) H_2O_2 from Control, D, and DG groups at the first, second, and third different visits are shown here in the box plots. The representations of the data and comparison between visits are similar to those in Figure 3.3.



(a) Estimated GSH influx in the elder study groups



(b) Estimated H₂O₂ in the elder study groups

Figure 5.13: **Longitudinal changes in the GSH influx and H₂O₂ in elder diabetic subjects.** The model estimated values for (a) GSH influx and (b) H₂O₂ from elder diabetic subjects in D, and DG groups at the first, second, and third different visits are shown here in the box plots. The representations of the data and comparison between visits are similar as in Figure 3.3.

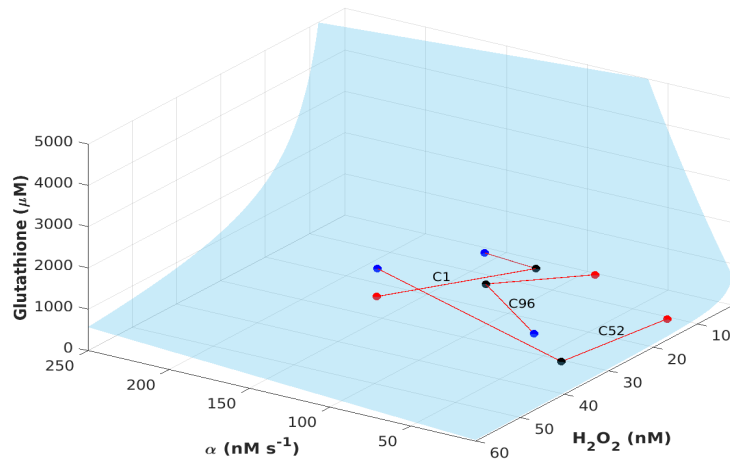


Figure 5.14: **Trajectories of control group individuals in the clinical trial.** The model predicted surface for erythrocytic GSH is plotted here against α (range of 50-200 nM/s) and H_2O_2 values (range of 2-60 nM) for control group individuals. Measured erythrocytic GSH with model-estimated GSH influx and H_2O_2 are marked for the first (red circle), second (black circle), and third (blue circle) visits for ($n=3$) individuals from each group. Trajectories connecting these steady-state points during the clinical trial period are overlaid on these surfaces here, representing the individual's recovery path. The subject IDs of these individuals in the clinical trial for control (C1, C52, C96) are also marked on the corresponding trajectory.

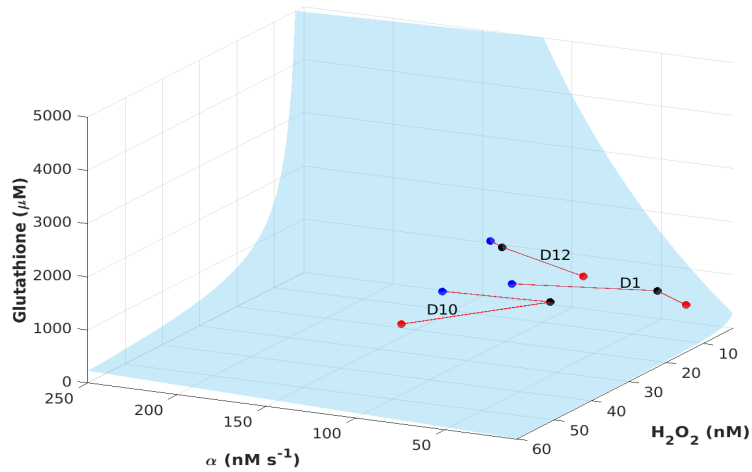


Figure 5.15: **Trajectories of D group individuals in the clinical trial.** The model predicted surface for erythrocytic GSH is plotted here against a α (range of 50-200 nM/s) and H_2O_2 values (range of 2-60 nM) for D group individuals. Measured erythrocytic GSH with model-estimated GSH influx and H_2O_2 are marked for the first (red circle), second (black circle), and third (blue circle) visits for ($n=3$) individuals from each group. Trajectories connecting these steady-state points during the clinical trial period are overlaid on these surfaces here, representing the individual's recovery path. The subject IDs of these individuals in the clinical trial diabetic without GSH supplementation (D1, D10, D12) are also marked on the corresponding trajectory.

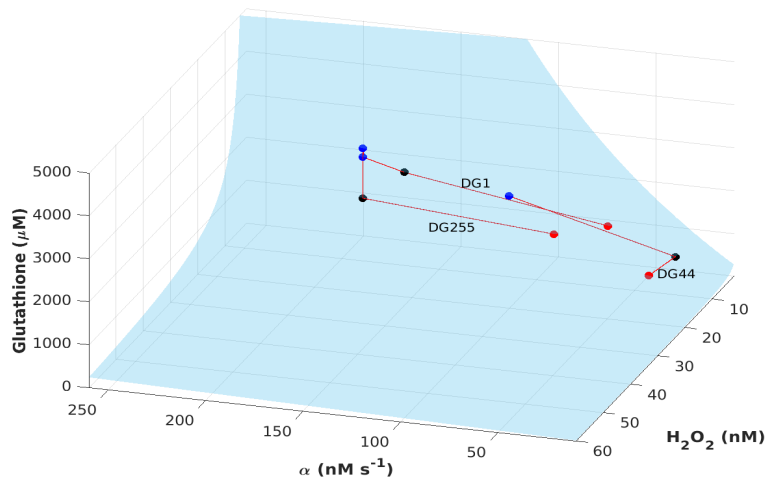


Figure 5.16: **Trajectories of DG group individuals in the clinical trial.** The model predicted surface for erythrocytic GSH is plotted here against a α (range of 50-200 nM/s) and H_2O_2 values (range of 2-60 nM) for DG group individuals. Measured erythrocytic GSH with model-estimated GSH influx and H_2O_2 are marked for the first (red circle), second (black circle), and third (blue circle) visits for ($n=3$) individuals from each group. Trajectories connecting these steady-state points during the clinical trial period are overlaid on these surfaces here, representing the individual's recovery path. The subject IDs of these individuals in the clinical trial with GSH supplementation (DG1, DG44, DG255) are also marked on the corresponding trajectory.

5.4 Discussion

In this chapter, we formulated a minimal mathematical model for the dynamics of GSH turnover in erythrocytes to understand their dose-response behaviors. We utilized this model to study how intracellular GSH respond to different extracellular treatment conditions and how their dynamics differ with different diabetic status. We further explained the experimentally measured effects of different extracellular stimuli with GSH, GSSG, and H_2O_2 in nondiabetic, prediabetic, and diabetic individuals.

Glutathione turnover in erythrocytes is driven by various enzymes involved in the glutamyl cycle and GSH synthesis pathways, namely, γ -glutamyl transpeptidases, glutamate-cysteine ligase, glutathione synthase (GS), oxoprolinase, glutathione peroxidase, glutathione reductase enzymes, membrane transporters of precursor amino acids, and GSSG transporters, etc. (Meister and Anderson, [76], Meister [179], Wu *et al.* [33], Bachhawat and Yadav [180]). While there are some existing modeling studies on glutathione turnover (Reed *et al.* [125], Adimora *et al.* [181], Raftos *et al.* [126]), there is a scarcity of research in the literature focused on using models to understand the data and physiology, especially in T2D conditions. Here, we proposed a minimal model for comprehending the GSH turnover on the basis of some of the major reactions directly involved, namely GSH influx, GSH, GSSG interconversions, and GSSG export reaction in erythrocytes. The model needed to be able to accurately predict erythrocytic GSH responses in order for it to be considered valid based on the physiology of the processes and experimental observations. Our model was constructed sequentially from the bottom up, beginning with the kinetic descriptions of these relevant processes in GSH turnover for which reasonable descriptions are given. Then, we added new components and assumptions to simulate the biochemical patterns observed in treatment

experiments performed on human erythrocytes.

We assumed constant GSH influxes as the primary source for intracellular GSH into the cellular pool. Interconversions between reduced and oxidized forms of glutathione were majorly driven by GPx and GR enzymes, for which Michaelis-Menten kinetics was a suitable choice to describe the kinetics of these reactions. The cellular export of GSSG was known to be a concentration-dependent reaction for which the rate increases with the increasing concentration of GSSG. Therefore, we modeled this export through first-order kinetics with a constant. The model parameters were optimized carefully to fit the model with data available from treatment experiments. This obtained an optimal best fit for the parameters that predict the model steady states close to the data available from different treatments in each group with different diabetic status. The optimization was performed independently for different study groups by fitting for the parameter values and predicted steady states of GSH and GSSG. The optimization results for the model fitted with the data indicated that the construction of the model was reasonably well to be able to capture both the physiology and give a good description of the data.

The physiological conditions and prolonged glycemic stress levels could alter enzymatic activities and transporters across different groups. Therefore, it was reasonable to allow different values for these parameters in the optimization across the study groups with different diabetic status. The results obtained by fitting the model for GSH influx and intracellular H_2O_2 levels at different treatments describe that the intracellular GSH and GSSG responses were influenced by available GSH and their efficiency in clearing the H_2O_2 -induced stress in erythrocytes.

While analyzing the fitted results from treatment experiments, we observed interesting trends in GSH influx and H_2O_2 values that explain the differences in

their physiology under different diabetic conditions. We expect these estimates can be explored clinically in understanding the effectiveness of extracellular stimulus, especially in planning treatments in diabetic conditions.

The model estimated GSH influx in the untreated control samples of the diabetic group to be lower than in the control and prediabetic groups. This might have been observed due to the increased oxidative stress in the diabetic group. On examining the effects of an increased dose of extracellular GSH, the influx of GSH improved in all erythrocytes. It also resulted in an improvement in their H_2O_2 clearance capacity. Fitted H_2O_2 levels in the diabetic erythrocytes were observed to have similar trends as in the nondiabetic erythrocytes when treated with increasing extracellular GSH. The diabetic individuals were already on glucose control treatment, possibly altering H_2O_2 clearance to almost similar levels as to nondiabetic samples.

Increasing extracellular H_2O_2 also seemed to have altered GSH influx and H_2O_2 clearance at different extents depending on the diabetic conditions. GSH influx was observed to be decreasing with increasing extracellular H_2O_2 in the nondiabetic samples. There are known membrane-bound aquaporin proteins on RBCs that help H_2O_2 molecules diffuse across membranes. As a result, extracellular H_2O_2 treatment can directly influence the redox balance between GSH and GSSG couple inside the cells. The control group subjects are relatively rich in their erythrocytic GSH stores. The transported H_2O_2 could be involved in the oxidation of precursor amino acids for GSH synthesis, which further results in a reduced GSH influx and a decrease in the intracellular H_2O_2 . Thus, extracellular H_2O_2 could be inhibiting the GSH influx of the control group. However, to meet the need for oxidative challenges induced by H_2O_2 , the other routes of GSH production could be becoming more active. For instance, GSSG is getting reduced easily by GR with the help of readily

available NADPH in the RBCs of control group individuals.

Interestingly, in nondiabetic erythrocytes, intracellular H_2O_2 is cleared even when they are exposed to high concentrations of extracellular H_2O_2 . Whereas in prediabetic erythrocytes, intracellular H_2O_2 is gradually increasing in response to extracellular H_2O_2 . This clearly indicated that while nondiabetic erythrocytes protect themselves by clearing intracellular H_2O_2 , prediabetic erythrocytes failed to do that. Diabetic erythrocytes could clear intracellular H_2O_2 in response to 1, 10 μM of extracellular H_2O_2 , possibly due to the glucose control treatments but failed to do so at 100 μM H_2O_2 .

The effects of changing external conditions on the model steady states were possible to comprehend carefully through the 3-dimensional surfaces presented. We interpret this representation of the model in such a way that each surface describes GSH steady states for an individual with a particular diabetic status can move along the corresponding surface under the changing extracellular conditions. The trace of this movement with changing conditions is determined by GSH influx and H_2O_2 . This can be further explored to understand the recovery path from low GSH and stress conditions, especially in diabetic individuals.

Although, we have observed steady increases in GSH influx and a decrease in H_2O_2 with increasing doses of GSH in all three study groups. The observed trajectories were not showing steady changes as a result of GSSG treatments for different groups. Additional treatment experiments with different doses will provide more data to understand and strengthen the evidence about the effect of changes in GSH influx and H_2O_2 with different conditions. The presented model is not the best representation of the GSH turnover, however, it provides a decent description of the systems involved. The model formulated needs to be refined further if additional cellular measurements are available. We can

incorporate the GSH synthesis reactions from component amino acids into the model to improve the understanding.

In the extended analysis, we analyzed the erythrocytic GSH data published earlier to examine the effect of oral GSH supplementation in altering erythrocytic GSH stores in diabetic patients. By using the fitted model, we intended to estimate how oral GSH supplementation affects diabetic subjects in terms of their GSH influx and H_2O_2 . This analysis also provided a way to sequentially trace the progression of individual subjects throughout the period of GSH supplementation. This approach can be extended to examine the trajectory corresponding to a patient under any interventions. By tracking the progression of estimates from the diabetic individuals through the surface determined, the GSH model is used to examine the effectiveness of clinical interventions. This approach is crucial for understanding disease conditions, particularly the dynamics of GSH-mediated cellular redox status in diabetes, and will greatly influence future clinical interventions with GSH.

To summarize, we have developed an evidence-based model, which is a simplified analytical description of processes relevant to GSH turnover in erythrocytes. We demonstrated the use of this model to generate predictions for experimental observations on intracellular GSH and GSG in subjects with different diabetic conditions. This model is helpful for analyzing the mechanisms of cellular-level GSH turnover in diabetes and planning clinical interventions to understand improvement in systemic redox status on extracellular stimuli. Tracking improvements through the fitted trajectories gives a large scope to extend them to continuous assessment of the clinical interventions. The methodology we present here can potentially aid in easing personal therapy design. However, we emphasize that individualized treatment designs have to involve multiple considerations. This work also supports the development of

similar cellular-systemic models and reinforces their utility as a foundation for further exploration in GSH-mediated interventions.

5.5 Appendix

5.5.1 Detailed models for GPx and GR enzyme kinetics

As discussed earlier, the interconversion of reduced and oxidized forms of glutathione is driven by glutathione peroxidase (GPx) and glutathione reductase (GR) enzymes. These enzymes play crucial roles in maintaining the redox status of cells, and therefore, it is worth looking at the detailed kinetics of these enzymes for the dynamics of these reactions involved. We have attempted to formulate a detailed theoretical model for the mechanism involved in these enzymatic reactions and to ask how erythrocytic GSH and GSSG concentrations may change in diabetic subjects. The derivations of this alternate model for GPx and GR systems and model equations are described here for the completeness of this work report.

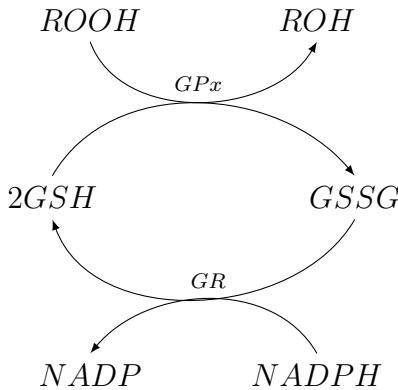


Figure 5.17: Reaction pathways for GSH turnover in RBCs.

An alternative model derived here could be used in identifying the role of individual reaction steps or possible rate-determining steps in the enzymatic mechanism of GPx and GR theoretically. However, our primary objectives for the analysis were not addressed using this model, considering the limited data

sets and model complexities. The reaction schemes of GPx and GR enzymes are shown below in Figure 5.17. The model equations for this will be derived further. In order to do this, we formulate the models for GPx and GR enzyme kinetics individually further.

5.5.2 Glutathione Reductase

A scheme for reactions with glutathione reductase (GR) is shown below. The enzyme GR is represented with the symbol E_1 in this scheme. The intermediates formed as the complex of enzymes with X reactant are denoted as $E_1.X$ in the following representation. The rate of change in species concentrations

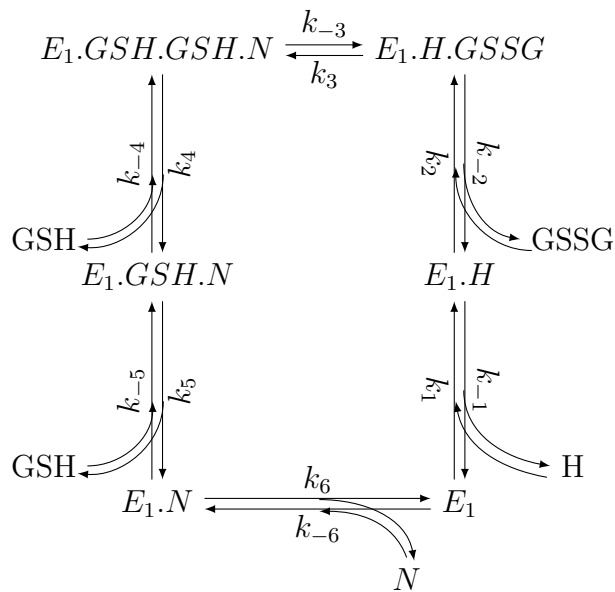


Figure 5.18: Enzymatic kinetics for Glutathione Reductase.

in this scheme is given by following differential equations

$$\frac{d[E_1]}{dt} = -k_1 \cdot [E_1] \cdot [H] + k_{-1} \cdot [E_1.H] + k_6 \cdot [E_1.N] - k_{-6} \cdot [E_1] \cdot [N]$$

$$\frac{d[E_1.H]}{dt} = k_1 \cdot [E_1] \cdot [H] - k_{-1} \cdot [E_1.H] - k_2 \cdot [E_1.H] \cdot [GSSG] + k_{-2} \cdot [E_1.H.GSSG]$$

$$\frac{d[E_1.H.GSSG]}{dt} = k_2.[E_1.H].[GSSG] - k_{-2}.[E_1.H.GSSG] - k_3.[E_1.H.GSSG] + k_3.E_1.GSH.GSH.N$$

$$\frac{d[E_1.GSH.GSH.N]}{dt} = k_3.[E_1.H.GSSG] - k_{-3}.[E_1.GSH.GSH.N] - k_4.[E_1.GSH.GSH.N] + k_{-4}.[E_1.GSH.N].[GSH]$$

$$\frac{d[E_1.GSH.N]}{dt} = k_4.[E_1.GSH.GSH.N] - k_{-4}.[E_1.GSH.N].[GSH] - k_5.[E_1.GSH.N] + k_{-5}.[E_1.N].[GSH]$$

where the total enzyme

$$[E_1] + [E_1.H] + [E_1.H.GSSG] + [E_1.GSH.GSH.N] + [E_1.GSH.N] + [E_1.N] = E_1^0 \quad (5.9)$$

The steady-state solution of the flux (J_{GR}) in this system of equations is obtained as

$$J_{GR} = k_6[E_1.N] - k_{-6}[E_1].[N]$$

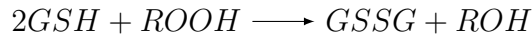
$$J_{GR} = \frac{\left(k_1 k_2 k_3 k_4 k_5 k_6 [GSSG].[H] - k_{-1} k_{-2} k_{-3} k_{-4} k_{-5} k_{-6} [GSH]^2.[N] \right) E_1^0}{DEN1} \quad (5.10)$$

where

$$\begin{aligned}
DEN1 = & k_{-1}k_3k_4k_5k_6 + k_{-1}k_{-2}k_4k_5k_6 + k_{-1}k_{-2}k_{-3}k_5k_6 + k_{-1}k_{-2}k_{-3}k_{-4}k_{-5}[GSH]^2 \\
& + k_2k_3k_4k_5k_6[GSSG] + k_{-1}k_{-2}k_{-3}k_{-4}k_6.[GSH] + k_1k_3k_4k_5k_6[H] + k_1k_{-2}k_4k_5k_6[H] \\
& + k_1k_{-2}k_{-3}k_5k_6[H] + k_{-1}k_3k_4k_5k_{-6}[N] + k_{-1}k_{-2}k_4k_5k_{-6}[N] + k_{-1}k_{-2}k_{-3}k_5k_{-6}[N] \\
& + k_1k_2k_3k_4k_5[GSSG].[H] + k_1k_2k_3k_4k_6[GSSG].[H] + k_1k_2k_4k_5k_6[GSSG].[H] \\
& + k_1k_2k_{-3}k_5k_6[GSSG].[H] + k_1k_{-2}k_{-3}k_{-4}k_6[GSH].[H] + k_2k_3k_4k_5k_{-6}[GSSG].[N] \\
& + k_{-1}k_3k_4k_{-5}k_{-6}[GSH].[N] + k_{-1}k_{-2}k_4k_{-5}k_{-6}[GSH].[N] + k_{-1}k_{-2}k_{-3}k_{-4}k_{-6}[GSH].[N] \\
& + k_{-1}k_{-2}k_{-3}k_{-5}k_{-6}[GSH].[N] + k_{-1}k_{-2}k_{-3}k_{-4}k_{-5}[GSH]^2.[H] + k_{-1}k_3k_{-4}k_{-5}k_{-6}[GSH]^2.[N] \\
& + k_{-1}k_{-2}k_{-4}k_{-5}k_{-6}[GSH]^2.[N] + k_{-1}k_{-3}k_{-4}k_{-5}k_{-6}[GSH]^2.[N] + k_{-2}k_{-3}k_{-4}k_{-5}k_{-6}[GSH]^2.[N] \\
& + k_1k_2k_3k_4k_{-5}[GSH].[GSSG].[H] + k_1k_2k_3k_{-4}k_6[GSH].[GSSG].[H] \\
& + k_1k_2k_{-3}k_{-4}k_6[GSH].[GSSG].[H] + k_2k_3k_4k_{-5}k_{-6}[GSH].[GSSG].[N] \\
& + k_1k_2k_3k_{-4}k_{-5}[GSH]^2.[GSSG].[H] + k_1k_2k_{-3}k_{-4}k_{-5}[GSH]^2.[GSSG].[H] \\
& + k_2k_3k_{-4}k_{-5}k_{-6}[GSH]^2.[GSSG].[N] + k_2k_{-3}k_{-4}k_{-5}k_{-6}[GSH]^2.[GSSG].[N]
\end{aligned} \tag{5.11}$$

5.5.3 Glutathione Peroxidase

In the presence of reactive oxygen species (eg: ROOH), GSH gets oxidized into GSSG with the help of the enzyme glutathione peroxidase (GPx) enzyme.



This reaction takes place in three steps. In the first step, oxidation of the selenocysteine residue of the *GPx* enzyme takes place. In the next two steps, GSH molecules react with the intermediates and produce GSSG. A scheme for reactions is shown below. Here, E_2 denotes the enzyme in the ground state, F denotes the intermediate formed after the first step of oxidation, and G

is a half-reduced intermediate. The intermediates formed as the complex of enzymes with X reactant are denoted as $E_2.X$ in the following representation. The rate of change in species concentrations in this scheme is given by

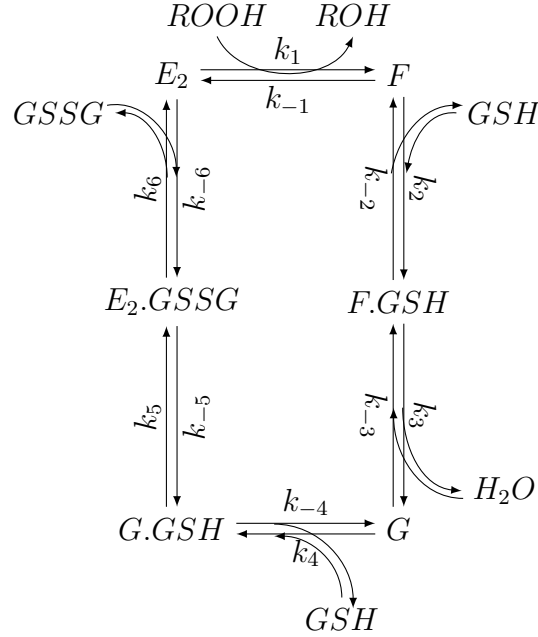


Figure 5.19: Enzymatic kinetics for Glutathione Peroxidase.

$$\frac{d[E_2]}{dt} = -k_1.[E_2].[ROOH] + k_{-1}.[F].[ROH] + k_6.[E_2.GSSG] - k_{-6}.[E_2].[GSSG]$$

$$\frac{d[F]}{dt} = k_1.[E_2].[ROOH] - k_{-1}.[F].[ROH] - k_2.[F].[GSH] + k_{-2}.[F.GSH]$$

$$\frac{d[F.GSH]}{dt} = k_2.[F].[GSH] - k_{-2}.[F.GSH] - k_3.[F.GSH] + k_{-3}.[H_2O].[G]$$

$$\frac{d[G]}{dt} = k_3.[F.GSH] - k_{-3}.[H_2O].[G] - k_4.[G].[GSH] + k_{-4}.[G.GSH]$$

$$\frac{d[G.GSH]}{dt} = k_4.[G].[GSH] - k_{-4}.[G.GSH] - k_5.[G.GSH] + k_{-5}.[E_2.GSSG]$$

where the total enzyme concentration is given by

$$[E_2] + [F] + [F.GSH] + [G] + [G.GSH] + [E_2.GSSG] = E_2^0$$

The steady-state solution of the flux (J_{GPx}) in this system of equations is obtained as

$$J_{GPx} = k'_1[E_2].[ROOH] - k'_{-1}[F].[ROH]$$

$$J_{GPx} = \frac{\left(k'_1k'_2k'_3k'_4k'_5k'_6.[GSH]^2.[ROOH] - k'_{-1}k'_{-2}k'_{-3}k'_{-4}k'_{-5}k'_{-6}.[GSSG].[ROH].[H_2O]\right)E_2^0}{DEN2} \quad (5.12)$$

where the denominator is given by

$$\begin{aligned}
DEN2 = & k'_2 k'_3 k'_4 k'_5 k_6 [GSH]^2 + k'_2 k'_3 k'_4 k'_5 k'_6 [GSH] \cdot [GSSG] \\
& + k'_{-2} k'_{-3} k'_{-4} k'_{-5} k'_{-6} \cdot [GSSG] \cdot [H_2O] + k'_1 k'_2 k'_3 k'_5 k'_6 [GSH] \cdot [ROOH] \\
& + k'_1 k'_3 k'_4 k'_5 k'_6 \cdot [GSH] \cdot [ROOH] + k'_{-1} k'_3 k'_4 k'_5 k'_6 \cdot [GSH] \cdot [ROH] \\
& + k'_1 k'_2 k'_3 k'_{-4} k'_6 \cdot [GSH] \cdot [ROOH] + k'_1 k'_{-2} k'_4 k'_5 k'_6 \cdot [GSH] \cdot [ROOH] \\
& + k'_{-1} k'_{-2} k'_4 k'_5 k'_6 \cdot [GSH] \cdot [ROH] + k'_1 k'_2 k'_3 k'_{-4} k'_5 \cdot [GSH] \cdot [ROOH] \\
& + k'_{-1} k'_3 k'_{-4} k'_5 k'_6 \cdot [GSSG] \cdot [ROH] + k'_{-1} k'_{-2} k'_{-4} k'_5 k'_6 \cdot [GSSG] \cdot [ROH] \\
& + k'_1 k'_{-2} k'_{-3} k'_5 k'_6 \cdot [H_2O] \cdot [ROOH] + k'_{-1} k'_{-2} k'_{-3} k'_5 k'_6 \cdot [H_2O] \cdot [ROH] \\
& + k'_1 k'_{-2} k'_{-3} k'_{-4} k'_6 [H_2O] \cdot [ROOH] + k'_{-1} k'_{-2} k'_{-3} k'_{-4} k'_6 [H_2O] \cdot [ROOH] \\
& + k'_1 k'_{-2} k'_{-3} k'_{-4} k'_5 [H_2O] \cdot [ROOH] + k'_{-1} k'_{-2} k'_{-3} k'_{-4} k'_5 [H_2O] \cdot [ROH] \\
& + k'_2 k'_3 k'_4 k'_5 k'_6 [GSH]^2 [GSSG] + k'_2 k'_3 k'_4 k'_5 k'_6 [GSH]^2 [GSSG] + k'_1 k'_2 k'_3 k'_4 k'_5 [GSH]^2 [ROOH] \\
& + k'_1 k'_2 k'_3 k'_4 k'_6 [GSH]^2 [ROOH] + k'_1 k'_2 k'_4 k'_5 k'_6 [GSH]^2 [ROOH] + k'_1 k'_2 k'_3 k'_4 k'_5 [GSH]^2 \cdot [ROOH] \\
& + k'_2 k'_{-3} k'_{-4} k'_{-5} k'_6 [GSH] \cdot [GSSG] \cdot [H_2O] + k'_{-1} k'_3 k'_4 k'_5 k'_6 [GSH] \cdot [GSSG] \cdot [ROH] \\
& + k'_{-1} k'_{-2} k'_4 k'_5 k'_6 [GSH] \cdot [GSSG] \cdot [ROH] + k'_{-1} k'_3 k'_4 k'_5 k'_6 [GSH] \cdot [GSSG] \cdot [ROH] \\
& + k'_{-1} k'_{-2} k'_4 k'_{-5} k'_6 [GSH] \cdot [GSSG] \cdot [ROH] + k'_1 k'_2 k'_{-3} k'_5 k'_6 [GSH] \cdot [H_2O] \cdot [ROOH] \\
& + k'_1 k'_2 k'_{-3} k'_{-4} k'_6 [GSH] \cdot [H_2O] \cdot [ROOH] + k'_1 k'_2 k'_{-3} k'_{-4} k'_5 [GSH] \cdot [H_2O] \cdot [ROOH] \\
& + k'_{-1} k'_{-2} k'_{-3} k'_5 k'_6 [GSSG] \cdot [H_2O] \cdot [ROOH] + k'_{-1} k'_{-2} k'_{-3} k'_{-4} k'_6 [GSSG] \cdot [H_2O] \cdot [ROOH] \\
& + k'_{-1} k'_{-2} k'_{-3} k'_{-5} k'_6 [GSSG] \cdot [H_2O] \cdot [ROOH] + k'_{-1} k'_{-3} k'_{-4} k'_{-5} k'_6 [GSSG] \cdot [H_2O] \cdot [ROOH]
\end{aligned} \tag{5.13}$$

Based on the flux balances, the rate of changes in GSH and GSSG can be written in terms of steady-state fluxes of GPx and GR enzymes (J_{GPx} and J_{GR}) as

$$\frac{d[GSH]}{dt} = 2J_{GR} - 2J_{GPx} \tag{5.14}$$

$$\frac{d[GSSG]}{dt} = J_{GPx} - 2J_{GR} \tag{5.15}$$

This model was used to conduct an initial theoretical analysis, and we tried to optimize the model using our clinical data and relevant literature. However, the complexity of the model made it challenging to obtain any meaningful results. As a result, we have decided not to include these findings in the main text of the thesis.

5.5.4 Use of $\frac{GSSG}{GSH^2}$ ratio: perspectives

The relative ratio between the reduced and oxidized forms, GSH and GSSG based on redox potentials, is frequently used to explain redox regulation and other biological processes (Sarsour *et al.* [182], Jones [183], Millis *et al.* [184]). GSH is a significant reactant for reactive oxygen species; therefore, redox status is expressed as the ratio of the concentrations of GSH and GSSG. These studies support that GSH-GSSG redox potential drives several cellular biological processes (Zitika, [185]). It is often used in the literature as one of the markers for explaining oxidative stress in several disease conditions. The total concentration of GSH couple was reported to be present in normal cells in the ranges of 1-10 *mM* (Zitika, [185]). In normal conditions, the GSH: GSSG ratio was found to be of the order of 100:1, whereas the ratio values were of the order of 10:1 or 1:1 under the oxidative stress conditions.

We highlight the rationale behind the use of relative ratio between the concentrations does not address the contribution of enzymes and enzyme kinetics. There is consensus in the literature pointing out the drawbacks of this approach only based on the thermodynamic principles (Flohe *et al.* [186]). Redox potential can not be used directly to explain the extent of reactions involved or their velocities. These GPx and GR activities contribute to the cellular defense against different stress conditions. Therefore, we think a sufficient understanding needs to be obtained from the models of enzyme kinetics.

The redox potential of a reaction can be expressed as the Nernst equation, which is given by

$$\Delta E_{cell} = \Delta E_{cell}^0 - \frac{RT}{zF} \log Q$$

where E_{cell} is the cell potential and Q is the reaction quotient. For the following conversion reaction



the reaction quotient will be given by $Q = \frac{GSSG}{GSH^2 H_2O_2}$. We define a variable called G -ratio, which is given by $\frac{GSSG}{GSH^2}$, which will be used for the further analysis below.

5.5.5 Model-derived relationships for $\frac{GSSG}{GSH^2}$ ratio

The expressions for fluxes, J_{GPx} and J_{GR} obtained using steady-state assumptions are given in 5.14-5.15. Here $k_i, i = 1, \dots, 6$ and $k'_i, i = 1, \dots, 6$ are unitary rate constants. Rewriting J_{GPx} and J_{GR} using $K_i = \frac{k_{-i}}{k_i}$ and $K'_i = \frac{k'_{-i}}{k'_i}$ as

$$J_{GPx} = \frac{k'_1 k'_2 k'_3 k'_4 k'_5 k'_6 \left([GSH]^2 \cdot [ROOH] - K'_1 K'_2 K'_3 K'_4 K'_5 K'_6 \cdot [GSSG] \cdot [ROH] \cdot [H_2O] \right) E_2^0}{DEN2} \quad (5.16)$$

$$J_{GR} = \frac{k_1 k_2 k_3 k_4 k_5 k_6 \left([GSSG] \cdot [H] - K_1 K_2 K_3 K_4 K_5 K_6 [GSH]^2 \cdot [N] \right) E_1^0}{DEN1} \quad (5.17)$$

Steady-state assumptions $\frac{d[GSH]}{dt} = 0$ and $\frac{d[GSSG]}{dt} = 0$, gives $J_{GPx} = J_{GR}$, thereby,

$$\begin{aligned} & \frac{k'_1 k'_2 k'_3 k'_4 k'_5 k'_6 \cdot \left([GSH]^2 \cdot [H_2O_2] - K'_1 K'_2 K'_3 K'_4 K'_5 K'_6 \cdot [GSSG] \cdot [H_2O] \right) E_2^0}{DEN2} \\ &= \frac{k_1 k_2 k_3 k_4 k_5 k_6 \cdot \left([GSSG] \cdot [H] - K_1 K_2 K_3 K_4 K_5 K_6 [GSH]^2 \cdot [N] \right) E_1^0}{DEN1} \end{aligned} \quad (5.18)$$

\Rightarrow

$$\begin{aligned} & \left([GSH]^2 \cdot [H_2O_2] - K'_1 K'_2 K'_3 K'_4 K'_5 K'_6 \cdot [GSSG] \cdot [H_2O] \cdot [H_2O] \right) \\ &= \left(\frac{k_1 k_2 k_3 k_4 k_5 k_6}{k'_1 k'_2 k'_3 k'_4 k'_5 k'_6} \right) \left(\frac{DEN2}{DEN1} \right) \frac{E_1^0}{E_2^0} \left([GSSG] \cdot [H] - K_1 K_2 K_3 K_4 K_5 K_6 [GSH]^2 \cdot [N] \right) \end{aligned} \quad (5.19)$$

Which can be divided with GSH^2 on both sides and rearranged to obtain

$$\begin{aligned} & \left([H_2O_2] - K'_1 K'_2 K'_3 K'_4 K'_5 K'_6 \cdot \frac{[GSSG]}{[GSH]^2} \cdot [H_2O] \cdot [H_2O] \right) \\ &= \left(\frac{k_1 k_2 k_3 k_4 k_5 k_6 E_1^0}{DEN1} \right) \left(\frac{[GSSG]}{[GSH]^2} \cdot [H] - K_1 K_2 K_3 K_4 K_5 K_6 \cdot [N] \right) \end{aligned} \quad (5.20)$$

The most abundant *ROOH* species in cells are hydrogen peroxide (H_2O_2). The expression will be rewritten by replacing *ROOH* with H_2O_2 and *ROH* with H_2O below. The concentration for water will be assumed to be unity ($[H_2O] = 1$). Therefore, we rewrite the expression as

$$\begin{aligned} & \left([H_2O_2] - K'_1 K'_2 K'_3 K'_4 K'_5 K'_6 \cdot \frac{[GSSG]}{[GSH]^2} \right) \\ &= \left(\frac{k_1 k_2 k_3 k_4 k_5 k_6 E_1^0}{k'_1 k'_2 k'_3 k'_4 k'_5 k'_6 E_2^0} \right) \left(\frac{DEN2}{DEN1} \right) \left(\frac{[GSSG]}{[GSH]^2} \cdot [H] - K_1 K_2 K_3 K_4 K_5 K_6 \cdot [N] \right) \end{aligned} \quad (5.21)$$

Studying the behavior of $\frac{[GSSG]}{[GSH]^2}$ ratio on different conditions, using the estimates of the unitary rate constants for GPx and GR enzymes, can be beneficial in understanding the kinetics and rate-limiting steps in detail, if any.

5.5.6 8-OHdG and G-ratio comparisons

We further attempted to understand the relevance of the G-ratio between GSH and GSSG concentrations in erythrocytes using the insights from the clinical trial data. In agreement with Flohe *et al.* [186], we think it is not obvious to expect a relation between G-ratio and 8-OHdG. 8-OHdG is an oxidized de-oxy-guanosine derivative known to be the major product of DNA oxidation. Their cellular concentration has been widely used as an alternative measurement of oxidative stress. 8-OHdG has been measured for subjects from each group in the clinical trial at all three visits. We obtained G-ratio and analyzed them with the measured 8-OHdG for individuals from all three study groups at different visits through regressions. We asked whether a relationship exists between oxidative stress marker 8-OHdG and whether the G-ratio of GSH and GSSG are related.

We performed both OLS and robust regressions to understand the relationships between 8-OHdG and G-ratio for each control, D, and D group visit from the data. Results of these comparisons are shown in Figure A.2-5.22 below. We note that linear regression with ordinary least squares (OLS) gives a model with poor R^2 values. This could be happening due to outliers in the data. Linear regressions were also performed by considering the threshold Cook's distance for being an outlier at $4/\text{sample size}$. These fit as well, producing poor R^2 values for all groups. However, robust regressions provided fit with higher R^2 values here. 95% CI for the slope of the regression line contains zero in all fits. The slope is not significantly different from zero. Together, this could be suggestive that 8-OHdG levels have no effect on G-ratio.

The clinical data reveals a counterintuitive observation: the correlation between the marker for oxidative stress, 8-OHdG, and the $\frac{GSSG}{GSH^2}$ values is weak, contrary to popular belief and the traditional use of GSH to GSSG

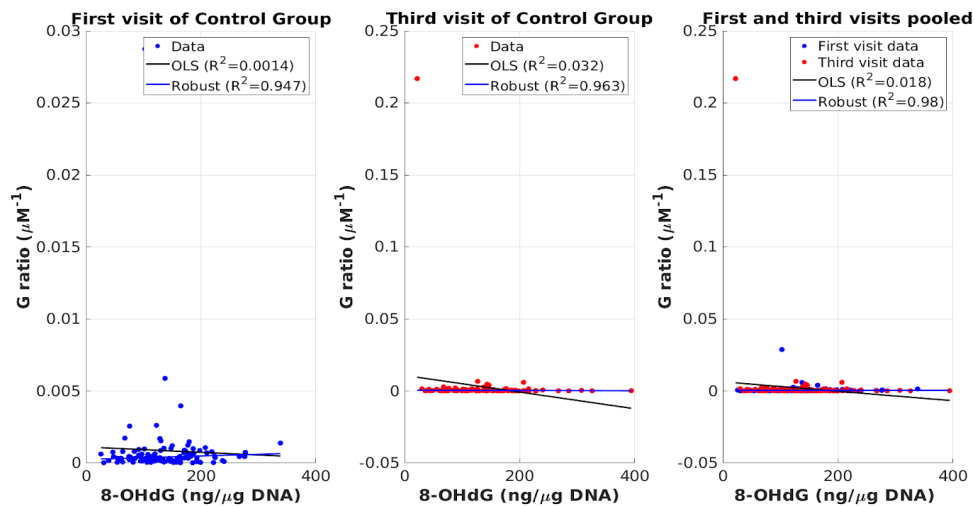


Figure 5.20: **Regression between 8-OHdG and G-ratio in the control group at the first and third visits.** Results of ordinary least squares and robust regressions first (left), third (middle), and pooled (right) visits between 8-OHdG and G-ratio are plotted here for individuals in the control group.

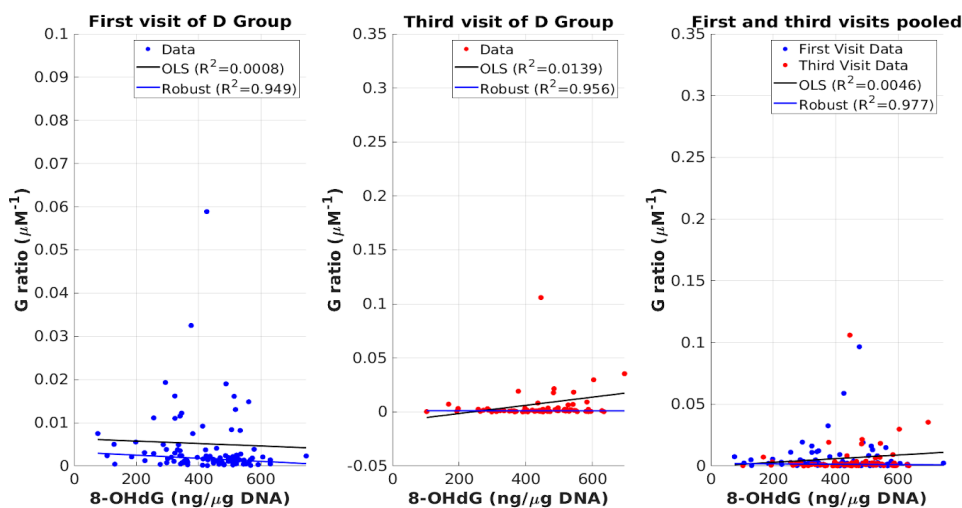


Figure 5.21: **Regression between 8-OHdG and G-ratio in the D group at the first and third visits.** Results of ordinary least squares and robust regressions first (left), third (middle), and pooled (right) visits between 8-OHdG and G-ratio are plotted here for individuals in the D group.

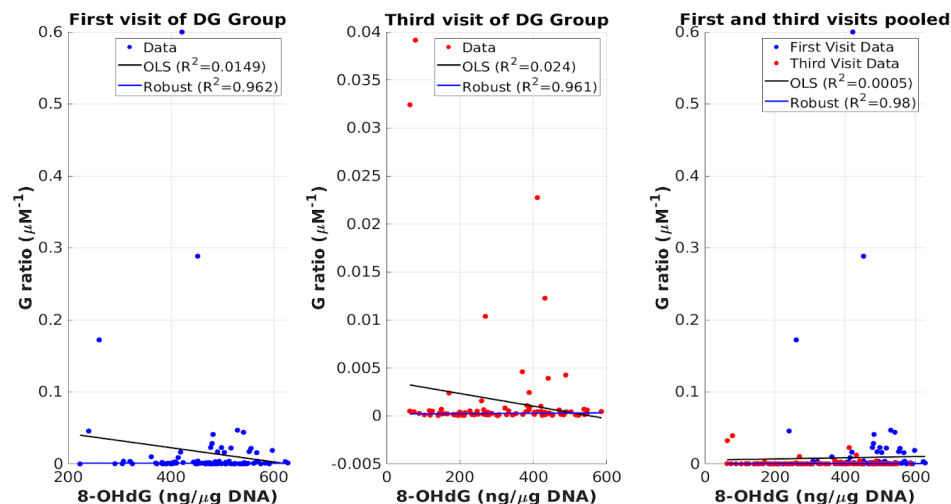


Figure 5.22: **Regression between 8-OHdG and G-ratio in the DG group at the first and third visits.** Results of ordinary least squares and robust regressions first (left), third (middle), and pooled (right) visits between 8-OHdG and G-ratio are plotted here for individuals in the DG group.

ratios. This observation challenges the consensus and is in line with Flohe *et al.* [186]. To better understand the ratio and relative concentrations of GSH and GSSG and their relevance in tracking various disease conditions, we propose constructing detailed models based on the enzyme kinetics involved in their interconversions.

Chapter 6

Conclusions and future directions

Interventions aimed at controlling hyperglycemia have been the primary line of treatment for individuals with T2D. Several studies have reported the critical roles of GSH in maintaining adequate cellular redox status. It is also known from earlier studies that low GSH is associated with different pathological conditions in T2D. In light of the ADA position, routine supplementation of antioxidants has not been recommended due to insufficient evidence about their safety and efficacy in T2D, and therefore, antioxidant supplements may not be advisable for everyone. It is very important to understand the effects of supplementation in T2D, and if it does benefit, who might benefit better, and what effective ways/doses of administration also need to be established. Considering the potential benefits of restoring redox balance, exploring the effects of GSH supplementation in counteracting the detrimental impact of hyperglycemia-induced oxidative stress is worthwhile.

In this thesis, we have utilized diverse approaches to comprehensively investigate the role of GSH metabolism in T2D and gain a deeper understanding

of the significance of redox balance in diabetes treatment, and potentially uncover novel targets for therapeutic interventions. Our research has focused explicitly on developing strategies to evaluate the impact of GSH supplementation, with the goal of enhancing personalized care for individuals with T2D.

In **Chapter 3**, we study the effect of oral GSH supplementation in individuals with T2D by conducting an extensive longitudinal and randomized controlled clinical trial. We provide evidence that oral supplementation of GSH restores the body's GSH stores and markedly diminishes oxidative DNA damage in individuals with T2D. GSH supplementation showed a stabilization effect, reducing HbA1c within three months and maintaining it thereafter in the diabetic population. Results from the clinical trial strongly suggest that GSH supplementation leads to a systemic redox improvement in T2D. Further, the augmented antioxidant reserves may help in relieving oxidative assault. Thus, we demonstrate that supplementing with GSH improves the effectiveness of standard anti-diabetic treatment for maintaining normoglycemia in individuals with T2D. The subgroup of elder individuals with T2D appears to experience substantial benefits compared to the overall diabetic population, demonstrated by a significant reduction in HbA1c. Moreover, we believe an increase in insulin secretion by β -cells was also achieved over a six-month period. A clinical application arising from our study suggests that orally administering GSH can serve as a supplementary therapy alongside anti-diabetic treatment, contributing to the efficient attainment of targets, particularly in the elderly population. These findings provide substantial evidence for the use of GSH supplementation as an adjunct therapy benefitting the regular anti-diabetic treatment in individuals with T2D.

We point out that age, type of interventions, and additionally diet modifications, etc., could be important factors determining the effectiveness of

GSH supplementation in T2D. Customized anti-diabetic treatment is necessary to achieve efficient glycemic targets rather than a one-size-fits-all approach. However, limited algorithms are available to describe how to achieve this goal. Adding GSH supplementation to the clinician’s toolkit is crucial, as it has been shown to have significant positive effects and is well-tolerated by patients. It would be necessary to understand how long the effect of GSH intervention lasts since individual antioxidant status can significantly affect the effectiveness of exogenous supplementation. Longer intervention with GSH might result in additional enhancements in glycemic parameters, such as fasting glycemia. Further research involving diverse population cohorts is needed to gain a better understanding of these effects. The insights from **Chapter 3** motivate in developing more personalized strategies for GSH supplementation considering the relevant factors, which are addressed through modeling approaches in the succeeding chapters.

In **Chapter 4**, we studied the dynamics of individual responses to oral GSH supplementation with mix-effects models to explain the longitudinal responses in patients with T2D. We modeled the average linear trajectories to explain how biochemical parameters progress during the clinical trial. Further, the model estimated the effects of GSH supply on the rate of biochemical changes after accounting for inter-individual and intra-individual variations. To the best of our understanding, this is the first model-based analysis of the inter-individual impacts of GSH supplementation in individuals with T2D. The primary findings of this study are centered around identifying the differences in biochemical responses between individuals, particularly influenced by their age group. The model findings strongly suggest that GSH supplementation improves the rate of replenishments in erythrocytic GSH stores and the rate of reduction in oxidative DNA damage in individuals with diabetes.

Furthermore, we modeled the trajectories for elder and younger diabetics independently and examined their differences in the early onset of diabetes in response to GSH supplementation. Elder and younger individuals with T2D responded differently to GSH supplementation. Notably, GSH supplementation improves the HbA1c reduction rates and fasting insulin secretion in elder individuals with T2D. The changes in GSH correlated strongly and beneficially to HbA1c, 8-OHdG, and fasting insulin changes in elder individuals with T2D. Results in this chapter also provide a way to make predictions of the recovery trajectory for individuals undergoing GSH supplementation. Furthermore, this aids in identifying the extent of recovery and examines whether individuals in these subgroups on GSH supplementation are in a better or worse regime than the average profile. This analysis could establish novel benchmarks with direct clinical use in individuals with T2D. By providing clinicians with model predictions and results, this study can assist in personalizing treatment objectives for employing oral GSH supplementation as a supplementary therapy for T2D.

In **Chapter 5**, we propose a minimal mathematical model to describe the dynamics of erythrocytic GSH turnover in response to varying extracellular conditions in T2D. We demonstrate that this model can accurately capture GSH response profiles in experimental data by conducting various cellular treatment experiments in nondiabetic, prediabetic, and diabetic individuals. The model allows straightforward estimation of relevant parameters to describe the restoration of cellular GSH pools and H_2O_2 clearance under varying conditions. Later in this chapter, we used this model to describe how different extracellular conditions affect intracellular GSH, which can help plan appropriate interventions. Using this model, we demonstrate recovery from stress and oxidative conditions in T2D as a quantal response to GSH supplementa-

tion. This model enables personalizing interventions by tracking cellular-level responses through model-parameter estimates. Our analysis of data from the GSH supplementation clinical trial showcases this capability of the model. The work done in this chapter serves as a foundation for future studies aimed at understanding interventions for improving the cellular redox state in diabetes.

The minimal model describing GSH turnover in erythrocytes has some drawbacks, as it oversimplifies the process and physiology. The observed relationships between external conditions and steady states inside cells may be influenced by multiple mechanisms involving amino acid transporters, γ -glutamyl cycle, GSH synthase, γ -glutamate cysteine ligase enzymes, etc. Nevertheless, due to its simple, functional form, the minimal model remains useful for predicting steady states. Both modeling procedures showed robustness to small but significant perturbations in GSH and GSSG concentrations. A major strength of this modeling and optimization is that from the measurements of GSH and GSSG, we provided a quantitative measure of cellular GSH influx and H_2O_2 at steady states inside erythrocytes of nondiabetic, prediabetic, and diabetic individuals. However, the study is limited by the availability of only a few data points from treatment experiments, which is why the minimal model was used for the data analysis to avoid overfitting. An approach with detailed models will require more frequent measurements of GSH over a longer duration to obtain model estimates and make precise inferences about dose-response relationships under different extracellular conditions.

Chapter 6 summarizes key findings, conclusions, and deliverables from this thesis study. We brief the outcomes of our clinical trial and its strong positioning in the T2D research to establish the effectiveness of GSH supplementation in individuals with T2D. The evidence from the clinical trial demonstrated GSH supplementation could improve erythrocytic GSH stores,

enhance antioxidant defenses, and expedite the achievement of normoglycemia in individuals with T2D. The results of our statistical and mathematical models formulated in **Chapter 4** and **Chapter 5** help in planning glutathione-based strategies with personalization goals in the development and progression of T2D. Our rigorous approaches with patient-level and cellular-level models show how biochemical and pathophysiological characteristics of patients can be used in guiding the personalization of their anti-diabetic therapy with GSH supplementation. The mixed-effects modeling approaches help decipher individual differences in the effects of GSH supplementation in individuals with T2D. We showed how GSH supplementation influences intrinsic responses to their anti-diabetic treatment through trajectories describing recovery paths and model estimates in individuals with T2D. The mathematical models formulated for describing erythrocytic GSH turnover at extracellular conditions obtained relevant model estimates in individuals with different diabetic statuses. Despite some limitations, this modeling work reveals the potential to develop complex physiological models that can differentiate between individual variations at the cellular and biochemical levels in the efficacy of GSH supplementation. We emphasize that our models informed these insights and can be used in guiding the development of more effective GSH-based interventions for diabetes management.

By gaining a comprehensive understanding of GSH turnover, we understand that there is scope to explain the redox balances and the impact of various sources of GSH, which could contribute to developing models for monitoring continuous redox status in individuals with T2D. Based on the insights from this study, we also propose to further investigate cellular GSH turnover by studying detailed enzymatic pathways in future research for a better understanding. A depiction of the reaction pathways, which can be modeled for

an improved description of GSH turnover in erythrocytes, is constructed in Figure 6.1 below. As the complexity of the model increases, obtaining the necessary experimental data for parameter estimations will also become difficult. Nevertheless, it is worthy to thoroughly examine the theory behind cellular GSH turnover and its responses in T2D conditions. Various studies

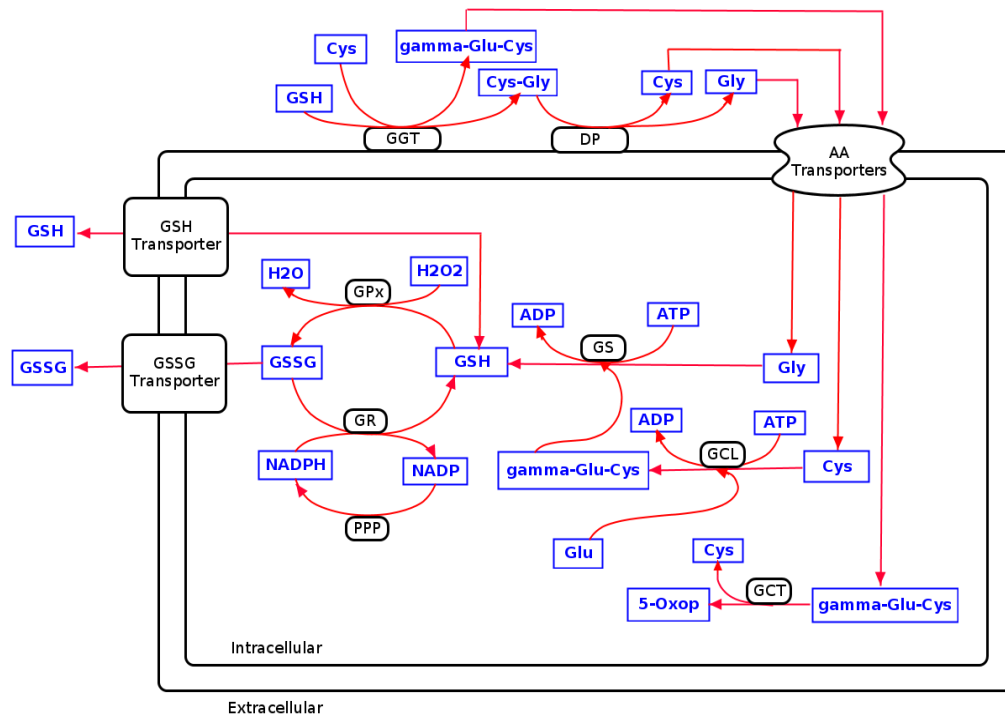


Figure 6.1: Reaction diagram for transport, intracellular synthesis, and turnover of GSH in RBCs. The enzymes involved here are glutathione peroxidase (GPx), glutathione reductase (GR), γ -glutamyl transpeptidase (GGT), glutathione synthase (GS), glutamyl-cysteine ligase (GCL), dipeptidases (DP). There are membrane-bound transporters for amino acids and glutathione export. The other abbreviations for amino acids used in the figure are glutamate (Glu), glycine (Gly), and cysteine (Cys). The reaction diagram in this figure was primarily formulated based on the concepts of [76] and [53]

have indicated that GSH depletion in individuals with diabetes can cause ROS-mediated apoptosis of β -cells, resulting in the accumulation of reactive oxygen species (ROS) that inhibit insulin secretion (Franco *et al.* [187]). To examine

the impact of GSH supplementation on systemic changes, future studies must be planned to develop compartmental models in a framework that incorporates both the dynamics of systemic glucose-insulin levels and cellular biochemical changes. The dynamics of systemic variables like glucose and insulin are popularly modeled with the Topp model (Topp *et al.* [98]). This model has been further developed to explain the physiological basis of Type 2 diabetes, for instance, hyper-secretion theory, continuous glucose, insulin monitoring, etc. (Goel [109]). A possible approach by using Topp-like models to study the mechanism of how cellular GSH status modifies the systemic measurements of individuals with T2D. This could be used to answer how GSH supplementation helped significantly lower HbA1c and increase fasting insulin levels in elder individuals with T2D.

In conclusion, our quantitative approaches have yielded results that can be readily applied in a clinical setting to define therapeutic targets using GSH-based interventions for treating individuals with T2D. Our model predictions provide valuable insights for defining personalized treatment targets and optimizing recovery. Understanding the role of GSH-mediated redox regulation in controlling the development and progression of complications and preventive measures against oxidative damage are shown to have the potential to improve T2D treatments. While our model-informed insights are intriguing and show promise for personalized diabetes target setting, further research is needed to evaluate and refine the effectiveness of our approach. Gaining a better quantitative understanding of the role of GSH in redox regulation in diabetes through this work opens ways to personalize targets in T2D treatment more effectively. Our simple yet powerful models for profiling changes in GSH metabolism at different levels stand out as significant to help in personalizing anti-diabetic interventions.

Bibliography

- [1] American Diabetes Association. Diagnosis and classification of diabetes mellitus. *Diabetes Care*, 34(Supplement_1):S62–S69, 2011.
- [2] JD Rockefeller. *Diabetes: symptoms, causes, treatment, and prevention*. Create Space Independent Publishing Platform, 2015.
- [3] Ralph A DeFronzo, Ele Ferrannini, Leif Groop, Robert R Henry, William H Herman, Jens Juul Holst, Frank B Hu, C Ronald Kahn, Itamar Raz, Gerald I Shulman, et al. Type 2 diabetes mellitus. *Nature Reviews Disease Primers*, 1(1):1–22, 2015.
- [4] Centers for Disease Control and Prevention. Diabetes report card 2019. *Centers for Disease Control and Prevention, US Dept of Health and Human Services*, 2020.
- [5] Bin Zhou, Yuan Lu, Kaveh Hajifathalian, James Bentham, Mariachiara Di Cesare, Goodarz Danaei, Honor Bixby, Melanie J Cowan, Mohammed K Ali, Cristina Taddei, et al. Worldwide trends in diabetes since 1980: a pooled analysis of 751 population-based studies with 4· 4 million participants. *The Lancet*, 387(10027):1513–1530, 2016.
- [6] International diabetes federation. Atlas, diabetes. *IDF Diabetes Atlas*, 7th edn., 33:2, 2015.

- [7] Mohammad G Saklayen. The global epidemic of the metabolic syndrome. *Current Hypertension Reports*, 20(2):1–8, 2018.
- [8] Ranjit Unnikrishnan, Rajendra Pradeepa, Shashank R Joshi, and Viswanathan Mohan. Type 2 diabetes: demystifying the global epidemic. *Diabetes*, 66(6):1432–1442, 2017.
- [9] Sarah Wild, Gojka Roglic, Anders Green, Richard Sicree, and Hilary King. Global prevalence of diabetes: estimates for the year 2000 and projections for 2030. *Diabetes Care*, 27(5):1047–1053, 2004.
- [10] Pouya Saeedi, Inga Petersohn, Paraskevi Salpea, Belma Malanda, Suvi Karuranga, Nigel Unwin, Stephen Colagiuri, Leonor Guariguata, Ayesha A Motala, Katherine Ogurtsova, et al. Global and regional diabetes prevalence estimates for 2019 and projections for 2030 and 2045: Results from the international diabetes federation diabetes atlas. *Diabetes Research and Clinical Practice*, 157:107843, 2019.
- [11] Priya Shetty. Public health: India’s diabetes time bomb. *Nature*, 485(7398):S14–S16, 2012.
- [12] Seema Abhijeet Kaveeshwar and Jon Cornwall. The current state of diabetes mellitus in india. *The Australasian Medical Journal*, 7(1):45, 2014.
- [13] Iciar Martín-Timón, Cristina Sevillano-Collantes, Amparo Segura-Galindo, and Francisco Javier del Cañizo-Gómez. Type 2 diabetes and cardiovascular disease: have all risk factors the same strength? *World Journal of Diabetes*, 5(4):444, 2014.

- [14] Christian Rask-Madsen and George L King. Vascular complications of diabetes: mechanisms of injury and protective factors. *Cell metabolism*, 17(1):20–33, 2013.
- [15] Barry Commoner, Jonathan Townsend, and George E Pake. Free radicals in biological materials. *Nature*, 174:689–691, 1954.
- [16] Celia Andrés Juan, José Manuel Pérez de la Lastra, Francisco J Plou, and Eduardo Pérez-Lebeña. The chemistry of reactive oxygen species (ros) revisited: outlining their role in biological macromolecules (dna, lipids and proteins) and induced pathologies. *International Journal of Molecular Sciences*, 22(9):4642, 2021.
- [17] Dmitry B Zorov, Magdalena Juhaszova, and Steven J Sollott. Mitochondrial reactive oxygen species (ros) and ros-induced ros release. *Physiological Reviews*, 94(3):909–950, 2014.
- [18] Jérôme Roy, Jean-Marie Galano, Thierry Durand, Jean-Yves Le Guennec, and Jetty Chung-Yung Lee. Physiological role of reactive oxygen species as promoters of natural defenses. *The FASEB Journal*, 31(9):3729–3745, 2017.
- [19] Marian Valko, Dieter Leibfritz, Jan Moncol, Mark TD Cronin, Milan Mazur, and Joshua Telser. Free radicals and antioxidants in normal physiological functions and human disease. *The International Journal of Biochemistry & Cell Biology*, 39(1):44–84, 2007.
- [20] Sanaa K Bardaweel, Mustafa Gul, Muhammad Alzweiri, Aman Ishaqat, Husam A Alsalamat, and Rasha M Bashatwah. Reactive oxygen species: The dual role in physiological and pathological conditions of the human body. *The Eurasian Journal of Medicine*, 50(3):193, 2018.

- [21] Sheldon Magder. Reactive oxygen species: toxic molecules or spark of life? *Critical Care*, 10(1):1–8, 2006.
- [22] Sergio Di Meo, Tanea T Reed, Paola Venditti, Victor Manuel Victor, et al. Role of ros and rns sources in physiological and pathological conditions. *Oxidative Medicine and Cellular Longevity*, 2016, 2016.
- [23] Ferdinando Giacco and Michael Brownlee. Oxidative stress and diabetic complications. *Circulation Research*, 107(9):1058–1070, 2010.
- [24] Roberto Marchioli, Guido Finazzi, Raffaele Landolfi, Jack Kutti, Heinz Gisslinger, Carlo Patrono, Raphael Marilus, Ana Villegas, Gianni Tognoni, and Tiziano Barbui. Vascular and neoplastic risk in a large cohort of patients with polycythemia vera. *Journal of Clinical Oncology*, 23(10):2224–2232, 2005.
- [25] Cristina Fernández-Mejía. Oxidative stress in diabetes mellitus and the role of vitamins with antioxidant actions. *Oxidative stress and chronic degenerative diseases-a role for antioxidants*, 209, 2013.
- [26] Joseph L Evans, Ira D Goldfine, Betty A Maddux, and Gerold M Grodsky. Oxidative stress and stress-activated signaling pathways: a unifying hypothesis of type 2 diabetes. *Endocrine Reviews*, 23(5):599–622, 2002.
- [27] Cristina Espinosa-Diez, Verónica Miguel, Daniela Mennerich, Thomas Kietzmann, Patricia Sánchez-Pérez, Susana Cadenas, and Santiago Lamas. Antioxidant responses and cellular adjustments to oxidative stress. *Redox Biology*, 6:183–197, 2015.
- [28] John W Baynes. Role of oxidative stress in development of complications in diabetes. *Diabetes*, 40(4):405–412, 1991.

- [29] Esra Birben, Umit Murat Sahiner, Cansin Sackesen, Serpil Erzurum, and Omer Kalayci. Oxidative stress and antioxidant defense. *World Allergy Organization Journal*, 5:9–19, 2012.
- [30] Ergul Belge Kurutas. The importance of antioxidants which play the role in cellular response against oxidative/nitrosative stress: current state. *Nutrition Journal*, 15(1):1–22, 2015.
- [31] Gabriele Pizzino, Natasha Irrera, Mariapaola Cucinotta, Giovanni Pallio, Federica Mannino, Vincenzo Arcoraci, Francesco Squadrito, Domenica Altavilla, Alessandra Bitto, et al. Oxidative stress: harms and benefits for human health. *Oxidative Medicine and Cellular Longevity*, 2017, 2017.
- [32] Martin R Bennett, Sanjay Sinha, and Gary K Owens. Vascular smooth muscle cells in atherosclerosis. *Circulation Research*, 118(4):692–702, 2016.
- [33] Guoyao Wu, Yun-Zhong Fang, Sheng Yang, Joanne R Lupton, and Nancy D Turner. Glutathione metabolism and its implications for health. *The Journal of Nutrition*, 134(3):489–492, 2004.
- [34] Helmut Sies. Glutathione and its role in cellular functions. *Free Radical Biology and Medicine*, 27(9-10):916–921, 1999.
- [35] Danyelle M Townsend, Kenneth D Tew, and Haim Tapiero. The importance of glutathione in human disease. *Biomedicine & Pharmacotherapy*, 57(3-4):145–155, 2003.
- [36] Shelly C Lu. Regulation of glutathione synthesis. *Current Topics in Cellular Regulation*, 36:95–116, 2001.

- [37] Owen W Griffith and Alton Meister. Glutathione: interorgan translocation, turnover, and metabolism. *Proceedings of the National Academy of Sciences*, 76(11):5606–5610, 1979.
- [38] Fallon K Lutchmansingh, Jean W Hsu, Franklyn I Bennett, Asha V Badaloo, Norma McFarlane-Anderson, Georgiana M Gordon-Strachan, Rosemarie A Wright-Pascoe, Farook Jahoor, and Michael S Boyne. Glutathione metabolism in type 2 diabetes and its relationship with microvascular complications and glycemia. *PLOS ONE*, 13(6):e0198626, 2018.
- [39] Katarzyna Gawlik, Jerzy Waław Naskalski, Danuta Fedak, Dorota Pawlica-Gosiewska, Urszula Grudzień, Paulina Dumnicka, MT Małcki, and Bogdan Solnica. Markers of antioxidant defense in patients with type 2 diabetes. *Oxidative Medicine and Cellular Longevity*, 2016, 2016.
- [40] PJ Thornalley, AC McLellan, TW Lo, J Benn, and PH Sönksen. Negative association between erythrocyte reduced glutathione concentration and diabetic complications. *Clinical Science*, 91(5):575–582, 1996.
- [41] Jhankar D Acharya, Amol J Pande, Suyog M Joshi, Chittaranjan S Yajnik, and Saroj S Ghaskadbi. Treatment of hyperglycaemia in newly diagnosed diabetic patients is associated with a reduction in oxidative stress and improvement in β -cell function. *Diabetes Metabolism Research and Reviews*, 30(7):590–598, 2014.
- [42] Rashmi Kulkarni, Jhankar Acharya, Saroj Ghaskadbi, and Pranay Goel. Thresholds of oxidative stress in newly diagnosed diabetic patients on intensive glucose-control therapy. *PLOS ONE*, 9(6):e100897, 2014.

- [43] Henry Jay Forman and Hongqiao Zhang. Targeting oxidative stress in disease: Promise and limitations of antioxidant therapy. *Nature Reviews Drug Discovery*, 20(9):689–709, 2021.
- [44] American Diabetes Association et al. Standards of medical care in diabetes—2018 abridged for primary care providers. *Clinical diabetes: a publication of the American Diabetes Association*, 36(1):14, 2018.
- [45] Saurabh Ram Bihari Lal Shrivastava, Prateek Saurabh Shrivastava, and Jegadeesh Ramasamy. Role of self-care in management of diabetes mellitus. *Journal of Diabetes & Metabolic Disorders*, 12(1):1–5, 2013.
- [46] Mary D Adu, Usman H Malabu, Aduli EO Malau-Aduli, and Bunmi S Malau-Aduli. Enablers and barriers to effective diabetes self-management: A multi-national investigation. *PLOS ONE*, 14(6):e0217771, 2019.
- [47] Shang-Jyh Chiou. Using patient profiles for sustained diabetes management among people with type 2 diabetes. *Preventing Chronic Disease*, 20, 2023.
- [48] Silvio E Inzucchi, Richard M Bergenstal, John B Buse, Michaela Diamant, Ele Ferrannini, Michael Nauck, Anne L Peters, Apostolos Tsapas, Richard Wender, and David R Matthews. Management of hyperglycemia in type 2 diabetes: a patient-centered approach: position statement of the american diabetes association (ada) and the european association for the study of diabetes (easd). *Diabetes Care*, 35(6):1364–1379, 2012.
- [49] Biplab Giri, Sananda Dey, Tanaya Das, Mrinmoy Sarkar, Jhimli Banerjee, and Sandeep Kumar Dash. Chronic hyperglycemia mediated physiological alteration and metabolic distortion leads to organ dysfunction,

- infection, cancer progression and other pathophysiological consequences: an update on glucose toxicity. *Biomedicine & pharmacotherapy*, 107:306–328, 2018.
- [50] Caroline Maria Oliveira Volpe, Pedro Henrique Villar-Delfino, Paula Martins Ferreira Dos Anjos, and José Augusto Nogueira-Machado. Cellular death, reactive oxygen species (ros) and diabetic complications. *Cell Death & Disease*, 9(2):119, 2018.
- [51] Sevgican Demir, Peter P Nawroth, Stephan Herzig, and Bilgen Ekim Üstünel. Emerging targets in type 2 diabetes and diabetic complications. *Advanced Science*, 8(18):2100275, 2021.
- [52] American Diabetes Association. Standards of medical care in diabetes—2016 abridged for primary care providers. *Clinical Diabetes*, 34(1):3, 2016.
- [53] Helmut Sies and E Cadenas. Oxidative stress: damage to intact cells and organs. *Philosophical Transactions of the Royal Society of London. B, Biological Sciences*, 311(1152):617–631, 1985.
- [54] Enrique Cadenas and Helmut Sies. Oxidative stress: excited oxygen species and enzyme activity. *Advances in Enzyme Regulation*, 23:217–237, 1985.
- [55] Helmut Sies, Carsten Berndt, and Dean P Jones. Oxidative stress. *Annual Review of Biochemistry*, 86:715–748, 2017.
- [56] Helmut Sies, Wilhelm Stahl, and Alex Sevanian. Nutritional, dietary and postprandial oxidative stress. *The Journal of Nutrition*, 135(5):969–972, 2005.

- [57] Helmut Sies, D P Jones, and G Fink. Encyclopedia of stress. *Oxidative Stress*, 3:45–8, 2007.
- [58] Helmut Sies. Biological redox systems and oxidative stress. *Cellular and Molecular Life Sciences*, 64:2181–2188, 2007.
- [59] Helmut Sies. Role of metabolic h₂o₂ generation: redox signaling and oxidative stress. *Journal of Biological Chemistry*, 289(13):8735–8741, 2014.
- [60] Helmut Sies. Oxidative stress: a concept in redox biology and medicine. *Redox Biology*, 4:180–183, 2015.
- [61] Fabrice Collin. Chemical basis of reactive oxygen species reactivity and involvement in neurodegenerative diseases. *International journal of molecular sciences*, 20(10):2407, 2019.
- [62] Jonas Nordberg and Elias SJ Arnér. Reactive oxygen species, antioxidants, and the mammalian thioredoxin system. *Free radical biology and medicine*, 31(11):1287–1312, 2001.
- [63] Kenneth B Storey. Oxidative stress: animal adaptations in nature. *Brazilian Journal of Medical and Biological Research*, 29:1715–1733, 1996.
- [64] Dean P Jones and Helmut Sies. The redox code. *Antioxidants & Redox Signaling*, 23(9):734–746, 2015.
- [65] Md Torequl Islam. Oxidative stress and mitochondrial dysfunction-linked neurodegenerative disorders. *Neurological Research*, 39(1):73–82, 2017.

- [66] Volodymyr I Lushchak. Interplay between bioenergetics and oxidative stress at normal brain aging. aging as a result of increasing disbalance in the system oxidative stress–energy provision. *Pflügers Archiv-European Journal of Physiology*, 473(5):713–722, 2021.
- [67] Enrique Cadenas, Lester Packer, and Maret G Traber. Antioxidants, oxidants, and redox impacts on cell function—a tribute to helmut sies—. *Archives of Biochemistry and Biophysics*, 595:94–99, 2016.
- [68] Barry Halliwell. Antioxidant defence mechanisms: from the beginning to the end (of the beginning). *Free Radical Research*, 31(4):261–272, 1999.
- [69] Barry Halliwell. Antioxidants in human health and disease. *Annual Review of Nutrition*, 16(1):33–50, 1996.
- [70] Daniela Salvemini, Zhi-Qiang Wang, Jay L Zweier, Alexandre Samouilov, Heather Macarthur, Thomas P Misko, Mark G Currie, Salvatore Cuzzocrea, James A Sikorski, and Dennis P Riley. A nonpeptidyl mimic of superoxide dismutase with therapeutic activity in rats. *Science*, 286(5438):304–306, 1999.
- [71] Andrea M Vincent, James W Russell, Kelli A Sullivan, Carey Backus, John M Hayes, Lisa L McLean, and Eva L Feldman. Sod2 protects neurons from injury in cell culture and animal models of diabetic neuropathy. *Experimental Neurology*, 208(2):216–227, 2007.
- [72] Paola Otero, Bartolomé Bonet, Emilio Herrera, and Alberto Rabano. Development of atherosclerosis in the diabetic balb/c mice: prevention with vitamin e administration. *Atherosclerosis*, 182(2):259–265, 2005.
- [73] Yanling Zhang, Jun Wada, Izumi Hashimoto, Jun Eguchi, Akihiro Yasuhara, Yashpal S Kanwar, Kenichi Shikata, and Hirofumi Makino.

- Therapeutic approach for diabetic nephropathy using gene delivery of translocase of inner mitochondrial membrane 44 by reducing mitochondrial superoxide production. *Journal of the American Society of Nephrology*, 17(4):1090–1101, 2006.
- [74] Renu A Kowluru, Vibhuti Kowluru, Ye Xiong, and Ye-Shih Ho. Over-expression of mitochondrial superoxide dismutase in mice protects the retina from diabetes-induced oxidative stress. *Free Radical Biology and Medicine*, 41(8):1191–1196, 2006.
- [75] Frederick R DeRubertis, Patricia A Craven, and Mona F Melhem. Acceleration of diabetic renal injury in the superoxide dismutase knockout mouse: effects of tempol. *Metabolism*, 56(9):1256–1264, 2007.
- [76] Alton Meister and Mary E Anderson. Glutathione. *Annual Review of Biochemistry*, 52(1):711–760, 1983.
- [77] Shelly C Lu. Regulation of glutathione synthesis. *Molecular Aspects of Medicine*, 30(1-2):42–59, 2009.
- [78] Minette Lagman, Judy Ly, Tommy Saing, Manpreet Kaur Singh, Enrique Vera Tudela, Devin Morris, Po-Ting Chi, Cesar Ochoa, Airani Sathananthan, and Vishwanath Venketaraman. Investigating the causes for decreased levels of glutathione in individuals with type ii diabetes. *PLOS ONE*, 10(3):e0118436, 2015.
- [79] Rajagopal V Sekhar, Siripoom V McKay, Sanjeet G Patel, Anuradha P Guthikonda, Vasumathi T Reddy, Ashok Balasubramanyam, and Farook Jahoor. Glutathione synthesis is diminished in patients with uncontrolled diabetes and restored by dietary supplementation with cysteine and glycine. *Diabetes Care*, 34(1):162–167, 2011.

- [80] Réjeanne Gougeon, José A Morais, Stéphanie Chevalier, Sandra Pereira, Marie Lamarche, and Errol B Marliss. Determinants of whole-body protein metabolism in subjects with and without type 2 diabetes. *Diabetes Care*, 31(1):128–133, 2008.
- [81] Panagiotis Halvatsiotis, Kevin R Short, Maureen Bigelow, and K Sreekumar Nair. Synthesis rate of muscle proteins, muscle functions, and amino acid kinetics in type 2 diabetes. *Diabetes*, 51(8):2395–2404, 2002.
- [82] Dan Nguyen, W Hsu Jean, Farook Jahoor, and V Sekhar Rajagopal. Effect of increasing glutathione with cysteine and glycine supplementation on mitochondrial fuel oxidation, insulin sensitivity, and body composition in older hiv-infected patients. *The Journal of Clinical Endocrinology & Metabolism*, 99(1):169–177, 2014.
- [83] Katherine Esposito, Francesco Nappo, Raffaele Marfella, Giovanni Giugliano, Francesco Giugliano, Myriam Ciotola, Lisa Quagliari, Antonio Ceriello, and Dario Giugliano. Inflammatory cytokine concentrations are acutely increased by hyperglycemia in humans: role of oxidative stress. *Circulation*, 106(16):2067–2072, 2002.
- [84] American Diabetes Association. Standards of medical care in diabetes: 2012. *Diabetes Care*, 35(1):S11–S63, 2012.
- [85] Nazzareno Ballatori, Suzanne M Krance, Sylvia Notenboom, Shujie Shi, Kim Tieu, and Christine L Hammond. Glutathione dysregulation and the etiology and progression of human diseases. 2009.
- [86] Hisham Waggiallah, Mohammed Alzohairy, et al. The effect of oxidative stress on human red cells glutathione peroxidase, glutathione reductase

- level, and prevalence of anemia among diabetics. *North American Journal of Medical Sciences*, 3(7):344, 2011.
- [87] Rajagopal V Sekhar, Sanjeet G Patel, Anuradha P Guthikonda, Marvin Reid, Ashok Balasubramanyam, George E Taffet, and Farook Jahoor. Deficient synthesis of glutathione underlies oxidative stress in aging and can be corrected by dietary cysteine and glycine supplementation-. *The American Journal of Clinical Nutrition*, 94(3):847–853, 2011.
- [88] Giuseppe Paolisso, Giosue Di Maro, Gennaro Pizza, Anna D’Amore, Saverio Sgambato, Paola Tesauro, Michele Varricchio, and Felice D’Onofrio. Plasma gsh/gssg affects glucose homeostasis in healthy subjects and non-insulin-dependent diabetics. *American Journal of Physiology-Endocrinology And Metabolism*, 263(3):E435–E440, 1992.
- [89] Giuseppe Paolisso, Dario Giugliano, Gennaro Pizza, Antonio Gambardella, Paola Tesauro, Michele Varricchio, and Felice D’Onofrio. Glutathione infusion potentiates glucose-induced insulin secretion in aged patients with impaired glucose tolerance. *Diabetes Care*, 15(1):1–7, 1992.
- [90] John P Richie, Sailendra Nichenametla, Wanda Neidig, Ana Calcagnotto, Jeremy S Haley, Todd D Schell, and Joshua E Muscat. Randomized controlled trial of oral glutathione supplementation on body stores of glutathione. *European Journal of Nutrition*, 54:251–263, 2015.
- [91] Jason Allen and Ryan D Bradley. Effects of oral glutathione supplementation on systemic oxidative stress biomarkers in human volunteers. *The Journal of Alternative and Complementary Medicine*, 17(9):827–833, 2011.

- [92] Daniela Buonocore, Matteo Grosini, Silvana Giardina, Angela Micheli, Mariaelena Carrabetta, Antonio Seneci, Manuela Verri, Maurizia Dossena, and Fulvio Marzatico. Bioavailability study of an innovative orobuccal formulation of glutathione. *Oxidative Medicine and Cellular Longevity*, 2016, 2016.
- [93] Brianna K Bruggeman, Katharine E Storo, Haley M Fair, Andrew J Wommack, Colin R Carriker, and James M Smoliga. The absorptive effects of orobuccal non-liposomal nano-sized glutathione on blood glutathione parameters in healthy individuals: A pilot study. *PLOS ONE*, 14(4):e0215815, 2019.
- [94] Yuki Ueno, Miho Kizaki, Ryusuke Nakagiri, Toshikazu Kamiya, Hiroyuki Sumi, and Toshihiko Osawa. Dietary glutathione protects rats from diabetic nephropathy and neuropathy. *The Journal of Nutrition*, 132(5):897–900, 2002.
- [95] Johanna T Dwyer, Paul M Coates, and Michael J Smith. Dietary supplements: regulatory challenges and research resources. *Nutrients*, 10(1):41, 2018.
- [96] Richard N Bergman, Y Ziya Ider, Charles R Bowden, and Claudio Cobelli. Quantitative estimation of insulin sensitivity. *American Journal of Physiology-Endocrinology And Metabolism*, 236(6):E667, 1979.
- [97] Andrea De Gaetano and Ovide Arino. Mathematical modelling of the intravenous glucose tolerance test. *Journal of Mathematical Biology*, 40:136–168, 2000.
- [98] Brian Topp, Keith Promislow, Gerda Devries, Robert M Miura, and Diane T Finegood. A model of β -cell mass, insulin, and glucose kinetics:

- pathways to diabetes. *Journal of Theoretical Biology*, 206(4):605–619, 2000.
- [99] Chiara Dalla Man, Robert A Rizza, and Claudio Cobelli. Meal simulation model of the glucose-insulin system. *IEEE Transactions on biomedical engineering*, 54(10):1740–1749, 2007.
- [100] Petra M Jauslin, Nicolas Frey, and Mats O Karlsson. Modeling of 24-hour glucose and insulin profiles of patients with type 2 diabetes. *The Journal of Clinical Pharmacology*, 51(2):153–164, 2011.
- [101] Roy Malka, David M Nathan, and John M Higgins. Mechanistic modeling of hemoglobin glycation and red blood cell kinetics enables personalized diabetes monitoring. *Science Translational Medicine*, 8(359):359ra130–359ra130, 2016.
- [102] Eugene Ackerman, Laël C Gatewood, John W Rosevear, and George D Molnar. Model studies of blood-glucose regulation. *The Bulletin of Mathematical Biophysics*, 27:21–37, 1965.
- [103] M Della Corte, S Romano, MR Voeghelin, and M Serio. On a mathematical model for the analysis of the glucose tolerance curve. *Diabetes*, 19(6):445–449, 1970.
- [104] G Segre, G Turco, and G Vercellone. Modeling blood glucose and insulin kinetics in normal, diabetic and obese subjects. *Diabetes*, 22(2):94–103, 1973.
- [105] R Srinivasan, Arnold H Kadish, and R Sridhar. A mathematical model for the control mechanism of free fatty acid-glucose metabolism in normal humans. *Computers and Biomedical Research*, 3(2):146–165, 1970.

- [106] Ewart R Carson, L Finkelstein, and C Cobelli. Mathematical modeling of metabolic and endocrine systems: Model formulation, identification, and validation. *John Wiley & Sons, Inc., 1983, 394*, 1983.
- [107] Claudio Cobelli, G Federspil, G Pacini, A Salvan, and C Scandellari. An integrated mathematical model of the dynamics of blood glucose and its hormonal control. *Mathematical Biosciences*, 58(1):27–60, 1982.
- [108] Pranay Goel, Durga Parkhi, Amlan Barua, Mita Shah, and Saroj Ghaskadbi. A minimal model approach for analyzing continuous glucose monitoring in type 2 diabetes. *Frontiers in Physiology*, 9:673, 2018.
- [109] Pranay Goel. Insulin resistance or hypersecretion? the β ig picture revisited. *Journal of Theoretical Biology*, 384:131–139, 2015.
- [110] Katharina Fritzen, Lutz Heinemann, and Oliver Schnell. Modeling of diabetes and its clinical impact. *Journal of Diabetes Science and Technology*, 12(5):976–984, 2018.
- [111] James E Bailey. Mathematical modeling and analysis in biochemical engineering: past accomplishments and future opportunities. *Biotechnology Progress*, 14(1):8–20, 1998.
- [112] David Fell and Athel Cornish-Bowden. *Understanding the control of metabolism*, volume 2. Portland press London, 1997.
- [113] JG Reich and EE Sel'kov. Energy metabolism of the cell academic press, 1981.
- [114] Tom A Rapoport, Reinhart Heinrich, Gisela Jacobasch, and Samuel Rapoport. A linear steady-state treatment of enzymatic chains: A math-

- ematical model of glycolysis of human erythrocytes. *European Journal of Biochemistry*, 42(1):107–120, 1974.
- [115] Fazoil I Ataulakhanov, Victor M Vitvitsky, Anatoly M Zhabotinsky, Aleksei V Pichugin, Olga V Platonovo, Boris N Kholodenko, and Lev I Ehrlich. The regulation of glycolysis in human erythrocytes: the dependence of the glycolytic flux on the atp concentration. *European Journal of Biochemistry*, 115(2):359–365, 1981.
- [116] Neema Jamshidi, Jeremy S Edwards, Tom Fahland, George M Church, and Bernhard O Palsson. Dynamic simulation of the human red blood cell metabolic network. *Bioinformatics*, 17(3):286–287, 2001.
- [117] Abhay Joshi and Bernhard O Palsson. Metabolic dynamics in the human red cell: Part i—a comprehensive kinetic model. *Journal of Theoretical Biology*, 141(4):515–528, 1989.
- [118] Yoichi Nakayama, Ayako Kinoshita, and Masaru Tomita. Dynamic simulation of red blood cell metabolism and its application to the analysis of a pathological condition. *Theoretical Biology and Medical Modelling*, 2(1):1–11, 2005.
- [119] Hermann-Georg Holzhutter, Gisela Jacobaxch, and Alex Bisdorff. Mathematical modelling of metabolic pathways affected by an enzyme deficiency: A mathematical model of glycolysis in normal and pyruvate-kinase-deficient red blood cells. *European Journal of Biochemistry*, 149(1):101–111, 1985.
- [120] Abhay Joshi and Bernhard O Palsson. Metabolic dynamics in the human red cell: Part ii—interactions with the environment. *Journal of Theoretical Biology*, 141(4):529–545, 1989.

- [121] Abhay Joshi and Bernhard O Palsson. Metabolic dynamics in the human red cell. part iii—metabolic reaction rates. *Journal of Theoretical Biology*, 142(1):41–68, 1990.
- [122] Abhay Joshi and Bernhard O Palsson. Metabolic dynamics in the human red cell. part iv—data prediction and some model computations. *Journal of Theoretical Biology*, 142(1):69–85, 1990.
- [123] Masaru Tomita, Kenta Hashimoto, Koichi Takahashi, Thomas Simon Shimizu, Yuri Matsuzaki, Fumihiko Miyoshi, Kanako Saito, Sakura Tanida, Katsuyuki Yugi, J Craig Venter, et al. E-cell: software environment for whole-cell simulation. *Bioinformatics*, 15(1):72–84, 1999.
- [124] Peter J Mulquiney, William A Bubb, and Philip W Kuchel. Model of 2, 3-bisphosphoglycerate metabolism in the human erythrocyte based on detailed enzyme kinetic equations1: in vivo kinetic characterization of 2, 3-bisphosphoglycerate synthase/phosphatase using ^{13}C and ^{31}P nmr. *Biochemical Journal*, 342(3):567–580, 1999.
- [125] Michael C Reed, Rachel L Thomas, Jovana Pavisic, S Jill James, Cornelia M Ulrich, and H Frederik Nijhout. A mathematical model of glutathione metabolism. *Theoretical Biology and Medical Modelling*, 5(1):1–16, 2008.
- [126] Julia E Raftos, Stephney Whillier, and Philip W Kuchel. Glutathione synthesis and turnover in the human erythrocyte: alignment of a model based on detailed enzyme kinetics with experimental data. *Journal of Biological Chemistry*, 285(31):23557–23567, 2010.
- [127] Richard N Bergman. Minimal model: perspective from 2005. *Hormone Research in Paediatrics*, 64(Suppl. 3):8–15, 2005.

- [128] Karina W Davidson, Michael J Barry, Carol M Mangione, Michael Cabana, Aaron B Caughey, Esa M Davis, Katrina E Donahue, Chyke A Doubeni, Alex H Krist, Martha Kubik, et al. Screening for prediabetes and type 2 diabetes: Us preventive services task force recommendation statement. *JAMA*, 326(8):736–743, 2021.
- [129] Karla I Galaviz, KM Venkat Narayan, Felipe Lobelo, and Mary Beth Weber. Lifestyle and the prevention of type 2 diabetes: a status report. *American Journal of Lifestyle Medicine*, 12(1):4–20, 2018.
- [130] Erica J Graham and Frederick R Adler. Long-term models of oxidative stress and mitochondrial damage in insulin resistance progression. *Journal of Theoretical Biology*, 340:238–250, 2014.
- [131] Michael Brownlee. The pathobiology of diabetic complications: a unifying mechanism. *Diabetes*, 54(6):1615–1625, 2005.
- [132] Bernard Schmitt, Morgane Vicenzi, Catherine Garrel, and Frédéric M Denis. Effects of n-acetylcysteine, oral glutathione (gsh) and a novel sublingual form of gsh on oxidative stress markers: A comparative crossover study. *Redox Biology*, 6:198–205, 2015.
- [133] Raghu Sinha, Indu Sinha, Ana Calcagnotto, Neil Trushin, Jeremy S Haley, Todd D Schell, and JP Richie. Oral supplementation with liposomal glutathione elevates body stores of glutathione and markers of immune function. *European Journal of Clinical Nutrition*, 72(1):105–111, 2018.
- [134] Saurabh Kalamkar, Jhankar Acharya, Arjun Kolappurath Madathil, Vijay Gajjar, Uma Divate, Sucheta Karandikar-Iyer, Pranay Goel, and Saroj Ghaskadbi. Randomized clinical trial of how long-term glutathione

- supplementation offers protection from oxidative damage and improves hba1c in elderly type 2 diabetic patients. *Antioxidants*, 11(5):1026, 2022.
- [135] Saurabh Kalamkar, Jhankar Acharya, Arjun Kolappurath Madathil, Vijay Gajjar, Uma Divate, Sucheta Karandikar-Iyer, Pranay Goel, and Saroj Ghaskadbi. Randomised clinical trial of long term glutathione supplementation offers protection from oxidative damage, improves hba1c in elderly type 2 diabetic patients. *medRxiv*, 2021.
- [136] Torsten Hothorn, Kurt Hornik, Mark A Van De Wiel, and Achim Zeileis. Implementing a class of permutation tests: the coin package. *Journal of Statistical Software*, 28:1–23, 2008.
- [137] Jacob Cohen. *Statistical power analysis for the behavioral sciences*. Academic press, 2013.
- [138] Shlomo S Sawilowsky. New effect size rules of thumb. *Journal of Modern Applied Statistical Methods*, 8(2):26, 2009.
- [139] Mine Erden-İnal, Emine Sunal, and Güngör Kanbak. Age-related changes in the glutathione redox system. *Cell Biochemistry and Function*, 20(1):61–66, 2002.
- [140] Jennifer Kovacs-Nolan, Prithy Rupa, Toshiro Matsui, Mitsuru Tanaka, Toru Konishi, Yusuke Sauchi, Kenji Sato, Shin Ono, and Yoshinori Mine. In vitro and ex vivo uptake of glutathione (gsh) across the intestinal epithelium and fate of oral gsh after in vivo supplementation. *Journal of Agricultural and Food Chemistry*, 62(39):9499–9506, 2014.
- [141] Marie H Hanigan. Gamma-glutamyl transpeptidase: redox regulation and drug resistance. *Advances in cancer research*, 122:103–141, 2014.

- [142] Kowluru Anjaneyulu, Renu Anjaneyulu, Abdullah Sener, and WJ Malaisse. The stimulus-secretion coupling of glucose-induced insulin release. thiol: disulfide balance in pancreatic islets. *Biochimie*, 64(1):29–36, 1982.
- [143] Manisha A Modak, Pradeep Bhaskar Parab, and Saroj S Ghaskadbi. Pancreatic islets are very poor in rectifying oxidative dna damage. *Pancreas*, 38(1):23–29, 2009.
- [144] Slgurd Lenzen, Jens Drinkgern, and Markus Tiedge. Low antioxidant enzyme gene expression in pancreatic islets compared with various other mouse tissues. *Free Radical Biology and Medicine*, 20(3):463–466, 1996.
- [145] HPT Ammon, S Klumpp, A Fuss, EJ Verspohl, H Jaeschke, A Wendel, and P Müller. A possible role of plasma glutathione in glucose-mediated insulin secretion: in vitro and in vivo studies in rats. *Diabetologia*, 32:797–800, 1989.
- [146] Rashmi B Prasad, Olof Asplund, Sharvari R Shukla, Rucha Wagh, Pooja Kunte, Dattatrey Bhat, Malay Parekh, Meet Shah, Sanat Phatak, An-nemari Käräjämäki, et al. Subgroups of patients with young-onset type 2 diabetes in india reveal insulin deficiency as a major driver. *Diabetologia*, 65:65–78, 2022.
- [147] Jitai Zhang, Hui An, Kaidi Ni, Bin Chen, Hui Li, Yanqin Li, Guilian Sheng, Chuanzan Zhou, Mengzhen Xie, Saijing Chen, et al. Glutathione prevents chronic oscillating glucose intake-induced β -cell dedifferentiation and failure. *Cell Death & Disease*, 10(4):321, 2019.
- [148] Silvia Del Guerra, Roberto Lupi, Lorella Marselli, Matilde Masini, Marco Bugliani, Simone Sbrana, Scilla Torri, Maria Pollera, Ugo Boggi, Franco

- Mosca, et al. Functional and molecular defects of pancreatic islets in human type 2 diabetes. *Diabetes*, 54(3):727–735, 2005.
- [149] Sunil Mathur and Joseph Sutton. Personalized medicine could transform healthcare. *Biomedical Reports*, 7(1):3–5, 2017.
- [150] Kevin B Johnson, Wei-Qi Wei, Dilhan Weeraratne, Mark E Frisse, Karl Misulis, Kyu Rhee, Juan Zhao, and Jane L Snowdon. Precision medicine, ai, and the future of personalized health care. *Clinical and Translational Science*, 14(1):86–93, 2021.
- [151] Alessandro Gasparini, Keith R Abrams, Jessica K Barrett, Rupert W Major, Michael J Sweeting, Nigel J Brunskill, and Michael J Crowther. Mixed-effects models for health care longitudinal data with an informative visiting process: A monte carlo simulation study. *Statistica Neerlandica*, 74(1):5–23, 2020.
- [152] Nan M Laird and James H Ware. Random-effects models for longitudinal data. *Biometrics*, pages 963–974, 1982.
- [153] Helen Brown and Robin Prescott. *Applied mixed models in medicine*. John Wiley & Sons, 2015.
- [154] Geert Verbeke, Geert Molenberghs, and Dimitris Rizopoulos. Random effects models for longitudinal data. In *Longitudinal research with latent variables*, pages 37–96. Springer, 2010.
- [155] Andrew Gelman, Jennifer Hill, and Masanao Yajima. Why we (usually) don’t have to worry about multiple comparisons. *Journal of Research on Educational Effectiveness*, 5(2):189–211, 2012.

- [156] Andrew Bell, Daniel Holman, and Kelvyn Jones. Using shrinkage in multilevel models to understand intersectionality. *Methodology*, 2019.
- [157] Dale J Barr, Roger Levy, Christoph Scheepers, and Harry J Tily. Random effects structure for confirmatory hypothesis testing: Keep it maximal. *Journal of Memory and Language*, 68(3):255–278, 2013.
- [158] Scott A Baldwin, Zac E Imel, Scott R Braithwaite, and David C Atkins. Analyzing multiple outcomes in clinical research using multivariate multilevel models. *Journal of Consulting and Clinical Psychology*, 82(5):920, 2014.
- [159] Guoqiao Wang, Andrew J Aschenbrenner, Yan Li, Eric McDade, Lei Liu, Tammie LS Benzinger, Randall J Bateman, John C Morris, Jason J Hassenstab, and Chengjie Xiong. Two-period linear mixed effects models to analyze clinical trials with run-in data when the primary outcome is continuous: Applications to alzheimer’s disease. *Alzheimer’s & Dementia: Translational Research & Clinical Interventions*, 5:450–457, 2019.
- [160] Patrick Schober and Thomas R Vetter. Linear mixed-effects models in medical research. *Anesthesia & Analgesia*, 132(6):1592–1593, 2021.
- [161] Arjun Kolappurath Madathil, Saroj Surendra Ghaskadbi, Pranay Goel, and Saurabh Kalamkar. Pune gsh supplementation study: Analyzing longitudinal changes in type 2 diabetic patients using linear mixed-effects models. *Frontiers in Pharmacology*, 14:603.
- [162] Douglas Bates, Reinhold Kliegl, Shravan Vasishth, and Harald Baayen. Parsimonious mixed models. *arXiv Preprint arXiv:1506.04967*, 2015.

- [163] Charles R Henderson. Estimation of genetic parameters. In *Biometrics*, volume 6, pages 186–187. International Biometric Soc, 1950.
- [164] Charles R Henderson. Best linear unbiased estimation and prediction under a selection model. *Biometrics*, pages 423–447, 1975.
- [165] Douglas Bates, Martin Mächler, Ben Bolker, and Steve Walker. Fitting linear mixed-effects models using lme4. *arXiv Preprint arXiv:1406.5823*, 2014.
- [166] Johannes Titz. mimosa: A modern graphical user interface for 2-level mixed models. *Journal of Open Source Software*, 5(49):2116, 2020.
- [167] Carlo Bonferroni. Teoria statistica delle classi e calcolo delle probabilita. *Pubblicazioni del R Istituto Superiore di Scienze Economiche e Commerciali di Firenze*, 8:3–62, 1936.
- [168] William B Kannel and Daniel L McGee. Diabetes and cardiovascular disease: the framingham study. *Jama*, 241(19):2035–2038, 1979.
- [169] William Duckworth, Carlos Abaira, Thomas Moritz, Domenic Reda, Nicholas Emanuele, Peter D Reaven, Franklin J Zieve, Jennifer Marks, Stephen N Davis, Rodney Hayward, et al. Glucose control and vascular complications in veterans with type 2 diabetes. *New England Journal of Medicine*, 360(2):129–139, 2009.
- [170] Karl Pearson. Vii. note on regression and inheritance in the case of two parents. *Proceedings of the Royal Society of London*, 58(347-352):240–242, 1895.
- [171] M Sue Kirkman, Vanessa Jones Briscoe, Nathaniel Clark, Hermes Florez, Linda B Haas, Jeffrey B Halter, Elbert S Huang, Mary T Korytkowski,

- Medha N Munshi, Peggy Soule Odegard, et al. Diabetes in older adults. *Diabetes Care*, 35(12):2650–2664, 2012.
- [172] KM Baker, WH Barry, D Bets, M Bond, M Bristow, JH Brown, F Brozovich, E Carmeliet, HE Cingolani, WS Colucci, et al. Editorial board: J. abe p. anversa m. avkiran.
- [173] Thomas V Perneger. What’s wrong with bonferroni adjustments. *Bmj*, 316(7139):1236–1238, 1998.
- [174] Robert J Cabin and Randall J Mitchell. To bonferroni or not to bonferroni: when and how are the questions. *Bulletin of the ecological society of America*, 81(3):246–248, 2000.
- [175] Kenneth J Rothman. No adjustments are needed for multiple comparisons. *Epidemiology*, pages 43–46, 1990.
- [176] Abhay Joshi and Bernhard O Palsson. Metabolic dynamics in the human red cell: Part i—a comprehensive kinetic model. *Journal of Theoretical Biology*, 141(4):515–528, 1989.
- [177] Aristidis S Veskoukis, Nikos V Margaritelis, Antonios Kyparos, Vassilis Paschalis, and Michalis G Nikolaidis. Spectrophotometric assays for measuring redox biomarkers in blood and tissues: the nadph network. *Redox Report*, 23(1):47–56, 2018.
- [178] Margaret A Baker, George J Cerniglia, and Aziza Zaman. Microtiter plate assay for the measurement of glutathione and glutathione disulfide in large numbers of biological samples. *Analytical Biochemistry*, 190(2):360–365, 1990.

- [179] Alton Meister. On the discovery of glutathione. *Trends in Biochemical Sciences*, 13(5):185–188, 1988.
- [180] Anand Kumar Bachhawat and Shambhu Yadav. The glutathione cycle: Glutathione metabolism beyond the γ -glutamyl cycle. *Iubmb Life*, 70(7):585–592, 2018.
- [181] Nnenna J Adimora, Dean P Jones, and Melissa L Kemp. A model of redox kinetics implicates the thiol proteome in cellular hydrogen peroxide responses. *Antioxidants & Redox Signaling*, 13(6):731–743, 2010.
- [182] Ehab H Sarsour, Maneesh G Kumar, Leena Chaudhuri, Amanda L Kalen, and Prabhat C Goswami. Redox control of the cell cycle in health and disease. *Antioxidants & Redox Signaling*, 11(12):2985–3011, 2009.
- [183] Dean P Jones. [11] redox potential of gsh/gssg couple: assay and biological significance. In *Methods in Enzymology*, volume 348, pages 93–112. Elsevier, 2002.
- [184] Kevin K Millis, Kim H Weaver, and Dallas L Rabenstein. Oxidation/reduction potential of glutathione. *The Journal of Organic Chemistry*, 58(15):4144–4146, 1993.
- [185] Ondrej Zitka, Sylvie Skalickova, Jaromir Gumulec, Michal Masarik, Vojtech Adam, Jaromir Hubalek, Libuse Trnkova, Jarmila Kruseova, Tomas Eckschlager, and Rene Kizek. Redox status expressed as gsh: Gssg ratio as a marker for oxidative stress in paediatric tumour patients. *Oncology Letters*, 4(6):1247–1253, 2012.
- [186] Leopold Flohé. The fairytale of the gssg/gsh redox potential. *Biochimica et Biophysica Acta (BBA)-General Subjects*, 1830(5):3139–3142, 2013.

- [187] R Franco, OJ Schoneveld, A Pappa, and MI Panayiotidis. The central role of glutathione in the pathophysiology of human diseases. *Archives of Physiology and Biochemistry*, 113(4-5):234–258, 2007.

Appendix A

Copyrights and License

Copyrights and license information for the two following published articles,

1. Kalamkar, S.; Acharya, J.; Kolappurath Madathil, A.; Gajjar, V.; Divave, U.; Karandikar Iyer, S.; Goel, P.; Ghaskadbi, S. *Randomized Clinical Trial of How Long-Term Glutathione Supplementation Offers Protection from Oxidative Damage and Improves HbA1c in Elderly Type 2 Diabetic Patients*. *Antioxidants* 2022, 11, 1026. doi:10.3390/antiox11051026.
2. Kolappurath Madathil, A.; Ghaskadbi, S.; Kalamkar, S.; Goel, P. Pune GSH supplementation study: *Analyzing longitudinal changes in type 2 diabetic patients using linear mixed-effects models*. *Frontiers in Pharmacology* 2023, 14:1139673. doi:10.3389/fphar.2023.1139673.

are provided in Figure A.1 and A.2, respectively.

Article

Randomized Clinical Trial of How Long-Term Glutathione Supplementation Offers Protection from Oxidative Damage and Improves HbA1c in Elderly Type 2 Diabetic Patients

Saurabh Kalamkar ^{1,*}, Jhankar Acharya ^{1,*}, Arjun Kolappurath Madathil ^{2,†}, Vijay Gajjar ³, Uma Divite ⁴, Sucheta Karandikar-Iyer ⁵, Pranay Goel ^{2,*} and Saroj Ghaskadbi ^{1,*}

¹ Department of Zoology, Savitribai Phule Pune University, Pune 411007, India; sdikalamkar@unipune.ac.in (S.K.); jhankaracharya@unipune.ac.in (J.A.)

² Biology Division, Indian Institute of Science Education and Research, Pune 411008, India; k.marjun@students.iiserpune.ac.in

³ Department of Medicine, Jehangir Hospital, Pune 411001, India; vijaygajjar2008@gmail.com

⁴ Jehangir Clinical Development Centre, Pune 411001, India; umadivite@jcdc.co.in

⁵ Iyer Clinic, Pune 411030, India; academics@imhospital.org

* Correspondence: pgoel@iiserpune.ac.in (P.G.); ssg@unipune.ac.in (S.G.); Tel.: +91-202-569-0617 (S.G.)

† These authors contributed equally to this work.



Citation: Kalamkar, S.; Acharya, J.; Kolappurath Madathil, A.; Gajjar, V.; Divite, U.; Karandikar-Iyer, S.; Goel, P.; Ghaskadbi, S. Randomized Clinical Trial of How Long-Term Glutathione Supplementation Offers Protection from Oxidative Damage and Improves HbA1c in Elderly Type 2 Diabetic Patients. *Antioxidants* **2022**, *11*, 1026. <https://doi.org/10.3390/antiox11051026>

Academic Editors: Vanessa Routh, Xavier Fioramonti and Anstra Carr

Received: 21 April 2022

Accepted: 20 May 2022

Published: 23 May 2022

Publisher's Note: MDPI stays neutral with regard to jurisdictional claims in published maps and institutional affiliations.



Copyright © 2022 by the authors. Licensee MDPI, Basel, Switzerland. This article is an open access article distributed under the terms and conditions of the Creative Commons Attribution (CC BY) license (<https://creativecommons.org/licenses/by/4.0/>).

Abstract: Complications in type 2 diabetes (T2D) arise from hyperglycemia-induced oxidative stress. Here, we examined the effectiveness of supplementation with the endogenous antioxidant glutathione (GSH) during anti-diabetic treatment. A total of 104 non-diabetic and 250 diabetic individuals on anti-diabetic therapy, of either sex and aged between 30 and 78 years, were recruited. A total of 125 diabetic patients were additionally given 500 mg oral GSH supplementation daily for a period of six months. Fasting and PP glucose, insulin, HbA1c, GSH, oxidized glutathione (GSSG), and 8-hydroxy-2-deoxy guanosine (8-OHdG) were measured upon recruitment and after three and six months of supplementation. Statistical significance and effect size were assessed longitudinally across all arms. Blood GSH increased (Cohen's $d = 1.01$) and 8-OHdG decreased (Cohen's $d = -1.07$) significantly within three months ($p < 0.001$) in diabetic individuals. A post hoc sub-group analysis showed that HbA1c (Cohen's $d = -0.41$; $p < 0.05$) and fasting insulin levels (Cohen's $d = 0.56$; $p < 0.05$) changed significantly in diabetic individuals above 55 years. GSH supplementation caused a significant increase in blood GSH and helped maintain the baseline HbA1c overall. These results suggest GSH supplementation is of considerable benefit to patients above 55 years, not only supporting decreased glycated hemoglobin (HbA1c) and 8-OHdG but also increasing fasting insulin. The clinical implication of our study is that the oral administration of GSH potentially complements anti-diabetic therapy in achieving better glycemic targets, especially in the elderly population.

Keywords: GSH supplementation; type 2 diabetes; HbA1c; oxidative stress; 8-OHdG; elderly diabetic population

1. Introduction

Hyperglycemia causes micro- and macrovascular complications in type 2 diabetes (T2D) through oxidative stress. This is mediated by the overproduction of reactive oxygen species (ROS) through four pathways, namely advanced glycation end products, polyol, hexosamine, and protein kinase C [1]. Animal studies have shown that scavenging hyperglycemia-mediated ROS with antioxidants such as N-acetyl-cysteine (NAC), lipoic acid, and glutathione (GSH), or precursors of GSH, such as glycine and cysteine [2–5], not only partially improved blood glucose levels, the functionality of β -cells, and insulin sensitivity, but also reduced diabetic complications. However, there are few human studies that confirm the role of antioxidants as a potential supplementary treatment in diabetes.

Figure A.1: Copyright information for Kalamkar et al. (2022) reused in chapter 3



OPEN ACCESS

EDITED BY
Takeo Nakanishi,
Takasaki University of Health and Welfare,
Japan

REVIEWED BY
Eugenia Piragine,
University of Pisa, Italy
Dateng Li,
Morgan Stanley, United States

*CORRESPONDENCE
Arjun Kolappurath Madathil,
✉ k.marjun@students.iiserpune.ac.in

[†]These authors share first authorship

SPECIALTY SECTION

This article was submitted to Drug
Metabolism and Transport,
a section of the journal
Frontiers in Pharmacology

RECEIVED 18 January 2023

ACCEPTED 27 February 2023

PUBLISHED 13 March 2023

CITATION

Madathil AK, Ghaskadbi S, Kalamkar S and
Goel P (2023), Pune GSH
supplementation study: Analyzing
longitudinal changes in type 2 diabetic
patients using linear mixed-
effects models.
Front. Pharmacol. 14:1139673.
doi: 10.3389/fphar.2023.1139673

COPYRIGHT

© 2023 Madathil, Ghaskadbi, Kalamkar
and Goel. This is an open-access article
distributed under the terms of the
Creative Commons Attribution License
(CC BY). The use, distribution or
reproduction in other forums is
permitted, provided the original author(s)
and the copyright owner(s) are credited
and that the original publication in this
journal is cited, in accordance with
accepted academic practice. No use,
distribution or reproduction is permitted
which does not comply with these terms.

Pune GSH supplementation study: Analyzing longitudinal changes in type 2 diabetic patients using linear mixed-effects models

Arjun Kolappurath Madathil ^{1*}, Saroj Ghaskadbi²,
Saurabh Kalamkar² and Pranay Goel¹

¹Biology Division, Indian Institute of Science Education and Research, Pune, India, ²Department of
Zoology, Savitribai Phule Pune University, Pune, India

Oral GSH supplementation along with antidiabetic treatment was shown to restore the body stores of GSH significantly and reduce oxidative DNA damage (8-OHdG) in Indian Type 2 diabetic (T2D) patients over 6 months in our recent clinical study. Post hoc analysis of the data also suggested that elder patients benefit from improved HbA1c and fasting insulin. We modeled longitudinal changes in diabetic individuals using a linear mixed-effects (LME) framework and obtained i) the distribution of individual trajectories with and without GSH supplementation and ii) the overall rates of changes in the different study arms. Serial changes in elder and younger diabetic individuals were also modeled independently to examine differences in their progression. The average linear trajectories obtained from the model explain how biochemical parameters in T2D patients progress over 6 months on GSH supplementation. Model estimates show improvements in erythrocytic GSH of 108 μM per month and a reduction in 8-OHdG at a rate of 18.5 ng/ μg DNA per month in T2D patients. GSH replenishes faster in younger people than in the elder. 8-OHdG reduced more rapidly in the elder (24 ng/ μg DNA per month) than in younger (12 ng/ μg DNA per month) individuals. Interestingly, elder individuals show a substantial reduction in HbA1c (0.1% per month) and increased fasting insulin (0.6 $\mu\text{U}/\text{mL}$ per month). Changes in GSH correlate strongly with changes in HbA1c, 8-OHdG, and fasting insulin in the elder cohort. The model estimates strongly suggest it improves the rate of replenishment in erythrocytic GSH stores and reduces oxidative DNA damage. Elder and younger T2D patients respond differently to GSH supplementation: It improves the rate of reduction in HbA1c and increases fasting insulin in elder patients. These model forecasts have clinical implications that aid in personalizing treatment targets for using oral GSH as adjuvant therapy in diabetes.

Figure A.2: Copyright information for Madathil et al. (2023) reused in chapter 4

Appendix B

List of Publications

The research work presented in this thesis has been done entirely during this PhD period at IISER Pune. Different parts of this work have been published in the articles listed below:

B.1 Publications

1. Kalamkar, S.; Acharya, J.; Kolappurath Madathil, A.; Gajjar, V.; Divate, U.; Karandikar Iyer, S.; Goel, P.; Ghaskadbi, S. *Randomized Clinical Trial of How Long-Term Glutathione Supplementation Offers Protection from Oxidative Damage and Improves HbA1c in Elderly Type 2 Diabetic Patients*. *Antioxidants* 2022, 11, 1026. doi:10.3390/antiox11051026.
2. Kolappurath Madathil, A.; Ghaskadbi, S.; Kalamkar, S.; Goel, P. Pune GSH supplementation study: *Analyzing longitudinal changes in type 2 diabetic patients using linear mixed-effects models*. *Frontiers in Pharmacology* 2023, 14:1139673. doi:10.3389/fphar.2023.1139673.

B.2 Conference Abstracts

1. Kolappurath Madathil, A.; Ghaskadbi, S.; Kalamkar, S.; Goel, P. *Investigating the Effect of Oral Glutathione Supplementation to Improve the Standards of Personalized Type 2 Diabetes Care*. Clinical Sciences. Chronicles of Diabetes Research and Practice 2023;2, Suppl S1:9-29.

B.3 Preprints

1. Kalamkar, S.; Acharya, J.; Kolappurath Madathil, A.; Gajjar, V.; Divate, U.; Karandikar Iyer, S.; Goel, P.; Ghaskadbi, S. *Randomised clinical trial of long term glutathione supplementation offers protection from oxidative damage, improves HbA1c in elderly type 2 diabetic patients*. medRxiv 2021. doi:10.1101/2021.04.27.21256157

This is now published in the Antioxidants and available at doi:10.3390/antiox11051026.

Article

Randomized Clinical Trial of How Long-Term Glutathione Supplementation Offers Protection from Oxidative Damage and Improves HbA1c in Elderly Type 2 Diabetic Patients

Saurabh Kalamkar ^{1,†}, Jhankar Acharya ^{1,†}, Arjun Kolappurath Madathil ^{2,†}, Vijay Gajjar ³, Uma Divate ⁴, Sucheta Karandikar-Iyer ⁵, Pranay Goel ^{2,*} and Saroj Ghaskadbi ^{1,*}

¹ Department of Zoology, Savitribai Phule Pune University, Pune 411007, India;

sdkalamkar@unipune.ac.in (S.K.); jhankaracharya@unipune.ac.in (J.A.)

² Biology Division, Indian Institute of Science Education and Research, Pune 411008, India;

k.marjun@students.iiserpune.ac.in

³ Department of Medicine, Jehangir Hospital, Pune 411001, India; vijaygajjar2008@gmail.com

⁴ Jehangir Clinical Development Centre, Pune 411001, India; umadivate@jcdc.co.in

⁵ Iyer Clinic, Pune 411030, India; academics@dmhospital.org

* Correspondence: pgoel@iiserpune.ac.in (P.G.); ssg@unipune.ac.in (S.G.); Tel.: +91-202-569-0617 (S.G.)

† These authors contributed equally to this work.



Citation: Kalamkar, S.; Acharya, J.; Kolappurath Madathil, A.; Gajjar, V.; Divate, U.; Karandikar-Iyer, S.; Goel, P.; Ghaskadbi, S. Randomized Clinical Trial of How Long-Term Glutathione Supplementation Offers Protection from Oxidative Damage and Improves HbA1c in Elderly Type 2 Diabetic Patients. *Antioxidants* **2022**, *11*, 1026. <https://doi.org/10.3390/antiox11051026>

Academic Editors: Vanessa Routh, Xavier Fioramonti and Anitra Carr

Received: 21 April 2022

Accepted: 20 May 2022

Published: 23 May 2022

Publisher's Note: MDPI stays neutral with regard to jurisdictional claims in published maps and institutional affiliations.



Copyright: © 2022 by the authors. Licensee MDPI, Basel, Switzerland. This article is an open access article distributed under the terms and conditions of the Creative Commons Attribution (CC BY) license (<https://creativecommons.org/licenses/by/4.0/>).

Abstract: Complications in type 2 diabetes (T2D) arise from hyperglycemia-induced oxidative stress. Here, we examined the effectiveness of supplementation with the endogenous antioxidant glutathione (GSH) during anti-diabetic treatment. A total of 104 non-diabetic and 250 diabetic individuals on anti-diabetic therapy, of either sex and aged between 30 and 78 years, were recruited. A total of 125 diabetic patients were additionally given 500 mg oral GSH supplementation daily for a period of six months. Fasting and PP glucose, insulin, HbA1c, GSH, oxidized glutathione (GSSG), and 8-hydroxy-2-deoxy guanosine (8-OHdG) were measured upon recruitment and after three and six months of supplementation. Statistical significance and effect size were assessed longitudinally across all arms. Blood GSH increased (Cohen's $d = 1.01$) and 8-OHdG decreased (Cohen's $d = -1.07$) significantly within three months ($p < 0.001$) in diabetic individuals. A post hoc sub-group analysis showed that HbA1c (Cohen's $d = -0.41$; $p < 0.05$) and fasting insulin levels (Cohen's $d = 0.56$; $p < 0.05$) changed significantly in diabetic individuals above 55 years. GSH supplementation caused a significant increase in blood GSH and helped maintain the baseline HbA1c overall. These results suggest GSH supplementation is of considerable benefit to patients above 55 years, not only supporting decreased glycosylated hemoglobin (HbA1c) and 8-OHdG but also increasing fasting insulin. The clinical implication of our study is that the oral administration of GSH potentially complements anti-diabetic therapy in achieving better glycemic targets, especially in the elderly population.

Keywords: GSH supplementation; type 2 diabetes; HbA1c; oxidative stress; 8-OHdG; elderly diabetic population

1. Introduction

Hyperglycemia causes micro- and macrovascular complications in type 2 diabetes (T2D) through oxidative stress. This is mediated by the overproduction of reactive oxygen species (ROS) through four pathways, namely advanced glycation end products, polyol, hexosamine, and protein kinase C [1]. Animal studies have shown that scavenging hyperglycemia-mediated ROS with antioxidants such as N-acetyl-cysteine (NAC), lipoic acid, and glutathione (GSH), or precursors of GSH, such as glycine and cysteine [2–5], not only partially improved blood glucose levels, the functionality of β -cells, and insulin sensitivity, but also reduced diabetic complications. However, there are few human studies that confirm the role of antioxidants as a potential supplementary treatment in diabetes.

Clinical trials of GSH supplementation, in particular, have received a great deal of attention. GSH is an endogenous antioxidant necessary to detoxify free radicals and maintain the redox homeostasis of the cell. Low levels of GSH are associated with many pathological conditions, such as cancer, arthritis, cardiovascular and neurodegenerative diseases, and diabetes [6]. Several reports, including work from our lab, have confirmed that GSH levels are significantly lower in diabetic patients [7–9], and controlling hyperglycemia over a period of two months increases blood GSH levels and reduces oxidative damage significantly [8]. The compensation of GSH insufficiency through supplementation may help in further arresting the development of complications in T2D by improving the redox state.

GSH has been orally administered in forms such as sublingual [10], orobuccal [11,12], and liposomal [13] for rapid absorption. We note that these forms of GSH are not only not easily available commercially but also sublingual and orobuccal formulations include GSH as one of the (primary) ingredients, which makes it difficult to attribute the effects to GSH alone. Richie et al. (2015) [14] demonstrated that oral GSH supplementation in 20 healthy individuals led to a significant increase in blood GSH. In a somewhat larger study conducted on 40 healthy American adults, however, Allen and Bradley (2011) [15] reported that oral GSH supplementation did not change GSH levels and biomarkers of oxidative stress. Precursor amino acids of GSH administered orally have also demonstrated enhanced body stores of GSH [16] in humans. Sekhar et al. [17] showed that dietary supplementation with cysteine and glycine, precursors of GSH, increased the rate of GSH synthesis and reduced lipid peroxidation in 12 American diabetic individuals without any change in glycated hemoglobin (HbA1c). They claimed that the deficient synthesis of GSH was restored by the oral supplementation with cysteine and glycine in eight older patients, but not in young individuals [17]. GSH has an added advantage over its precursor amino acids, for instance, cysteine, which has an unpleasant taste, in ensuring better patient compliance. Paolisso et al. [18] reported that GSH infusion led to increased GSH and total body glucose disposal in 10 Italian diabetic subjects; this effect was more pronounced in elderly individuals with impaired glucose tolerance [19]. Infusion is clearly difficult to implement in clinical practice. Most of these clinical studies have been carried out with small sample sizes and are often inconclusive. Discrepancies in the outcomes of these studies could be due to differences in the dose and duration of GSH, and the site of measurement of GSH being plasma instead of an erythrocyte fraction. Moreover, while most of these studies have focused on restoring body stores of GSH in both healthy and diabetic individuals, few have reported their effects on alleviating oxidative stress, or for that matter, glycemic stress itself. A detailed summary of all these trials is provided in Table S1.

Since we intended to measure HbA1c as a marker in our study (RBC lifespan is typically taken as 120 days), the overall study duration was chosen to be 6 months, which allowed two measurements of change in HbA1c, 3 months apart. This allowed us to establish long-term effects and study the stability of the observations to prolonged supplementation.

We conducted a pragmatic clinical trial prospectively in 200 Indian diabetic patients to assess whether supplementation with oral GSH improves body stores of GSH. We further asked if GSH supplementation for a relatively prolonged duration (six months) co-administered with ongoing anti-diabetic treatment supports glycemic control by minimizing oxidative damage. We serially measured concentrations of GSH, 8-hydroxy-2-deoxyguanosine (8-OHdG; an oxidative damage marker), and glycemic parameters in diabetic patients receiving GSH supplementation in addition to anti-diabetic treatment, and compared them with serial measurements in those receiving anti-diabetic treatment alone. Our study results show that oral GSH supplementation not only improved body stores of GSH and significantly reduced oxidative damage but also helped maintain lower HbA1c in elderly diabetic patients. We noted that this effect of GSH supplementation was more pronounced in elderly individuals.

2. Subjects, Materials, and Methods

2.1. Ethical Approval

This study was approved by the Institutional Ethical Committee of Jehangir Hospital Development Center, Pune (JCDC ECN- ECR/352/Inst/NIH/2013); Institutional Biosafety Committee of SPPU (Bot/27A/15), Pune; and the Institutional Ethical Committee of IISER, Pune (IECHR/Admin/2019/001). Signed informed consent was obtained from all the subjects at the time of enrollment in the study after explaining the purpose and nature of the study. All participants in this study were de-identified using a numbered code. This study is registered with the Clinical Trials Registry—India (CTRI/2018/01/011257). This study was conducted in compliance with CONSORT guidelines and guidelines of the Helsinki declaration.

2.2. Study Design

We conducted a pragmatic clinical trial designed as a case-control cohort study to assess the effect of oral GSH supplementation on blood GSH levels and glucose homeostasis in diabetic patients.

2.3. Inclusion/Exclusion Criteria for Study Participants

We recruited healthy non-diabetic controls ($n = 104$) with HbA1c $< 6.5\%$, and known T2D subjects ($n = 250$) with HbA1c $\geq 6.5\%$ [20] visiting Jehangir Hospital and Iyer clinic, Pune. Pregnant women, heavy smokers, individuals with excessive alcohol intake, individuals with any clinical infection or with a history of a recent cardiovascular event, and those receiving antioxidants or herbal formulations were excluded from the study. Body weight, height, anti-diabetic treatment, and family history of diabetes were noted for each subject.

2.4. Recruitment and Randomization for GSH Intervention

We recruited known diabetic subjects ($n = 250$) who were already on anti-diabetic regimen and study physician randomly categorized them into two groups based on coin-toss method: 125 diabetic patients were advised to continue with their anti-diabetic regimen (Group D), and the other 125 diabetic patients were given oral 500 mg glutathione (Jarrow Formulas, Los Angeles, CA, USA) supplementation once daily in addition to their anti-diabetic treatment (Table S2A,B) for a period of six months (Group DG) (Figure 1). At the time of randomization, concentrations of covariates, fasting and postprandial (PP) glucose and insulin, HbA1c, GSH and oxidized glutathione (GSSG), and 8-OHdG were not available, and therefore did not influence the assignment of diabetic patients in D or DG groups. Compliance to medical treatment by patients of D and DG group and consumption of GSH by patients of the DG was emphasized by maintaining continuous communication between the physician and patients. Out of 125 diabetic patients in D and DG group, 23 were lost to follow-up in the D group and 21 in DG group for not complying with the treatment regimen. We also recruited healthy non-diabetic control subjects who were followed for six months, during which they were advised to continue with their regular diet and exercise regimen. Blood samples were collected at the time of enrollment 0 (α visit), 3 (β visit), and 6 (γ visit) months after the date of enrollment.

2.4.1. Sample Size Calculation

Sample Size ($n = 100$) is calculated based on a two-sided t -test, at 0.1 type 1 error and 80% power, to detect a mean difference of 35 in GSH with a standard deviation of 100.

2.4.2. Sample Collection

At each visit, a total of 10 mL fasting and postprandial (PP) blood samples were collected from all the subjects at Golwilkar Metropolis, Pune. Blood samples were centrifuged at 4000 rpm for 10 min to separate erythrocyte fraction from whole blood. Plasma was stored at $-80\text{ }^{\circ}\text{C}$ (Thermo Fisher Scientific, Asheville, NC, USA) for further analysis.

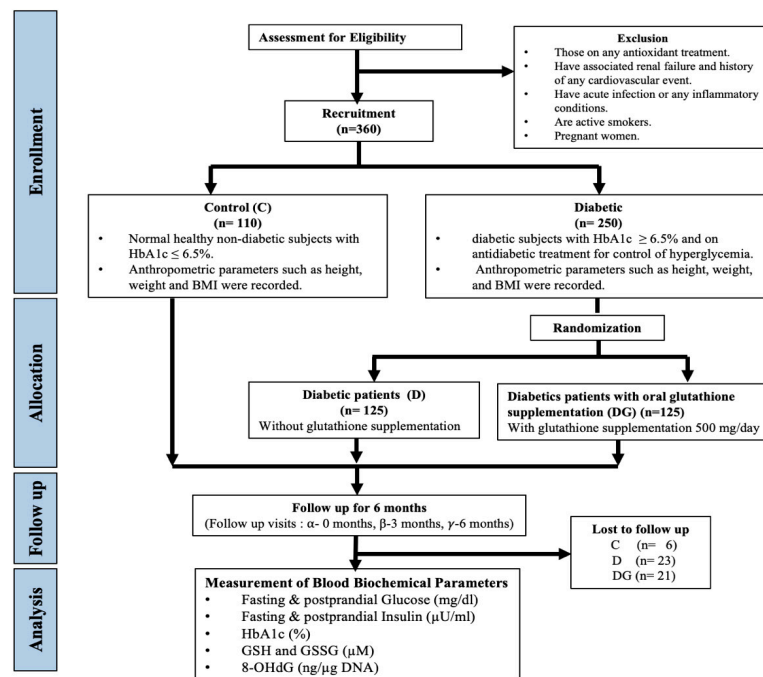


Figure 1. Flowchart for study design.

2.5. Estimation of Blood Biochemical Parameters

Measurement of fasting plasma glucose (FPG), postprandial blood glucose (PPG), fasting plasma insulin (FPI), postprandial insulin (PPI), and HbA1c was performed on an automated analyzer at Golwilkar Metropolis, Pune, following CLSI (Clinical and Laboratory Standards Institute, Malvern, PA, USA) guidelines. Erythrocyte hemolysate was prepared by washing it twice with cold saline and hemolyzing by adding ice-cold ultrapure water [8]. This was stored at -80°C for further analysis.

2.6. Estimation of GSH and GSSG

Reduced and total glutathione content in erythrocyte hemolysate was estimated using glutathione assay kit (Cayman Chemical, Ann Arbor, MI, USA). This kit follows DTNB (5,5'-dithio-bis-2 nitrobenzoic acid, Ellman's reagent) method for estimation of GSH [21], where DTNB reacts with reduced GSH, yielding yellow-colored 2-nitro-5-thiobenzoate, which is read at 405 nm on ELISA reader. Briefly, 50 μL of erythrocyte lysate was deproteinized using an equal volume of metaphosphoric acid at 4°C . After vigorous vortexing, the resulting mixture was centrifuged at $2000 \times g$ for 2 min at 4°C . The supernatant was separated and aliquoted in two parts and used for estimation of total GSH (TGSH) and GSSG. The pH of the samples was adjusted to 8 by addition of triethanolamine (5 $\mu\text{L}/100 \mu\text{L}$ of the sample). One of the aliquots was diluted 50 times with $1 \times$ MES buffer (0.4 M (N-morpholino) ethanesulphonic acid, 0.1 M phosphate buffer, and 2 mM EDTA pH 6) and used for estimation of TGSH. In the second aliquot, 2 μL of vinyl pyridine was added and diluted 25 times with $1 \times$ MES buffer and 50 μL of this sample was used for estimation of GSSG. Both the aliquots were then incubated for 1 h at room temperature. The reaction was started by adding 150 μL assay cocktail (11.25 mL MES (N-morpholino) ethanesulphonic acid, 0.1 M phosphate buffer, and 2 mM EDTA pH 6) buffer, 0.45 mL cofactor mixture containing NADP^+ and glucose-6-phosphate, 2.1 mL enzyme mixture containing glutathione reductase and glucose-6-phosphate dehydrogenase, 2.3 mL water, and 0.45 mL DTNB. Increase in TNB formation was determined by measuring absorbance at 405 nm at 5 min interval for 30 min. GSSG was used as a standard for estimating the concentration of TGSH and GSSG in samples. Absorbance values of samples and standard (0, 0.5, 1.0, 2.0, 4.0, 8.0, 12.0, and

16.0 μM) were plotted as a function of time, and slope for each sample was calculated. This was called i-slope. The i-slope of each concentration of standard was plotted against the concentration of GSH and the slope of this curve was called f-slope. Values for total GSH and GSSG were calculated by using the formula given below. GSH concentration was determined by subtracting GSSG from total GSH.

$$\text{GSH } (\mu\text{M}) = \frac{(\text{i-slope for sample}) - (\text{y intercept})}{\text{f-slope}} \times \text{sample dilution}$$

2.7. Estimation of 8-OHdG

DNA was isolated from whole blood by standard phenol–chloroform isoamyl alcohol extraction method and quantitated on nanodrop. Amount of 8-OHdG in DNA was determined by competitive enzyme-linked immunosorbent assay using standard protocol of Modak et al. (2009) [22]. Briefly, 96-well plate was coated with 100 μL 0.003% protamine sulphate (Sigma, St. Louis, MO, USA) and then incubated at 37 $^{\circ}\text{C}$ for 5–6 h. Protamine sulphate solution was removed and 100 ng of 8-OHdG was added to each well and incubated at 4 $^{\circ}\text{C}$ overnight. The plate was washed with phosphate-buffered saline (PBS) and incubated with monoclonal antibody against 8-OHdG (1 mg/mL) (1:5000) already mixed with either standard 8-OHdG or experimental DNA samples and incubated for 3–4 h at 37 $^{\circ}\text{C}$. Experimental samples consisted of 100 ng genomic DNA of the individuals from three study groups (C, D, and DG) at α , β , and γ visits. After washing the plate with PBS containing Tween-20 (PBST) 5 times, it was incubated with 100 μL (1:2500) of goat anti-mouse antibody conjugated with a biotin Fab fragment per well at 37 $^{\circ}\text{C}$ for 30 min. The plate was then washed 5 times with PBST and incubated with 100 μL (1:5000) of avidin conjugated with horseradish peroxidase enzyme at 37 $^{\circ}\text{C}$ for 30 min. Finally, after 3 washings of PBST and 3 washings of phosphate citrate buffer, pH 5, 100 μL of ABTS substrate solution containing 0.06% H_2O_2 was added to each well incubated for 10 min and the absorbance was measured at 405 nm using Multiskan plate reader (Thermo scientific, Shanghai, China) and expressed as ng 8-OHdG/ μL DNA.

Statistical Methods

Biochemical parameters of subjects in Control, D, and DG groups at the first visit were represented using the descriptive statistics (Median, 25th percentile, and 75th percentile). All intra- and inter-group comparisons of biochemical parameters at different visits were performed using permutation tests, using the “Coin” package in R [23]. Statistical significance was set at p -value < 0.05. The results of permutation tests were confirmed with two-sample, two-sided t -tests. The results obtained from permutation tests were presented here. Effect size analysis was used to quantify the difference between 6-month biochemical changes in D and DG groups. All calculations and parametric t -tests were carried out using Matlab version 2019.

Effect Size Calculations

Biochemical measurements of variables are available at α , β , and γ visits. Changes in the biochemical variables, HbA1c, fasting glucose (FPG), fasting insulin (FPI), PP glucose (PPG), PP insulin (PPI), GSH, GSSG, and 8-OHdG in during the study period from α to γ visit (6 months) in a group were estimated by taking their paired differences between those visits. Let the 6-month changes in D for a variable x be denoted by \mathbf{D}_x , and similarly for DG group by \mathbf{DG}_x . The effect size of 6-month changes in the concentration of a particular biochemical variable x (x can be HbA1c, FPG, FPI, PPG, PPI, GSH, GSSG, and 8-OHdG) between D and DG groups is estimated using Cohen’s d [24] as

$$d = \frac{\text{mean of } \mathbf{DG}_x - \text{mean of } \mathbf{D}_x}{s}$$

where, s is the pooled standard deviation of changes in the x variable in D and DG groups. Cohen (1969) described an effect size of 0.2, 0.5, and 0.8 as “Small”, “Medium”, and “Large”

effects respectively, and Sawilowsky [25] classified an effect of sizes 1.2 and 2 as “Huge” and “Very large” effects, respectively.

3. Results

3.1. Baseline Characteristics

The study population included diabetic subjects with a mean age of 54 years and a BMI of 26.9 kg/m², and the Control group included individuals with a mean age of 41 years and a BMI of 26 kg/m². The D group consisted of 57 males and 45 females, the DG group consisted of 49 males and 55 females, and the Control group consisted of 62 males and 42 females.

The baseline characteristics of subjects in each group are presented in Table 1. Concentrations of FPG, PPG, FPI, HbA1c, and 8-OHdG were significantly high and that of GSH was significantly low in D and DG compared to Control ($p < 0.001$, all parameters). Levels of PPI in D and DG were not found to be significantly different compared to the Control group (Table 1).

Table 1. Baseline characteristics of Control, D, and DG groups. Data from each group at the α visit are presented here as median and IQR, inter-quartile ranges (25th percentile–75th percentile). * indicates the significance of the comparison between baseline measurements of Control versus D or Control versus DG groups. Significance levels are * $p < 0.05$, ** $p < 0.01$, and *** $p < 0.001$. Similarly, significance levels for comparisons between D versus DG groups are denoted with ##, or ### for $p < 0.05$, $p < 0.01$, and $p < 0.001$, respectively. We did not observe any significant differences in the levels of FPG, PPG, FPI, PPI, HbA1c, and GSH within the D and DG groups, thus confirming covariate balance in the two groups at baseline (Table S4). Abbreviations used here are BMI—body mass index, HbA1c—glycated hemoglobin, GSH—reduced glutathione, PP glucose—postprandial glucose, PP insulin—postprandial insulin, and 8-OHdG—8-hydroxy-2-deoxy guanosine.

Biochemical Variables	Control	D	DG
	Median (25th–75th Percentile)	Median (25th–75th Percentile)	Median (25th–75th Percentile)
Age (years)	39.5 (33.5–49)	55.5 (47–61) ***	56 (48–61) ***
BMI (kg/m ²)	26.1 (23.5–28.2)	26.3 (22.7–29.2)	26.8 (23.8–29.8)
HbA1c (%)	5.6 (5.4–5.8)	8.1 (7.1–9.6) ***	8 (7.1–9.7) ***
Fasting Glucose (mg/dL)	90 (85–95)	147 (120–190) ***	140.5 (109–182) ***
Fasting Insulin (μ U/mL)	9.4 (6.8–12.3)	11.9 (7.4–17.1) **	10.4 (7.5–16.1) *
PP Glucose (mg/dL)	104 (96–117)	220 (169–285) ***	209 (168–258) ***
PP Insulin (μ U/mL)	36 (18.1–71.7)	36.2 (24–54.8)	32.4 (18.1–60.4)
GSH (μ M)	801 (548–1068)	379 (243–533) ***	440 (176–635) ***
GSSG (μ M)	205 (124–303)	215 (139–326)	137 (89–209) ***,###
8-OHdG (ng/ μ g DNA)	129.97 (97.2–175.2)	442.33 (340.26–514) ***	481.71 (412.23–535.11) **,##

3.2. Oral GSH Supplementation Increases Erythrocyte GSH and Decreases Oxidative Damage to DNA but Does Not Alter Glycemia in Diabetic Patients over a Period of Six Months

GSH levels increased significantly over a period of six months, from the α to γ visit in both DG ($p < 0.001$) and D ($p < 0.001$) groups, while they remained unchanged in the Control. We further estimated the effect size of GSH supplementation within the diabetic groups: A “Large” effect (Cohen’s $d = 1.01$; $p < 0.001$) indicated that the increase in GSH is significantly high in DG compared to D (Figure 2). GSSG was similarly increased in DG compared to D (Cohen’s $d = 0.61$, $p < 0.001$).

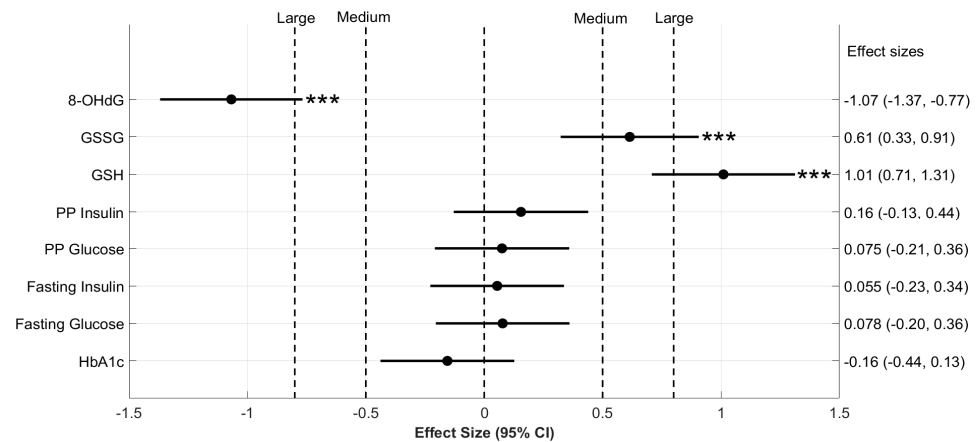


Figure 2. The effect size of changes in blood biochemical parameters. Six-month changes in the biochemical parameters of D and DG groups were compared here on a forest plot with effect size and corresponding 95% confidence intervals (CI). Effect size (Cohen's *d*) calculated between 6-month changes in the concentration of biochemical variables are denoted on the *x*-axis. The group-wise means of 6-month changes in the concentration of these variables were compared using two-sample permutation tests. The significance of these comparisons is denoted by the *p* values mentioned to the right of horizontal lines for CI. Significance level is *** $p < 0.001$ for respective comparisons. Effect size takes either a positive or negative sign based on the direction of change: a positive effect size increases towards the right and a negative effect towards the left. Vertical dotted lines represent different classifications of effect size. In particular, "Medium" effects are labeled at 0.5 and -0.5 , and "Large" effects at 0.8 and -0.8 . Abbreviations used here are, HbA1c—glycated hemoglobin, GSH—reduced glutathione, PP glucose—postprandial glucose, PP insulin—postprandial insulin, and 8-OHdG—8-hydroxy-2-deoxy guanosine.

We also observed a significant decrease in the concentrations of 8-OHdG from the α to γ visit with a "Large" effect in DG (Cohen's $d = -1.07$; $p < 0.001$) but not in the D and Control groups ($p > 0.05$) (Figure 2).

We then analyzed the effect of oral GSH supplementation on the glyceic parameters in diabetic patients. We observed that HbA1c levels decreased significantly over six months in both D and DG; however, the extent to which it decreased in DG was comparable to the D group, as indicated by a small Cohen's $d = -0.16$ ($p > 0.05$) (Figure 2). FPG, PPG, FPI, and PPI decreased over a period of six months in D and DG; however, changes in DG were comparable to those in D ($p > 0.05$, Cohen's $d < 0.2$, all parameters).

Overall, our results indicate that GSH supplementation leads to a significant increase in the erythrocyte GSH and GSSG and a decrease in 8-OHdG in diabetic patients. However, the changes in the glyceic parameters of D and DG were to similar extents.

Next, we investigated whether the effect of GSH supplementation is accomplished rapidly and stabilized thereafter, or whether their levels change gradually over a period of six months (Table S1).

3.3. Oral GSH Supplementation Enhances Erythrocyte GSH in Diabetic Subjects within Three Months

Figure 3a,b show serial changes in the concentrations of GSH and GSSG, respectively, from the α to β and γ visits in the three study groups. In Control, GSH and GSSG remained unchanged over a period of six months. GSH supplementation in DG led to a significant increase in GSH within the first three months ($p < 0.001$) and remained stable thereafter for up to six months (Figure 3a). In the D group, on the other hand, GSH increased marginally from 0 to 3 and 6 months. In the DG group (Figure 3b), GSSG also increased significantly within the first three months ($p < 0.001$), and did not change further. In D, GSSG remained unchanged during the study period. Thus, oral GSH supplementation in diabetic patients

increased GSH significantly within three months and stabilized it thereafter. On the other hand, in D, anti-diabetic therapy alone led to a small increase in GSH.

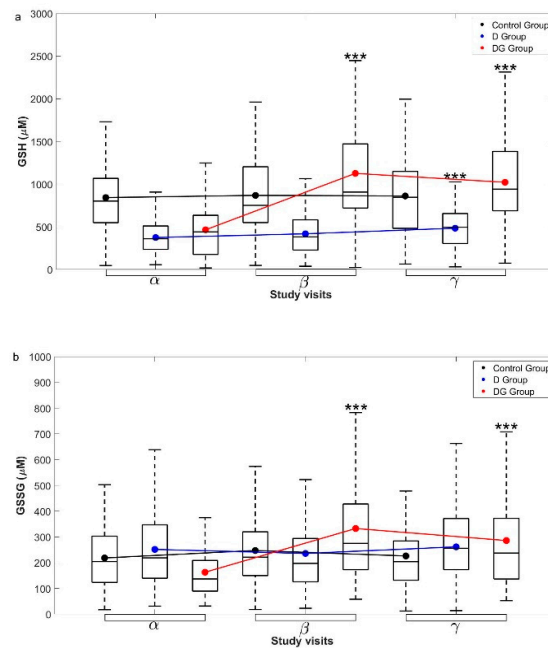


Figure 3. Longitudinal changes in the concentration of (a) GSH and (b) GSSG in different groups. The measured data for (a) GSH and (b) GSSG concentrations from Control, D, and DG groups at α , β , and γ visits are shown here with box and whiskers plots. Mean (black circles for Control, blue for D, and red for DG groups, respectively) and inter-quartile ranges (IQR) of the data are overlaid over the corresponding box plots. The group-wise means at different visits are connected using solid lines with the same color. Significance levels displayed above β , and γ visits denote the comparisons with α visit using permutation tests. Significance level is *** $p < 0.001$ for respective comparisons. Abbreviations used here are, GSH—reduced glutathione, and GSSG—oxidized glutathione.

3.4. Oral GSH Supplementation Significantly Reduces 8-OHdG in Diabetic Subjects

In the Control group, concentrations of 8-OHdG remained unchanged over a period of six months, while GSH supplementation in diabetic patients led to a significant decrease in 8-OHdG within the first three months, which continued to reduce significantly thereafter ($p < 0.001$) (Figure 4a). However, in the D group, its concentrations did not change significantly.

3.5. HbA1c Levels Are Stabilized by Oral GSH Supplementation in Diabetic Patients

We examined serial changes in the levels of glycemic parameters in D and DG groups in greater detail. FPG levels lowered significantly within three months in D ($p < 0.01$) and DG ($p = 0.05$); however, they recovered to the baseline levels by the end of six months (Figure 4b). PPG levels, on the other hand, did not change significantly in D and DG over a period of six months ($p > 0.05$, all) (Figure 4c). HbA1c rapidly decreased from 0 to 3 months in both D ($p < 0.01$) and DG ($p < 0.001$) (Figure 4d). Thereafter, HbA1c levels were maintained until 6 months in DG, while they appear to have returned to the baseline in the D group.

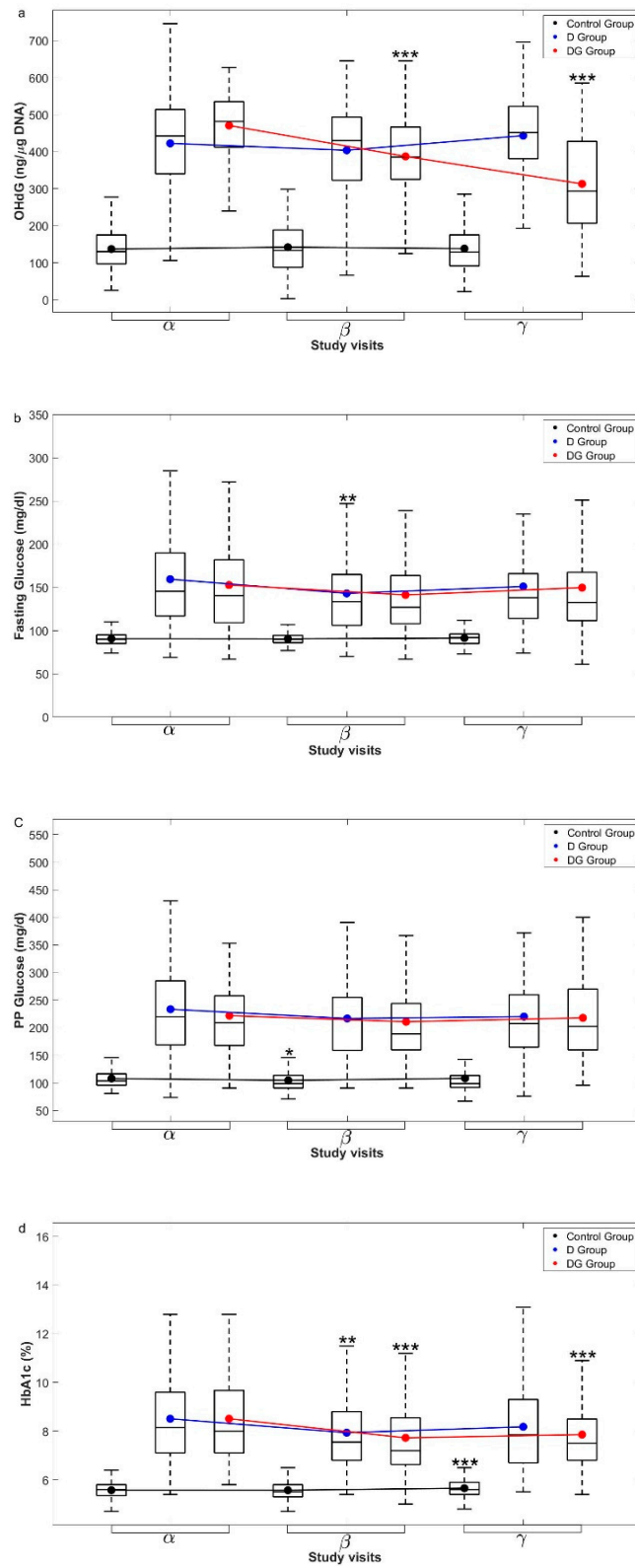


Figure 4. Cont.

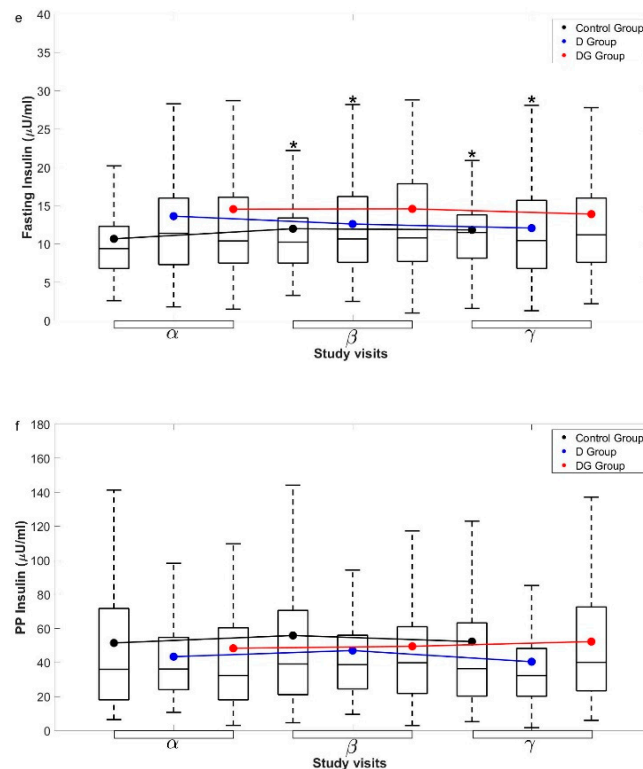


Figure 4. Longitudinal changes in glycemic parameters. The measured data for (a) 8-OHdG, (b) fasting glucose, (c) PP glucose, (d) HbA1c, (e) fasting insulin, and (f) PP insulin concentrations from Control, D, and DG groups at α , β , and γ visits are shown here with box and whiskers plots. Mean (black circles for Control, blue for D, and red for DG groups) and IQR of the data are overlaid over the corresponding box plot. The group-wise means at different visits of a group are connected using solid lines with the same color. Significance levels (*) displayed above β , and γ visits denote the comparisons with α visit using permutation tests. Significance levels are * $p < 0.05$, ** $p < 0.01$, and *** $p < 0.001$ for respective comparisons. Abbreviations used here are, 8-OHdG—8-hydroxy-2-deoxy guanosine, PP glucose—postprandial glucose, HbA1c—glycated hemoglobin, PP insulin—postprandial Insulin.

FPI levels changed significantly from 0 to 3 and 6 months in D ($p < 0.05$), while they remained unchanged in DG ($p > 0.05$) (Figure 4e). PPI levels remained unaltered in D and DG throughout the study period (Figure 4f). Taken together, oral GSH supplementation in diabetic patients appears to have a “stabilizing effect” on HbA1c, i.e., it decreases rapidly within three months and continues thereafter.

3.6. A Oral GSH Supplementation Significantly Reduces HbA1c in Elderly Diabetic Patients

Earlier reports suggest that the concentration of GSH decreases with age in healthy adults [17,26]. Therefore, we assessed the effect of GSH supplementation in elderly diabetic patients.

Diabetic patients in our study ranged from 31 to 78 years of age. The median age in these cohorts is about 55 years in the D and DG groups. We used this age as a threshold to isolate an elder sub-group. We then re-examined the effect of GSH supplementation in this sub-group diabetic population to assess whether they respond differently to oral GSH supplementation compared to the younger population.

Mean values for all the biochemical parameters and serial changes from 0 to 3 and 6 months in their concentrations in the D ($n = 44$) and DG ($n = 54$) groups are shown in Figures S1 and S2, respectively. Similar to results obtained for diabetic patients overall, the

concentration of GSH and GSSG increased significantly over a period of 6 months in both the D and DG sub-groups (Figure S1). Changes in the mean GSH and GSSG over a period of 6 months in the DG group (Figure 5) were significantly higher compared to the D group (Cohen's $d = 1.14$ and 0.67 for GSH and GSSG, respectively, $p < 0.001$).

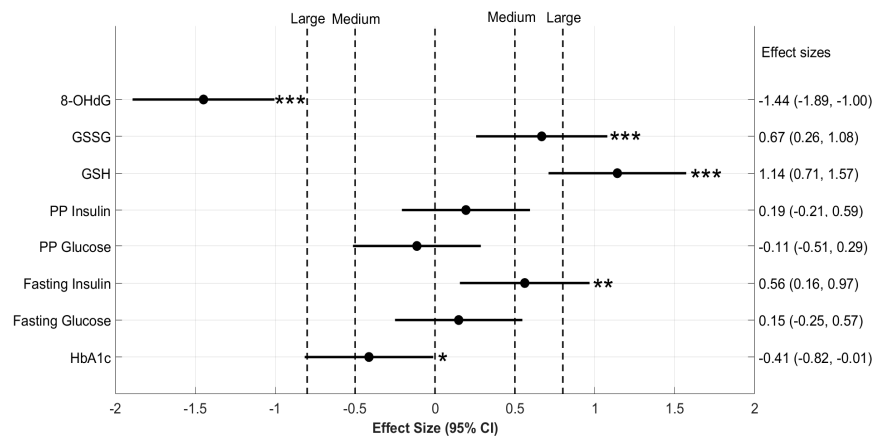


Figure 5. The effect size of changes in blood biochemical parameters of elderly diabetic patients. Six-month changes in the biochemical parameters of those in D and DG sub-groups were compared here on a forest plot with effect size and 95% confidence intervals. Effect size (Cohen's d) calculated between 6-month changes in the concentration of biochemical variables are denoted on the x -axis. The group-wise means of 6-month changes in the concentration of these variables were compared using two-sample permutation tests. The significance of these comparisons is denoted by the p values mentioned to the right of horizontal lines for CI. Significance levels are * $p < 0.05$, ** $p < 0.01$, and *** $p < 0.001$ for respective comparisons.

GSH supplementation also resulted in a "Very large" effect (Cohen's $d = -1.45$, $p < 0.001$) in the reduction of 8-OHdG in the elderly sub-group of diabetic patients (Figure 5), suggesting that oral GSH supplementation in the elderly diabetic population results in a significant reduction in the accumulation of oxidative DNA damage.

Next, we examined the effect size of blood glyceemic parameters in response to oral GSH supplementation in the elderly sub-group of diabetic patients (Figure 5). In contrast to the results observed in the diabetic population overall, GSH supplementation in the DG sub-group led to a significant reduction in HbA1c over a period of 6 months compared to D (Cohen's $d = -0.41$, $p < 0.05$).

Interestingly, FPI levels also increased significantly in the DG sub-group from the α to γ visit compared to D (Cohen's $d = 0.56$, $p < 0.05$). GSH supplementation had a small effect on levels of FPG, PPG, and PPI in the DG sub-group (Cohen's $d < 0.2$, $p < 0.05$, all parameters).

Thus, GSH supplementation in the DG sub-group of elderly diabetic patients over a period of 6 months led to a significant increase in the erythrocyte GSH, GSSG, and FPI and a decrease in HbA1c and 8-OHdG levels (Figure S2), suggesting that the elderly diabetic population responds better to GSH supplementation in conjunction with anti-diabetic therapy. The effect of GSH supplementation has been also analyzed in the younger sub-groups of D and DG and the results are shown in the supplementary documents (Figures S3–S5).

HbA1c levels changed significantly from the baseline in the younger sub-group of DG (Figure S3D); however, the 6-month changes in the younger sub-group of DG did not show any significant difference when compared to the 6-month changes in the younger sub-group of D as a result of GSH supplementation (Figure S5).

4. Discussion

GSH, a water-soluble tri-peptide, is an important endogenous antioxidant required for maintaining the redox homeostasis of the cell. It is synthesized by glutathione synthetase and utilized by glutathione peroxidase and glutaredoxin to detoxify free radicals. Several studies have reported low levels of GSH in different pathological conditions [6]. GSH insufficiency can be due to increased exposure to oxidants, drugs, excess nutrients, or decreased rate of synthesis of GSH. In our earlier studies, we found a significant decrease in GSH in T2D individuals, and among 12 different markers of OS measured, GSH impressively correlated with changes in HbA1c [27], suggesting that altering hyperglycemia rapidly results in changes in GSH.

Interventions aiming at controlling hyperglycemia are the primary line of treatment for diabetic patients. It is interesting to ask if improving redox status by GSH supplementation can help counteract the deleterious effects of hyperglycemia-induced OS. Results from earlier clinical trials of oral GSH supplementation have been contrasting and debatable. Our study provides clear evidence that long-term oral GSH supplementation not only improves body stores of GSH but significantly decreases the accumulation of oxidative DNA damage in Indian T2D patients. It also helps increase the efficiency of anti-diabetic treatment in maintaining normoglycemia in diabetic patients.

GSH is known to be either transported in its intact form from the intestinal epithelial cells into the blood lumen [28] or broken down by gamma-glutamyl transferase to its constituent amino acids [29]. It is unclear whether GSH was either directly absorbed or broken down into its constituent amino acids and re-synthesized by glutathione synthetase. Additionally, we find a significant increase in the concentration of erythrocytic GSSG. This is possibly due to the conversion of erythrocytic GSH into GSSG, in line with previous reports; for instance, Nolan et al. [28] show that ¹³C-GSH administered to mice is rapidly converted to GSSG and accumulated in red blood cells and liver. Thus, oral GSH supplementation not only increases body stores of GSH but a fraction is stored as GSSG. These results strongly suggest that GSH supplementation results in a systemic improvement of the redox state in diabetic individuals. The augmentation of antioxidant reserves, by elevating GSH levels, also resulted in a significant reduction in the accumulation of oxidative DNA damage implicated in the pathophysiology of diabetic complications.

HbA1c levels typically fluctuate despite regular anti-diabetic treatment in diabetic patients. We found that GSH supplementation helped maintain lowered HbA1c within three months. This effect was more pronounced in elderly patients over 55 years of age. Other characteristics of the glycemic state, such as FPG, PPG, FPI, and PPI, did not change in the diabetic patients overall; however, interestingly, we observed an increase in FPI levels in elderly diabetic patients. The exact mechanism by which GSH helps in maintaining normoglycemia in diabetic patients requires further investigation.

Preserving β -cell function is essential to glucose control in diabetic patients. It is crucial to maintain a healthy redox state of pancreatic β -cells, as their ability to secrete insulin in response to glucose is dependent on intracellular thiols [30]. It is well established that β -cells are more vulnerable to ROS due to their low antioxidant capacity and poor ability to repair oxidatively damaged DNA [22,31]. Thus, one potential strategy for improving β -cell function is to provide antioxidant support to pancreatic β -cells. Enhancing extracellular GSH levels improved β -cell response to glucose in rats [32]. Infusion with GSH [12] also enhanced β -cell function and consequently improved glucose disposal in patients with impaired glucose tolerance. Our results also indicate that oral GSH supplementation supports anti-diabetic treatment in reducing hyperglycemia. It is difficult at this stage to establish a causal sequence of events that underlie these observations. For instance, while it is generally believed that the etiology of diabetes in Southeast Asian diabetic patients points to especially poor insulin resistance [33], recent reports have indicated that a large sub-group of patients belong to an insulin-deficient phenotype [34]. We note, in particular, that HOMA indices were only one component of a more comprehensive clustering pattern that included age at diagnosis, HbA1c, HOMA2- β , HOMA2-IR, and BMI. We further point

out that there are there few patients in this study ($n = 7$) who were on insulin, hence it is unclear if the observations described here extend to those in whom insulin insufficiency is severe.

It is known that concentration of GSH declines with aging [17,26] and this could be further aggravated in elderly diabetic patients. We indeed observed that elderly diabetic patients benefited more from GSH supplementation both in terms of reducing oxidative DNA damage and improving glycemic status. Interestingly, we also observed a significant increase in FPI in these elderly patients. Recently Zhang et al. [35] reported restoration of β -cell function by administration of oral GSH in diabetic rats. Islets isolated from T2D cadaveric organ donors showed impaired insulin secretion in response to glucose and increased levels of oxidative damage markers. Treating these islets with GSH led to an improvement in their functionality and also alleviated oxidative damage markers [36], suggesting that reducing OS in islets could be a potential target for treating diabetes. We speculate that a systemic increase in GSH in diabetic patients resulted in a significant reduction in oxidative DNA damage, improved the pancreatic β -cell function, and concomitantly reduced HbA1c, prominently so in elderly diabetic individuals. However, these results need to be further validated in large clinical settings.

T2D is a multifactorial, complex disease and can be controlled by diet modifications, control of physical activity, weight reduction, etc. These factors need to be considered for the personalization of therapy. It would also be interesting to see how long the effect of GSH intervention persists; since the antioxidant status of an individual varies widely, it is plausible that this can significantly influence the effect of exogenous supplementation. This might even explain why the changes in HbA1c observed in DG have shown limited effect sizes. It is also conceivable that longer intervention with GSH may show further improvements in glycemic parameters, such as fasting glycemia. In our study, due to sample size limitations, we do not have enough statistical power to perform such analyses. However, our work lays the foundation for further studies with various population cohorts to understand these effects better.

Our results have provided support for significant, if modest, effects of GSH supplementation on HbA1c. This is very important, especially in light of the ADA position [37], which recognizes that the personalization of anti-diabetic therapy—rather than a one-size-fits-all treatment—is necessary to achieve successful glycemic targets. However, few algorithms exist that describe how to achieve this ambitious goal. For this reason, we reiterate that GSH supplementation is an important addition to this toolbox. We have shown significant positive benefits of GSH, and importantly, it is tolerated very well by patients; this makes it a very useful therapeutic agent to add to the clinician's arsenal.

5. Conclusions

Our results strongly suggest that oral GSH supplementation replenishes the body's stores of GSH and significantly reduces oxidative DNA damage in Indian T2D patients. It also reduces HbA1c within three months and maintains it thereafter in the diabetic population overall. An elderly sub-group seems to benefit greatly, as evidenced by a significant decrease in HbA1c and an increase in insulin secretion by β -cells over a period of six months. A clinical implication of our study is that the oral administration of GSH can be used as an adjunct therapy to anti-diabetic treatment in achieving better glycemic targets, especially in the elderly population.

Supplementary Materials: The following supporting information can be downloaded at: <https://www.mdpi.com/article/10.3390/antiox11051026/s1>, Figure S1: Serial changes in the concentration of (A) GSH and (B) GSSG in elderly diabetic subjects. Figure S2: Longitudinal changes in the concentration of biochemical parameters (A) 8-OHdG, (B) Fasting Glucose, (C) PP Glucose, (D) HbA1c, (E) Fasting Insulin, and (F) PP Insulin in elderly diabetic subjects. Figure S3: Serial changes in the concentration of (A) GSH and (B) GSSG in diabetic subjects younger than 55 years. Figure S4: Longitudinal changes in the concentration of biochemical parameters (A) 8-OHdG, (B) Fasting Glucose, (C) PP Glucose, (D) HbA1c, (E) Fasting Insulin, and (F) PP Insulin in subjects younger than 55 years of

age. Figure S5: The effect size of changes in blood biochemical parameters of subjects younger than 55 years of age. Figure S6: The effect size of changes in blood biochemical parameters in (A) females and (B) males in the study. Figure S7: The effect size of changes in blood biochemical parameters, HOMA IR and HOMA β (A) between D and DG groups and (B) elder sub-groups of D and DG. Table S1: Summary of clinical trials conducted using GSH/different forms of GSH/precursors of GSH. Table S2: Number of subjects in (A) D and (B) DG groups with different types of anti-diabetic treatment. Table S3: Biochemical measurements at different visits in Control, D, and DG groups. Table S4: Inter-group comparisons of baseline characteristics.

Author Contributions: S.K. collected the samples and performed the biochemical assays. J.A. designed the biochemical assays, supervised the data collection, and wrote the manuscript. V.G., U.D. and S.K.-I. helped in the recruitment of study participants. A.K.M. and P.G. analyzed the data and performed the statistical analysis. S.G. and P.G. contributed to the design and implementation of the study and the editing of the manuscript. All authors have read and agreed to the published version of the manuscript.

Funding: This work was financially supported by the UGC-XIIth Plan-Innovation Grant, SPPU, Pune. We also acknowledge partial financial support from UGC-CAS and the DST-PURSE program of the Department of Zoology, SPPU. S.K. is a recipient of a Junior Research Fellowship from CSIR, India. A.K.M. is financially supported by DST-Inspire, from the Government of India.

Institutional Review Board Statement: This study was approved by the Institutional Ethical Committee of Jehangir Hospital Development Center, Pune (JCDC ECN- ECR/352/Inst/NIH/2013); Institutional Biosafety Committee of SPPU (Bot/27A/15), Pune; and the Institutional Ethical Committee of IISER, Pune (IECHR/Admin/2019/001). This study is registered with the Clinical Trials Registry—India (CTRI/2018/01/011257).

Informed Consent Statement: Signed informed consent was obtained from all the subjects at the time of enrollment in the study after explaining the purpose and nature of the study. All participants in this study were de-identified using a numbered code. This study is registered with the Clinical Trials Registry—India (CTRI/2018/01/011257).

Data Availability Statement: All data generated or analyzed during this study are included in this published article, including supplementary files, and can be downloaded from <https://figshare.com/s/0803267e1d38c054cee6> (accessed on 24 August 2019). Please note that the folder also contains scripts that can be used to conveniently reproduce the analysis in the manuscript.

Acknowledgments: We thank all patients for their whole-hearted participation in the study. We acknowledge the financial help from all the funding agencies mentioned above.

Conflicts of Interest: The authors declare no conflict of interest. The funders had no role in the design of the study; in the collection, analyses, or interpretation of data; in the writing of the manuscript, or in the decision to publish the results.

References

1. Brownlee, M. The Pathobiology of Diabetic Complications: A Unifying Mechanism. *Diabetes* **2005**, *54*, 1615–1625. [[CrossRef](#)] [[PubMed](#)]
2. Haber, C.A.; Lam, T.K.T.; Yu, Z.; Gupta, N.; Goh, T.; Bogdanovic, E.; Giacca, A.; Fantus, I.G. N-acetylcysteine and taurine prevent hyperglycemia-induced insulin resistance in vivo: Possible role of oxidative stress. *Am. J. Physiol. Endocrinol. Metab.* **2003**, *285*, E744–E753. [[CrossRef](#)] [[PubMed](#)]
3. Ueno, Y.; Kizaki, M.; Nakagiri, R.; Kamiya, T.; Sumi, H.; Osawa, T. Dietary Glutathione Protects Rats from Diabetic Nephropathy and Neuropathy. *J. Nutr.* **2002**, *132*, 897–900. [[CrossRef](#)] [[PubMed](#)]
4. Jain, S.K.; Velusamy, T.; Croad, J.L.; Rains, J.L.; Bull, R. L-Cysteine supplementation lowers blood glucose, glycated hemoglobin, CRP, MCP-1, and oxidative stress and inhibits NF- κ B activation in the livers of Zucker diabetic rats. *Free Radic. Biol. Med.* **2002**, *46*, 1633–1638. [[CrossRef](#)] [[PubMed](#)]
5. El-Hafidi, M.; Franco, M.; Ramírez, A.R.; Sosa, J.S.; Flores, J.A.P.; Acosta, O.L.; Salgado, M.C.; Cardoso-Saldaña, G. Glycine Increases Insulin Sensitivity and Glutathione Biosynthesis and Protects against Oxidative Stress in a Model of Sucrose-Induced Insulin Resistance. *Oxid. Med. Cell. Longev.* **2018**, *2018*, 2101562. [[CrossRef](#)] [[PubMed](#)]
6. Townsend, D.M.; Tew, K.D.; Tapiero, H. The importance of glutathione in human disease. *Biomed. Pharmacother.* **2003**, *57*, 145–155. [[CrossRef](#)]

7. Song, F.; Jia, W.; Yao, Y.; Hu, Y.; Lei, L.; Lin, J.; Sun, X.; Liu, L. Oxidative stress, antioxidant status and DNA damage in patients with impaired glucose regulation and newly diagnosed Type 2 diabetes. *Clin. Sci.* **2007**, *112*, 599–606. [[CrossRef](#)]
8. Acharya, J.D.; Pande, A.J.; Joshi, S.M.; Yajnik, C.S.; Ghaskadbi, S.S. Treatment of hyperglycaemia in newly diagnosed diabetic patients is associated with a reduction in oxidative stress and improvement in β -cell function: Glucose Control Reduces Oxidative Stress. *Diabetes Metab. Res. Rev.* **2014**, *30*, 590–598. [[CrossRef](#)]
9. Picu, A.; Petcu, L.; Ștefan, S.; Mitu, M.; Lixandru, D.; Ionescu-Tîrgoviște, C.; Pîrcălăbioru, G.G.; Ciulu-Costinescu, F.; Bubulica, M.-V.; Chifiriuc, M.C. Markers of Oxidative Stress and Antioxidant Defense in Romanian Patients with Type 2 Diabetes Mellitus and Obesity. *Molecules* **2017**, *22*, 714. [[CrossRef](#)]
10. Schmitt, B.; Vicenzi, M.; Garrel, C.; Denis, F.M. Effects of N-acetylcysteine, oral glutathione (GSH) and a novel sublingual form of GSH on oxidative stress markers: A comparative crossover study. *Redox Biol.* **2017**, *6*, 198–205. [[CrossRef](#)]
11. Buonocore, D.; Grosini, M.; Giardina, S.; Michelotti, A.; Carrabetta, M.; Seneci, A.; Verri, M.; Dossena, M.; Marzatico, F. Bioavailability study of an innovative orobuccal formulation of glutathione. *Oxid. Med. Cell. Longev.* **2016**, *2016*, 3286365. [[CrossRef](#)] [[PubMed](#)]
12. Bruggeman, B.K.; Storo, K.E.; Fair, H.M.; Wommack, A.J.; Carriker, C.R.; Smoliga, J.M. The absorptive effects of orobuccal non-liposomal nano-sized glutathione on blood glutathione parameters in healthy individuals: A pilot study. *PLoS ONE* **2019**, *14*, e0215815. [[CrossRef](#)] [[PubMed](#)]
13. Sinha, R.; Sinha, I.; Calcagnotto, A.; Trushin, N.; Haley, J.S.; Schell, T.D.; Richie, J.P. Oral supplementation with liposomal glutathione elevates body stores of glutathione and markers of immune function. *Eur. J. Clin. Nutr.* **2018**, *72*, 105–111. [[CrossRef](#)] [[PubMed](#)]
14. Richie, J.P.; Nichenametla, S.; Neidig, W.; Calcagnotto, A.; Haley, J.S.; Schell, T.D.; Muscat, J.E. Randomized controlled trial of oral glutathione supplementation on body stores of glutathione. *Eur. J. Nutr.* **2015**, *54*, 251–263. [[CrossRef](#)] [[PubMed](#)]
15. Allen, J.; Bradley, R.D. Effects of Oral Glutathione Supplementation on Systemic Oxidative Stress Biomarkers in Human Volunteers. *J. Altern. Complement. Med.* **2011**, *17*, 827–833. [[CrossRef](#)]
16. Sekhar, R.V.; Patel, S.G.; Guthikonda, A.P.; Reid, M.; Balasubramanyam, A.; Taffet, G.E.; Jahoor, F. Deficient synthesis of glutathione underlies oxidative stress in aging and can be corrected by dietary cysteine and glycine supplementation. *Am. J. Clin. Nutr.* **2011**, *94*, 847–853. [[CrossRef](#)]
17. Sekhar, R.V.; McKay, S.V.; Patel, S.G.; Guthikonda, A.P.; Reddy, V.T.; Balasubramanyam, A.; Jahoor, F. Glutathione Synthesis Is Diminished in Patients With Uncontrolled Diabetes and Restored by Dietary Supplementation With Cysteine and Glycine. *Diabetes Care* **2011**, *34*, 162–167. [[CrossRef](#)]
18. Paolisso, G.; Di Maro, G.; Pizza, G.; D'Amore, A.; Sgambato, S.; Tesauro, P.; Varricchio, M.; D'Onofrio, F. Plasma GSH/GSSG affects glucose homeostasis in healthy subjects and non-insulin-dependent diabetics. *Am. J. Physiol. Endocrinol. Metab.* **1992**, *263*, E435–E440. [[CrossRef](#)]
19. Paolisso, G.; Giugliano, D.; Pizza, G.; Gambardella, A.; Tesauro, P.; Varricchio, M.; D'Onofrio, F. Glutathione Infusion Potentiates Glucose-Induced Insulin Secretion in Aged Patients With Impaired Glucose Tolerance. *Diabetes Care* **1992**, *15*, 1–7. [[CrossRef](#)]
20. ADA. Classification and Diagnosis of Diabetes. *Diabetes Care* **2016**, *39*, S13–S22. [[CrossRef](#)]
21. Baker, M.A.; Cerniglia, G.J.; Zaman, A. Microtiter plate assay for the measurement of glutathione and glutathione disulfide in large numbers of biological samples. *Anal. Biochem.* **1990**, *190*, 360–365. [[CrossRef](#)]
22. Modak, M.A.; Parab, P.B.; Ghaskadbi, S.S. Pancreatic Islets Are Very Poor in Rectifying Oxidative DNA Damage. *Pancreas* **2009**, *38*, 23–29. [[CrossRef](#)] [[PubMed](#)]
23. Hothorn, T.; Hornik, K.; van de Wiel, M.A.; Zeileis, A. A Lego System for Conditional Inference. *Am. Stat.* **2006**, *60*, 257–263. [[CrossRef](#)]
24. Cohen, J. *Statistical Power Analysis for the Behavioral Sciences*, 2nd ed.; Routledge: New York, NY, USA, 2013. [[CrossRef](#)]
25. Sawilowsky, S.S. A Different Future For Social And Behavioral Science Research. *J. Mod. Appl. Stat. Methods* **2003**, *2*, 128–132. [[CrossRef](#)]
26. Erdennal, M.; Sunal, E.; Kanbak, G. Age-related changes in the glutathione redox system. *Cell Biochem. Funct.* **2002**, *20*, 61–66. [[CrossRef](#)] [[PubMed](#)]
27. Kulkarni, R.; Acharya, J.; Ghaskadbi, S.; Goel, P. Thresholds of Oxidative Stress in Newly Diagnosed Diabetic Patients on Intensive Glucose-Control Therapy. *PLoS ONE* **2014**, *9*, e100897. [[CrossRef](#)] [[PubMed](#)]
28. Kovacs-Nolan, J.; Rupa, P.; Matsui, T.; Tanaka, M.; Konishi, T.; Sauchi, Y.; Sato, K.; Ono, S.; Mine, Y. In Vitro and ex Vivo Uptake of Glutathione (GSH) across the Intestinal Epithelium and Fate of Oral GSH after in Vivo Supplementation. *J. Agric. Food Chem.* **2014**, *62*, 9499–9506. [[CrossRef](#)]
29. Hanigan, M.H. Gamma-Glutamyl Transpeptidase. In *Advances in Cancer Research*; Townsend, D.M., Tew, K.D., Eds.; Elsevier: Amsterdam, The Netherlands, 2014; pp. 103–141.
30. Anjaneyulu, K.; Anjaneyulu, R.; Sener, A.; Malaisse, W.J. The stimulus-secretion coupling of glucose-induced insulin release. Thiol: Disulfide balance in pancreatic islets. *Biochimie* **1982**, *64*, 29–36. [[CrossRef](#)]
31. Lenzen, S.; Drinkgern, J.; Tiedge, M. Low antioxidant enzyme gene expression in pancreatic islets compared with various other mouse tissues. *Free Radic. Biol. Med.* **1996**, *20*, 463–466. [[CrossRef](#)]
32. Ammon, H.P.T.; Klumpp, S.; Fuss, A.; Verspohl, E.J.; Jaeschke, H.; Wendel, A.; Müller, P. A possible role of plasma glutathione in glucose-mediated insulin secretion: In Vitro and In Vivo studies in rats. *Diabetologia* **1989**, *32*, 797–800. [[CrossRef](#)]

33. Yabe, D.; Seino, Y. Type 2 diabetes via β -cell dysfunction in east Asian people. *Lancet Diabetes Endocrinol.* **2016**, *4*, 2–3. [[CrossRef](#)]
34. Prasad, R.B.; Asplund, O.; Shukla, S.R.; Wagh, R.; Kunte, P.; Bhat, D.; Parekh, M.; Shah, M.; Phatak, S.; Käräjämäki, A.; et al. Subgroups of patients with young-onset type 2 diabetes in India reveal insulin deficiency as a major driver. *Diabetologia* **2022**, *65*, 65–78. [[CrossRef](#)] [[PubMed](#)]
35. Zhang, J.; An, H.; Ni, K.; Chen, B.; Li, H.; Li, Y.; Sheng, G.; Zhou, C.; Xie, M.; Chen, S.; et al. Glutathione prevents chronic oscillating glucose intake-induced β -cell dedifferentiation and failure. *Cell Death Dis.* **2019**, *10*, 321. [[CrossRef](#)] [[PubMed](#)]
36. Del Guerra, S.; Lupi, R.; Marselli, L.; Masini, M.; Bugliani, M.; Sbrana, S.; Torri, S.; Pollera, M.; Boggi, U.; Mosca, F.; et al. Functional and molecular defects of pancreatic islets in human type 2 diabetes. *Diabetes* **2005**, *54*, 727–735. [[CrossRef](#)] [[PubMed](#)]
37. Inzucchi, S.E.; Bergenstal, R.M.; Buse, J.B.; Diamant, M.; Ferrannini, E.; Nauck, M.; Peters, A.L.; Tsapas, A.; Wender, R.; Matthews, D.R. Management of hyperglycemia in type 2 diabetes: A patient-centered approach: Position statement of the American Diabetes Association (ADA) and the European Association for the Study of Diabetes (EASD). *Diabetes Care* **2012**, *35*, 1364–1379. [[CrossRef](#)] [[PubMed](#)]



OPEN ACCESS

EDITED BY

Takeo Nakanishi,
Takasaki University of Health and Welfare,
Japan

REVIEWED BY

Eugenia Piragine,
University of Pisa, Italy
Dateng Li,
Morgan Stanley, United States

*CORRESPONDENCE

Arjun Kolappurath Madathil,
✉ k.marjun@students.iiserpune.ac.in

[†]These authors share first authorship

SPECIALTY SECTION

This article was submitted to Drug
Metabolism and Transport,
a section of the journal
Frontiers in Pharmacology

RECEIVED 18 January 2023

ACCEPTED 27 February 2023

PUBLISHED 13 March 2023

CITATION

Madathil AK, Ghaskadbi S, Kalamkar S and
Goel P (2023), Pune GSH
supplementation study: Analyzing
longitudinal changes in type 2 diabetic
patients using linear mixed-
effects models.
Front. Pharmacol. 14:1139673.
doi: 10.3389/fphar.2023.1139673

COPYRIGHT

© 2023 Madathil, Ghaskadbi, Kalamkar
and Goel. This is an open-access article
distributed under the terms of the
[Creative Commons Attribution License
\(CC BY\)](https://creativecommons.org/licenses/by/4.0/). The use, distribution or
reproduction in other forums is
permitted, provided the original author(s)
and the copyright owner(s) are credited
and that the original publication in this
journal is cited, in accordance with
accepted academic practice. No use,
distribution or reproduction is permitted
which does not comply with these terms.

Pune GSH supplementation study: Analyzing longitudinal changes in type 2 diabetic patients using linear mixed-effects models

Arjun Kolappurath Madathil ^{1*†}, Saroj Ghaskadbi²,
Saurabh Kalamkar² and Pranay Goel¹

¹Biology Division, Indian Institute of Science Education and Research, Pune, India, ²Department of
Zoology, Savitribai Phule Pune University, Pune, India

Oral GSH supplementation along with antidiabetic treatment was shown to restore the body stores of GSH significantly and reduce oxidative DNA damage (8-OHdG) in Indian Type 2 diabetic (T2D) patients over 6 months in our recent clinical study. Post hoc analysis of the data also suggested that elder patients benefit from improved HbA1c and fasting insulin. We modeled longitudinal changes in diabetic individuals using a linear mixed-effects (LME) framework and obtained i) the distribution of individual trajectories with and without GSH supplementation and ii) the overall rates of changes in the different study arms. Serial changes in elder and younger diabetic individuals were also modeled independently to examine differences in their progression. The average linear trajectories obtained from the model explain how biochemical parameters in T2D patients progress over 6 months on GSH supplementation. Model estimates show improvements in erythrocytic GSH of 108 μM per month and a reduction in 8-OHdG at a rate of 18.5 ng/ μg DNA per month in T2D patients. GSH replenishes faster in younger people than in the elder. 8-OHdG reduced more rapidly in the elder (24 ng/ μg DNA per month) than in younger (12 ng/ μg DNA per month) individuals. Interestingly, elder individuals show a substantial reduction in HbA1c (0.1% per month) and increased fasting insulin (0.6 $\mu\text{U}/\text{mL}$ per month). Changes in GSH correlate strongly with changes in HbA1c, 8-OHdG, and fasting insulin in the elder cohort. The model estimates strongly suggest it improves the rate of replenishment in erythrocytic GSH stores and reduces oxidative DNA damage. Elder and younger T2D patients respond differently to GSH supplementation: It improves the rate of reduction in HbA1c and increases fasting insulin in elder patients. These model forecasts have clinical implications that aid in personalizing treatment targets for using oral GSH as adjuvant therapy in diabetes.

KEYWORDS

GSH supplementation, type 2 diabetes, HbA1c, 8-OHdG, elderly diabetic population, mixed-effects models

Abbreviations: T2D, Type 2 diabetes; HbA1c, glycated hemoglobin; GSH, reduced glutathione; GSSG, oxidized glutathione; PP glucose, postprandial glucose; PP insulin, postprandial insulin; 8-OHdG, 8-hydroxy-2-deoxy guanosine; LME, Linear Mixed-Effects; EA, Elder Adults.

Introduction

A large number of clinical and experimental studies have demonstrated the role of oxidative stress in developing type 2 diabetes (T2D) complications (Brownlee, 2005; Volpe et al., 2018; Burgos-Morón et al., 2019). However, the use of antioxidants as therapy isn't recommended in healthcare practice due to the lack of evidence about their long-term safety and efficacy. Glutathione (GSH) is a major endogenous antioxidant in all cells and determines their redox status and is significantly low in T2D individuals (Townsend et al., 2003). Therefore, replenishing GSH should be a good strategy to improve systemic redox status. However, few clinical trials with GSH supplementation have been conducted in healthy and diabetic individuals. Most of these studies have concentrated on the effect of GSH supplementation on replenishing body stores of GSH; few have studied its impact on reducing oxidative stress, and even fewer on glycemic stress. Results of these trials (Allen and Bradley, 2011; Sekhar et al., 2011; Ritchie et al., 2015) have been difficult to interpret due to differences in the dose and duration of GSH supplementation and the site of outcome measurements, making the clinical recommendations difficult.

Our recent work (Kalamkar et al., 2022) has provided the most conclusive evidence regarding the effects of GSH supplementation in conjunction with antidiabetic treatment. The evidence from this clinical trial suggested that the long-term GSH supplementation offered protection from oxidative damage and improved HbA1c and fasting insulin, especially in elderly T2D patients. We, therefore, believe that GSH should be used as an adjunct therapy for T2D individuals. In our data, we observed significant differences in how individuals respond to GSH intervention. In addition to the factors such as age, diet, physical activity, dose, and length of GSH intervention, the basal amount of endogenous GSH is also responsible for this differential response among individuals. Therefore, we feel that the personalization of GSH supplementation based on endogenous GSH for T2D individuals could be an important addition to current clinical practices. To formulate effective personalized interventions of GSH with antidiabetic treatment, it is essential to understand the dynamics of longitudinal biochemical change and the variations between individual responses to GSH supplementation in detail. This would be largely useful in evaluating the progress of treatment and understanding the glucose control targets for diabetic individuals.

In this work, we have formulated longitudinal mixed-effects models (Laird and Ware, 1982; Brown and Prescott, 2006) to analyze the clinical data of diabetic individuals. Our mixed-effects (ME) models are hierarchical models, where the units of analysis are subject-level predictors (level two) with fixed and random effects. The framework of LME models also performs 'shrinkage' for estimating model parameters; that is, individual estimates obtained from LME models are shrunk towards a grand mean of the population level estimate compared to fitting separate linear models to each subject's data (Bell et al., 2019). ME models have a long history of use in health and medicine since these models treat each patient not only as a member of a population but as an individual with unique characteristics (Gelman et al., 2012; Barr et al., 2013; Baldwin et al., 2014; Wang et al., 2019; Schober and Vetter, 2021). ME models thus allow estimating model parameters that describe between- and within-subject variability of individual responses. A two-level LME model provides reliable estimates in absolute, not just relative, physical units of the variables.

This is beneficial for direct clinical use rather than the effect-size-based estimates of treatment effects obtained in our earlier work. We formulated two different LME models, namely, 1) with random intercepts and fixed slopes and 2) random intercepts and random slopes for each variable. These models were evaluated using best likelihood by Akaike's Information Criteria (AIC) and non-singularity criteria and selected for optimal performance (Bates D. M. et al., 2015).

In our earlier study, we pointed out that the response in elder and younger cohorts was markedly different. We, therefore, analyzed these data separately with LME models.

Materials and methods

Clinical trial data

This study has been carried out using the data published in our work (Kalamkar et al., 2022), which was collected from the clinical trial entitled "Effect of glutathione supplementation on glucose homeostasis in diabetic patients" and registered with the Clinical Trials Registry -India (CTRI/2018/01/011257). The data set is freely available online (on the link: <https://figshare.com/s/0803267e1d38c054cee6>). The analysis of the clinical trial data was conducted with ethical approvals from the Institutional Ethical Committee (IEC) of Jehangir Hospital Development Center, Pune (JCDC ECN- ECR/352/Inst/NIH/2013), IEC of IISER Pune (IECHR/Admin/2019/001); and the Institutional Biosafety Committee (IBC) of SPPU (Bot/27A/15).

The dataset published in the trial comprised 250 known Indian diabetic individuals recruited between February 2016 and January 2018 who were already on anti-diabetic treatment. The clinical trial consisted of three groups: A control group comprising healthy, non-diabetic subjects and two groups of diabetic patients; in one of those, GSH supplementation (500 mg/day for 6 months) was carried out, namely, the DG group, and the other group without supplementation, the D group. The only difference between this D and DG group is the intervention, that is, supplementation with GSH. More importantly, D and DG are similar in nearly all respects, and covariate balance at the baseline has already been shown (Kalamkar et al., 2022).

Measured variables and follow-up visits

Blood samples of each individual were collected at the time of recruitment and three and 6 months post-GSH supplementation. The dataset used in this study consists of the amounts of reduced (GSH) and oxidized (GSSG) glutathione, fasting and postprandial glucose (FPG and PPG), fasting and postprandial insulin (FPI and PPI), HbA1c, and 8-hydroxy-deoxy-guanosine (8-OHdG), a marker of oxidative DNA damage measured from all individuals.

Statistical analysis

Descriptive statistics with the mean and standard deviation (SD) were used to describe different study groups in terms of metabolic outcomes at baseline and each subsequent follow-up. Biochemical

parameters at different visits were compared using two-sample t-tests. The statistical significance of the comparisons was set at a p -value less than 0.05.

Formulation of linear mixed-effect models

The formulation of linear mixed-effect (LME) models for each biochemical variable (GSH, GSSG, HbA1c, 8-OHdG, FPG, FPI, PPG, and PPI) assumed fixed and random effect parameters at different levels (Level 1: time, Level 2: individuals) in the study. The composite form of the model was written by combining the model equations from these different levels. This form of the model was further used to study the dependency of each effect at different levels and their nested structure in one another. The response variable Y_{ij} from subject i on the j^{th} visit was modeled with subject-specific intercepts (b_{i0}) and subject-specific slopes (b_{i1}) against treatment time t_{ij} (where $t_{ij} = 0, 3, 6$ months for $j = 1, 2, 3$ visits respectively). An indicator variable T_i was assumed to take a value of 0 for the D group and one for the DG group (control and treatment with GSH supplementation, respectively). We denote the average intercept of diabetic individuals when all predictors are 0 by β_0 (mean expected value of the response variable Y). β_1 represents the average rate of change in Y during the treatment for the D group. $\beta_1 + \beta_2$ represents the average rate of change in the DG group. The difference in the rates of change between D and DG β_2 represents the average treatment effect of GSH supplementation on Y .

We considered two candidate models of biochemical variables, namely, 1) random intercept and random slope (RIRS) model and 2) random intercept and fixed slope (RIFS) model for explaining the measured longitudinal data. We formulated RIRS models for the outcome variable Y_{ij} as $Y_{ij} = b_{i0} + b_{i1} \times t_{ij} + \epsilon_{ij}$ with subject-specific random slopes and intercepts b_{i0} and b_{i1} defined by $b_{i0} = \beta_0 + b_{i0}$ and $b_{i1} = \beta_1 + \beta_2 \times T_i + b_{i1}$ where b_{i0} , and b_{i1} were assumed to be distributed as $N(0; \sigma_0^2)$ and $N(0, \sigma_1^2)$, with covariance σ_{01} , respectively. In the RIRS model, fixed effects are $\beta_0, \beta_1, \beta_2$ and random effects are b_{i0}, b_{i1} . The residual errors were assumed to be normally distributed with a variance of σ_e^2 . The composite form of the RIRS model for Y_{ij} is given by, $Y_{ij} = \beta_0 + b_{i0} + (\beta_1 + \beta_2 \times T_i + b_{i1}) \times t_{ij} + \epsilon_{ij}$.

RIFS models for outcome variable Y_{ij} were formulated with random intercepts and fixed slopes at subject level (level 2) defined by intercept, $b_{i0} = \beta_0 + b_{i0}$ and slope; $b_{i1} = \beta_1 + \beta_2 \times T_i$. The random intercepts b_{i0} in the model were assumed to be distributed as $b_{i0} \sim N(0; \sigma_0^2)$. The composite forms of the RIFS model for Y_{ij} is given by $Y_{ij} = \beta_0 + b_{i0} + (\beta_1 + \beta_2 \times T_i) \times t_{ij} + \epsilon_{ij}$.

The design matrices for model equations and covariance matrices are described in further detail in [Supplementary Sections S1.1, S1.2](#).

Model parameters and fitting

The formulated models have been tested and fitted using the **lme4** package in R (Bates D. et al., 2015); these calculations were confirmed using the **fitlme** package in Matlab and the **mimoso** package (Titz, 2020) for mixed effects models. Other packages, ggplot2, and tidyverse in R, were used for analysis and plots. RIFS and RIRS models were fitted for GSH, GSSG, 8-OHdG, HbA1c, FPG, FPI, PPG, and PPI. A suitable RIFS

or RIRS model was selected for each response variable using the best AIC and non-singularity criteria (Bates D. M. et al., 2015).

RIFS models were fitted for five parameters, $\beta_0, \beta_1, \beta_2, \sigma_0, \sigma_e$ and RIRS models were fitted with seven parameters, $\beta_0, \beta_1, \beta_2, \sigma_0, \sigma_1, \sigma_{01}, \sigma_e$. The fitted estimates for β and b , the vectors of fixed effect parameters, random effect parameters, respectively, are given by the Best Linear Unbiased Estimator (BLUE) of $\hat{\beta}$, and Best Linear Unbiased Predictor (BLUP) of \hat{b} , (Refer to [Supplementary Section S1.3](#) for further details). The components of \hat{b} , b_{i0} , and b_{i1} , random effects represent person-specific intercepts (in both RIFS and RIRS) at the baseline and person-specific differences in the rate of change in the slopes (in RIRS only), respectively.

The statistical significance of the results of the LME estimates was determined as $p < 0.05$. We have followed the uncorrected p -value to interpret the results through. To ensure completeness, we have performed corrections for multiple comparisons using the Bonferroni method. We applied these corrections for the estimates from LME models for each variable and across all results in both main and supplementary analyses. Those results, which continued to be statistically significant even after the corrections, were marked with a “#” in the corresponding tables. The reader should take this into consideration when evaluating the statistical findings.

Analysis of elder and younger patients

The variation in response to GSH supplementation with age was studied as follows: The data was divided into 1) a subgroup of elder adults (EA) above 55 years and 2) the subgroup of younger adults (YA) below 55 years.

The model for EA is given by $Y_{ij} = \beta_0 + b_{i0} + (\beta_1 + \beta_2 \times T_i) \times t_{ij} + \epsilon_{ij}$. The treatment variable T_i takes the value of 0 for EA in the D group and one for the EA in the DG group. The model was formulated similarly for YA as well.

Analysing the age effects on outcomes

We studied the effects of the age of individuals on the outcome variables Y with different LME models by incorporating 1) continuous variable for the age of individuals at the recruitment and 2) categorical variable for elder and younger age groups. These model formulations are described in [Supplementary Section S1.4](#).

The models considered in this analysis are the following:

- (i) Model 1: The original RIRS model in the study without age variables
- (ii) Model 2: RIRS model with a treatment-time interaction term, and three-way interaction term with age, treatment indicator, and time at the patient level (Level 2)
- (iii) Model 3: RIRS model with a three-way interaction term with age, treatment indicator, and time at the patient level (Level 2)
- (iv) Model 4: RIRS model with age groups as a categorical variable for pooling EA and YA at the patient level (Level 2)

These models were fitted for all eight variables, and their performances were compared using AIC and BIC estimates after the likelihood ratio test.

The structure of the data from the D and DG groups

A sample structure of the data from the clinical trial is given in [Supplementary Table S1](#). This data format was prepared for analysis using the lme4 package. The dataset consisted of eight different measured variables of 201 individuals (100 in D, 101 in DG) who completed both the follow-up visits (3 and 6 months post-GSH supplementation). The Group IDs are encoded as 0 for D and one for DG.

Estimating correlations between longitudinal changes in different variables

The correlation between individual-specific slopes of variables obtained from RIRS models was estimated using the Pearson correlation coefficient (Pearson, 1895). Correlation diagrams were obtained between all variables using the slopes for RIRS models fitted with 1) the whole data sets and 2) the unpooled data sets from elder individuals and younger individuals. The size of the circle in each cell of the correlation diagram represents the extent of correlation between compared variables. The blue color represents a positive correlation, and the brown represents a negative correlation.

Making predictions for virtual individuals

The fitted model estimates were utilized to predict responses in virtual individuals with diabetes. We considered three new virtual individuals (V1, V2, and V3) and assumed arbitrary but reasonable baseline measurements of GSH, 8-OHdG, and HbA1c. We thus predicted trajectories in these subjects over 6 months. The scheme used for this purpose is described in [Supplementary Section S1.5](#). The steps in this scheme perform the following:

- (i) The baseline values assumed for virtual subjects are shrunk towards the average intercept estimated by our LME model, and the individual specific random effects are obtained.
- (ii) Using the LME model estimates of the average intercept, random effect of the intercept, and the rate of changes in the slopes, we obtained the average linear trajectory for each virtual individual in the presence and absence of GSH supplementation.

Results

Observational summary of longitudinal changes in the D and DG groups

Group-wise statistics (mean and standard deviation) of the measured variables (GSH, GSSG, 8-OHdG, HbA1c, FPG, FPI, PPG, and PPI) for both D and DG in each of the three visits are described in [Kalamkar et al. \(2022\)](#); these are summarized here for completeness in [Table 1](#).

GSH and GSSG were significantly increased, and 8-OHdG and HbA1c significantly decreased ($p < 0.001$) within 3 months in DG and continued to be so at 6 months as well. FPI of DG increased significantly within 6 months ($p < 0.001$). FPG, PPG, and PPI didn't show significant changes. GSH in the third visit was also significantly increased in D, but not as much compared to the corresponding change in DG.

LME estimates of the rates of change for the whole population

We fit RIRS and RIFS models for GSH, GSSG, 8-OHdG, HbA1c, FPG, PPG, FPI, and PPI (as described in [Model parameters and fitting](#)). These subject-wise trajectories obtained from RIRS models are shown in [Figure 1](#). Individual trajectories are distributed around the group-wise average trajectory. Group-wise average intercepts are determined by β_0 ; these are equal for both D and DG. The average slopes in D and DG are β_1 and $\beta_1 + \beta_2$, respectively. This β_2 denotes the difference between the average slopes in the two groups, that is, the treatment effect of GSH supplementation on outcomes. These estimates (β_0 , β_1 , and β_2) are detailed in [Table 2](#). Estimated random effects, that is, within-individual and between-individual variations, are described in [Supplementary Tables S2, S3](#).

We find that β_2 is significant for GSH, GSSG, and 8-OHdG ([Table 2](#)). Among the glycemic variables, β_2 is significant only for FPI, and PPI but not for HbA1c, FPG, and PPG.

The mean erythrocytic GSH is estimated as 492 μM in individuals with diabetes. It increased slightly, at an average rate of 0.04 μM per month from the baseline during the study period in D. In DG, GSH increased at an average rate of 107.7 μM per month. Therefore GSH supplementation significantly improved GSH by about 22 percent (107.7 μM , $p < 0.001$) per month relative to baseline. Mean GSSG is estimated as 221 μM . In D and DG, GSSG increased at average rates of 4.7 and 17.7 μM per month, respectively, from the baseline ([Figure 1](#)). Thus GSSG rates are significantly improved ($p < 0.001$) by about six percent per month of the baseline (13.02 μM , $p < 0.001$). 8-OHdG is estimated to be 442 ng/ μg DNA in diabetic individuals. It decreased in D and DG at average rates of 2.8 and 21.3 ng/ μg DNA per month, respectively. Thus the effect of GSH supplementation significantly reduced 8-OHdG by four percent per month of the baseline (18.5 ng/ μg DNA, $p < 0.001$).

HbA1c, FPG, and PPG changed at similar rates in D and DG ([Figure 1](#)), suggesting that the effect was negligible ($p > 0.05$). FPI and PPI are found to be affected significantly. Mean FPI is estimated as 13.4 $\mu\text{U}/\text{mL}$. FPI decreased at an average rate of 0.3 $\mu\text{U}/\text{mL}$ per month in D. GSH supplementation significantly improved FPI at a rate of 0.2 $\mu\text{U}/\text{mL}$ in DG. The average PPI is estimated as 48.8 $\mu\text{U}/\text{mL}$ in individuals with diabetes. It decreased at average rates of 0.8 and 4.9 $\mu\text{U}/\text{mL}$ per month in D and DG, respectively ([Figure 1](#)). GSH supplementation significantly enhanced FPI by four percent (0.5 $\mu\text{U}/\text{mL}$, $p < 0.001$) and reduced PPI rates by eight percent (4.1 $\mu\text{U}/\text{mL}$, $p < 0.001$) of the baseline per month.

Results obtained from RIFS models are shown in [Supplementary Figure S1](#) and [Supplementary Table S3](#). The parameter estimates of β_2 from RIFS models are also found to be significant for GSH, GSSG,

TABLE 1 0-, 3- and 6- month changes of subjects in D and DG groups. Group-wise means and standard deviations (SD) of blood concentrations of GSH, GSSG, 8-OHdG, HbA1c, FPG, FPI, PPG, and PPI are shown for D and DG groups at different visits. The significance of change is determined for the second (3 months from the first visit) and third visits (6 months from the first visit) relative to the first visit using two-sample t-tests. The significance levels used are * $p < 0.05$, ** $p < 0.01$, and *** $p < 0.001$. Abbreviations of the variables used here are: HbA1c—glycated hemoglobin, GSH—reduced glutathione, GSSG—oxidized glutathione, PP glucose—postprandial glucose, PP insulin—postprandial insulin, and 8-OHdG—8-hydroxy-2-deoxy guanosine.

Variable	Mean (SD) in the D group			Mean (SD) in the DG group		
	Baseline visit	Second visit	Third visit	Baseline visit	Second visit	Third visit
GSH (μM)	395 (225)	428 (263)	484 (255)***	465 (352)	1,129 (668)***	1,021 (518)***
GSSG (μM)	249 (150)	236 (157)	262 (137)	163 (104)	333 (214)***	286 (204)***
8-OHdG (ng/ μg DNA)	422 (124)	404 (124)	443 (110)	471 (83)	387 (112)***	313 (135)***
HbA1c (%)	8.4 (1.9)	7.9 (1.7)**	8.2 (1.8)	8.5 (1.9)	7.7 (1.5)***	7.9 (1.5)***
FPG (mg/dL)	160 (61)	143 (47)*	151 (58)*	153 (59)	141 (47)	150 (59)
FPI ($\mu\text{U/mL}$)	14.2 (10.4)	12.7 (6.8)	12.1 (7.7)	12.6 (8.06)	14.6 (13.8)	13.9 (10.5)***
PPG (mg/dL)	233.6 (84.1)	216.9 (70.9)	220.3 (83.6)	221.9 (77)	211 (80.4)	218 (83.2)
PPI ($\mu\text{U/mL}$)	43.4 (26.9)	47.03 (33.3)	40.5 (29.9)	48.3 (47.7)	49.5 (39.6)	52.3 (43.8)

8-OHdG, FPI, and PPI, leading to similar conclusions about the effects of GSH supplementation as in RIRS models.

We note that these results largely coincide with the results from previous work (Kalamkar et al., 2022). However, FPI and PPI, which were earlier reported not to be affected by GSH supplementation, are found to have a significant effect through the LME model-based analysis.

Independent LME model estimates for ages above and below 55 years

Diabetes is an age-onset disease; an early diagnosis leads to an increased chance for complications to set in relatively early. We have earlier demonstrated that the effectiveness of GSH supplementation differed between the younger and elder populations using an age cutoff of 55 years, which was the median age of the study population (Kalamkar et al., 2022). We fit a separate LME for each of these two age groups. Model estimates obtained by fitting LME models independently for EA and YA are detailed in [Supplementary Table S4](#).

GSH supplementation significantly affected GSH, 8-OHdG, HbA1c, FPI, and PPI in EA, and GSH, GSSG, 8-OHdG, and PPI in YA (β_2 in [Table 3](#), $p < 0.001$).

GSH

Mean erythrocytic GSH in EA (488 μM) is estimated to be less than YA (497 μM). In YA of D, it decreased at an average rate of 6.9 μM per month, whereas in DG, GSH increased at an average rate of 104 μM per month ([Supplementary Figure S2](#)). In EA of D and DG, GSH increased at average rates of 6.5 and 111 μM per month, respectively ([Figure 2](#)). This clearly indicates that GSH supplementation resulted in a significant improvement in GSH by about 21 percent per month of their baseline in YA (111 μM , $p < 0.001$) and 22 percent per month in EA (105 μM , $p < 0.001$) with diabetes.

GSSG

Interestingly, the effect on GSSG was significant in YA ($p < 0.01$) but not in EA. The mean GSSG in EA (231 μM) was estimated to be higher than YA (209 μM). When YA of D and DG were examined, GSSG increased at average rates of 1.9 and 18.4 μM per month, respectively ([Supplementary Figure S2](#)). It increased at average rates of 7.6 and 17.1 μM per month in EA of D and DG, respectively ([Figure 2](#)). This shows that GSH supplementation enhanced GSSG significantly per month by eight percent of the baseline (17.5 μM , $p < 0.001$) per month only in YA.

8-OHdG

The average 8-OHdG estimate is higher in EA (445 ng/ μg DNA) than in YA (438 ng/ μg DNA). In EA of both D and DG, 8-OHdG decreased at average rates of 3.3 and 27 ng/ μg DNA per month during the study period ([Figure 2](#)). Similarly, it decreased at average rates of 2.1 and 14.16 ng/ μg DNA per month in the YA of D and DG groups ([Supplementary Figure S2](#)). Thus, we find that GSH supplementation significantly reduced 8-OHdG from the baseline by 12.06 ng/ μg DNA per month (3%) in YA and 23.7 ng/ μg DNA per month (5%) in EA. These results suggest that oral GSH administration rapidly offers better protection from oxidative DNA damage in EA compared to YA.

HbA1c

GSH supplementation was earlier reported to affect the HbA1c in the elder cohort significantly (Kalamkar et al., 2022). We examined LME estimates of both YA and EA to quantitate the effect on HbA1c. The average HbA1c is estimated at 8.3% and 8.4% in YA and EA, respectively. In EA of D, HbA1c decreased at an average rate of 0.02% per month, while in DG, it decreased at an average rate of 0.12% per month ([Figure 2](#)), suggesting that GSH supplementation improved HbA1c rates significantly by about 0.1% per month in EA. Estimated HbA1c rates are not significantly different between YA of D and DG ([Supplementary Figure S2](#)).

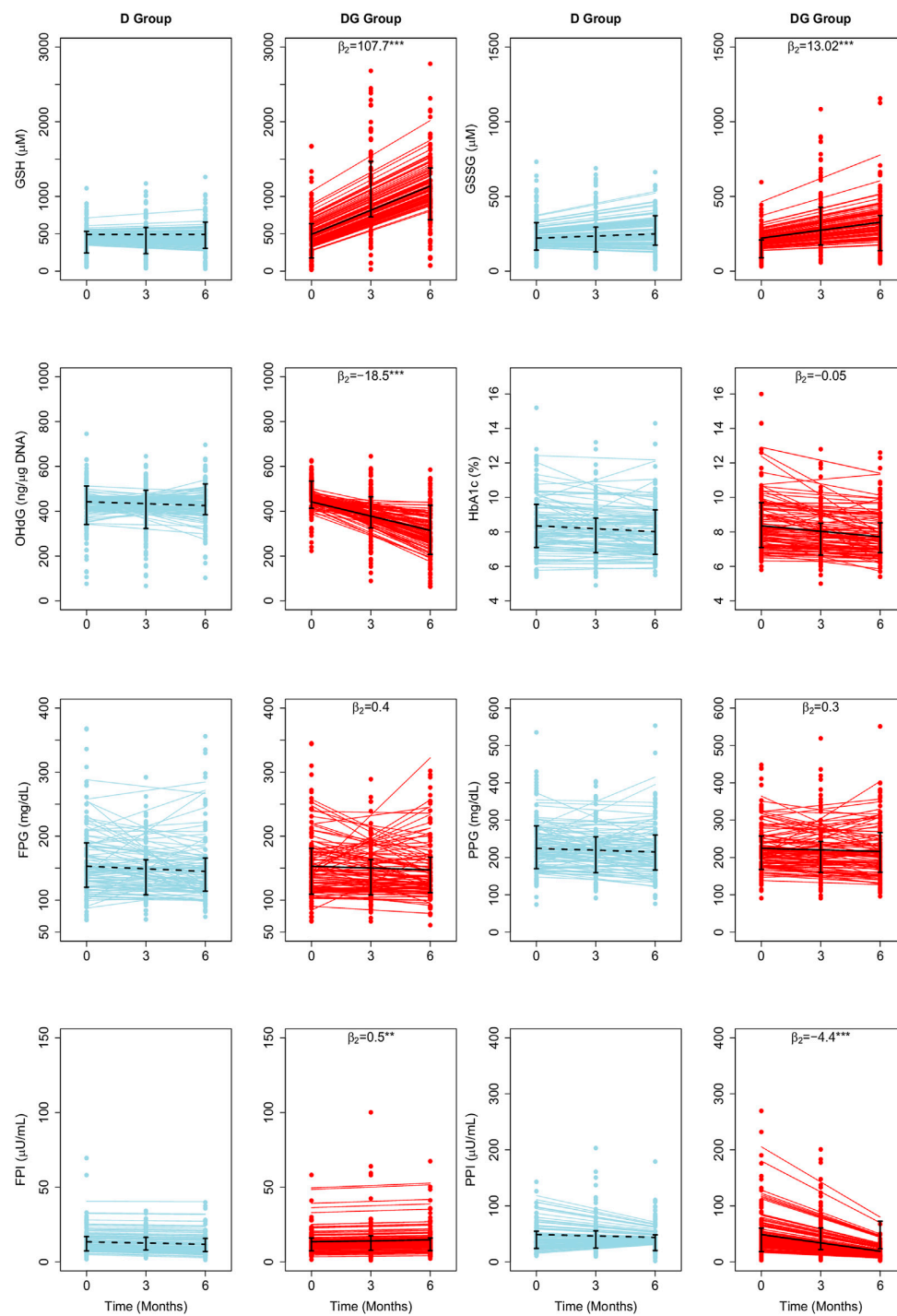


FIGURE 1

Average treatment effects of GSH supplementation on biochemical changes estimated using LME Models. The fitted results of RIRS models for GSH, GSSG, 8-OHdG, HbA1c, FPG, FPI, PPG, and PPI (RIFS model fits are shown in [Supplementary Figure S1](#)) in D group and DG groups (figure panels marked with titles D and DG) are overlaid here with the longitudinal data from 201 individuals (100 D subjects in blue circles, 101 DG subjects in red circles) at different visits. Solid blue and red lines depict the fitted subject-specific mean trajectories in the D group and the DG group, respectively. The black dotted and solid lines represent the group-wise means for D and DG, respectively. Interquartile ranges of the data for D and DG groups are shown with vertical interval plots (25th–75th quartiles) at each visit. The average treatment effects of GSH supplementation (β_2) are denoted on top of each panel corresponding to the DG group. The estimated β_2 was significant on the rate of changes in GSH ($\beta_2 = 107.7 \mu\text{M}$ per month), GSSG ($\beta_2 = 13.02 \mu\text{M}$ per month), 8-OHdG ($\beta_2 = -18.5 \text{ ng}/\mu\text{g DNA}$ per month), FPI ($\beta_2 = 0.5 \mu\text{U}/\text{mL}$ per month) and PPI ($\beta_2 = -4.1 \mu\text{U}/\text{mL}$ per month) levels. The significance levels of parameter estimate are given by $^*p < 0.05$, $^{**}p < 0.01$, and $^{***}p < 0.001$. Abbreviations of the variables used here are HbA1c—glycated hemoglobin, GSH—reduced glutathione, GSSG—oxidized glutathione, PP glucose—postprandial glucose, PP insulin—postprandial insulin, and 8-OHdG—8-hydroxy-2-deoxy guanosine.

TABLE 2 Fixed-effects parameter values obtained by fitting LME models of RIRS form for GSH, GSSG, 8-OHdG, HbA1c, FPG, FPI, PPG, and PPI variables are presented here with standard error associated with the estimates. Random-effects parameter values are given in [Supplementary Table S2](#). The fitted results from the corresponding RIFS model are shown in [Supplementary Table S3](#). Average treatment effects (β_2) of GSH supplementation were observed to be significant on the rate of changes (slopes) for GSH, GSSG, 8-OHdG, FPI, and PPI levels. Statistical significance levels of parameter estimates are given by * $p < 0.05$, ** $p < 0.01$, and *** $p < 0.001$. Abbreviations of the variables used here are the same as in [Table 1](#).

Variable	Fixed effect parameters		
	β_0 (SE)	β_1 (SE)	β_2 (SE)
GSH (μM)	492.2 (27.4)***#	0.04 (8.6)	107.8 (10.3)***#
GSSG (μM)	221 (11.3)***#	4.9 (3.1)	12.7 (3.8)***#
8-OHdG (ng/ μg DNA)	442 (7.5)***#	-2.8 (2.6)	-18.5 (2.9)***#
HbA1c (%)	8.4 (0.1)***#	-0.06 (0.03)	-0.05 (0.04)
FPG (mg/dL)	152.9 (3.9)***#	-1.33 (1.09)	0.4 (1.3)
FPI ($\mu\text{U}/\text{mL}$)	13.4 (0.66)***#	-0.3 (0.14)*	0.5 (0.2)**
PPG (mg/dL)	224.4 (5.4)***#	-1.6 (1.6)	0.3 (1.9)
PPI ($\mu\text{U}/\text{mL}$)	48.8 (2.3)***#	-0.7 (0.6)	-4.4 (0.7)***#

TABLE 3 Baseline assumptions for virtual individuals. The concentrations of GSH, 8-OHdG, and HbA1c assumed at the baseline for virtual individuals (V1, V2, and V3) to make predictions using RIFS models are shown in the table.

Subject ID	GSH (μM)	8-OHdG (ng/ μg DNA)	HbA1c (%)
V1	200	500	10
V2	500	400	8
V3	800	300	6

Fasting Insulin

Our earlier work (Kalamkar et al., 2022) found that oral GSH supplementation significantly changed FPI in elder patients. We quantitated the effect on FPI using LME model estimates ([Supplementary Table S4](#)). The average FPI is estimated to be 12.9 $\mu\text{U}/\text{mL}$ in YA and 14 $\mu\text{U}/\text{mL}$ in EA. In both EA and YA of D, FPI decreased at rates of 0.4 $\mu\text{U}/\text{mL}$ and 0.1 $\mu\text{U}/\text{mL}$ per month, respectively ([Figure 2](#)). The estimated rates were similar between the YA of the D and DG, indicating that the effect on FPI is negligible ($p > 0.05$). On the other hand, in EA of DG, FPI increased at a rate of 0.2 $\mu\text{U}/\text{mL}$ per month, suggesting that GSH supplementation improved FPI rates significantly by 0.6 $\mu\text{U}/\text{mL}$ per month. FPI increased by 4.3% of the baseline per month in EA and negligibly in YA.

Postprandial Insulin

Using LME models to fit the data, PPI was found to decrease in both YA and EA. The average PPI in YA and EA is estimated to be 46 and 51 $\mu\text{U}/\text{mL}$, respectively. In YA of D, PPI increased at a rate of 0.1 $\mu\text{U}/\text{mL}$ per month, whereas in DG, it decreased at a rate of 4.7 $\mu\text{U}/\text{mL}$ per month. PPI decreased at average rates of 1.6 $\mu\text{U}/\text{mL}$ and 5.2 $\mu\text{U}/\text{mL}$ per month in EA of D and DG, respectively.

Fasting and Postprandial Glucose

The average FPG estimated in YA and EA are 156 and 150 mg/dL, respectively. In both YA and EA, the GSH supplementation effect wasn't found to be significant. In both EAs of D and DG, FPG decreased at average rates of 1.7 and 0.9 mg/dL per month, respectively. Similarly, in YAs of D and DG, it decreased at average rates of 1.3 and 0.8 mg/dL per month, respectively. PPG estimated in YA and EA at the time of recruitment is 227 and 223 mg/dL, respectively. GSH supplementation decreased PPG by 2.5 mg/dL per month in EAs and increased PPG by 3.5 mg/dL per month in YA.

For exploratory purposes, we also analyzed the effects of the age using new candidate models as incorporated with age as a model variable (Model 2, Model 3, and Model four in [Supplementary Section S1.4](#)) for GSH, GSSG, 8-OHdG, HbA1c, FPG, FPI, PPG, and PPI. Results obtained by fitting with these models are shown in [Supplementary Tables S5A–C](#). When we compared model fits from all four models using AIC and BIC estimates, our original RIRS model (Model 1) was found to be the better-fit model for all variables ([Supplementary Table S5D](#)).

Changes in GSH correlate strongly with changes in HbA1c and 8-OHdG in EA

We estimated pairwise correlations between subject-specific slopes of GSH, GSSG, 8-OHdG, HbA1c, FPG, FPI, PPG, and PPI obtained from RIRS models. These correlation diagrams for the full population (pooled data) are shown in [Figure 3A](#). Changes in GSH are found to be strongly correlated positively with GSSG ($r > 0.6$) and FPI ($r > 0.9$). Changes in GSH correlated negatively with 8-OHdG and PPI ($r < -0.6$). The other correlations are found to be relatively weaker.

Correlation plots for EAs alone are shown in [Figure 3B](#). GSH slopes are strongly negatively correlated with 8-OHdG slopes ($r = -0.71$) and HbA1c slopes at moderate levels ($r = -0.43$). GSH slopes are strongly negatively correlated with PPI slopes ($r = -0.74$, [Figure 3B](#)); however, they are strongly positively correlated with FPI ($r = 0.75$).

In YAs ([Supplementary Figure S3](#)), GSH slopes are negatively correlated at moderate levels with 8-OHdG ($r = -0.43$) and PPI ($r = -0.57$) slopes. The correlation between GSH slopes and HbA1c slopes is negligibly small.

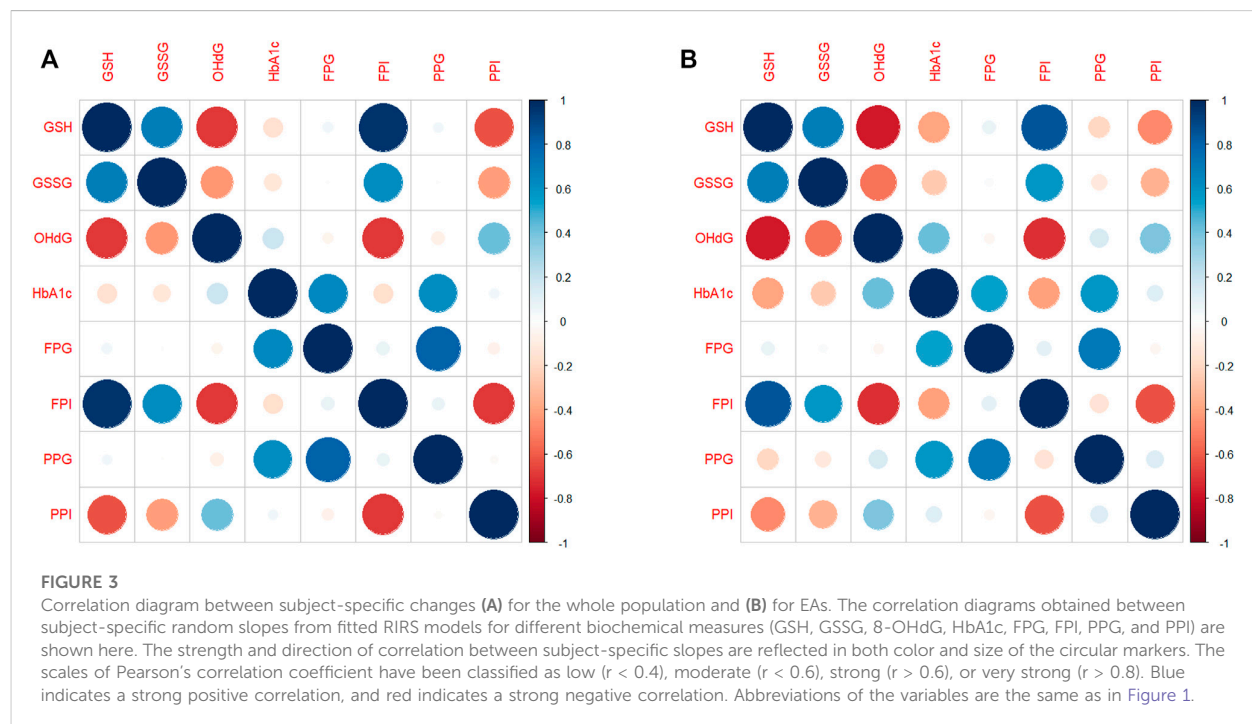
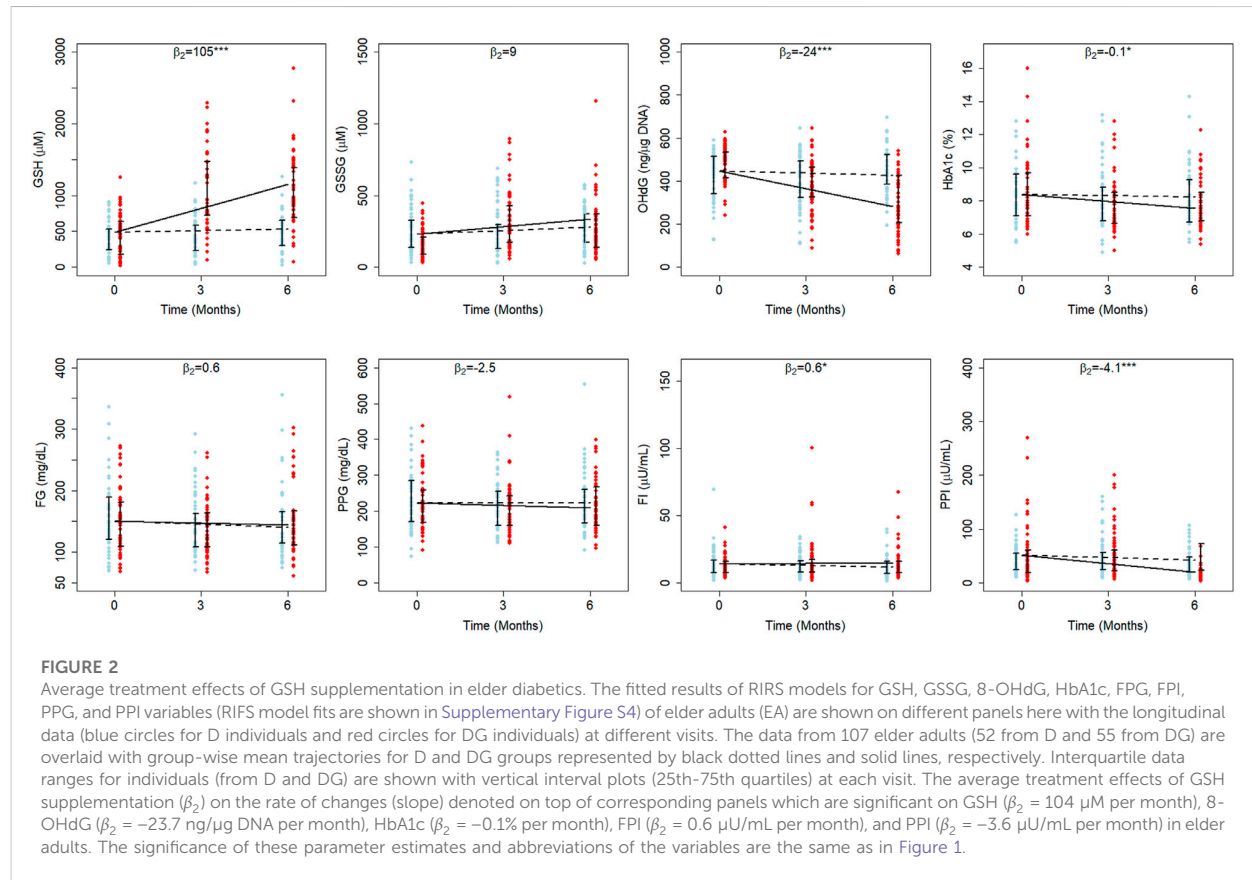
Taken together, the strengths of the correlations between the changes in GSH and outcome variables are evidently different between EAs and YAs.

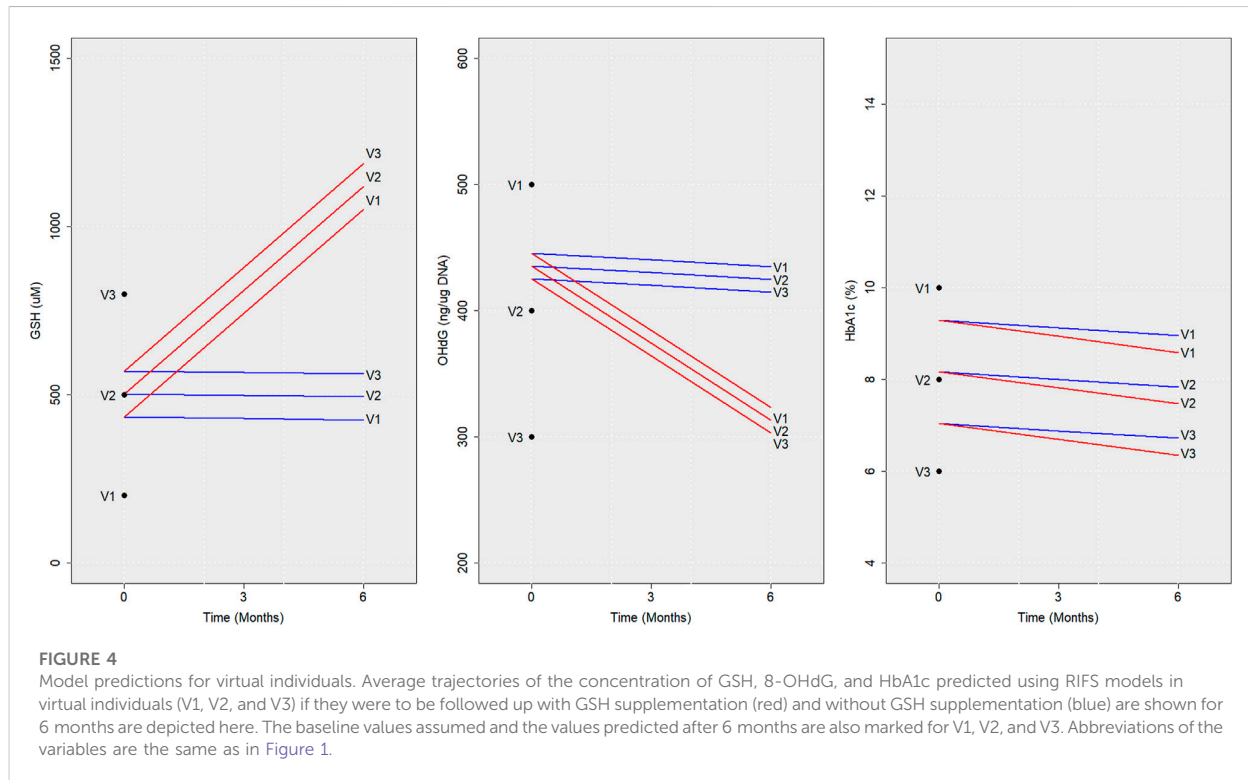
We next use LME model estimates to help quantify the overall rates of changes that can be expected of individuals.

Predicted trajectories for virtual diabetic individuals

Next, we describe the sample predictions obtained for three virtual individuals (V1, V2, and V3) using RIFS models. Baseline values assumed for these virtual individuals are given in [Table 3](#).

The trajectories of GSH, 8-OHdG, and HbA1c obtained if they were with or without GSH supplementation are shown in [Figure 4](#).





RIFS models predicted the GSH of V1 close to 429 μM by the end of 6 months, whereas, on GSH supplementation, V1 ended up at 1,079 μM . Similar predictions were made for 8-OHdG and HbA1c for all these individuals (Figure 4).

This can also be modified to estimate 1) the average time required for a recruited individual to reach a particular level of a biochemical parameter given the baseline value and 2) the expected change in the level of a particular biochemical parameter with time.

Finding a patient's potential trajectory has direct clinical and academic uses. This method, therefore, can be used on newly added subjects to predict different outcomes during 6 months, with or without GSH supplementation.

Discussion

Our earlier study demonstrated *population-level* changes in GSH, GSSG, HbA1c, 8-OHdG, FPG, FPI, PPG, and PPI; these changes were further studied for younger and elder subgroups of the patients. The response in individual patients is, unsurprisingly, considerably varied; however, analyzing individual responses was beyond the scope of that study. In the present study, we are focused on explaining *individual-level* responses to GSH supplementation over the full study period of 6 months. We addressed this through a linear mixed-effects model framework. The major results of this study are to characterize the variability in the inter-individual biochemical response, in particular, determined by the age group of an individual. To the best of our knowledge, this is the first inter-individual analysis of the effects of GSH supplementation in patients with diabetes.

The response to GSH supplementation was analyzed in the earlier work (Kalamkar et al., 2022) by comparing 6-month changes in D and DG groups through population-level Cohen's-d-based estimates. GSH supplementation was found to significantly affect GSH, GSSG, and 8-OHdG levels (at moderate levels of Cohen's $d > 0.6$) and not for HbA1c, FPG, FPI, and PPG variables. The LME model framework helped analyze biochemical responses longitudinally and obtain more refined estimates that account for inter-individual and within-individual variations at two levels of hierarchy. We note that LME models describe linear trajectories over a 6-month duration. The estimates show that D and DG average trajectories lie between the 25th and 75th percentiles of the data at all visits; that is, these models are a good description of the data.

Model estimates were consistent with the effect size estimates in the earlier study (Kalamkar et al., 2022) for GSH, GSSG, 8-OHdG, HbA1c, FPG, FPI, and PPG variables but not for PPI. LME estimates determined that the GSH supplementation markedly enhanced the rate of replenishments in erythrocytic GSH stores by about 22%, GSSG stores by about 6%, and reduced oxidative DNA damage by about 4% of the baseline month in diabetic patients. Importantly, these estimates are in the actual (not relative) physical units and are, therefore, directly interpretable for use in clinical applications.

We had identified an older subgroup separate from a younger diabetic population that benefits better from GSH supplementation through a *post hoc* subgroup analysis in our earlier study. That study wasn't designed to evaluate this analysis explicitly, and as such, it was a weaker form of evidence. LME models provided a more formal way of comparing their differential responses; that is, two independent models described the responses in each of these two

age classes. GSH supplementation improved the rates of 8-OHdG and HbA1c reduction in elder diabetic individuals more than in younger diabetic cohorts. LME models estimated the effect to be significant for FPI in elder patients, which supported our claims of a beneficial elder cohort. Model estimates for GSSG suggested a significant effect of GSH supplementation in younger patients (by 17 μ M per month) but not in elder ones. In contrast to the earlier results, PPI model estimates were found to be significant in both elder and younger cohorts. Thus, our model-based analysis describes the extent to which diabetic patients above 55 can be expected to benefit from GSH supplementation.

LME model estimates further allow for examining the strength of the association between covariates. The results of the correlation analysis (in Figure 3; Supplementary Figure S3) show to what extent GSH intervention improves erythrocytic GSH stores and reduces DNA damage. Estimates from the elder and younger individuals also revealed that GSH changes were correlated strongly with changes in HbA1c and 8-OHdG in elder adults.

Finally, we have formulated a scheme (in Supplementary Section S1.5) that makes individual-specific *predictions* for newly recruited subjects with diabetes, given a baseline measurement by using the LME model estimates of the fixed-effects and random-effects parameters. In particular, this scheme can be utilized to make predictions of what changes might be expected in the biochemical levels. Alternatively, the average time required for a recruited patient to reach a particular range of biochemical parameters in diabetic subjects can be estimated. The fitted LME model estimates can be used to identify the extent of each subject's response, whether they are in a better or worse condition than the average population response (Inzucchi et al., 2012; Kirkman et al., 2012). These schemes are of direct clinical and academic use to predict prospective trajectories, which can be a powerful addition to the clinician's toolbox.

Strengths of this study include that it is based on the data available from diabetic individuals on a well-conducted, randomized control trial, which is one of the most extensive GSH supplementation studies so far. Using LME models, we evaluated the individual trajectories and associated variations within individuals and between individuals, which has not been done before in GSH intervention studies.

It is particularly important to keep in mind that our understanding of the results is based on the uncorrected *p* values. The practice of correcting for multiple comparisons has been a topic of debate among statisticians for several years now. Various opinions were found in the literature in opposition regarding the conditions under which a correction for multiple testing should be applied. We note that several highly cited reports over the years (Poole, 1991; Perneger, 1998; Cabin and Mitchell, 2000) recommend dismissing the usage of corrections with multiple comparisons. It was shown that when trying to reduce the rate of false positives (Type I error) for null associations, often leads to an increase in the rate of false negatives (Type II error) for those that are not null (Rothman, 1990). Also, these comparisons were often complained of being unnecessarily conservative, which makes this approach frequently fails to identify actual differences. However, for the interest of all readers, we have also incorporated significance levels after corrections for each comparison. Those readers who prefer statistically corrected results should follow the corresponding

tables to determine which findings still retain significance and which did not after correction for multiple comparisons.

We had earlier identified the differential effects of GSH supplementation in elder and younger subgroups (Kalamkar et al., 2022). This study analyzed the longitudinal responses of GSH supplementation observed in these subgroups of diabetic individuals rigorously with a framework of the LME models. The subgroup of subjects above the median age of 55 is consistent with previous studies that show an increased risk of diabetes-related complications in individuals around this age. Several organizations have already developed guidelines specific to, or including, older adults on their annual Standards of Medical Care in Diabetes (American Diabetes Association, 2012). These reports also discuss the severity of diabetes complications in elders and the lack of high-level evidence on the effectiveness of different medications in diabetics (Leung et al., 2018). We think the onset of diabetes and complications should be addressed differently for elder and younger diabetic individuals, and treatments need to be planned separately from each other. The two independent LME models formulated for analyzing the longitudinal trajectories of elder and younger adults provided estimates of the treatment effect of GSH supplementation on each endpoint separately. This helps in identifying their extent of recovery and examining whether individuals are in a better or worse condition than the average profile in these subgroups on GSH supplementation for direct clinical use. We recommend planning large-scale clinical trials to examine these insights about GSH supplementation, especially in elder diabetic individuals. This could help in establishing novel benchmarks for caring for elder patients with diabetes. We have also analyzed different possible models to study the effect of the age of individuals on GSH supplementation. This will form the basis and motivate a number of future studies to examine many of the finer nuances of the effect of age on supplementation.

Some limitations of this study also need to be considered. Although antidiabetic treatments were not changed during the period of the study, patients did use different types of medication. We have not analyzed the combinatorial complexity of treatments further due to a lack of sufficient statistical power. It is possible that future work may uncover if GSH supplementation is particularly more effective with certain treatments than others. The results presented here can be the basis for future GSH intervention studies that advance precision diabetes research.

Data availability statement

Publicly available datasets were analyzed in this study. This data can be found here: 10.6084/m9.figshare.21786518.

Ethics statement

The studies involving human participants were reviewed and approved by the Institutional Ethical Committee (IEC) of Jehangir Hospital Development Center, Pune (JCDC ECN- ECR/352/Inst/NIH/2013); Institutional Biosafety Committee (IBC) of SPPU (Bot/27A/15), Pune; and the Institutional Ethical Committee (IEC) of IISER, Pune (IECHR/Admin/2019/001). The clinical trial is registered with the Clinical Trials Registry-India (CTRI/2018/01/

011257). Written informed consent to participate in this study was provided by the participants and a legal guardian/next of kin.

Author contributions

AM and PG designed the study and performed the model computations. SG, PG, AM, and SK contributed to the analysis of the results and the editing of the manuscript. All authors have read and confirmed the published version of the manuscript.

Funding

AM is financially supported by a Senior Research Fellowship from DST-Inspire, Government of India, and SK was supported by Senior Research Fellowship from CSIR, India, during the study.

Acknowledgments

We acknowledge the above-mentioned funding agencies for all financial help.

References

- Allen, J., and Bradley, R. D. (2011). Effects of oral glutathione supplementation on systemic oxidative stress biomarkers in human volunteers. *J. Altern. Complement. Med.* 17, 827–833. doi:10.1089/acm.2010.0716
- American Diabetes Association (2012). Standards of medical care in diabetes-2012. *Diabetes Care* 35 (1), S11–S63. doi:10.2337/dc12-s011
- Baldwin, S. A., Imel, Z. E., Braithwaite, S. R., and Atkins, D. C. (2014). Analyzing multiple outcomes in clinical research using multivariate multilevel models. *J. Consult. Clin. Psychol.* 82 (5), 920–930. doi:10.1037/a0035628
- Barr, D. J., Levy, R., Scheepers, C., and Tily, H. J. (2013). Random effects structure for confirmatory hypothesis testing: Keep it maximal. *J. Mem. Lang.* 68 (3), 255–278. doi:10.1016/j.jml.2012.11.001
- Bates, D., Mächler, M., Bolker, B., and Walker, S. (2015b). Fitting linear mixed-effects models Using lme4. *J. Stat. Softw.* 67 (1). doi:10.18637/jss.v067.i01
- Bates, D. M., Kliegl, R., Vasishth, S., and Baayen, H. (2015a). *Parsimonious mixed models*. ArXiv Methodology. doi:10.48550/arXiv.1506.04967
- Bell, A., Holman, D., and Jones, K. (2019). Using shrinkage in multilevel models to understand intersectionality: A simulation study and a guide for best practice. *Methodology* 15 (2), 88–96. doi:10.1027/1614-2241/a000167
- Brown, H., and Prescott, R. (2006). “Applied mixed models in medicine,” in *Applied mixed models in medicine*. Second Edition (John Wiley & Sons).
- Brownlee, M. (2005). The pathobiology of diabetic complications: A unifying mechanism. *Diabetes* 54, 1615–1625. doi:10.2337/diabetes.54.6.1615
- Burgos-Morón, E., Abad-Jiménez, Z., Martínez de Marañón, A., Iannantuoni, F., Escribano-López, I., López-Domènech, S., et al. (2019). Relationship between oxidative stress, ER stress, and inflammation in type 2 diabetes: The battle continues. *J. Clin. Med.* 8, 1385. doi:10.3390/jcm8091385
- Cabin, R. J., and Mitchell, R. J. (2000). To Bonferroni or not to Bonferroni: When and how are the questions. *Bull. Ecol. Soc. Am.* 81 (3), 246–248.
- Gelman, A., Hill, J., and Yajima, M. (2012). Why we (usually) don't have to worry about multiple comparisons. *J. Res. Educ. Eff.* 5 (2), 189–211. doi:10.1080/19345747.2011.618213
- Inzucchi, S. E., Bergenstal, R. M., Buse, J. B., Diamant, M., Ferrannini, E., Nauck, M., et al. (2012). Management of hyperglycemia in type 2 diabetes: A patient-centered approach: Position statement of the American diabetes association (ada) and the European association for the study of diabetes (easd). *Diabetes Care* 35, 1364–1379. doi:10.2337/dc12-0413
- Kalamkar, S., Acharya, J., Kolappurath, M. A., Gajjar, V., Divate, U., Karandikar-Iyer, S., et al. (2022). Randomized clinical trial of how long-term glutathione

Conflict of interest

The authors declare that the research was conducted in the absence of any commercial or financial relationships that could be construed as a potential conflict of interest.

Publisher's note

All claims expressed in this article are solely those of the authors and do not necessarily represent those of their affiliated organizations, or those of the publisher, the editors and the reviewers. Any product that may be evaluated in this article, or claim that may be made by its manufacturer, is not guaranteed or endorsed by the publisher.

Supplementary material

The Supplementary Material for this article can be found online at: <https://www.frontiersin.org/articles/10.3389/fphar.2023.1139673/full#supplementary-material>

- supplementation offers protection from oxidative damage and improves HbA1c in elderly type 2 diabetic patients. *Antioxidants* 11 (5), 1026. doi:10.3390/antiox11051026
- Kirkman, M. S., Briscoe, V. J., Clark, N., Florez, H., Haas, L. B., Halter, J. B., et al. (2012). Diabetes in older adults. *Diabetes Care* 35 (12), 2650–2664. doi:10.2337/dc12-1801
- Laird, N. M., and Ware, J. H. (1982). Random-effects models for longitudinal data. *Biometrics* 38, 963–974. doi:10.2307/2529876
- Leung, E., Wongrakpanich, S., and Munshi, M. N. (2018). Diabetes management in the elderly. *Diabetes Spectr.* 31 (3), 245–253. doi:10.2337/ds18-0033
- Pearson, K. (1895). Notes on regression and inheritance in the case of two parents. *Proc. R. Soc. Lond.* 58, 240–242. doi:10.1098/rspl.1895.0041
- Perneger, T. V. (1998). What's wrong with Bonferroni adjustments. *BMJ* 316 (7139), 1236–1238. doi:10.1136/bmj.316.7139.1236
- Poole, C. (1991). Editorial. *Epidemiology* 2 (4), 241–243. doi:10.1097/00001648-199107000-00001
- Ritchie, J. P., Nichenametta, S., Neidig, W., Calcagnotto, A., Haley, J. S., Schell, T. D., et al. (2015). Randomized controlled trial of oral glutathione supplementation on body stores of glutathione. *Eur. J. Nutr.* 54, 251–263. doi:10.1007/s00394-014-0706-z
- Rothman, K. J. (1990). No adjustments are needed for multiple comparisons. *Epidemiology* 1 (1), 43–46. doi:10.1097/00001648-199001000-00010
- Schober, P., and Vetter, T. R. (2021). Linear mixed-effects models in medical research. *Anesth. Analg.* 132 (6), 1592–1593. doi:10.1213/ANE.0000000000005541
- Sekhar, R. V., Patel, S. G., Guthikonda, A. P., Reid, M., Balasubramanyam, A., Taffet, G. E., et al. (2011). Deficient synthesis of glutathione underlies oxidative stress in aging and can be corrected by dietary cysteine and glycine supplementation. *Am. J. Clin. Nutr.* 94, 847–853. doi:10.3945/ajcn.110.003483
- Titz, J. (2020). Mimosas: A modern graphical user interface for 2-level mixed models. *J. Open Source Softw.* 5, 2116. doi:10.21105/joss.02116
- Townsend, D. M., Tew, K. D., and Tapiero, H. (2003). The importance of glutathione in human disease. *Biomed. Pharmacother.* 57, 145–155. doi:10.1016/s0753-3322(03)00043-x
- Volpe, C. M. O., Villar-Delfino, P. H., Dos Anjos, P. M. F., and Nogueira-Machado, J. A. (2018). Cellular death, reactive oxygen species (ROS) and diabetic complications. *Cell. Death Dis.* 9, 119. doi:10.1038/s41419-017-0135-z
- Wang, G., Aschenbrenner, A. J., Li, Y., McDade, E., Liu, L., Benzinger, T. L. S., et al. (2019). Two-period linear mixed effects models to analyze clinical trials with run-in data when the primary outcome is continuous: Applications to Alzheimer's disease. *Alzheimers. Dement.* 5 (5), 450–457. doi:10.1016/j.trci.2019.07.007

Appendix C

Ethics statement

The Institutional Ethical Committee (IEC) of IISER Pune approved the studies discussed in this thesis. These studies are listed below:

1. The work described in **Chapter 3** and **Chapter 4** was a part of the project titled, **Mathematical Modeling and Statistical analysis of the Role of GSH in Diabetic Treatment** approved by the IEC (Ref: IECHR/Admin/2019/001).
2. The work described in **Chapter 5** was a part of the project titled, **Mathematical Modeling and Statistical analysis of erythrocytic GSH/GSSG levels under extracellular treatments with GSH, GSSG, and Hydrogen Peroxide** approved by the IEC (Ref: IECHR/Admin/2021/009).

The approval documents are attached below respectively.

भारतीय विज्ञान शिक्षा एवं अनुसंधान संस्थान पुणे
INDIAN INSTITUTE OF SCIENCE EDUCATION AND RESEARCH PUNE

डॉ. होमी भाभा मार्ग, पुणे 411008, महाराष्ट्र, भारत | Dr. Homi Bhabha Road, Pune 411008, Maharashtra, India
T +91 20 2590 8001 W www.iiserpune.ac.in



IECHR CERTIFICATE

Date: 28th February 2019

Ref.: IECHR/Admin/2019/001

To,

Dr. Pranay Goel
IISER, Pune

Dear Dr. Goel,

This is with reference to your project proposal titled *Mathematical Modeling and Statistical analysis of the Role of GSH in Diabetic Treatment* submitted to the IISER Ethics Committee for Human Research. It was considered by the committee in its meeting held on *February 21st, 2019*.

Since this is a proposal for secondary data analysis and no direct data collection is involved in the study, a waiver from the IECHR is being issued.

Yours sincerely

A handwritten signature in blue ink, appearing to read "Vineeta Bal".

[Vineeta Bal]
Member Secretary

भारतीय विज्ञान शिक्षा एवं अनुसंधान संस्थान पुणे

INDIAN INSTITUTE OF SCIENCE EDUCATION AND RESEARCH PUNE

डॉ. होमी भाभा मार्ग, पुणे 411008, महाराष्ट्र, भारत | Dr. Homi Bhabha Road, Pune 411008, Maharashtra, India
T +91 20 2590 8001 W www.iiserpune.ac.in



IECHR APPROVAL CERTIFICATE

Date: 22nd March 2021

Ref.: IECHR/Admin/2021/009

To
Dr. Pranay Goel
IISER, Pune

Dear Dr. Goel,

This is with reference to your project proposal titled "*Mathematical modeling and statistical analysis of erythrocytic GSH/GSSG levels under extracellular treatments with GSH, GSSG, and Hydrogen peroxide.*" submitted to the IISER Ethics Committee for Human Research. It was considered by the committee in its meeting held on March 10, 2021.

Since this is a proposal for secondary data analysis and no direct data collection is involved in the study, a waiver from the IECHR is being issued.

Sincerely

A handwritten signature in black ink, appearing to read "Aurnab Ghose".

[Aurnab Ghose]
Convenor